Harnessing the Potential of MAIT Cells as Cellular Adjuvants in Mucosal Vaccines

Kaitlin Buick

2020

A thesis submitted to Victoria University of Wellington in fulfilment of the requirements of the degree of Master of Biomedical Science

Abstract

The development of vaccines is considered one of the most successful medical interventions to date, preventing millions of deaths every year. However, the majority of vaccines are administered peritoneally, despite the vast majority of pathogens invade the human host at mucosal sites. By vaccinating at distal sites, little to no protection is developed at the mucosa where the initial invasion occurs. There are however, a handful of licenced mucosally administered vaccines against infections such as poliovirus, influenza and *Salmonella* Typhi that are able to induce both a systemic and mucosal protective immune response. All but one of the current licenced mucosal vaccines are live attenuated due in part to the difficulty of developing new mucosal adjuvants. Recombinant cholera toxin subunit B is the only adjuvant used in the current licenced mucosal vaccines. While inactivated and subunit vaccines are considered safer as they are unable to revert back to virulent pathogens, adjuvants are required to boost their immunogenicity. This thesis therefore explores whether mucosal-associated invariant T (MAIT) cells which are found in mucosal tissues, are invariant in nature and have rapid activation, could be exploited as cellular adjuvants in mucosal vaccines.

This thesis was able to show that intranasally administered MAIT cell agonist components, 5-A-RU and methylglyoxal (MG), are able to induce both MAIT cell and conventional dendritic cell (cDC) activation in the lung tissue and mediastinal lymph node (mLN). In this model CD40L and RANKL co-stimulatory interactions are involved in ICOSL expression on cDCs in the lung and associated with cDC activation. The MAIT cells within this model also maintained a RORγT and GATA3 phenotype after both one and three doses of the 5-A-RU + MG vaccine. Furthermore, a prime-boost intranasal vaccine scheme of 5-A-RU + MG and the model antigen OVA, was able to induce MR1-dependent accumulation of T_{FH} cells and antigen-specific germinal center B cells in the mLN along with systemic antigen-specific IgG antibody production. This humoral response was also dependent on the presence of both cDC1 and cDC2 populations. Together, this thesis suggests MAIT cells have the potential to be utilised as cellular adjuvants in mucosal vaccines.

Acknowledgements

Firstly, I would like to thank my supervisor Dr. Lisa Connor for kindly taking me on during unexpected circumstances. You have always given me your support, time and guidance which has allowed me to produce a thesis of which I'm proud of. Thank you for also showing me your passion for science and always seeing the positive side of everything. And of course, thank you to the rest of the LC team, especially Theresa, Olga and Kaileen for helping on long harvest days and giving me your support and laughter along the way, plus for maintaining a spotless lab space. Also thank you to the TTR mouse facility for looking after the mice required for this thesis.

Thank you to everyone at the Malaghan Institute for always making me feel welcome and sharing your knowledge and expertise, and a big thank-you to the Huge Green Cytometry Centre and Biomedical Research Unit staff for providing the resources to improve my science. I would also like to thank the Young Researchers Club for always providing an enjoyable end to the week. Additionally, thank-you to the Ferrier Research Institute for providing the compounds to make this project possible.

I would also like to thank the funding bodies. To the Health Research Council of New Zealand for providing the funds for this project, the Research For Life Wellington Medical Research Foundation and the Centre for Biodiscovery for supporting my attendance at conferences over the last year and to Victoria University for awarding the scholarships that have made my study possible.

To Phoebe and Palak, I cannot thank you enough. You have helped me through a crazy and stressful time, you have given me your support, advice, laughter and above all your friendship. You have always been there to just listen and made the last two years so enjoyable. You are both hard working intelligent scientists and I can't wait to see where your scientific careers take you.

Thank you to Storm for being my home away from home and for putting up with me for so many years. Thank you for your unwavering friendship, being an ear to listen and

making me laugh and smile. You will always be a forever friend. Also, to John, for the support, laughter and relaxing times amid the stress, and Brigette, for the much-needed catch ups, debriefs and bubble tea sessions.

And finally, to my family. Thank you to Mum and Dad for always allowing me to pursue my interests and your continuous support in the decisions and pathways I take. You have both always shown me love and support. Also thank you to Jason and Nicole for being amazing siblings who I can always look up to. Especially to Nicole, for always looking out for me over the years I have been studying in Wellington, for the movie nights and dinner dates and the constant wealth of support and advice. And lastly to my sister Shannon, for sparking my love for science xx

Disclosure Statement

This thesis was done in collaboration with the Malaghan Institute of Medical Research and the Ferrier Research Institute. The prime-boost experiments were also done in collaboration with PhD candidate Theresa Pankhurst.

Table of Contents

List of Figures

List of Tables

Abbreviations

5-A-RU	5-amino-6-D-ribitylaminouracil
5-OE-RU	5-(2-oxoethylideneamino)-6-D-ribitylaminouracil
5-OP-RU	5-(2-oxopropylideneamino)-6-D-ribitylaminouracil
6-FP	6-formylpterin
α-GalCer	α-galactosylceramide
Ac-6-FP	Acetyl-6-formylpterin
ACT	Tris-Buffered Ammonium Chloride
Alum	Aluminium salts
AP-1	Activator protein 1
APC	Antigen presenting cell
APRIL	A proliferation-inducing ligand
BAFF	B cell-activating factor
BALT	Bronchus-associated lymphoid tissue
BATF3	Basic leucine zipper transcriptional factor ATF-like 3
BCL6	B-cell lymphoma 6 protein
BCR	B cell receptor
CCL	C-C motif chemokine ligand
CCR	C-C motif chemokine receptor
CD	Cluster of differentiation
cDC	Conventional dendritic cell
Clec9A	C-type lectin domain family 9 member A
CLR	C-type lectin receptor
CT	Cholera toxin
CTL	Cytotoxic T lymphocytes
CTLA-4	Cytotoxic T-lymphocyte-associated protein 4
CXCR	C-X-C motif chemokine receptor
D	Diversity genes
DAMPs	Damage-associated molecular patterns
DAP	DNAX-activating protein

DC	Dendritic cell
DNA	Deoxyribonucleic acid
EDTA	Ethylenediaminetetraacetic acid
ELISA	Enzyme-linked immunosorbent assay
ER	Endoplasmic reticulum
FAE	Follicle-associated epithelium
FBS	Foetal bovine serum
FMO	Fluorescence minus one
FoxP3	Forkhead box P3
GALT	Gut-associated lymphoid tissue
GATA3	GATA binding protein 3
GC	Germinal center
GFP	Green fluorescent protein
GM-CSF	Granulocyte-macrophage colony-stimulating factor
HIV	Human immunodeficiency virus
HLA	Human leukocyte antigen
HSV-1	Herpes simplex virus-1
IFN	Interferon
ICOS	Inducible T cell co-stimulator ligand
Ig	Immunoglobulin
Ii	Invariant chain
IL	Interleukin
i.n.	Intranasal
i.p.	Intraperitoneal
IPS-1	IFN-β promoter stimulator-1
IRF	Interferon regulatory factor
J	Joining genes
LCMV	Lymphocytic choriomeningitis virus
LFA-1	Lymphocyte function-associated antigen 1
LN	Lymph node
LPS	Lipopolysaccharide
Lys	Lysine

MAIT cell	Mucosal -associated invariant T cell
MALT	Mucosal-associated lymphoid tissue
MARCH1	MHCII ubiquitin by membrane associated ring-CH-type finger 1
M cell	Multifenestrated cell
MFI	Median fluorescence intensity
MG	Methylglyoxal
MHC	Major histocompatibility complex
mLN	Mediastinal lymph node
MPL	3-O-desacyl-4'-monophosphoryl lipid A
MR1	Major histocompatibility complex-related molecule 1
MS	Multiple sclerosis
Mtb	*Mycobacterium tuberculosis*
MyD88	Myeloid differentiation primary response protein 88
NALT	Nasopharynx-associated lymphoid tissue
NF-AT	Nuclear factor of activated T-cells
NF-κB	Nuclear factor kappa-light-chain-enhancer of activated B cells
NKT cell	Natural killer T cell
NLR	NOD-like receptors
NOD1	Nucleotide-binding oligomerization domain-containing 1
Nur77	Nuclear receptor 77
OPV	Oral polio vaccine
OVA	Ovalbumin
Pam2Cys	dipalmitoyl-S-glyceryl cysteine
PAMPs	Pathogen-associated molecular patterns
PBS	Phosphate buffered saline
PD-1	Programmed cell death protein 1
PDL-1	Programmed death-ligand 1
PRRs	Pattern recognition receptors
qPCR	Quantitative polymerase chain reaction
RANK	Receptor activator of nuclear factor kapa-B
RBC	Red blood cell
RIP2	Receptor-interacting-serine/threonine-protein kinase 2

RLR	Retinoic acid-inducible gene-I-like receptors
RNA	Ribonucleic acid
RORγt	Retinoic-acid-receptor-related orphan nuclear receptor gamma
Sags	Superantigens
S-IgA	Secretory immunoglobulin A
SIRPα	Signal-regulatory protein α
STAT6	Signal transducer and activator of transcription 6
TACI	transmembrane activator and calcium-modulating cyclophilin ligand interactor
T_{EM}	Effector memory T cells
T_{CM}	Central memory T cells
TCR	T cell receptor
TF	Transcription factor
T_{FH}	T follicular helper cell
TGF-β	Transforming growth factor beta
T_H	T helper cells
TLR	Toll-like receptor
TNF	Tumor necrosis factor
TRAF	Tumour necrosis factor receptor associated factors
T_{Reg}	T regulatory cell
TRIF	TIR-domain-containing adaptor-inducing interferon-β
TRIM21	Tripartite motif-containing protein 21
T_{RM}	Tissue-resident memory T cell
Ty21A	Oral *Salmonella* Typhi vaccine
V	Variable genes
YF-17D	Yellow fever vaccine

1 General Introduction

1.1 Vaccination

Vaccination is considered one of the most effective medical interventions developed by humans to date[1]. In lay terms, a vaccination is when a weakened, killed or component of a microbe is injected into the body and induces a protective immune response upon future re-exposure to the microbe subsequently preventing or reducing severity of the disease[2]. Since Edward Jenner's experimentation with a smallpox vaccination over two centuries ago, vaccines are now estimated to prevent 2-3 million deaths per year by the World Health Organisation[3]. The success of vaccinations is further highlighted through the eradication of smallpox and the extensive reduction in incidence (over 95%) in diseases such as tetanus, rubella and diphtheria[4]. Vaccination schemes are not only based on an individual's protection but also on the practice of herd immunity. Herd immunity allows for the protection of individuals that are immunocompromised, unvaccinated and/or immunologically naïve due to the majority of the population being vaccinated and therefore reducing the likelihood of transmission to susceptible individuals[5]. With the growing understanding of the immune system and the immune mechanisms involved in vaccination, the approach to vaccine design has become more rational and directed.

Vaccines can be classified into four different categories, live attenuated, killed/inactivated, subunit and toxoid vaccines. These categories are dependent on the vaccine antigens origin and nature[6]. The widely used live attenuated vaccines involve attenuating the pathogen to produce a non-virulent form that still remains viable, either through passage of the pathogen in a foreign host or by growing the pathogen in media at temperatures lower than the human body. This results in mutants that have a low virulence in the human host allowing for the development of an adaptive memory immune response and clearance of the pathogen[6,7]. killed (bacterial) or inactivated (viral) vaccines are produced by killing the pathogen through either heat, chemicals or radiation and unlike live attenuated vaccines, are unable to replicate within the host. However, they are still able to provide the whole pathogens array of antigens to induce an immune response[8]. The third vaccine category, subunit vaccines, comprise of only a

specific or several specific antigens from the pathogen[9]. Lastly, toxoid vaccines facilitate formaldehyde to alter a pathogens toxin both by changing specific amino acids and causing conformational changes. These changes lead to a non-toxic toxoid which still has similar physciochemically properties to induce cross-protective antibodies to the naïve toxin[6,10].

Each of the vaccine categories have their advantages and disadvantages. Live attenuated vaccines such as the smallpox, polio and measles vaccines are able to induce a strong, long lasting response due to the ability to replicate and provide a wide range of danger and pathogen signals, resulting in a highly immunogenic vaccine[11]. However, a live pathogen can be unstable in environmental conditions and there is a small risk of the pathogen reverting back to a virulent form in the human host[12]. To combat this virulence risk, killed/inactivated, subunit and toxoid vaccines use either killed pathogens or a select number of antigens to induce an immune response, respectively. Additionally, these vaccines are also usually more stable and last longer when out in the environment. However, due to the low immunogenicity, they often require multiple doses and the addition of an adjuvant to provide a strong protective response[6]. Furthermore, while inactivated and subunit vaccines are considered safer, they don't actively infect, therefore they can be limited in their ability to access the appropriate tissues and induce a local immune response. For example, the intramuscular administered inactivated polio vaccine provides a systemic humoral response but only induces a limited mucosal response[13].

1.1.1 Vaccine Adjuvants

A vaccine adjuvant is defined as a substance that enhances, accelerates and prolongs an antigen specific immune response to a vaccine antigen, and is required by some vaccine categories to improve the efficacy of the vaccine[14,15]. Additionally, adjuvants can be used to drive favourable immune responses and allows for reduced doses of antigen and fewer vaccine doses[16]. Adjuvants can be divided based on their mechanism, they can either provide help through improving delivery of the vaccine antigen or through

directly stimulating the immune system[17]. One of the first scientists to explore the idea of vaccine adjuvants was veterinarian, Gaston Ramon, in the 1920's, who by injecting foodstuffs such as tapioca and starch along with a vaccine was able to enhance the adaptive antiserum yield[15,18]. This technique was able to induce a local inflammatory response and therefore, boost the subsequent adaptive response. Alexander Glenny was another scientist around the same time who was exploring the use of aluminium potassium sulphate as an adjuvant in 1926. He along with his colleagues were able to show an enhanced antibody response compared to antigen alone when antigen was precipitated with aluminium potassium sulphate. This research kick started the use of aluminium salts (alum) as adjuvants in human vaccines against tetanus and diphtheria beginning in 1932 and is still the most widely used vaccine adjuvant today, nearly 100 years after its discovery[15,19,20].

Despite the long history and continued use of alum as a vaccine adjuvant, the mechanism of action remains unclear. Initially it was believed that alum caused a depot effect by which the alum allowed the slow release of the vaccine antigen and therefore the persistent activation of the immune system[19]. However, the removal of the vaccination site after administration of alum plus antigen has no effect on the adaptive response[21], suggesting this depot effect is not the underlying mechanism. Recent research has investigated alternative mechanisms and has suggested a requirement of elements such as the Nalp3 inflammasome[22] and the danger signal uric acid[23]. However these pathways have failed to be consistently required in follow up studies[19]. Hence, the mechanism behind alum adjuvanticity remains to be elucidated, highlighting the difficulty in determining adjuvants modes of action.

Since the discovery of alum as an adjuvant, few other adjuvants have become licenced for use in human vaccines. Oil-in-water emulsions are another form of adjuvant including MF59 and AS03. These adjuvants began with Jules Freund's, 'Freund's complete adjuvant', a mixture of paraffin oil and mycobacterial cells. Using this adjuvant, Freund was able to show a long term antibody response in guinea pigs and

rabbits[24]. Freund's incomplete adjuvant, which excludes the bacterial component has also been used in both veterinary and human vaccines, however, the adjuvant caused local reactions in trials and so was discontinued[25,26]. The first successful oil-in-water emulsion and second vaccine adjuvant to be licenced for use in humans was MF59 in 1997. This was almost 70 years after the licencing of alum. MF59 is made up of squalene oil combined with surfactants Tween 80 and Span 85 and has been used in influenza vaccines[26]. The adjuvant effect of MF59 requires the oil-in-water formulation[27] and leads to a chemokine gradient at the site of vaccination which recruits antigen presenting cells (APCs) such as monocytes and granulocytes resulting in an amplification of the chemokine gradient. This inflammatory response increases the APCs and subsequently the trafficking to the draining lymph nodes for T cell priming[28–31]. AS03 is another oil-in-water emulsion comprised of α-tocopherol, squalene and polysorbate 80. It has been successfully licenced for two influenza vaccines, a H1N1 pandemic[32] and a H5N1 pre-pandemic[33] vaccine. Similar to MF59, AS03 stimulates cytokine and chemokine production at the injection site, resulting in recruitment of monocytes and granulocytes to the local site and the draining lymph node, leading to an antibody response[34].

Virosomes are a novel delivery system which can also be used as an adjuvant. A virosome is derived from an influenza envelope minus the virus's genetic material. It forms a vesicle that is comprised of lipids and also contains the hemagglutinin and neuraminidase proteins found in influenza envelopes. This allows the virosome to maintain the same binding and membrane fusion properties as influenza[35]. Therefore, virosomes are able to be used as antigen delivery systems which are safe as they are unable to replicate but also maintain some of the viral signals so are able to stimulate the immune system and stabilise the antigen. Virosomes can display the antigen on the outer surface to prime a B cell response and/or a cluster of differentiation (CD)4^+ helper T cell response through the major histocompatibility complex (MHC) II. Alternatively, if the antigen is internalised within the virosome, it can be delivered into the cytoplasm of APCs and induce a cytotoxic $CD8^+$ T cells response through MHCI. Virosomes allow for

a diverse adaptive response and are licenced as vaccine adjuvants for influenza and hepatitis A[36].

In contrast to using adjuvants as delivery systems, some adjuvants are able to directly stimulate the immune system such as AS04. There are many immunoenhancer adjuvants that are currently being investigated, however, there are safety concerns as the direct stimulation of the immune system can lead to toxic side effects. AS04 is able to combat these concerns as it's a combination of detoxified immunoenhancer 3-O-desacyl-4'-monophosphoryl lipid A (MPL) and aluminium hydroxide. MPL is a detoxified form of lipopolysaccharide (LPS) derived from *Salmonella Minnesota* which binds Toll-like receptor 4 (TLR4). Unlike LPS, which can induce a detrimental cytokine storm, MPL has reduced toxicity but maintains the immunostimulatory factors through TLR4[37–39]. AS04 is able to induce the transcription factor complex, nuclear factor kappa-light-chain-enhancer of activated B cells (NF-κB), and subsequently cytokine release, this helping to activate antigen specific dendritic cells (DCs) and monocytes both at the injection site and in the draining lymph node. This activation of the innate system improves the activation of antigen specific T cells. Although the alum component of the adjuvant doesn't synergies with MPL it allows for a prolonged response at the injection site[40]. AS04 is currently licenced as an adjuvant in vaccines against hepatitis B virus and human papillomavirus[41].

The selection of adjuvant is of importance as adjuvants not only impact the innate response[30,34,40] but different adjuvants also skew the protective adaptive response to vaccine antigen. For example, adjuvants such as alum induce a dominant T_H2 response, whereas AS04 skews more of a T_H1 response[40]. The addition of an adjuvant also impacts the B cell and antibody response, with the increase in antigen specific B cells and higher titers of neutralising and cross-reactive antibodies with an adjuvanted vaccine compared to no adjuvant[42]. Moreover, unlike alum adjuvants, oil-in-water emulsions are able to enhance the immunogenicity of influenza vaccines, with adjuvants such as MF59 being able to induce epitope spreading from HA2 to HA1 in influenza infection

compared to alum and non-adjuvanted vaccines[43]. The epitope spreading allows for protection against strains that may have gone through antigenic drift, therefore the vaccine is more advantageous as it is able to protect against more than one strain. These findings emphasise the importance of adjuvant selection in vaccine design.

1.1.2 Mucosal Vaccines

The majority of human vaccines are administered parenterally, either intramuscularly or subcutaneously via a needle injection[44]. However, despite the fact that over 90% of pathogens invade the human host through mucosal routes there are comparatively very few mucosally delivered vaccines. Parenteral vaccination leads to minimal or even a complete absence of immunity at the mucosa. This highlighting the benefit of mucosally administered vaccines which improve protection and prevent invasion at the local site of infection[44,45].

Mucosal vaccines also have advantages in terms of manufacturing and administration compared to injected parenteral vaccines. As the gut and other mucosal surfaces are already populated by the microbiome, containing vast amounts of bacteria, the endotoxin level in a vaccine is of less concern for a mucosal vaccine. This reducing the amount of purification required, saving on cost and time[46]. Additionally, the needleless administration reduces the transmission risk of blood-borne diseases from contaminated needles[47], allows painless administration[48] with the potential to improve compliance and doesn't require trained medical staff to administer[46].

Mucosal routes include oral, nasal, ocular, sublingual, rectal and genital tract. The administration of vaccines at a specific mucosal site also leads to adaptive antibody responses at other distal mucosal sites[49,50]. Furthermore, mucosal delivery of antigen has been shown to induce circulating antibody producing cells giving a systemic protection[51,52]. The mucosal route that is chosen can also alter the resulting immune response at other mucosal sites, showing a preference for specific sites. For example, oral vaccination has been shown to lead to a stronger immune response in the saliva

and virginal secretions whereas, rectal vaccination gives a heightened response in the nasal and ocular secretions as well as the rectum. However, both have equivalent serum or systemic effects[53]. This shows that the administration route of vaccines can alter the immune response and is therefore an important consideration for vaccination schemes.

There are a handful of mucosal vaccines licenced for use in humans including vaccines against influenza, rotavirus, poliovirus, *Salmonella Typhi* and cholera[46]. The oral polio vaccine (OPV) is one of the most successful mucosal vaccines. Categorised as a trivalent vaccine, its comprised of the three live attenuated serotypes of poliovirus and provides a strong prolonged antibody response both systemically and mucosally[54]. Cases of polio have decreased by over 99% due to the launch of a global vaccination scheme in 1988 based on OPV. However, due to the vaccine being live attenuated, there has been some rare cases of vaccine-derived poliovirus caused by genetic drift back to virulent strains[55]. This emphasising that although the vaccine is highly effective, new alternatives or adjuvants to live attenuation are required.

1.1.2.1 Challenges of Mucosal Vaccines

The majority of licenced mucosal vaccines are live attenuated. Currently there is only one mucosal vaccine that doesn't follow this trend, the inactivated *Vibrio cholerae* Dukoral® vaccine, which has the addition of cholera toxin B subunit as an adjuvant[45,48]. Despite, many mucosal adjuvants being under continued research or clinical trials as candidate adjuvants, only cholera toxin B and virus envelope particles can be used in licenced mucosal vaccines[46]. The challenge in adjuvant design is being able to maintain improved immunogenicity while having minimal toxic side effects. The added challenge of the mucosa is the harsh mucosal conditions that the adjuvants need to navigate through. The mucosa is armed with an array of physical barriers such as mucus, tight junctions between epithelial cells, protease and nuclease enzymes, acidic conditions and peristalsis. All of these factors aim to prevent pathogens invading the human host and in doing so also provide barriers for vaccine administration and delivery across the mucosa. This is where live attenuated vaccines have an upper hand, as the pathogen is

able to readily invade the host. Additionally, the mucosal secretions dilute and trap vaccine components, making vaccine dose variable and challenging[56,57].

Another major challenge that mucosal adjuvants must overcome is the induction of tolerance. Tolerance is a protective mechanism that naturally occurs at the mucosa, whereby the immune system fails to respond to soluble antigens to prevent a detrimental immune response[58], particularly to innocuous antigens such as food antigens. Failure to induce tolerance can lead to food allergies[59] and autoimmune diseases[60]. Tolerance in the mucosal system is also involved in maintaining homeostasis with the microbiome[61]. Despite the protective role of mucosal tolerance, this system can be unfavourable to vaccine design by inducing tolerance to vaccine components instead of inducing a protective immune response to the antigen[62].

1.1.2.2 Improvements for Mucosal Vaccines

To attempt to combat the challenges of mucosal vaccines, new delivery systems are being investigated. These systems are designed to both protect the vaccine from degradation in the mucosa and also to improve uptake by immune cells[57]. Some of these delivery systems include encapsulating the vaccine in a capsule or coat. For example, the Ty21a vaccine against *Salmonella typhi* used an enteric-coated capsule to protect against the acidic conditions of the gut and improve protection[63]. Furthermore, vaccines coated by alginate microspheres[64], liposomes[65], proteasome vesicles[66] and the polysaccharide chitosan[67], have all been shown to improve circulating IgG and secretory IgA antibody responses when administered mucosally.

Once the vaccines have evaded the mucosa's secreted defences, the next hurdle is to get from the lumen of the mucosal system, through the epithelial barrier and into the host. One route to bypass this barrier is through multifenestrated (M) cells. M cells are located on the luminal side of Peyer's patches in the small intestine. They are able to endocytose antigen from the gut lumen and transfer it to the underlying lymphocytes for further processing[68]. This specialised mucosal delivery pathway can be targeted to improve vaccine uptake. Eldridge, J. *et al.* (1989) were able to show microspheres were

able to be processed through the Peyer's patches and when associated with a vaccine, were able to induce circulating antigen specific antibodies and secretory IgA. Whereas the soluble vaccine alone was ineffective at inducing these responses[69]. The addition of microspheres is able to direct the vaccine to the M cell and subsequently allow interaction with the host immune system, prompting an adaptive response. Furthermore, smaller nanometer particles may also have the potential to passively pass through the epithelial cells, improving mucosal uptake[70].

1.2 Mucosal Immune System

The mucosal immune system is comprised of organised inductive sites generally called mucosal-associated lymphoid tissues (MALT) which can be split into the gut-associated lymphoid tissue (GALT), bronchus-associated lymphoid tissue (BALT) and the nasopharynx-associated lymphoid tissue (NALT). This excluding the urogenital tract and the salivary and mammary glands[57]. These inductive sites initially interact with the antigen and begin the immune response which is then interconnected with effector sites such as the lamina propria where the antigen primed cells migrate[48]. Studies have suggested pathways between the different mucosal tissues forming a common mucosal immune system. Czerkinsky, C. *et al.* (1986), was able to show that after oral ingestion of bacterial antigen, antigen specific IgA producing cells were found in circulation at day 7, this was followed by antigen specific secretory IgA in the saliva and tears at 2 weeks[52]. Furthermore, McDermott, M., & Bienenstock, J., (1979), found that an adoptive lymphocyte transfer from donor mesenteric lymph nodes, resulted in the donor cells seeding the recipient gut, urogenital tract, mammary glands and mesenteric lymph nodes. These cells had a preference for IgA immunoglobulin receptor, whereas, cells transferred from peripheral lymph nodes mainly seeded the same lymph nodes in the recipient, but the majority of immunoglobulin was IgG isotype. This suggesting that lymphocytes of mucosal origin are able to move into different mucosal sites forming this common mucosal immune system[71]. However, it may be that the different origins of mucosal lymphocytes results in differing abilities for migration to distal mucosal sites, as in the same study, when lymphocytes from the mediastinal lymph nodes were

transferred, they showed preference for lung localisation[71]. This compartmentalisation or preference between different mucosal sites has also been shown with vaccination. An oral vaccination leads to stronger immune responses at different mucosal sites compared to rectal vaccination[53]. Together, it seems that the mucosal immune system is linked to distal mucosal tissues but select mucosal sites have differing migration abilities and tissue preferences to other mucosal sites.

Despite the vulnerable nature of the mucosal system, only thin epithelial barriers separate the body from the environment to allow for adsorption of nutrients and the exchange of gasses. However, these epithelial cells are able to recognise bacteria and bacterial products and stimulate the immune system through the release of chemoattractants such as C-C motif chemokine ligand 20 (CCL20)[72], interleukin 8 (IL-8)[73], granulocyte-macrophage colony-stimulating factor (GM-CSF) and tumor necrosis factor alpha (TNF-α)[74]. These chemoattractants are subsequently able to recruit a wide range of innate immune cells, including immature dendritic cells, macrophages, monocytes and polymorphonuclear leukocytes[72,73].

In the MALT of the distal ileum, highly organised lymphoid follicles aggregate together to form Peyer's patches. Similar less complex, isolated lymphoid follicles are found in the lamina propria of mucosal tissues[75] such as the colon, rectum and appendix. Above these follicles and Peyer's patches, sits a specialised epithelium called follicle-associated epithelium (FAE) which includes M cells. M cells are able to sample the antigens in the lumen of the mucosa and deliver the antigen via vesicular transport to DCs or a pocket directly below the FAE. The antigen positive DCs are able to process the antigen and present it as a peptide to naïve $CD4^+$ T cells and induce the consequent adaptive immune response, much like in a lymph node[48,56,57]. Not all mucosal epithelium contains M cells and organised lymphoid structures. Another route for antigens to cross the epithelium is directly through DC capture. DCs are able to protrude dendrites between epithelial cells and into the lumen and directly sample antigen[76–78]. The DCs are then able to either interact with T cells at the local site or migrate to draining lymph nodes to induce an

adaptive response[79]. Intact protein can also be found in the lymph and blood following ingestion, suggesting a role for passive antigen diffusion[80,81].

1.2.1 Microbiome

The human body is home to an estimated 38 trillion bacterial cells, compared to the estimated 30 trillion human cells[82]. These bacterial cells along with other microorganisms including fungi, archaea, protozoa and viruses make up the human microbiome[83]. Mammalian hosts and their microbiota share a mutualistic relationship, in which the host provides a specialised niche for the microorganisms to thrive and the microorganisms help to maintain homeostasis of the host. Unlike the human host, the microbiota are able to carry out anaerobic fermentation of undigestible dietary material together with endogenous compounds, which provides the host with metabolites they would otherwise not naturally produce[84]. The microbiota is also able to provide the human host with essential vitamins that cannot be synthesised by host cells[85]. Furthermore, the microbiota is able to prevent pathogen infection either through direct mechanisms such as the release of anti-microbials[86] and also indirect mechanisms including maintaining the homeostatic mucus conditions required for barrier function[87].

The maintenance of a homeostatic mucosal immune system is also reliant on the microbiota. Germ-free mice born and raised in sterile conditions consequently have no microbiome or microbial stimulus. These mice have a significantly reduced number of isolated lymphoid follicles in the gut, with their normal development and structure requiring microbiota stimulus via innate receptor nucleotide-binding oligomerization domain-containing 1 (NOD1), TLRs and C-C motif chemokine receptors CCR6[88] and CCR7[89], among others. Furthermore, bacterial species of the gut are required for the development and maturation of T_H17 cells[90,91], T regulatory (T_{Reg}) cells[92,93], IgA-producing B cells[94,95] and innate lymphoid cells[96]. In turn, the mucosal immune cells are able to maintain a mutualistic microbial population in the gut. For example, the T_{Reg} cells induced by the microbiome are also required to reduce any inflammatory responses to commensal bacteria[93]. Additionally, intestinal DCs are able to retain phagocytosed

commensal bacteria and induce an IgA response to maintain the microbiota in the intestinal lumen and prevent harmful systemic immune responses[97]. This allowing for a maintained mutualistic balance between the microbiota and host. Dysbiosis or changes of the microbiome have been associated with both local mucosal and systemic diseases such as allergic disease[98], type 1 diabetes[99], arthritis[100], inflammatory bowel disease[101] and multiple sclerosis[102]. Moreover, bacterial metabolites such as short-chain fatty acids have been linked to prevention of diseases such as allergic airway inflammation[103] and obesity[104]. It is evident that the microbiome not only effects the mucosal system and the associated mucosal immune system, but also has far reaching effects on systemic immunity. It is therefore paramount to consider its influence when investigating mucosal immunity.

1.3 Innate Immune System

Vaccinology and immunology are tightly linked disciplines as one does not occur without the other, however, despite the successes of vaccinations over the last two centuries', they have been developed with an absence of knowledge for the immunological mechanisms that allow for their success. This is evident by the lack of protective vaccines for diseases such as human immunodeficiency virus (HIV), and highlights the need for understanding of the immune systems response to vaccination[7]. Research has identified the innate immune system to hold a pivotal role in identifying and processing vaccine antigens and adjuvants and consequently stimulating a protective and long-lasting response to the associated pathogen. The innate immune system is the first arm of the immune system and first responder to pathogens identified through common pathogen-associated molecular patterns (PAMPs) binding to a wide range of pattern recognition receptors (PRRs) on the innate cells. Activation of these receptors, allows innate cells such as macrophages, monocytes, neutrophils and DCs to either produce molecules that directly kill invading pathogens or mediators which prime other immune cells to initiate a protective response[105].

The second arm of the immune system is the adaptive system. The adaptive system is critical for immunological memory and therefore the underlying principle of vaccination. However, the majority if not all adaptive responses to vaccination fundamentally begin with the innate immune system[16]. The mechanism behind the innate systems ability to recognise vaccine antigens and adjuvants is through germ-line encoded PRRs. These PRRs include TLRs, NOD-like receptors (NLR), retinoic acid-inducible gene-I-like receptors (RLR) and C-type lectin receptors (CLR). TLRs are either transmembrane receptors or located intracellularly, with the ability to identify lipopeptides[106], lipopolysaccharides[107], nucleic acids[108,109] and proteins[110]. Another transmembrane receptor, CLR, recognises carbohydrates[111], whereas, cytoplasmic receptors NLR and RLR recognise PAMPs such as peptidoglycans[112] and double-stranded RNA[113] respectively. Once these receptors are engaged with their respective ligands, adaptor molecules such as myeloid differentiation primary response protein 88 (MyD88), TIR-domain-containing adaptor-inducing interferon-β (TRIF), IFN-β promoter stimulator-1 (IPS-1), receptor-interacting-serine/threonine-protein kinase 2 (RIP2), DNAX-activating protein (DAP) 10 and DAP12 become associated and result in the downstream activation and translocation of transcription factors into the nucleus, including interferon regulatory factor (IRF) 7, IRF3, activator protein 1 (AP-1), NF-κB and nuclear factor of activated T-cells (NF-AT). These transcription factors are then able to initiate the production of chemokines, proinflammatory cytokines, type 1 interferons (IFNs), co-stimulatory molecules and antimicrobial proteins[114], leading to either killing of the pathogen or recruitment of additional innate and adaptive immune cells.

Damage-associated molecular patterns (DAMPs) are another signal that can activate innate cells and can be involved in vaccine responses. DAMPs are associated with damaged or dying host cells and can initiate signalling pathways via inflammasomes. NLRs allow a frame work for the inflammasome signalling complex to form, leading to activation of inflammatory caspases. Caspase-1 is a protease enzyme which cleaves pro-IL-1β and pro-IL-18, into their active inflammatory cytokines IL-1β and IL-18 respectively[115,116]. Inflammasomes can be initiated through NLRs binding to ligands such

as bacterial proteins[117], the release of factors such as ATP[118] and uric acid[119] from necrotic and stressed cells, or through DMAPs released by host lysosomal damage, with the latter being associated with the adjuvant aluminium and NALP3 signalling[120].

Antigen presenting cells (APCs) are a fundamental link between the innate and adaptive immune response. APCs are required to present endogenous peptides on MHCI and phagocytosed exogenous peptides on MHCII to specific T cell receptors (TCR) on $CD8^+$ and $CD4^+$ T cells respectively[105]. Although, APCs such as macrophages vastly outnumber DCs, DCs are still considered the immune systems superior antigen presenting cell[121,122], due to their ability to transport antigen from the periphery to draining lymph nodes and provide the required signals for T cell activation[123]. DCs are divided into subsets based on their lineage, location and the expression of markers and select pattern recognition receptors which result in specialised functions[124]. One characterisation of DCs is to divide them into non-lymphoid tissue migratory DCs (migratory DCs) and lymphoid tissue resident DCs (resident DCs)[125]. Migratory DCs patrol the peripheral tissues and survey the tissue environment through phagocytosis. Upon exposure to pathogenic antigens, these DCs upregulate MHCII[126], co-stimulatory molecules such as B7[127] and chemokine receptor CCR7[128–130]. CCR7 binds to ligands CCL21 and CCL19 expressed on endothelial lymphatic cells, high endothelial venules and stromal cells in the T cell zone of the lymph node[128]. This allows mature antigen positive DCs to traffic to the draining lymph nodes via the afferent lymphatics where they can interact with the T cell zone[131]. However, antigen can also freely travel through the lymphatics to the draining lymph node where resident DCs can phagocytosis and present it to T cells[132].

The type of adaptive response induced is dependent on the signals provided by the DC due to the stimulation of different PRRs. For example, specific pathogens such as *Staphylococcus aureus* can induce IL-12 producing DCs and subsequent T_H1 polarisation of $CD4^+$ helper T cells that produce interferon-γ (IFN-γ)[133]. Alternatively, helminth infections can drive DCs to induce T_H2 polarisation and IL-4 production[134]. This $CD4^+$ T cell polarisation can also be seen in a vaccination setting, such that adjuvant MF59,

maintains the antigen induced polarisation into a balanced T_H1/T_H2 response but aids in boosting the response by stimulating the migration of granulocytes and monocyte differentiation to DCs[135] and increasing DC uptake of antigen[16,31]. Whereas, AS04 stimulate adaptor molecule TRIF through TLR4 and gives a T_H1 response, and Complete Freund's adjuvant drives a T_H1/T_H17 response through MyD88 signalling[16]. DCs are also able to support humoral responses by targeting specific DC subsets that preferentially support T follicular helper (T_{FH}) cell development and subsequent B cell responses[136]. The type of adaptive response initiated shows a dependence on the innate response and stimulus, thus having implications in vaccine design as different polarisations of the adaptive system is required for the clearance of different pathogens.

Adjuvants are just one way to enhance a vaccines ability to stimulate the innate immune system. Current research is now investigating other ways to enhance this response. One of these being conjugate vaccines. In a natural infection and live attenuated vaccine setting, the innate cells are exposed to the PAMPs and pathogen antigens for MHC delivery simultaneously. This allowing for the appropriate cytokine release, co-stimulatory upregulation and antigen presentation from individual innate cells to prime and activate an adaptive response. However, for some subunit vaccines, the antigen and adjuvant are separate, so may not directly target the same cell[16]. This can be combated by conjugating the antigen with the adjuvant component via a covalent linker. Wille-Reece, A. *et al.* (2005) were able to show in nonhuman primates, a HIV Gag protein conjugated to an agonist for TLR7/8 was able to significantly increase the magnitude and cytokine production of the T_H1 response compared to an admix or peptide alone. Additionally, the conjugate vaccine was able to induce an antigen specific $CD8^+$ T cell response suggesting induction of cross-presentation by the vaccine[137]. Co-delivery can also be carried out using fusion proteins[138] and delivery systems such as microparticles[139] and virus-like particles[140]. Another way to improve the adaptive response through the innate system, is using vaccines that directly target specific DCs to induce the desired adaptive response. Park, H. *et al.* (2017), linked influenza and enterovirus antigens to C-type lectin domain family 9 member A (Clec9A) antibodies

which showed an enhanced antibody response. Due to Clec9A expression on conventional DC1s (cDC1s), this vaccine was able to directly target these specialised cross-presenting DCs and induce this enhanced response[141]. Clec9A targeted vaccines have also been shown to enhance $CD4^+$ and $CD8^+$ T cells responses[142].

1.4 Adaptive Immune System

The adaptive immune system is comprised of two main lymphocyte populations, T and B cells. Two defining characteristics that sets the adaptive response apart from the innate, is their repertoires of diverse receptors and their ability to induce long term memory responses, among other things. Both T and B cell receptors (TCR and BCR respectively), contain variable regions that interact with antigen. As the name suggests, these regions are highly variable, with each individual lymphocyte having slight alterations due to somatic recombination of germline variable (V), diversity (D) and joining (J) gene segments. This allows for a diverse repertoire of receptors that in theory can identify almost any pathogen associated antigen[143]. After the resolution of an infection, the expanded adaptive immune system contracts back down to almost baseline levels, however, a small proportion of antigen-specific lymphocytes remain both in the central and peripheral system to provide future protection. Due to their previous priming, these memory cells are apt at inducing a rapid and fast response upon re-exposure of the pathogen, providing long-term protection[105,144,145]. This memory response is the mechanism behind the success of vaccinations.

1.4.1 B Cell Responses

B cells contribute to approximately 5-15% of lymphocytes within the human body. They circulate around the blood and secondary lymphatic system and are the sole producer of pathogen specific antibodies involved in the humoral immune response. One defining feature of B cells is their immunoglobulins (Igs) which come in two forms, either BCR bound on the B cells outer membrane or soluble antibodies found in the circulation and extracellular fluids or secreted in the lumen of the mucosal system[146]. As with TCRs, BCRs and antibodies are diverse and bind to specific antigens. However, unlike T cells,

B cells don't require antigen presentation, instead B cells can directly recognise antigen via crosslinking of their BCR. This direct recognition is also the case for antibodies[105]. To ensure B cells don't react to self-antigens, a secondary signal is required such as PAMPs or signals from other immune cells such as CD40L on $CD4^+$ T cells, to allow for activation and proliferation. The absence of this secondary signal results in death of B cells that are continuously exposed to antigen alone to prevent autoimmune reactions. However, in the case of transient exposure to antigen, B cells can return to naïve states[147]. Once activated, B cells proliferate and differentiate into effector plasma cells that secrete antibodies of the same antigen specificity as the BCR[105].

While B cells circulate through the blood, they can enter lymph nodes via the high endothelial venules and migrate to the B cell follicles[148]. Antigen can enter the lymph nodes through APC transport or alternatively soluble antigen from the tissue can freely enter the lymph nodes through tissue draining lymphatic vessels and readily enter the B cell follicles[149]. Once antigen is in the B cell follicle it can bind to the BCR and upon activation the B cell expresses CCR7, the receptor for chemokine CCL19 and CCL21 produced by T cells, and migrates to the boarder of the B cell follicle and T cell zone[150,151]. B cells are antigen presenting cells and can present peptide antigens to $CD4^+$ T cells through MHCII[152] and additional co-stimulatory interactions such as CD40L to CD40[153]. This interaction activates and causes proliferation of the B cells, which then either become short-lived plasma cells that migrate to the extrafollicular space and provide initial protection with low affinity antibodies or the B cells can migrate into the follicle to form germinal centers[154] with characteristic expression of GL7[155]. T_{FH} cells are also able to enter the germinal center and are characterised by BCL6, programmed cell death protein 1 (PD-1) and CXCR5 expression along with IL-21 production[156]. Within the germinal center, B cells, along with the help of T_{FH} cells, undergo somatic hypermutation of the V genes that form the variable Ig region. B cells that acquire higher affinity to antigen survive and become high-affinity memory B cells and long lived plasma cells[153]. Additionally, B cells undergo isotype switching in the germinal center through class-switch DNA recombination of the constant region in the heavy chain of the Ig. This

process which is largely dependent on CD40L:CD40 interactions and cytokines, drives Ig's to isotype switch. Naïve B cells commonly express IgD and IgM, upon isotype switching some will remain as IgM however the remainder as well as all IgD^+ B cells will switch to more specialised IgG, IgA and IgE isotypes with different localisations and efficacy to different pathogens[157]. Both the generation of memory B cells and the process of isotype switching can also occur independently of the germinal center[158,159]. This B cell development is not isolated to lymph nodes but also occurs in other secondary lymphoid organs such as the spleen and Peyer's patches.

Antibodies function to neutralise and opsonise specific pathogens and pathogen products as well as activating the complement system. Neutralisation is commonly elicited by vaccines, and results from antibodies binding directly to pathogens such as viruses to inhibit their entry into host cells, therefore their replication, and/or by binding to toxic products from bacteria or parasites to prevent their function. Opsonisation is where antibodies bind to the surface of pathogens such as bacteria and allows for their phagocytosis into innate cells via Fc receptors. Lastly, pathogen bound antibodies allow for more efficient complement activation and lysis of bacteria[105]. Each antibody isotype carries out specific roles based on these three effector functions. IgM takes either a pentamer or hexamer form and is mainly found in the circulation due to its large size. It results in complement activation through binding to repetitive motifs particularly on bacteria. The other antibody isotypes take monomeric forms with the addition of a dimeric IgA form, thus allows for dispersal into peripheral tissues as well as the circulation[157]. IgG antibodies can be further divided into IgG1, IgG2, IgG3 and IgG4 subsets and is the predominant antibody found in the blood with IgG1 as the predominant subset. IgG antibodies can conduct all three effector functions, they are able to neutralise viruses, bind to FcγR and induce phagocytosis and to C1q to activate complement[160]. IgG1 can respond to soluble proteins, bacteria, viruses and allergens, IgG2 reacts to bacterial capsular polysaccharides, IgG3 to viruses and soluble proteins and IgG4 to allergens and extracellular parasites, this among other stimuli[157,160]. IgE is found at very low levels during homeostasis but can bind to FcεR1 on granulocytes such

as mast cells and basophils to induce the release of toxic granules and histamines. This response is able to kill and expel extracellular parasites such as helminths but is also tightly linked to allergies[161]. IgA antibodies have the highest abundance and make up about 70% of all Ig's, this is due to the natural colonisation of the microbiome at the mucosa which induces continual IgA production. IgA producing B cells are predominantly found at mucosal sites where they can produce the dimeric secretory IgA (S-IgA) for transport across the mucosal boundary into the mucosa lumen. Pentamer IgM is also capable of secretion. S-IgAs primary role is to induce neutralisation of pathogens and toxins before they are able to invade the host cells through the mucosa[162].

Long lived B cell responses can be maintained within the human host for their entire lifetime. This is evident from the study by Yu, X. *et al.* (2008) who found that survivors of the 1918 H1N1 influenza pandemic, still maintained specific neutralising antibodies and circulating memory B cells to the virus almost 90 years later[163]. After induction, long lived plasma cells reside within the bone marrow and continuously secrete high affinity antigen specific antibodies into the blood circulation, independent of antigen and memory B cells[164–166]. However, memory B cells upon re-stimulation, proliferate and become antibody secreting cells[166]. Currently the majority of vaccines induce protection by driving a humoral response, where the long lived plasma cells and memory B cells are able to maintain lifelong protection, making frequent boosters redundant[163,167]. However, some individuals, especially the elderly are unable to induce protective B cell responses and antibody titres[168]. This can be improved with the addition of adjuvants. For example, the MF59 adjuvant is able to improve antibody titres as well as improve seroconversion and seroprotection against influenza in an elderly population compared to a non-adjuvanted vaccine[169]. Different vaccine routes are capable of inducing antibody responses both systemically and locally to different extents. A study by Moldoveanu, Z. *et al.* (1995), immunised individuals with influenza vaccines at different sites. They found that the oral route was unable to produce influenza specific antibodies in the serum, but serum antibodies were detected in both intramuscular and intranasal

administrations. The route also altered the antibody isotypes at mucosal sites, with orally and intranasally administered vaccines inducing a predominant IgA response over IgG in the saliva whereas, intramuscular increased the IgG response with lower IgA at this mucosal site. However, in the nasal secretions, there was a higher IgG response in the intramuscular and intranasally administered vaccines, but a comparable IgG to IgA response after oral administration[170]. This showing that the B cell response dissemination and isotype response to vaccination is dependent on the route of administration.

1.4.2 T Cell Responses

Conventional T cells can be further defined into either $CD4^+$ or $CD8^+$ T cells based on their expression of the CD4 and CD8 molecules along with their effector functions. Both $CD4^+$ and $CD8^+$ T cells have unique TCRs that are able to identify peptides presented on MHC molecules. $CD8^+$ T cells are able to recognise endogenous peptides presented on MHCI and upon activation form cytotoxic T lymphocytes (CTLs). The main role of CTLs is to kill virally infected or tumour cells, through the release of cytotoxic granules such as perforin and granzyme[171]. Unlike $CD8^+$ T cells, $CD4^+$ T cells recognise exogenous peptides presented on MHCII and mature into different T helper cell subsets driven by the provided stimulus. The main T helper cell subsets are T_H1, T_H2, T_H17, T regulatory cells (T_{Reg}) and T follicular helper cells (T_{FH}), which are categorised by their transcription factor (TF) expression, cytokine production and subsequent effector functions[105]. T-box transcription factor, T-bet, is considered the master TF for T_H1 cells and confers the production of cytokines such as IFN-γ which stimulates macrophages and drives B cells production of IgG antibodies[172]. T_H2 cells become differentiated through signal transducer and activator of transcription 6 (STAT6) activation and the activation of the downstream TF, GATA binding protein 3 (GATA3). GATA3 induces the production of cytokine such as IL-4, IL-5 and IL-13[173] which are associated with granulocytic eosinophils, mast cells and basophils and the production of IgE antibodies, orchestrating a response to clear parasitic infections with links to allergy and tissue repair[174]. The T_H17 subset is defined by IL-17 producing cells[175] and the TF, retinoic-acid-receptor-related

orphan nuclear receptor gamma (RORγt) with effector functions linked to macrophage and neutrophil recruitment during infection[176]. Aside from effector functions to clear pathogens, T_{Reg} cells are vital for dampening and limiting the immune response to self, commensal bacteria and foreign antigens. T_{Regs} can either be defined as thymic or induced based on where and how they were differentiated, however, both are associated with forkhead box P3 (FoxP3) and immunomodulatory cytokines such as transforming growth factor beta (TGF-β)[177]. Lastly, T_{FH} cells express B-cell lymphoma 6 protein (BCL6) and are involved in the formation and maintenance of germinal centers along with the differentiation of B cells into plasma cells and memory B cells[156]. However, these defined lineages are not so clear cut with plasticity occurring between the subsets and also the new characterisation of subset such as T_H9 and T_H22[178].

Concluding an infection, memory T cells remain in the secondary lymphoid tissues and circulate around the peripheral tissues[179]. Sallusto, F. *et al.* (1999), defined these two T cell memory populations as central memory (T_{CM}) and effector memory (T_{EM}) T cells based on their expression of the secondary lymphoid system homing chemokine receptor CCR7 or lack thereof, respectively. They were able to show that the $CD4^+$ T_{CM} (gated on $CD45RA^-CCR7^+$) don't produce effector cytokines, IFN-γ, IL-4 or IL-5 upon re-stimulation, compared to the $CD4^+$ T_{EM} (gated on $CD45RA^-CCR7^-$) cells which rapidly upregulate these cytokines. A similar trend was seen in the $CD8^+$ T_{CM} and T_{EM} cells, with IFN-γ and perforin being upregulated in the T_{EM} cells compared to the T_{CM} cells. Additionally, the T_{CM} cells were capable of greater responsiveness to TCR stimulus which strongly activated IL-12 producing DCs. This showed that the effector memory T cells which move through the circulation are capable of rapid effector functions upon re-activation, whereas the central memory T cells remain in the secondary lymphoid organs and circulation but prime effector DC activation[180]. Further research and characterisation has led to three subsets of memory T cells, T_{CM} which circulate in the blood and secondary lymphoid organs, T_{EM} which also circulate and can enter non-lymphoid tissues and lastly tissue-resident memory T cells (T_{RM}) which reside in non-lymphoid tissue, predominantly the skin and mucosa, with minimal recirculation. Due

to their location, T_{RM} cells would be the first memory cells to respond to re-infection, initiating strong responses to antigen and directing other immune cells[181]. The three subsets of memory cells give a wave like structure to the T cell memory response.

The majority of vaccines induce a B cell response and neutralising antibodies as protection, with antibody titres being the common measurement of vaccine immunogenicity. However, it is becoming clear that inducing T cell responses to vaccines can provide long term durable responses and also protection against intracellular pathogens, particularly viral infections[182,183]. The induction of a T cell response is dependent on the dose and route of administration. Hu, Z. *et al.* (2016), showed that $CD8^+$ T cell responses were dependent on $CD4^+$ T cell help more so when viral infections were administered intraperitoneally compared to intranasally. Additionally, the dose given could alter the resulting immune response with a smaller viral dose requiring $CD4^+$ T cell help to rescue the $CD8^+$ T cell response intranasally[184]. However, despite a higher dose improving the resulting T cell response and memory, balance is critical, as a dose too high can induce T cell exhaustion and poor vaccine responses[185]. Other important considerations for vaccine induced T cell responses are the type of memory response induced, whether the T cells are polyfunctional and the co-stimulatory signals provided. These can all effect the resulting memory response and vaccine efficacy[186].

Just as with a pathogenic infection, vaccination against different pathogens requires specific immune responses that are specialised to clear the pathogen. The different subsets of $CD4^+$ T cells allow for a range of responses. $CD4^+$ T cell responses are able to improve both $CD8^+$ T cell and antibody responses to vaccination. He, R. *et al.* (2018), were able to show an epitope based viral vaccine specific for $CD4^+$ T cells was able to not only induce anti-viral $CD4^+$ T cells but also enhance the number and quality of $CD8^+$ T cells specific for the virus. This leading to improved viral control upon subsequent infection[187]. Antibody responses are also enhanced by $CD4^+$ T cell activation. For example, $CD4^+$ T cell differentiation into T_{FH} cells helps to maintain the germinal center and B cell response to produce antibodies. Additionally, T helper subsets such as T_H1

helps to skewed responses towards IgG antibody production[188]. The polarisation of different T helper subsets can also be driven by the choice of adjuvant. The adjuvant aluminium drives a dominant T_H2 differentiation whereas, adjuvants such as AS04 has more of a T_H1 bias[40] and MF59 a mixed T_H1/T_H2 response[135]. On the other hand, $CD8^+$ T cell responses are required for intracellular pathogens. Unlike, live attenuated vaccines that directly infect host cells, subunit and killed vaccines that don't naturally infect cells face challenges with inducing CTL activation due to the reliance on MHCI pathways. Exogenous peptide can be presented to $CD8^+$ T cells on MHCI, but require cross-presentation, which is specific to only select innate cells, such as cDC1s[16]. Due to the cytotoxic effector functions of CTL cells, $CD8^+$ T cell targeted vaccines are also being investigated for use in cancer vaccines[189].

One challenge in childhood vaccinations is the inadequate or complete lack of B cell responses to T cell independent polysaccharide antigen under the age of two. This seems to be linked to the slow developmental rate of the marginal B cell zones with a lack of CD21 expression, which only begin to show characteristics of adult maturation around the age of two[190]. To improve antibody and vaccine responses, T cells can be employed through the use of conjugate polysaccharide vaccines. B cells are able to phagocytose the vaccine and cleave the protein portion off for processing and presentation via MHCII. The peptide is then recognised by $CD4^+$ T cells inducing both a T cell response as well as providing stimulation to the B cell, allowing for activation and polysaccharide specific antibody production[191]. These vaccines have already been successfully licenced for *Neisseria meningitidis, Haemophilus influenzae* and *Streptococcus pneumoniae* infections[192].

T cell targeted vaccines do have some draw backs. Due to T cells relying on antigen presentation for activation, the antigen must always be internalised within an APC and process through one of the MHC pathways. This means that even upon re-infection of a pathogen, the pathogen must infect host cells either directly or by phagocytosis to be presented to the memory cells[105]. This is unlike some antibody responses such as

secretory IgA (S-IgA) that neutralise pathogens before they are even able to invade the human host[193]. Another challenge for T cell immune responses is the variation within the human leukocyte antigen (HLA) complex which is formed from highly polymorphic genes to produce the human equivalent MHC molecules. Although the highly polymorphic nature allows for a variety of antigens to bind the MHC molecules, it also causes variation within the population, leading to variable vaccine responses between individuals[194]. Some individuals may lack the specific HLA complex required for presentation of vaccine peptides and therefore lack the T cell response. This is an issue in live attenuated vaccines[195] and also particularly subunit or peptide vaccines that carry minimal antigens for presentation[196]. To combat this, peptides that are capable of binding to a range of HLA complexes are required[196].

1.4.3 Mucosal-associated Invariant T (MAIT) Cells

1.4.3.1 Classification

Mucosal-associated invariant T (MAIT) cells, like natural killer T (NKT) cells and gamma-delta ($\gamma\delta$) T cells, are a subset of innate like T cells, that unlike conventional T cells, have restricted TCRs that bind to conserved non-peptide antigens[197]. MAIT cells are characterized by their semi-invariant T cell receptor, which consists of the α chain Vα7.2-Jα33 in humans and Vα19-Jα33 in mice[198], which associates with a limited range of β chains, either Vβ2 or Vβ13 in humans and Vβ6 or Vβ8 in mice[199]. In addition, the α chain can also be rearranged with Vα7.2-Jα12 and Vα7.2-Jα20 in humans[200]. MAIT cells can be further divided into subsets based on co-receptor expression of CD4 and CD8[200,201]. MAIT cells make up about 10% of peripheral blood T cells in humans, hence are found in the circulation, in addition to the liver and mucosal sites among other tissues[202]. They have also been shown to express specific receptors such as C-X-C motif chemokine receptor (CXCR) 3, CCR5 and CXCR1 as well as CCR3, CXCR4, CCR6 and $\alpha4\beta7$ integrin which are inflammatory chemokine receptors and receptors used for homing to hematopoietic organs and the gut respectively[201,203]. However, lymph node homing receptor CCR7 expression is low. These expression patterns, along with high expression

of CD45RO, CD127 and CD44 give MAIT cells a memory phenotype[203,204]. MAIT cells also express cytokine receptors such as IL-7Rα, IL-12R, IL-18Rα and IL-23R[205].

1.4.3.2 Antigen Presentation, Agonists and Antagonists

MAIT cell TCRs are able to recognize MHC-related molecule 1 (MR1) on antigen presenting cells[206]. MR1 is highly conserved[207] and has a low level of ubiquitous expression by a wide range of cells[208] including both bone marrow and non-bone marrow derived cells[209]. The MR1 structure is composed of 3 α domains, α1, α2 and α3 and a β_2m domain[210]. MAIT cells have been shown to respond to bacteria and yeast such as Enterobacteriaceae, Staphylococci and Mycobacterium, however, not Streptococci, *E. faecalis* and viruses, via a MR1 dependent presentation. In addition to this, in bacteria infected patients there is a reduction in MAIT cells present in the blood, this suggesting localization to the tissue and an antimicrobial function[198]. Kjer-Nielsen, L. *et al*. (2012) concluded that microbes with the riboflavin (vitamin B2) pathway were able to activate MAIT cells, whereas, microbes without this pathway were unable to. This is due to the vitamin B derivatives being presented on MR1 and initiating activation of MAIT cells. Interestingly, the folic acid derivative 6-formylpterin (6-FP) is capable of binding to MR1 but acts as a TCR antagonist, inhibiting MAIT cell activation[210].

It has been suggested that the folding and surface expression of MR1 is dependent on ligand binding to MR1 in the endoplasmic reticulum (ER), this making surface expression of MR1 difficult to detect via flow cytometry. MR1 that is awaiting ligand binding, associates with the peptide-loading complex in the ER, much like the classical MHCI. This occurs in both humans and mice. Further to this, stimulated increases in the peptide-loading complex by treatment with IFN-γ increases association of human MR1 with the peptide-loading complex[211]. However, other studies have found that MR1 expression does not require the protein-loading complex (including proteasome, TAP, tapsin and CRT) but instead chaperons such as the invariant chain (Ii) and HLA-DM, which are involved in MHCII antigen presentation. For example, overexpression of Ii and MR1 caused increased MAIT cell activation, whereas, disruption of endogenous Ii

alleviated this effect. Increased surface expression of MR1 can be associated with microbial infected cells and their antigens present in the late endosomes stabilising MR1[212].

The current known agonists include direct derivatives of the riboflavin pathway as well as 5-(2-oxopropylideneamino)-6-D-ribitylaminouracil (5-OP-RU) and 5-(2-oxoethylideneamino)-6-D-ribitylaminouracil (5-OE-RU) which form upon further processing steps[205]. Corbett, A. *et al*. (2014) found that genes encoding enzymes required for 5-amino-6-D-ribitylaminouracil (5-A-RU) production are necessary for MAIT cell activation. 5-A-RU is found in the riboflavin pathway of a wide range of microbes. Interestingly, 5-A-RU does not bind directly to MR1, but instead is further processed with small molecules, including glyoxal and methylglyoxal, which can be derived either from microbe or host cells. These combine to become unstable 5-OE-RU and 5-OP-RU, respectively, which can then bind MR1 at lysine 43 (Lys43) to create reversible covalent Schiff base complexes and activate MAIT cells via the invariant TCR[213]. Further studies have shown that small molecules such as drugs and drug metabolites can also bind to MR1, some of which inhibit and others that activate MAIT cells[214]. This indicates that MR1 is not completely restricted, with some plasticity to bind a range of ligands.

Like the agonists, 6-FP is able to bind covalently to the MR1 binding cleft at Lys43 and cause a conformational change required for correct folding and cell surface presentation. However, this doesn't bind the MAIT cell TCR and cause stimulation, but instead acts as an antagonist. The contacts between 6-FP and MR1, adjacent to the binding pocket are highly conserved across species. This indicates that the ligands that bind are also highly conserved[210]. Acetyl-6-formylpterin (Ac-6-FP) is another antagonist which binds MR1 with more potency than 6-FP[215].

1.4.3.3 Functions

MAIT cells are known to become activated and localize to bacterial infected tissues. For example, in *F. tularensis* pulmonary infection, MAIT cells produce proinflammatory

cytokines such as TNF, IFN-γ, IL-17A and help with the recruitment of active T cells to the site of infection. Not only do MAIT cells have this initial role but also continue to accumulate and produce cytokines such as IFN-γ throughout infection into the adaptive stage[216]. MAIT cells have also been associated with other infections such as *Mycobacterium abscessus*, *Escherichia coli*, *K. pneumoniae*, tuberculosis and *Vibrio cholerae*[217]. Furthermore, MAIT cells play a protective role against lethal doses of *Legionella*[218] and influenza[219] through MR1-dependent and independent pathways respectively. While MAIT cells have pro-inflammatory phenotypes, they also seem to be involved in homeostasis of the mucosa with links to the microbiome and gut integrity. For example, germ-free mice have an absence of MAIT cells[206] and $MR1^{-/-}$ mice that lack MAIT cells can have a loss of gut integrity.

1.4.3.4 Activation

1.4.3.4.1 MR1-Dependent

Microbes with the riboflavin pathway, are able to activate MAIT cells via the MR1-dependent pathway through the recognition of the metabolite by the invariant TCR. In response, MAIT cells upregulate CD25, CD69 and CD161 expression and secrete T_H1 and T_H17-like cytokines such as IFN-γ, TNF-α, IL-17 and IL-22 (figure 1.1). The production of these cytokines can be tissue specific[220]. MAIT cells are also capable of producing granzymes and perforin to lyse bacterially infected cells, providing cytotoxic functions[221]. Some studies have found that in addition to antigens, MAIT cell activation requires co-stimulation such as TLR ligands[222]. As MAIT cells are found in mucosal areas, they are in close proximity to commensal bacteria. Some commensal bacteria have the riboflavin pathway but this is not enough to stimulate MAIT cells and it is suggested that inflammatory cytokines are also required for activation[223].

1.4.3.4.2 Cytokine Mediated

MAIT cell MR1-independent activation requires cytokine mediated activation. $CD161^{++}$ $CD8^{+}$ MAIT cells can be activated by IL-12 plus IL-18, which then stimulates IFN-γ production[224] (figure 1.1). Whereas another study found a solely IL-18 dependent

activation of MAIT cells in influenza infection[225]. Cytokine mediated activation has also been shown to occur in non-infectious diseases such as systemic lupus erythematosus, where MAIT cells are activated by IL-6, IL-18 and IFN-γ[226]. This antigen independent pathway may also provide a mechanism for MAIT cells reactivity to viral infections as it doesn't require the microbial and/or fungal metabolites[219,227].

1.4.3.4.3 Superantigens

In addition to MR1-dependent and cytokine mediated activation, MAIT cells can be activated by superantigens (SAgs). SAgs bind to the Vβ subunit of the TCR and MHCII on the APC, activating the cell independent of antigens[228]. SEB produced by *Staphylococcus aureus* is a potent activator of MAIT cells, leading to production of IFN-γ, TNF-α, IL-2 and cytotoxic granules (figure 1.1). This manner of MAIT cell activation requires MHCII but not MR1 and is dependent on TCR Vβ interaction[229,230].

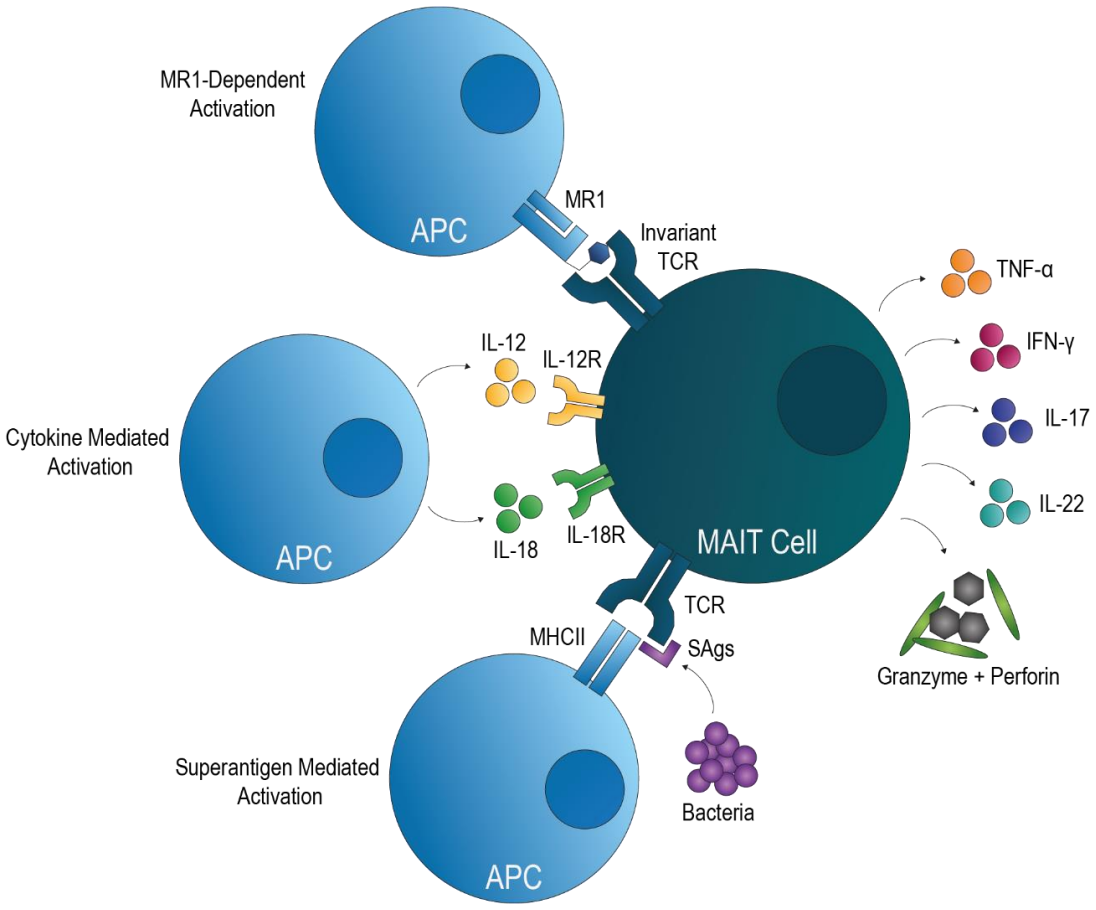

Figure 1.1: MAIT Cell Activation. The different ways in which MAIT cells can be activated.

1.5 Research proposal

Despite the success of modern vaccinations in reducing both infection rates and mortality, challenges of providing durable and cross protective immune responses remain evident. The mucosal tract provides the major entry site for pathogens to invade their human host. Vaccinating at the local site of mucosal invasion promotes the production of secretory IgA (SIgA), blocking pathogen invasion and neutralising microbial toxins[231]. Despite this, the majority of vaccines are administered parenterally away from natural sites of infection. The lack of effective mucosal vaccines is in part reflective of the limited development and availability of safe and effective mucosal adjuvants. Ideally, an adjuvant should induce a potent but low toxicity immune response[232].

The aim of my thesis is to investigate an entirely novel class of adjuvants that stimulate MAIT cells in mucosal tissues. We hypothesise that their apt location, rapid activation and low threshold provide a unique strategy to activate dendritic cells (DCs) and prime a subsequent adaptive immune response. Additionally, as the components of the MAIT cell agonist 5-OP-RU, are naturally found within the human body and unlike generalised adjuvants such as TLR stimulants which are potent and stimulate a wide expanse of cells, I hypothesise that MAIT cell agonists will allow for tight regulation of the initial response and will have low toxicity but provide ample stimulus for MAIT cell activation. This concept has shown promise in another 'innate-like' T cell subset, the natural killer-like T (NKT) cells. When a NKT cell agonist is conjugated to an antigen and taken up by DCs, the agonist activates the NKT cells to stimulate the DCs, increasing their expression of maturation markers and subsequently enhance the cytotoxic T lymphocyte response to the antigen[233–235]. Research focusing on MAIT cells in this context has revealed that MAIT cells in human whole blood cultured with 5-A-RU and methylglyoxal become activated, indicated by the downregulation of the TCR and increased expression of CD137 and IFN-γ. Additionally, Co-culture of DCs and MAIT cells with the agonist caused the maturation of DCs with the elevation in activation markers such as CD86 and

programmed death-ligand 1 (PDL-1)[236]. Together this illustrates cross-talk between DCs and MAIT cells and shows that 5-A-RU plus methylglyoxal can be used as a MAIT cell agonist enabling interaction with DCs and subsequent effector cytokine production by both cell types.

1.5.1 Hypothesis

Taken together, I hypothesis that intranasal administration of MAIT cell agonists alongside antigen will be presented via MR1 on an APC such as a DC to the MAIT cell invariant TCR. This will stimulate MAIT cell activation and induce enhanced activation of DCs through MAIT cell signals such as cytokines and co-stimulation interactions, therefore providing an adjuvant effect. The enhanced DCs will then have enhanced potential to licence an adaptive response through the presentation of vaccine antigen (figure 1.2). Therefore, I hypothesis that MAIT cells have the potential to be utilised as cellular adjuvants in mucosal vaccination.

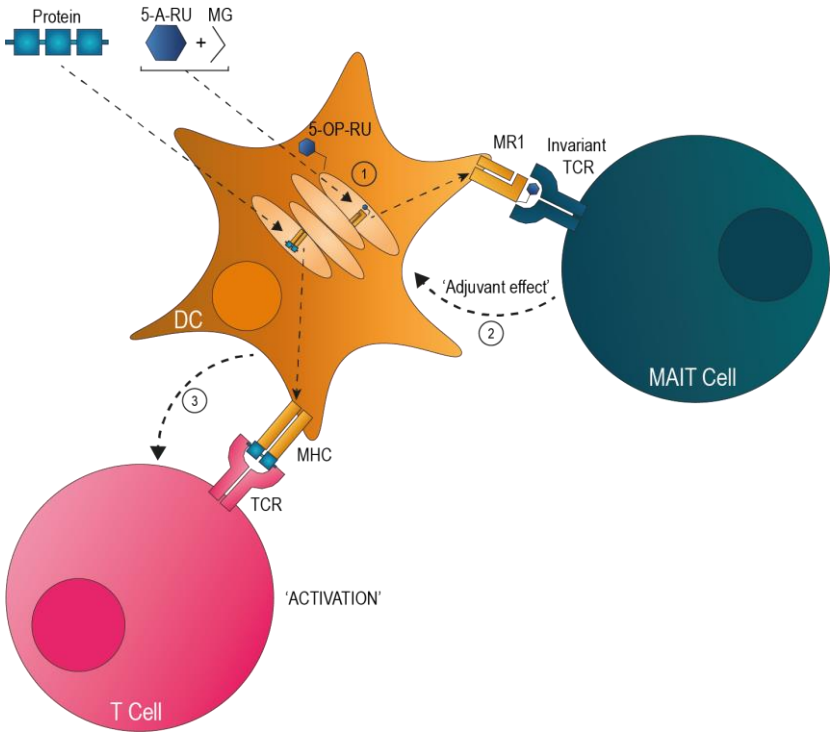

Figure 1.2: Hypothesised Mechanism. The intranasal administration of 5-A-RU + MG and an antigen is hypothesised to form the MAIT cell agonist 5-OP-RU, presented by a dendritic cell (DC) via MR1 to the MAIT cell through the invariant TCR. The MAIT cell will then provide stimulatory signals to the DC to enhance its ability to licence a T cell response to the antigen.

1.5.2 Aims

My thesis aims to characterise the early MAIT cell and DC response in the lung mucosa to intranasally administered MAIT cell agonists and to determine whether they can drive desired adaptive responses required for successful vaccines.

1) Determine whether mucosal administration of MAIT cell agonists can induce MAIT cell activation at local mucosal sites.
2) Assess whether mucosal administration of MAIT cell agonists can drive MAIT cell-dependent innate and adaptive immune responses that are desirable in a vaccination setting.
3) Explore the cell populations and mechanisms involved in driving the immune response induced by mucosal administration of MAIT cell agonists.

2 Materials and Methods

2.1 Materials

2.1.1 Laboratory Equipment

Table 2.1: Laboratory Equipment

Supplier/Manufacturer	Product
BD Biosciences, Auckland, New Zealand.	1, 3 and 10 mL syringes (REF 302100, 302113, 302149 respectively) 18, 25 and 27G PrecisionGlide Needles (REF 302032, 301805, 301801 respectively)
Lab Supply, Dunedin, New Zealand.	Cryovial 2 mL Ext. thread Natural cap skirted sterile, DNase and RNase free (REF GRE126261) Freezer Cryoboxes (REF BIO90-2281) Stir Bar Magnetic 30 mm X 6 mm (REF SCI12500005) Haemocytometer (REF MAR0610010) Parafilm 2 inch x 250 ft (REF BEMPM992) 250, 500 and 1000 mL Laboratory Bottles (REF MAR3607506, MAR3607507, MAR3607508 respectively)
Interlab Ltd, Porirua, New Zealand.	16 mm Polywire One Rack 10, 200 and 1250 µL Tips in Eclipse Sleeve (REF 1036-260, 1030-260, 1049-260 respectively) Bastion Nitrile Soft Powder Free, Blue, Small Gloves (REF 100-251) Rotarack for small tubes (REF HS29040B) 1.1 mL microtubes Empty cardboard freezer box for tubes (REF 2510-1472) 1.7 mL Flat cap tube (REF 3013-870) SPINWIN Centrifuge tube 15 mL (REF 546021) 5, 10 and 25 mL serological pipettes (REF KJ9052, KJ9102, KJ9252 respectively) Discovery Pro 12 Channel pipette 12-50 and 20-200 µL (REF DP12-50 and DP12-200 respectively) Reagent reservoirs (REF KJ411-1) 500 mL volumetric flask (REF 013.01.500)

	500 mL measuring cylinder (REF 3021012A) 1000 mL measuring cylinder (REF 345070)
Bio-Strategy, Auckland, New Zealand.	5 mL Polystyrene Round-Bottom Tube Falcon (REF 352054) 50 mL Polypropylene Conical Tube Falcon (REF 352070) Tissue Culture Plate, 12 well, flat bottom with lid (REF 353043) Tissue Culture Plate, 24 well, flat bottom with lid (REF 353047) Tissue Culture Plate, 96 well, U-Bottom with lid (REF 353077) Cell Strainer 70 µM White Frame IND ST (REF 144781) Microtube 0.6 mL Assorted (REF AXYGMCT-060-A) Microtube 1.7 mL Clear Maxyclear (REF AXYGMCT-175-C) Filter Tips 10, 20, 200, 1,000 µL (REF AXYGTXLF-10-L-R-S, AXYGTF-20-L-R-S, AXYGTF-200-L-R-S and AXYGTF-1000-L-R-S respectively)
MediRay, Auckland, New Zealand.	Eppendorf Research Plus 0.1-2.5, 0.5-10, 2-20, 20-200, 100-1000 µL single channel pipettes (REF EP3120000011, EP3120000020, EP3120000038, EP3120000054, EP3120000062 respectively) Easypet 3 Pipette Controller (REF EP4430000018)
Thermo Fisher Scientific, Auckland, New Zealand.	Nunc MaxiSorp flat-bottom 96 well ELISA Plate (REF 44-2404-21) Applied Biosystems MicroAmp™ Optical 8-Tube Strip (0.2 mL) (REF 4316567) and 8-Cap Strips (REF 4323032) Applied Biosystems MicroAmp™ Optical 96-Well Reaction Plate with Barcode (REF 4306737) Applied Biosystems Optical Adhesive Covers (REF 4360954)
Intermed, Auckland, New Zealand.	Dissecting Forceps 1/2 curved (REF MW-37.55.20) Iris Scissors Straight 11.5 cm (REF MW-02.20.11)

2.1.2 Laboratory Machines

Table 2.2: Laboratory Machines

Supplier/Manufacturer	Machine
Becton Dickinson,	Cytek Aurora Spectral Cytometer

San Jose, CA, USA.	BD LSRII SORP BD FACSMelody
Gyrozen, Gimpo, Korea.	Gyrozen 1730MR Centrifuge Gyrozen 1580MGR Centrifuge
Thermo Fisher Scientific, Auckland, New Zealand.	Balance mySPIN 6 Mini Centrifuge VELP Scientifica ZX3 Advanced Vortex Mixer Applied Biosystems Veriti™ 96-Well Thermal Cycler Applied Biosystems™ QuantStudio 7 Flex Real-Time PCR System
Thermo Scientific, New Zealand.	Heraeus Multifuge X3R Centrifuge
Olympus, Wellington, New Zealand.	Olympus CX41 Compound Microscope
Perkin Elmer, Massachusetts, USA.	Enspire 2300 Multilabel Reader
Labconco Corporation, Missouri, USA.	Purifier Biological Safety Cabinet
Grant Instruments, Cambridge, UK.	SUB Aqua 18Plus water bath
Marshall Scientific, New Hampshire, USA.	Sanyo CO_2 MCO-20AIC Incubator

2.1.3 Reagents and Buffers

2.1.3.1 Buffer Components

Dulbecco's Phosphate Buffered Saline (DPBS)

Purchased from Gibco by Life Technologies (Auckland, New Zealand) and stored at 4 °C (REF 14190-250).

Dulbecco's Phosphate Buffered Saline Powder (DPBS)

Purchased from Sigma-Aldrich (Auckland, New Zealand) in powder form (REF D5652-10X1L) and stored at 4 °C. 1 L bottles of PBS were made up using 1 packet DPBS powder into 1 L dH_2O and pH adjusted to 7.4. DPBS stock was either filter-sterilised or autoclaved and then stored at 4 °C.

Foetal Bovine Serum (FBS)

Manufactured by Invitrogen (New Zealand) and stored at -20 °C in 50 mL aliquots.

Sodium Azide

Purchased from Sigma-Aldrich (S2002-100G) as powder (Auckland, New Zealand) and stored at room temperature. Stock made up to 5% sodium azide in 100 mL milliQ H_2O and stored at room temperature.

Ethylenediaminetetraacetic Acid (EDTA)

Purchased from Simga-Aldrich (EDS-500G) (Auckland, New Zealand) and stored at room temperature. Stock made up to 0.5 M in 1 L milliQ H_2O and pH adjusted to 8 using NaOH pellets.

Liberase TL (Research Grade)

Purchased from Sigma-Aldrich (Auckland, New Zealand) as lyophilised powder (5401020001) stored at -20 °C. Then made into aliquots of 1mL at concentrations of 1 g/mL in IMDM and stored at -20°C.

Collagenase Type I

Purchased from Sigma-Aldrich (Auckland, New Zealand) as lyophilised powder (C0130) stored at -20 °C. Then made into aliquots of 1mL at concentrations of 24 mg/mL in IMDM and stored at -20°C.

DNase I (Grade II)

Purchased from Sigma-Aldrich (Auckland, New Zealand) as lyophilised powder (10104159001) which was then made into aliquots of 100 µL and 200 µL at concentrations of 10mg/mL in IMDM and stored at -20°C.

IMDM, GlutaMAX Supplement

Purchased from Gibco by Life Technologies (Auckland, New Zealand) in 500mL bottles (REF 31980-097) and stored at 4°C.

Tris Hydrochloride (Tris-HCl)

Purchased from Sigma-Aldrich (Auckland, New Zealand) and stored at room temperature. Tris-HCL stock was made to 0.17 M in a 500 mL bottle in, milliQ H_2O and pH adjusted to 7.65 and stored at room temperature.

Ammonium Chloride (NH_4Cl)

Purchased from Thermo Fisher Scientific (Auckland, New Zealand) and stored at room temperature (AJA31-550G). NH_4Cl stock was made to 0.16 M in a 1 L bottle in milliQ H_2O and pH adjusted to 7.4 and stored at room temperature.

FOXP3 Transcription Factor Stain Buffer Kit

Purchased from Thermo Fisher Scientific (Auckland, New Zealand) and stored at 4 °C (REF 00-5523-00).

Sodium Carbonate (Na_2CO_3)

Purchased from Sigma-Aldrich (Auckland, New Zealand) and stored at room temperature (S7795-500G).

Sodium Bicarbonate ($NaHCO_3$)

Purchased from Sigma-Aldrich (Auckland, New Zealand) and stored at room temperature (S5761 500G).

milliQ H_2O

Supplied from the filter system in Alan MacDiarmid level 3 labs at Victoria University of Wellington.

TWEEN 20

Purchased from Sigma Life Sciences (P1379-500mL) and stored at room temperature.

Ovalbumin (OVA)-Biotin

Ovalbumin and biotin were purchased from Sigma-Aldrich (Auckland, New Zealand). A stock solution of OVA-biotin was made in house at a concentration of 3.5 mg/mL and stored at -80 °C.

2.1.3.2 Flow Cytometry and Cell Sort Buffers and Reagents

FACS Buffer

Using a 1 L bottle of DPBS as a base and under sterile conditions, 20 mL FBS (2%), 2 mL 5% sodium azide and 4 mL 0.5 EDTA was added. The FACS buffer was mixed well then stored at 4 °C.

Digestion Buffer (Liberase TL)

The digestion buffer was used for both mLN and lung tissue. The digestion buffer was made by adding 0.1 mg/mL liberase TL and 0.10 mg/mL of DNase I in IMDM.

Digestion Buffer (Collagenase Type I)

The digestion buffer was used for optimising the lung tissue digestion protocol. The digestion buffer was made by adding 2.4 mg/mL Collagenase Type I and 120 µg/mL of DNase I in IMDM.

OVA-Biotin Staining Buffer

10% of FBS was added to DPBS under sterile conditions. OVA-biotin was then added at a 1:3000 dilution of the 3.5 mg/mL stock.

FOXP3 Transcription Factor Stain Fixative

As per manufacturer's instructions, 1 part of 4X fix concentrate was added to 3 parts fix diluent.

FOXP3 Transcription Factor Stain Permeabilisation Buffer

As per manufacturer's instructions, 5 mL of 1X permeabilization buffer was added to 45 mL milliQ H_2O.

Tris-Buffered Ammonium Chloride (ACT) Buffer

ACT buffer was made as required for individual experiments just before being added to the cells. 9-parts of the stock 0.16 M NH_4Cl was added to 1-part stock 0.17 M Tris-HCl.

UltraComp eBeads™ Compensation Beads

Purchased from Invitrogen by Thermo Fisher Scientific (Auckland, New Zealand) (Ref 01-2222-42) and stored at 4°C.

Rat anti-mouse CD16 (FcεRIII)/CD32 (FcεRIII) (Clone 2.4G2) (Fc Block)

Fc block was affinity-purified at Malaghan Institute of Medical Research (Wellington, New Zealand) from hybridoma culture supernatants via Hi Trap protein G Sepharose columns. Stored at 4 °C.

Trypan Blue Stain (0.4%)

Purchased from Gibco by Life Technologies (Auckland, New Zealand) (Ref 15250-061) and stored at room temperature.

Formalin Solution 10% neutral buffered (Contains formaldehyde 4%)

Purchased from Sigma-Aldrich (Auckland, New Zealand) and stored at room temperature (REF HT5012-60ml)

Sort Buffer

Made with the base of DPBS with addition of 5% FBS and 20 µg/mL DNase I and stored at 4 °C. Made and used on the same day.

BD FACSFlow™ Sheath Fluid

Purchased from BD Biosciences (Auckland, New Zealand) and stored at room temperature (REF 342003)

RNA Lysis Buffer

Purchased from Ngaio Diagnostics as part of the Zymo Research Quick-RNA™ MicroPrep kit (Cat No. R1050) and stored at room temperature.

BD FACS™ Accudrop RUO Beads

Purchased from BD Biosciences (Auckland, New Zealand) (Cat No. 661612) and stored at 4 °C. When used to set up the BD FACSMelody™ 1 drop of beads was added to 500 µL BD FACSFlow™ Sheath Fluid.

BD™ CS&T RUO Beads

Purchased from BD Biosciences (Auckland, New Zealand) (REF 661414) and stored at 4 °C. When used to set up the BD FACSMelody™ 2 drops of beads was added to 500 µL BD FACSFlow™ Sheath Fluid.

Table 2.3: Flow Cytometry and Cell Sort Antibodies, Biotins and Tetramers

Specificity	Fluorophore	Dilution	Clone	Supplier
B220	Biotin	1:1000	RA3-6B2	Biolegend
B220	BUV395	1:200	RA3-6B2	BD Biosciences
B220	PE Cy7	1:800	RA3-6B2	BD Biosciences
BCL6	AF647	1:50	K112-91	BD Biosciences
BST2	BV650	1:200	927	BD Biosciences
CD11b	BUV737	1:200	M1/70	BD Biosciences
CD11c	BV785	1:200	N418	Biolegend

CD4	APC H7	1:800	GK1.5	BD Biosciences
CD4	BV785	1:1600	GK1.5	Biolegend
CD44	AF700	1:200	IM7	Biolegend
CD44	APC Cy7	1:200	IM7	Biolegend
CD44	BUV737	1:400	IM7	BD Biosciences
CD64	AF647	1:200	X54-5/7.1	BD Biosciences
CD64	APC	1:200	X54-5/7.1	Biolegend
CD69	AF488	1:100	H1.2F3	Biolegend
CD69	BV650	1:100	H1.2F3	Biolegend
CD69	PE	1:100	H1.2F3	BD Biosciences
CD86	BUV395	1:200	GL-1	BD Biosciences
c-kit	PE CF594	1:500	2B8	BD Bioscience
CXCR5	Biotin	1:50	2G8	BD Biosciences
CXCR6	PE Cy7	1:100	SA051D1	Biolegend
FoxP3	APC	1:50	FJK-16s	ThermoFisher
GATA3	BV711	1:50	L50-823	BD Biosciences
GL7	FITC	1:600	GL7	Biolegend
IgD	APC H7	1:200	11-26c.2a	BD Bioscience
ICOS	APC	1:200	15F9	Biolegend
ICOSL	PE	1:200	B7H2	Biolegend
I-A(b)-HAAHAEINEA (MHCII-OVA peptide) Tetramer	PE	1:3	-	NIH
I-A(b)-AAHAEINEA (MHCII-OVA peptide) Tetramer	PE	1:3	-	NIH
Ki67	AF594	1:400	11F6	Biolegend
Ly6C	AF700	1:200	HK1.4	Biolegend
Ly6C	PE Cy7	1:1600	HK1.4	Biolegend
MHCII	AF488	1:200	3JP	MIMR made
MHCII (I-A/I-E)	APC	1:200	M5/114.15.2	Biolegend
MHCII (I-A/I-E)	FITC	1:200	M5/114.15.2	eBioscience

MR1 5-OP-RU Tetramer	BV421	1:200	-	NIH
Ovalbumin	Biotin	1:3000	-	Made in-house
PD-1	BV711	1:800	29F.1A12	Biolegend
PD-1	BV785	1:200	29F.1A12	Biolegend
PD-1	PE Cy7	1:400	29F.1A12	Biolegend
PDL-1	BV711	1:800	MIH5	BD Biosciences
RORγT	BV650	1:50	Q31-378	BD Biosciences
RORγT	PE CF594	1:50	Q31-378	BD Biosciences
SIRPα	Biotin	1:500	P84	Biolegend
Streptavidin	AF488	1:1000	-	Biolegend
Streptavidin	APC Cy7	1:800	-	Biolegend
Streptavidin	PE CF594	1:1200	-	BD Biosciences
Tbet	PE	1:50	O4-46	BD Biosciences
TCRβ	Biotin	1:400	H57-597	Biolegend
TCRβ	BV605	1:400	H57-597	Biolegend

Table 2.4: Flow Cytometry and Cell Sort Viability Dyes

Dye	Dilution	Supplier
Zombie Aqua™ Fixable Viability dye	1:1000	Biolegend
Fixable Viability Stain 700	1:3000	DB Biosciences
Zombie NIR™ Fixable Viability dye	1:1000	Biolegend

2.1.3.3 Enzyme-Linked Immunosorbent Assay (ELISA) Buffers and Reagents

Coating Buffer

Coating Buffer was made by adding 1.59 g Na_2CO_3 and 2.93 g $NaHCO_3$ into 1 L milliQ H_2O and stored at 4 °C. For the IgG_{Total} and IgG1 ELISAs, 20 µg/mL of EndoGrade® Ovalbumin was added to coating buffer to coat plates overnight.

Blocking Buffer

10% of FBS was added to 1 L DPBS under sterile conditions and stored at 4 °C.

Wash Buffer

0.05% (500 µL) Tween-20 was added to 1 L DPBS, mixed well and stored at 4 °C.

BD OptEIA™ TMB Substrate Reagent Set

Purchased from BD Biosciences (Auckland, New Zealand) and stored at 4 °C (Cat No. 555214). Used as per manufacturer's instructions with a 1:1 ratio of substrate A to substrate B at room temperature.

Goat anti-Mouse IgG (H+L) Cross-Adsorbed Secondary Antibody, HRP (IgG-HRP)

Purchased from Thermo Fisher Scientific (G21040) (Auckland, New Zealand) with stock made up to 1 mg/mL and stored at -80 °C. Then 1 µg/mL of stock IgG-HRP was diluted in blocking buffer for use in ELISA assays.

Goat anti-Mouse IgG1 Cross-Adsorbed Secondary Antibody, HRP (IgG1-HRP)

Purchased from Thermo Fisher Scientific (A10551) (Auckland, New Zealand) with stock made up to 1 mg/mL and stored at -80 °C. Then 1 µg/mL of stock IgG1-HRP was diluted in blocking buffer for use in ELISA assays.

BD OptEIA™ Mouse IgE ELISA Set

Purchased from BD Biosciences (Auckland, New Zealand) (Cat No. 555248) and stored at room temperature. When used for ELISAs, manufacturer's instructions were followed.

EndoGrade® Ovalbumin

Purchased from Lionex Diagnostics and Therapeutics as lyophilised powder (Braunschweig, Germany) (Cat No. LET0027) and stored at -20 °C under restricted biological protocols. Stock solutions of 25 mg/µL were made up and stored at -80 °C.

Stop Solution (Sulfuric Acid H_2SO_4)

Purchased from Sigma-Aldrich (Auckland, New Zealand) and stored at room temperature. Solution made up to 2 M and stored at room temperature.

2.1.3.4 Ribonucleic Acid (RNA) Extraction, Reverse Transcription, Pre-amplification and Quantitative Polymerase Chain Reaction (qPCR) Buffers and Reagents

Zymo Research Quick-RNA™ MicroPrep Kit

Purchased from Ngaio Diagnostics (Wellington, New Zealand) and stored at room temperature (Cat No. R1050).

Ethyl alcohol, Pure

Purchased from Sigma-Aldrich (Auckland, New Zealand) and stored at room temperature (E7023-500 mL).

Ambion™ Nuclease-free Water

Purchased from Thermo Fisher Scientific (Auckland, New Zealand) and stored at room temperature (REF AM9937).

Applied Biosystems™ High Capacity cDNA Reverse Transcription Kit

Purchased from Thermo Fisher Scientific (Auckland, New Zealand) and stored at -20 °C (REF 4368814).

SsoAdvanced™ PreAmp Supermix

Purchased from Bio-Rad (California, United States) and stored at -20 °C (Cat No. 1725160).

TE Buffer

Made up with 10 mM Tris-HCl and 1 mM EDTA in milliQ H_2O with a final pH of 8 and stored at room temperature.

PowerUp™ SYBR™ Green Master Mix

Purchased from Thermo Fisher Scientific (Auckland, New Zealand) and stored at -4 °C (Cat No. A25742).

PrimeTime® qPCR Primers

Purchased from Integrated DNA Technologies (Iowa, United States) as intercalating primers. Each primer was made up to a stock solution of 100 µM in nuclease-free water and stored at -20 °C.

Table 2.5: qPCR Primers

Assay ID	Gene Target	RefSeq Number	Exon Location	Sequence
Mm.PT.39a.1	Gapdh	NM_008084	2-3	5'-AATGGTGAAGGTCGGTGTG-3' 5'-GTGGAGTCATACTGGAACATGTAG-3'
Mm.PT.58.11809353	Csf2	NM_009969	1-3	5'-ATCAAAGAAGCCCTGAACCTC-3' 5'-TGAAATTGCCCCGTAGACC-3'
Mm.PT.58.28815139	Il15	NM_008357	4-5	5'-TCTCGTGCTACTTGTGTTTCC-3' 5'-CATCTATCCAGTTGGCCTCTG-3'
Mm.PT.39a.22214835	B2m	NM_009735	1-2	5'-TGGTCTTTCTGGTGCTTGTC-3' 5'-GGGTGGAACTGTGTTACGTAG-3'
Mm.PT.58.43894205	Rplp0	NM_007475	5-6	5'-TTATAACCCTGAAGTGCTCGAC-3' 5'-CGCTTGTACCCATTGATGATG-3'
Mm.PT.58.12575861	Tnf	NM_013693	2-4	5'-AGACCCTCACACTCAGATCA-3' 5'-TCTTTGAGATCCATGCCGTTG-3'
Mm.PT.58.10005566	Il6	NM_031168	4-5	5'-AGCCAGAGTCCTTCAGAGA-3' 5'-TCCTTAGCCACTCCTTCTGT-3'
Mn.PT.58.28778894	Lif	NM_008501	4-5	5'-GCAACCTCATGAACCAGATCA-3' 5'-GCACATAGCTTTTCCACGTTG-3'
Mn.PT.58.7853071	Il21	NM_021782	1-3	5'-TGACTTGGATCCTGAACTTCTATC-3' 5'-GGTTTGATGGCTTGAGTTTGG-3'
Mm.PT.58.6531092	Il17a	NM_010552	2-3	5'-AGACTACCTCAACCGTTCCA-3' 5'-GAGCTTCCCAGATCACAGAG-3'
Mm.PT.58.9739903	Il17f	NM_145856	2-3	5'-AATTCCAGAACCGCTCCAG-3' 5'-TTGATGCAGCCTGAGTGTC-3'
Mm.PT.58.16748291	Il23r	NM_144548	8-9	5'-CATCCCACGAACCTCAGAAG-3'

				5’-CAAGAAGACCATTCCCGACAA-3’
Mm.PT.58.41922174	Il12rb2	NM_008354	7-8	5’-TGAGTCACTGAGAACACGAAC-3’ 5’-GATCTGCTGTCTGTCATAGTCG-3’
Mm.PT.58.32192788	Il12rb1	NM_008353	9-10	5’-ACCTATGACCTGAATGTGCTC-3’ 5’-GATGTCATGTTGCCTCCCA-3’
Mm.PT.58.41769240	Ifng	NM_008337	1-2	5’-CTGAGACAATGAACGCTACACA-3’ 5’-TCCACATCTATGCCACTTGAG-3’
Mm.PT.58.30132453	Ifnb1	NM_010510	1-1	5’-ACTCATGAAGTACAACAGCTACG-3’ 5’-GGCATCAACTGACAGGTCTT-3’
Mm.PT.58.6938712	Icos	NM_017480	4-5	5’-GTGTGCATGACCCTAATAGTGA-3’ 5’-GAACTAGTCCATGCGTTTCCT-3’
Mm.PT.58. 32146263	Cd40lg	NM_011616	4-5	5’-GCGAAGCCAACAGTAATGC-3’ 5’-AGTCCTTCTCTTTTAACCGTCAG-3’
Mm.PT.58.29965375	Tnfsf13b	NM_033622	6-7	5’-GACCCTGTTCCGATGTATTCAG-3’ 5’-TCATCTCCTTCTTCCAGCCT-3’
Mm.PT.58.29202697	Tnfsf11	NM_011613	1-2	5’-TCCCGCTCCATGTTCCT-3’ 5’-AGTGCTGTCTTCTGATATTCTGT-3’
Mm.PT.58.32804456.g	Tnfrsf13c	NM_028075	2-3	5’-TCTAGTGAGTCTGGTGAGCTG-3’ 5’-GTAGGAGCTGAGGCATGAG-3’
Mm.PT.58.41807222	Tnfrsf13b	NM_021349	2-3	5’-CAGGTCAGACAACTCAGGAAG-3’ 5’-CACCAAGAAACAGCAGAAGATG-3’
Mm.PT.58.5492284.g	Tnfsf13	NM_023517	1-2	5’-GTCGCACTACTGATCCAACA-3’ 5’-TTCCAGGACATCAGGACTCT-3’
	IFNα (all genes)			5’-TCTGATGCAGCAGGTGGG-3’ 5’-AGGGCTCTCCAGACTTCTGCTCTG-3’

The RNA variations of IFNα were detected using custom primer sets described in Gautier, G. *et al*. (2005)[237].

2.1.3.5 Mouse Treatment Regime Reagents

Anaesthetic

Stock solution of 10x ketamine/xylazine anaesthetic was provided at a concentration of 86mg/mL ketamine and 2.6mg/mL xylazine and covered with tin foil and stored at 4°C. This was further diluted in sterile DPBS at a 1:10 dilution for a 1x working solution which was also stored at 4 °C.

5-amino-6-D-ribitylaminouracil (5-A-RU)

Manufactured and provided by the Ferrier Research Institute, Victoria University of Wellington in solution. Diluted using PBS to a stock of 12.7 mg/mL or 12.9 mg/mL depending on the batch used and stored at -80 °C.

Methylglyoxal (MG)

Purchased from Sigma-Aldrich (Auckland, New Zealand) and stored at 4°C (M0252). MG was used at a concentration of 750 nmol (diluted in DPBS) for vaccines.

Pro-5-A-RU

Manufactured and provided by the Ferrier Research Institute, Victoria University of Wellington as lyophilized powder. A stock was reconstituted in ddH_2O to 3 mg/mL and stored at -80°C.

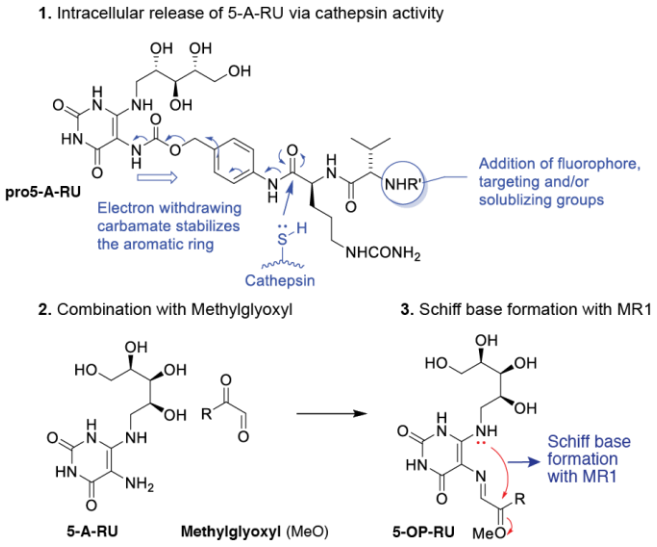

Figure 2.1: Pro-5-A-RU Structure and Mechanism. Diagram provided by the Ferrier Research Institute. Pro-5-A-RU contains a cathepsin-sensitive linker attached to an amino group required for the formation of the Schiff base attachment to MR1. Only once the pro-5-A-RU is inside a cell, is it exposed to cathepsin, whereby, cleavage and immolation of the linker can occur, allowing the released 5-A-RU to combine with methylglyoxal to form the agonist 5-OP-RU. 5-OP-RU is then able to form the Schiff base and attach to MR1, ready for cell surface presentation.

5-(2-oxopropylideneamino)-6-D-ribitylaminouracil (5-OP-RU)

Manufactured and provided by the Ferrier Research Institute, Victoria University of Wellington in solution. Diluted using ddH_2O to a stock of 10 mg/mL and stored at -80°C.

Dulbecco's Phosphate Buffered Saline (DPBS)

Purchased from Gibco by Life Technologies (Auckland, New Zealand) in 500mL bottles (Ref 14190-144) and stored at 4 °C.

Imject™ Alum Adjuvant (alum)

Purchased from Thermo Fisher Scientific (Auckland, New Zealand) and stored at room temperature (Cat No. 77161). Formulation of aluminum hydroxide and magnesium hydroxide.

EndoGrade® Ovalbumin

Purchased from Lionex Diagnostics and Therapeutics as lyophilised powder (Braunschweig, Germany) (Cat No. LET0027) and stored at -20 °C under restricted biological protocols. Stock solutions of 25 mg/µL were made up and stored at -80 °C.

Ovalbumin (OVA) is a protein abundantly found in avian egg-white and is well known as a model antigen in immunological studies[238]. In murine studies, it can be implemented as a foreign antigen with the ability to track the corresponding antigen-specific response due to the known TCR and BCR OVA epitopes[239,240]. This allowing me to determine whether our vaccine has the potential to induce an antigen specific adaptive response to a vaccine antigen.

Blocking Antibodies

Purchased from Bio X Cell (United States) and stored at 4 °C.

Table 2.6: Blocking Antibodies

InVivoMAb anti-mouse	*Clone*	*Cat No.*
CD40L	MR-1	BP0017-1
RANKL	IK22/5	BE0191

2.1.3.6 Vaccines

All vaccine components were kept sterile and vaccines were made up under a hood to ensure sterility until administration. All components were kept on ice.

5-A-RU + MG Admix

Vaccine components, 5-A-RU, MG and DPBS was aliquoted out into separate tubes. When mice were fully anaesthetised and placed on their backs, the MG was added to the DPBS then the 5-A-RU was added and the vaccine was resuspended until a faint yellow colour developed (lumazine formation). The mice were then administered 30 µL of the vaccine intranasally using a pipette. Unless otherwise specified 5-A-RU was at 75 nmols and the MG at 750 nmols.

Pro-5-A-RU

75 nmol of the pro-5-A-RU was added to DPBS to make up enough vaccine for 30 µL per mouse.

5-OP-RU

5-OP-RU was first filtered and then made up to 75 nmol in DPBS.

5-A-RU + MG Admix plus EndoGrade® Ovalbumin

Vaccine admix was prepared as described above but the DPBS also included 5 nmol EndoGrade® Ovalbumin.

Alum *+ EndoGrade® Ovalbumin*

This vaccine was made up to 100 µL per mouse for intraperitoneal injection. EndoGrade® Ovalbumin was added to DPBS at a concentration of 0.5 mg/mL and alum to a concentration of 10 mg/mL.

EndoGrade® Ovalbumin alone

This vaccine was made up to 100 µL per mouse for intraperitoneal injection. EndoGrade® Ovalbumin was added to DPBS at a concentration of 0.5 mg/mL.

CD40L and RANKL Monoclonal Antibodies

Monoclonal antibodies were made up to 100 µL per mouse for intraperitoneal injection. Each antibody was diluted into sterile DBPS at a concentration of either 500 µg or 250 µg.

2.1.4 Mice

Animal Care and Ethics

The mice used to carry out the experiments were either bred and housed in the Biomedical Research Unit at Malaghan Institute of Medical Research or in the mouse facility at Victoria University of Wellington. The mice were under specific-pathogen free conditions and were fed autoclaved meat-free rat and mouse diet (Specialty Feeds, Western Australia) and autoclaved acidified water. Both food and water were available ad libitum and mice were in a controlled 12 hr light 12 hr dark cycle. All mouse manipulations were approved by the Animal Ethics Committee at Victoria University of Wellington and followed the Code of Ethical Conduct for the Manipulation of Animals. Where possible, sex matched mice aged between 6-12 weeks at the onset of experiments were used. Treatment groups were also split across boxes in an attempt to avoid cage related effects. Experiments fell under either the 25790 protocol: Impact of microenvironment on dendritic cell function (approved 14/03/18), or the 26289 protocol: Antibody responses to invariant T cell adjuvant vaccines (approved 09/08/18).

Mouse Strains

C57BL/6J (referred to as C57BL/6)

Original breeding pairs were sourced from the Jackson Laboratory (Bar Harbour, ME, USA) and bred at the Biomedical Research Unit at the Malaghan Institute of Medical Research and the mouse facility at Victoria University of Wellington.

4C13R Homo x B6-SJ (referred to as 4C13R)

4C13R mice have transgenic expression of fluorescent AmCyan and dsRed reporters under the regulation of IL-4 and IL-13 elements respectively. These mice are generated through a bacterial artificial chromosome (BAC) system containing the control region of the T_H2 locus along with genes/regions encoding IL-13, CNS-1, IL-4 and kinesin-II subunit[241]. The 4C13R mice were obtained from Dr. William E. Paul (National Institutes of Health, United States) and were bred on a B6-SJ background at the Malaghan Institute of Medical Research, where they were also housed and genotyped for homozygous expression of the 4C13R genes.

MR1$^{-/-}$

MR1$^{-/-}$ mice lack MR1 which is required for MAIT cell development, therefore these mice lack MAIT cells. These mice are generated by gene targeting techniques that delete the α1 and α2 domains of MR1 and bred to maintain homozygous mice[242]. These mice were housed and bred at the Malaghan Institute of Medical Research.

Nur77^{GFP}

Nur77 is upregulated when T cells are activated through the TCR, but not by inflammatory stimuli. Nur77^{GFP} mice, allow identification of Nur77 expression through GFP fluorescence. These transgenic mice are generated through BAC that contains GFP inserted into the *Nr4a1* (Nur77) locus. The strength of TCR stimulation correlates with the GFP expression[243]. These mice were housed and bred at the Malaghan Institute of Medical Research.

BATF3$^{-/-}$

BATF3$^{-/-}$ mice lack the transcription factor BATF3, though the loss of exons 1-2 leading to elimination of gene expression. BATF3 is required in the development of some dendritic cell subsets such as CD8α$^+$ cDCs, therefore these mice lack these DC subsets[244]. Mice are homozygous and original breeding pairs were provided by Dr. K. Murphy (Washington University, United States). These mice were housed and bred at the Malaghan Institute of Medical Research.

IRF4$^{fl/fl}$ CD11c-Cre$^{+/-}$

IRF4$^{fl/fl}$ CD11c-Cre^{+} mice were created by crossing *IRF4*$^{fl/fl}$ mice (C57BL/6 background) with CD11c-Cre^{+} mice[245]. These mice utilise the Cre-lox system whereby, the P1 bacteriophage *cre* (cyclization recombination) recombinase gene is expressed along with the CD11c gene (*itgax).* Thus, when CD11c is expressed so is cre recombinase which targets the two *loxP* sites flanking IRF4 (termed the floxed locus). This Cre-lox system causes a lack of IRF4 in CD11c^{+} cells, thus a lack IRF4 in DCs. *IRF4*$^{fl/fl}$ CD11c-Cre^{-} mice (lack Cre recombinase) were used as control mice. The *IRF4*$^{fl/fl}$ CD11c-Cre$^{+/-}$ mice were housed and bred at the Malaghan Institute of Medical Research.

B6.129S2(C)-*Stat6*^{tm1Gru}/J (referred to as STAT6$^{-/-}$)

These mice were purchased from The Jackson Laboratory. They were generated by replacing the 505-584 amino acid region of the STAT6 endogenous gene with a vector cassette. This was electroporated into embryonic cells, which were in turn injected into BALB/c blastocysts. These mice were further bred with BALB/c mice for a BLAB/c background[246]. These mice were then bred with C57BL/6 mice for a C57BL/6 background. The C57.STAT6$^{-/-}$ mice were housed and bred at the Malaghan Institute of Medical Research.

2.2 Methods

2.2.1 Mouse Manipulations

Mouse manipulations included general handling and intraperitoneal injections of anaesthetic. Once anaesthetised, mice were administered intranasal vaccines of 30 µL volumes and in some cases, ear tagged.

Handling

General handling of the mice was required for intraperitoneal injections of anaesthetic. Once anaesthetised, mice were laid out on their back to allow for intranasal vaccination.

Mice were monitored during and directly after vaccination to ensure recovery and then returned to their box to fully recover from the anaesthetic.

Intraperitoneal Injections

For intraperitoneal injections the needle was inserted just off centre of the ventral side of the mouse to the left side and in line with the top of the flank. The dose of anaesthetic was dependent on the weight of the mice (100mg/kg of Ketamine and 3mg/kg of Xylazine) and generally totalled around 200-300 µL per mouse. Intraperitoneal injection of alum admixed with EndoGrade® Ovalbumin and EndoGrade® Ovalbumin alone was also carried out as described above.

Intranasal Administration of Vaccines

After mice were anaesthetised, they were placed on their backs with their faces up. 30 µL volumes were given via a pipette placed just above the nose and slowly expelling the vaccine into the nasal cavity. Mice were monitored during and after intranasal vaccination to ensure recovery.

Administration of CD40L and RANKL Monoclonal Antibodies

The initial 500 µg dose of each antibody was administered intraperitoneally 12 hrs prior to intranasal treatment. The second 250 µg dose was also administered intraperitoneally, 1 hr after mice had been anaesthetised and treated intranasally.

2.2.2 Endpoint

Euthanasia

Euthanasia was conducted by CO_2 asphyxiation and mice were checked to have no heart beat or reflexes before any further procedures were done.

2.2.3 Flow Cytometry

Mediastinal Lymph Node (mLN) Harvesting and Processing

After euthanasia, the mLN was retrieved on the left side under the lung using the vasculature architecture as a guide. Once collected the mLN was stored on ice in either 0.5 mL of IMDM or digestion buffer in a 24-well plate. Digestion buffer was used when experiments were investigating dendritic cells. To obtain a single cell suspension in experiments not investigating dendritic cells, mLN were filtered and mashed through a 70 μm cell strainer and then washed with 10 mL IMDM. When a digestion was required, the mLN's capsules were broken using two needles. This was followed by a 25-minute incubation at 37 °C. Digestion was ceased by adding 10 μL EDTA and the mLN further broken up by several resuspensions with a pipette. The resuspended mLNs were filtered through a 70 μm cell strainer, the well washed out with a further 0.5 mL IMDM and then the filter rinsed with 10 mL IMDM. Samples were finally centrifuged (250 x g at 4°C for 10 minutes), the supernatant removed, and the cell pellet resuspended in 200 μL IMDM, ready for transfer into a 96-well plate.

Cell Counting

Cell counting was used to determine the number of cells per mLN. Counting was done by diluting 10μl of sample into 90μl of Trypan blue in a 96-well plate. Once mixed, 10μl of the stained cells was loaded onto a haemocytometer. The live cells from the central squares were counted, while cells on the outside left and bottom line were excluded. The number of cells was calculated using this equation: cell concentration (cells/mL) = average cell count per square x dilution factor (10) x 10^4.

Lung Harvesting and Processing

Following the collection of the mLN, the lungs were perfused and collected. To perfuse the lung an incision in the top right ventricle of the heart was made and 5 mL of PBS was perfused through the right ventricle and the lung lobes were removed at the bronchioles. The lung lobes were stored on ice in 2.5 mL IMDM in a 12-well plate. The lungs were chopped finely in 2.5 mL digestion buffer and incubated at 37 °C for 45 minutes. The digestion was stopped using 50 μL EDTA. To obtain a single cell suspension, the lung samples were passed through a 3 mL syringe placed flat on the bottom of the

well to tease apart the lung tissue and release cells. Next the samples were filtered and mashed through a 70 μm cell strainer. The empty wells were then washed with 1 mL IMDM and filtered through the strainer followed by 20 mL IMDM. After centrifuging for 15 minutes (250 x g at 4 °C) and removing the supernatant, the cell pellet was incubated with ACT buffer at 37 °C for 10 minutes. Following red blood cell lysis, the samples were washed with 20 mL IMDM and centrifuged again for 15 minutes (250 x g at 4 °C). The supernatant was removed, and the cell pellet resuspended in 200 μL IMDM then filtered through a 70 μm cell strainer before being transferred into a 96-well plate.

Live Dead Staining and Fc Block

After the mLN and/or lung single cell suspensions were transferred into 96-well plates, the plates were centrifuged (250 x g at 4 °C for 2 minutes) and the supernatant removed ready for viability staining. BD Horizon™ Fixable Viability Stain 700 was used at a 1:3000 dilution, whereas the Zombie Aqua™ and NIR™ Fixable Viability dyes were used at 1:1000. In all cases the dyes were diluted in DPBS and 100 μL was added to each sample by resuspending the cell pellet. Following a 30-minute incubation at 4 °C, the samples were washed with 100 μL DPBS, centrifuged (250 x g at 4 °C for 2 minutes) and the supernatant removed. Next, 100 μL of a 1:300 dilution (in FACS buffer) of Fc block was resuspended with the cell pellet and left to incubate at 4 °C for 10 minutes. After incubation another wash, and centrifugation step was carried out as previously described.

I-A(b)-HAAHAEINEA and I-A(b)-AAHAEINEA Tetramer Staining (MHCII-OVA peptide)

Following Fc block staining, 5 μL of the MHC-II-OVA peptide (1:3 dilution of stock into FACS buffer) was added directly to the cell pellet, vortexed and left to incubate in the dark at room temperature for 30 minutes. Following incubation, the samples were washed 3 times with FACS buffer.

OVA-Biotin Staining

After Fc block or MHCII-OVA peptide tetramer staining, 50 μL of OVA-biotin (1:3000) diluted in 10% FCS PBS was resuspended with each sample. Plates were incubated for 30 minutes at 4 °C and then washed 3 times with FACS buffer. The corresponding streptavidin fluorophore was included in the cell surface antibody cocktail.

Cell Surface Staining

All antibodies were centrifuged at 17000 RPM for 1 minute at 4 °C before use. The cell surface antibody cocktails and fluorescence minus one (FMO) cocktails were made up in FACS buffer according to the dilutions in table 2.3. Each sample had 50 μL of the corresponding cocktail added. The MR1-5-OP-RU tetramer was also included in this staining cocktail. After addition of the antibodies, the plates were incubated at 4 °C for 15 minutes. Following incubation, the samples were washed 3 times with FACS buffer. If biotin was required for one of the markers a secondary stain was required for the streptavidin fluorophore. The streptavidin stain was also diluted in FACS buffer flowing the table 2.3 and 50 μL was added to each sample. Plates were incubated for 10 minutes on ice and washed 3 times as described above.

Transcription Factor Staining

When required, transcription factor staining was carried out as the last staining step using the FOXP3 Transcription Factor Staining Buffer Set. Cells were first fixed in 200 μL fixative following kit instructions. The plates were then incubated for 1 hour in the dark at room temperature. Following incubation, plates were centrifuged at 250 x g at 4°C for 5 minutes and washed 3 times with permeabilization buffer (kit instructions). After supernatant was removed, 50 μL of the transcription factor antibody cocktail and corresponding FMO cocktails were added to the cells. The cocktail was made in permeabilisation buffer with antibody dilutions following table 2.3. Plates were incubated for 2 hours in the dark at room temperature. Plates were washed another 3 times and then cells were resuspended in 200 μL FACS buffer and transferred to 1.1 mL microtubes. The tubes were covered with parafilm and tin foil, then stored at 4 °C overnight ready for flow cytometry the next day.

Fixing

Cells were fixed in all experiments and run on the LSRII the following day, excluding the experiment with 4C13R Homo x B6-SJ mice where samples were run the same day on the Cytek Aurora. When cells required to be fixed, fixation was carried out either using the FOXP3 transcription Factor Staining Buffer Set as described in the transcription factor staining section or with formalin solution after cell surface staining. The latter protocol involved incubating the cells with 100 μL formalin solution for 20 minutes at 4°C. The plates were then centrifuged (250 x g at 4 °C for 2 minutes), supernatant removed, and the cells resuspended in 200 μL FACS buffer and transferred to 1.1 mL microtubes. The samples were covered with parafilm and tin foil then stored at 4 °C overnight.

Compensation Controls

Single stain compensation controls were required for set up on the flow cytometers. All markers excluding MHCII and a live/dead control were made using UltraComp eBeads™. Each single stain had approximately half a drop of UltraComp eBeads™ to 100 μL FACS buffer and 0.5 μL of the corresponding antibody was added. After a 10-minute incubation in the dark, the beads were washed with 1 mL FACS buffer and centrifuged (250 x g at 4 °C for 5 minutes). Supernatant was removed, and the beads were resuspended in 200 μL FACS buffer and stored at 4 °C. For the MHCII and live/dead compensation controls, cells were used.

Flow Cytometers

Before experiments were run on the flow cytometers a CST was done by the Huge Green Cytometry Centre staff at the Malaghan Institute of Medical Research to check the cytometer performance, calculate the optimal voltages and laser delays for the day.

Before the samples were run on the cytometer they were filtered through 70 μm nylon gauze and vortexed. A short delay was given between acquiring the sample and

recording the sample, to allow for stabilisation. As the samples were running, the abort rate was monitored to ensure that no more than 5% of the sample was lost and the flow rate adjusted accordingly. The biological samples were run until all the sample was acquired.

LSRII – BD LSRII SORP (Becton Dickinson, San Jose, CA)

Firstly, the unstained sample was acquired, and the voltages were set so the peak fluorescence was at 10^2. The fully stained sample was then run to check it was on scale. Next, all the single stains were recorded, and the positive and negative peaks determined. Lastly, the required FMO's and fully stained samples were recorded.

Cytek Aurora Spectral Cytometer (Cytek Biosciences Inc., Fremont, CA)

The first step on the Aurora was to record the reference groups, this including the unstained cells and compensation single stains on beads. The unstained sample was used to adjust the FSC and SSC gains to make sure the cells were on scale. Next the fully stained sample that was expected to have the brightest signal was briefly run to check all signals were below 10^6. If the sample was above 10^6, the gains were reduced accordingly. This was repeated with the brightest single stains. Once the gains were checked, all the controls were recorded, and the positive and negative populations were then identified. The spectral plot was also checked to ensure the brightest peak was selected. Finally, the fully stained biological samples and FMO's were acquired and recorded.

2.2.4 Enzyme-Linked Immunosorbent Assay (ELISA)

Cardiac Puncture

Once mice were culled, they were placed ventral side up and a 1 mL syringe was inserted to the right side under the rib cage to conduct a cardiac puncture. The collected blood was placed in a 1.7 mL tube and left at room temperature for at least 30 minutes to allow clotting. The blood was then centrifuged for 10 minutes 3000 RPM. The serum was pipetted from the top layer and then stored at -80 °C.

Total IgG and IgG1 ELISA

96 well ELISA plates were coated overnight with 100 µL OVA coating buffer and stored at 4 °C. The next day, the plates were washed firstly with 100 µL wash buffer then 4 lots of 200 µL wash buffer. The blocking buffer was added (200 µL) into each well and incubated for 1 hour at room temperature. Serum fold dilutions were made in blocking buffer (from 1:10 to 1:100,000). After the 1-hour incubation, the blocking buffer was discarded, and the serum dilutions added to the corresponding wells. The serum was left to incubate for 2 hours at room temperature. Next the serum was washed from the plates follow the same wash steps as before. After washing the plates, 100 µL of IgG-HRP or IgG1-HRP conjugate was added and incubated for 1 hour at room temperature. The plates were again washed and then 100 µL of TMB substrate was added and left for the colour to develop (about 5 minutes). To stop the reaction, 50 µL of 2 M H_2SO_4 was added and then the plates read at 450 nm with an Enspire 2300 Multilabel Reader.

IgE ELISA

The IgE ELISA was completed using a BD Biosciences Mouse IgE ELISA Set (Cat. No. 555248). The manufacturer instructions were used to carry out the ELISA and the serum fold dilutions included 1:10 to 1:100,000. The positive and negative serum controls were kindly supplied by Prof Anne La Flamme (Victoria University of Wellington). The positive control was C57BL/6 mice infected with Schistosomiasis and the negative control serum was from naïve C57BL/6 mice. Plates were read at 450 nm with an Enspire 2300 Multilabel Reader.

2.2.5 Cell Sort

Lung Harvesting and Processing

Tissue processing of the lungs followed the same protocol as in the Flow Cytometry section.

Cell Surface Staining

The Cell surface staining (Live/dead staining, Fc block and cell surface antibody staining) methods followed the same protocols as in the Flow Cytometry section, with the only exception being the FACS buffer was replaced with the sort buffer.

Cell Sort

A BD FACSMelody™ (Becton Dickinson, San Jose, CA, USA) was used to sort and isolate the MAIT cells using the suggested set up work flow. The machine was set up using BD FACS™ Accudrop RUO Beads and BD™ CS&T RUO Beads. The stained single cells lung suspensions were diluted in 2.5 mL sort buffer and a pre-sort was conducted. The pre-sort was done on live $B220^{-}CD64^{-}Ly6C^{-}TCR\beta^{+}CD44^{hi}$ cells using the purity sort mode into 200 µL of sort buffer. The MAIT cells were then isolated from the pre-sort samples using the purity mode gating on live $B220^{-}CD64^{-}Ly6C^{-}TCR\beta^{+}CD44^{hi}$MR1-5-OP-RU tetramer^{+} cells and PD-1^{+} for the admix treated samples, whereas PD-1^{-} for the PBS treated samples. The MAIT cells were sorted into 100 µL RNA lysis buffer in 1.7 mL tubes, then vortexed and stored at -80 °C.

2.2.6 Quantitative Polymerase Chain Reaction (qPCR)

RNA Extraction

Once the MAIT cell samples frozen in lysis buffer were thawed, 100 µL of pure ethyl alcohol (molecular grade) was added to each sample. The samples were then vortexed followed by a quick centrifuge and transferred to spin columns in a collection tube. From this point the protocol followed the manufacturer's instructions from step 4 of the RNA Purification protocol in the Zymo Research Quick-RNA™ MicroPrep Kit. For the elution of the RNA, 11 µL of DNase/RNase free water was used. Samples were kept on ice and the reverse transcription was done immediately following RNA extraction.

Reverse Transcription

A master mix was made using the Applied Biosystems™ High Capacity cDNA Reverse Transcription Kit. This contained, 2 µL 10x RT Buffer, 0.8 µL 25x dNTP Mix, 2 µL 10x RT Random Primers, 1 µL MultiScribe Reverse Transcriptase and 4.2 µL nuclease-free water per sample. The master mix was vortexed and 10 µL added to 10 µL of extracted RNA in

MicroAmp™ Optical 8-Tube Strips. After vortexing and centrifuging the reactions, the tubes were placed in the Veriti™ 96-Well Thermal Cycler, using the following protocol:

Table 2.7: Reverse Transcription Cycling Conditions

	Step 1	Step 2	Step 3	Step 4
Temperature (°C)	25	37	85	4
Time (min)	10	120	5	∞

The resulting cDNA was stored at -20 °C.

Pre-amplification

Firstly, 2.5 µL of each primer (100 µM stock) was added to 500 µL of nuclease-free water to form a primer assay pool. Next a reaction mix was made containing 12.5 µL SsoAdvanced™ PreAmp Supermix, 2.5 µL of the primer assay pool and 3.75 µL nuclease-free water per sample. 18.75 µL of the reaction mix was then added to 6.25 µL of cDNA in MicroAmp™ Optical 8-Tube Strips. After vortexing and centrifuging the reactions, the tubes were placed in the Veriti™ 96-Well Thermal Cycler, using the following protocol:

Table 2.8: Pre-amplification Cycling Conditions

	Number of Cycles	Temperature (°C)	Time
Polymerase activation and DNA denaturation	Hold	95	3 min
Denaturation	12 cycles	95	15 sec
Annealing/Extension		58	4 min
	Hold	4	∞

The resulting amplified cDNA was stored at -20 °C.

qPCR

The amplified cDNA samples were diluted 10x in TE buffer. Each primer (100 µM stock) was further diluted in nuclease-free water to a stock of 10 µM for qPCR reactions (stored at -20 °C). A master mix for the amplified cDNA and nuclease free water, plus a master

mix of PowerUp™ SYBR™ Green Master Mix and the corresponding primers was made to allow for 5 µL PowerUp™ SYBR™ Green Master Mix, 0.5 µL primer (from 10 µM stock), 1 µL amplified diluted cDNA and 3.5 µL nuclease-free water per well. Master mixes were added to MicroAmp™ Optical 96-Well Reaction Plates with each sample in duplicate and each plate containing the housekeeping gene and a no template control (nuclease-free water) for each primer set. After vortexing and centrifuging the plates, they were placed in the Applied Biosystems™ QuantStudio 7 Flex Real-Time PCR System, using the following protocol with the addition of a melt curve:

Table 2.9: qPCR Cycling Conditions

Step	Temperature (°C)	Time	Cycles
UDG activation	50	2 min	Hold
Dual-Lock DNA polymerase	95	2 min	Hold
Denature	95	1 sec	50 cycles
Anneal/extend	60	30 sec	

Table 2.10: Melt Curve Cycling Conditions

Step	Ramp Rate (°C/sec)	Temperature (°C)	Time
1	1.6	95	15 sec
2	1.6	60	1 min
3	0.15	95	15 sec

Upon completion of the qPCRs the melt curves were checked for single peaks to confirm single product detection of the primers. For each sample duplicate, the housekeeping gene and target gene cycle threshold was averaged. A further average of the housekeeping gene and target gene cycle threshold was taken as there was also two samples of 100 MAIT cells per mouse. The relative expression of each target gene was then calculated for each mouse using the following equation, $2^{-\triangle CT}$.

2.2.7 Data Analysis

Flow Cytometry Data

FlowJo software (version 10, Treestar, Inc, CA, USA) was used to analyse the FACS data. Cells were gated based on the FMO's, unstained samples and experiment controls where appropriate. The flow cytometry plots displayed were generated from the FlowJo software.

Graphical Data

All graphical representation was constructed using Graph Pad Prism software (version 8, Graph Pad Software, CS, USA). The statistics displayed on the graphs were also conducted using Graph Pad Prism. Statistical analysis of $p<0.05$ was considered significant. When comparing a single parameter between three or more groups a One-way ANOVA test and Tukey's post-test was used. A two-way ANOVA was used when two parameters were being compared to the dependent variable, whereas, comparisons between two independent groups an unpaired t test was used.

3 MAIT and Dendritic Cell Phenotype Following Intranasal Administration of MAIT Cell Agonists

3.1 Introduction

Dendritic cells (DCs) play an integral role in linking the innate with the adaptive immune system. They are the immune systems superior antigen presenting cell with the ability to migrate to the draining lymph nodes upon maturation following antigen uptake[121–123]. Once in the lymph nodes, DCs are able to present antigen and drive specific adaptive responses, interacting with T cells and indirectly inducing B cell responses through T_{FH} cells[247]. The induction of adaptive immunity by a vaccine can be enhanced in a vaccine setting by targeting DCs. For example, OVA (antigen) conjugated to an antibody specific for CD11c, a molecule expressed on DCs, is able to target DCs and induce an elevated $CD4^+$ and $CD8^+$ T cell accumulation and increase their release of effector cytokine, IFN-γ[248]. DCs can also be targeted using specific antibodies targeting DEC-205, an endocytosis receptor on DCs. Much like with the CD11c targeting system, antigen conjugated to DEC-205 antibodies improves both $CD4^+$ and $CD8^+$ T cell responses[249]. It's important to note in these two experiments that additional DC stimulation through anergic CD40 antibodies was required for DC activation and the resulting adaptive response[248,249]. While targeting antigen to DCs improves the adaptive response, the DCs also need to become activated sufficiently to avoid tolerance induction. This highlights DCs important role in the induction of an adaptive immune response in vaccination.

DCs are comprised of an array of different subsets each with their own unique functions and locations within the body. Among others, these subsets include plasmacytoid DCs which have specialised viral responses by producing type 1 IFNs[250], Langerhans cells that reside within the skin[251], and conventional DCs (cDCs) with a broad range of functions. cDCs are specialised for antigen presentation with superior antigen processing and presentation which allows for the activation of naive T cells[252,253]. cDCs can be further divided into subsets which have been previously based on the expression of markers such as CD4, CD8α, CD103 and CD11b. These markers however are dependent on the location of the DCs, for example, CD4 and CD8α can be used in the murine spleen for cDC subset identification, whereas CD103 and CD11b can be used in peripheral tissues[253,254]. The complexity of defining these cDC subsets has led to the proposal of

dividing cDCs into cDC1s and cDC2s based on their dependency for different transcription factors. cDC1s express IRF8 which is required for survival and function[255] and also have a dependence on basic leucine zipper transcriptional factor ATF-like 3 (BATF3) for development[256,257], whereas cDC2s don't require BATF3 but are dependent on IRF4 for their survival and function[258–260]. In addition to these transcription factor markers, cDC1s and cDC2s can be identified through cell surface markers. The chemokine XCL1 receptor, XCR1, and signal-regulatory protein α (SIRPα/CD172α) can be used to discriminate cDC1s and cDC2s in both steady state and activated conditions[254]. cDC1s can be identified via XCR1^{+}SIRPα^{-} expression, whereas cDC2s by XCR1^{-}SIRPα^{+} expression[254,261]. Dividing cDC into cDC1s and cDC2s also reflects functional differences in the subsets. cDC1s are able to cross present exogenous antigen on MHCI to activate naïve CD8^{+} T cells in anti-viral and anti-tumour responses[256,262]. Conversely, cDC2s are apt at initiating a CD4^{+} T cell response through MHCII[263,264].

Conventional T cells are able to recognise peptides presented via MHC molecules on antigen presenting cells (APCs) such as DCs. These peptides are derived from larger proteins that have been digested intracellularly in an APC to release peptides that stabilise and bind to the polymorphic MHC molecules. This allows for extracellular presentation of the peptides to the diverse repertoire of T cell receptors (TCRs) on conventional T cells. Due to the diversity of TCRs, only a small proportion of T cells will be capable of recognising the peptide and inducing an antigen specific response. This response is also delayed due to the process of clonal expansion[265]. While a conventional T cell response can take several days to develop, non-conventional or 'innate-like' T cells can be activated rapidly, a characteristic of the innate immune system[266]. These non-conventional T cells overcome the delayed response due to their invariant TCRs which are non-MHC-restricted and instead recognise non-peptide antigens presented on non-polymorphic antigen presentation molecules. Together, this results in a T cell population whereby the majority are able to recognise the same antigen and induce a rapid response without the requirement for clonal expansion[265]. Additionally, non-conventional T cells are commonly but not restricted to barrier sites where they

frequently come into contact with environmental and microbial antigens[222,242,266–269]. This apt location aids in the rapid antigen recognition and activation upon insult.

Non-conventional T cells can be split into subsets including mucosal-associated invariant T (MAIT) cells and natural killer T (NKT) cells. Type 1 (or classical) NKT cells are able to recognise lipid-based antigens presented by the non-polymorphic MHC class I-like molecule, CD1d, on APCs. Just like in MAIT cells, NKT cells have a restricted TCR, with an invariant TCR-α chain (Vα14-Jα18 in mice and Vα24-Jα18 in humans) combined with a small range of TCR-Vβ chains (Vβ2, 7 and 8 in mice and Vβ11 in humans)[270]. NKT cells can respond to both microbial[271] and self-lipid based antigens[272] presented through CD1d or can become activated independent of antigen through pathogen induced cytokines[273]. Upon activation, NKT cells can produce both T_H1 and T_H2-like cytokines such as IFN-γ and IL-4[274]. Due to their conserved repertoire within a population and their bias towards restricted antigen recognition, NKT cells make ideal targets for immunotherapy and vaccination, as their activation and role is generalised throughout a population and would not require personalised adaptations. NKT cells have already shown promise in these areas. The NKT cell agonist, α-galactosylceramide (α-GalCer) when conjugated to an MHC binding peptide, has shown to induce DC activation and cytotoxic T cell activity, leading to an anti-tumour response in vivo. In this case the α-GalCer acts as a vaccine adjuvant to licence the immune response, as the cytotoxic T cell activity is lost in CD1d-deficient mice[275]. The enhanced adaptive response induced by administering antigen along with α-GalCer is dependent on DC interaction with NKT cells through CD40:CD40L interactions[276]. These studies suggest, the NKT cell agonist is processed by DCs along with the antigen, whereby the agonist stimulates NKT cells to become activated and helps to licence and enhance the DCs ability to activate a T cell response through the peptide presentation[277].

MAIT cells harbour similar characteristics to NKT cells. MAIT cells also have conserved TCRs, that are comprised of an invariant Vα chain (Vα7.2Jα33 in humans and Vα19Jα33 in mice) paired with a small range of β-chains (Vβ6 and 8 in mice and Vβ2 and 13 in

humans)[278]. These semi-invariant TCRs don't recognise lipids via CD1d, but instead bacterial and fungal metabolites presented on another non-polymorphic MHC class I-like protein, MR1. The metabolites presented on MR1 are commonly derived from the riboflavin pathway and upon activation[213], MAIT cells are able to release pro-inflammatory cytokines such as IFNγ, TNF and IL-17A[204]. As with the NKT cells, the MAIT cells invariant TCR and rapid activation, makes them an ideal target for immunotherapy[205] and vaccination[218]. Additionally, MAIT cells presence at the mucosa[222,242], allows for rapid interaction with pathogen metabolites. Furthermore, research has already identified interactions between MAIT cells and DCs, whereby MAIT cells co-incubated with immature DCs and 5-A-RU + MG (forms MAIT agonist 5-OP-RU), were able to induce DC maturation and activation, which led to IL-12 production. This DC maturation was depend on CD40L and MR1[236]. This shows parallels with the NKT cell DC interactions. This along with MAIT cells location at the mucosa, rapid activation ability and invariant nature provides rational for the investigation into MAIT cells ability to be used as a cellular adjuvant, especially with the need for new mucosal adjuvants being in high demand.

In order to investigate MAIT cells ability to be used as a mucosal cellular adjuvant, a model to identify MAIT cells at a mucosal site was first established. I was able to show that MAIT cells could be identified by flow cytometry using the MR1-5-OP-RU tetramer in the lung tissue and mediastinal lymph nodes (mLNs) of C57BL/6 mice after intranasal administration of MAIT cell agonists. Additionally, the admix of 5-A-RU and methylglyoxal (MG) was optimal and sufficient to activate MAIT cells and consequently conventional DCs through an MR1 dependent pathway in the lung and mLN. Furthermore, these MAIT cells showed a phenotypic bias towards RORγT and GATA3 expression in this model.

3.2 Aims

Based on the recent findings of non-conventional T cells adjuvant abilities such as with NKT cells, I hypothesised that MAIT cells could also harness this adjuvant activity. Additionally, MAIT cells mucosal location, invariant nature and rapid activation, make them ideal targets for mucosal vaccine cellular adjuvants. Therefore, this chapter aims to identify a model to investigate MAIT cells phenotype and ability to induce DC activation in the lung mucosal sites after intranasal vaccination of MAIT cell agonists.

Specific aims:

1) To determine whether MAIT cells can be activated at local mucosal tissue sites following intranasal administration of agonists
2) To access whether 5-A-RU plus methylglyoxal admix can induce DC maturation as a pivotal vaccine efficiency read out
3) To characterise the MAIT cell phenotype in the lung and mLN after intranasal admix administration

3.3 Results

3.3.1 MAIT and Dendritic Cell Activation is Induced Following Intranasal Administration of 5-A-RU plus MG Admix

MAIT cells have previously been identified using the MR1-5-OP-RU tetramer in a range of different tissue in C57BL/6 mice at steady state. Of these tissues, the lungs had one of the higher frequencies of MAIT cells among TCRβ^+ lymphocytes[222]. This identified the lung tissue as an ideal mucosal target for investigating MAIT cells. Additionally, the lung would be a primary tissue site for intranasal administration of vaccination. I initially wanted to determine whether two different MAIT cell agonists provided by the Ferrier Research Institute were able to be administered intranasally and drive MAIT cell activation in the lung tissue. The first agonist was an admix of the riboflavin derivative 5-amino-6-D-ribitylaminouracil (5-A-RU) mixed with methylglyoxal (MG), a product from glycolysis in mammalian cells and metabolism in microbe cells. These are well described components that form pyrimidines such as the potent MAIT cell agonist 5-(2-oxopropylideneamino)-6-D-ribitylaminouracil (5-OP-RU) through non-enzymatic condensation reactions. However, the resulting pyrimidines are unstable and rapidly go through dehydration to form the more stable lumazines. Both pyrimidines and lumazines are capable of binding and stabilising MR1 intracellularly, to allow for trafficking to the cell surface and presentation. Though both are able to activate MAIT cells through the TCR, pyrimidines such as 5-OP-RU are more potent activators compared to the weaker lumazines[210,213,279].

With this agonist formation pathway in mind, I had two MAIT cell agonist vaccines to investigate. For the admix vaccination, 75 nmol of 5-A-RU was mixed with 750 nmol MG in PBS just prior to intranasal administration. These components will begin to form 5-OP-RU but also the weaker lumazines in the exogenous vaccine mix. The lumazine formation becomes apparent as the vaccine mixture gradually becomes yellow in colour. As a slight yellow tinge starts to form, the vaccine is administered intranasally. The 5-OP-RU and resulting lumazines would be taken up by antigen presenting cells

(APCs) and presented via MR1 to the MAIT cell (figure 3.1A). Alternatively, the second agonist vaccine was also 5-A-RU (75 nmol in PBS) but contained a cathepsin-sensitive self-immolative linker attached to the amino group on 5-A-RU that allows for the Schiff formation with MR1 (structure provided in figure 2.1). This vaccine was termed pro-5-A-RU. The linker is only cleaved intracellularly once the vaccine has been taken up by APCs. This then allowing the release of 5-A-RU and formation of 5-OP-RU with endogenous sources of MG. The idea behind this vaccine is that lumazine formation will be limited as it is only once 5-A-RU is inside the cell can it start to form agonists for presentation via MR1 (figure 3.1B). Both the vaccines were administered intranasally (i.n.) in volumes of 30 μL to C57BL/6 mice. PBS was also given to a group of mice as a vehicle control. One day later the lung tissue and mediastinal lymph nodes (mLNs) were harvested, processed, stained with fluorescent antibodies and fixed for flow cytometry analysis the following day (figure 3.1C). To optimise the lung digestion protocol, both liberase TL and collagenase I enzymes were tested for cell yield. Liberase TL was used for all lung digestions due to having a higher cells of interest yield (Supplementary figure 1).

To determine which form of vaccination had stronger agonist effects on the MAIT cells, C57BL/6 mice were intranasally administered either PBS, 75 nmol 5-A-RU + 750 nmol MG (admix) or 75 nmol pro-5-A-RU. One day following vaccination, the lung tissue and mLNs were harvested and processed for flow cytometry analysis. The initial read out was whether the MAIT cells became activated in the primary lung tissue. After first gating on singlets, live cells and cells of interest, MAIT cells were identified as $B220^-$ $TCR\beta^+CD64^-$MR1-5-OP-RU $tetramer^+$ cells. The final MAIT cell gate was determined using both the MR1-6-FP control tetramer and a BV421 fluorescence minus one (FMO) (supplementary figure 2). Implementation of this gating strategy allowed for the identification of MAIT cells in the lung tissue following i.n. vaccination (figure 3.2A). The cells in the lung tissue were counted and showed an increase in total cell numbers after the admix vaccine but not the pro-5-A-RU (figure 3.2B), although, the number of MAIT cells did not change between the PBS control and both vaccines (figure 3.2C). After the

vaccine administration the MAIT cells were at a lower frequency (among TCRβ^+ cells) in the vaccine treated mice compared to the PBS, with the admix inducing a greater reduction compared to pro-5-A-RU (figure 3.2D). This reduction of the TCR is associated with MAIT cell activation, as these cells have an initial downregulation of their TCR when they become activated[236]. Of the MAIT cells that were able to be identified by the MR1-5-OP-RU tetramer, CD69 was used as an activation marker and showed an increased expression in only the admix treated group (figure 3.2D). However, the frequency of CD69$^+$ MAIT cells was increased in the pro-5-A-RU group (~30% of MAIT cells), but not to the same degree as the admix treated mice (~60% of MAIT cells) (figure 3.2A&F). Together this shows that the admix of 5-A-RU + MG when administered i.n. is more potent at activating lung MAIT cells than the pro-5-A-RU vaccine.

While the primary tissue is important to investigate as it is one of the first sites a vaccine comes in contact with, the activity in the draining lymph nodes is also an important measure of vaccine efficiency. The lymph node is where the innate system can interact with the conventional T cells and licence a T cell response and potentially a consequent B cell response through T_{FH} cells[105,136]. Hence, the mediastinal (mLN) or lung draining lymph node, was also harvested from the mice. Following the same gating strategy as the lung (B220$^-$TCRβ^+CD64$^-$MR1-5-OP-RU tetramer$^+$), MAIT cells could be identified in the mLN (figure 3.2G). There was no difference in the total cell number or MAIT cell numbers between the PBS control and the two MAIT cell agonist vaccines (figure 3.2H&I). There was also no change in the frequency of MAIT cells across the groups (figure 3.2J) but the 5-A-RU + MG admix, unlike the pro-5-A-RU vaccine, did induce MAIT cell activation, through the upregulation of CD69 in both median fluorescence intensity (MFI) and frequency of CD69$^+$ MAIT cells (figure 3.2G&K&L). Therefore, like in the lung tissue, the admix of 5-A-RU + MG was able to induce MAIT cell activation in the mLN, whereas the MAIT cells in the pro-5-A-RU treated mice remained at baseline levels.

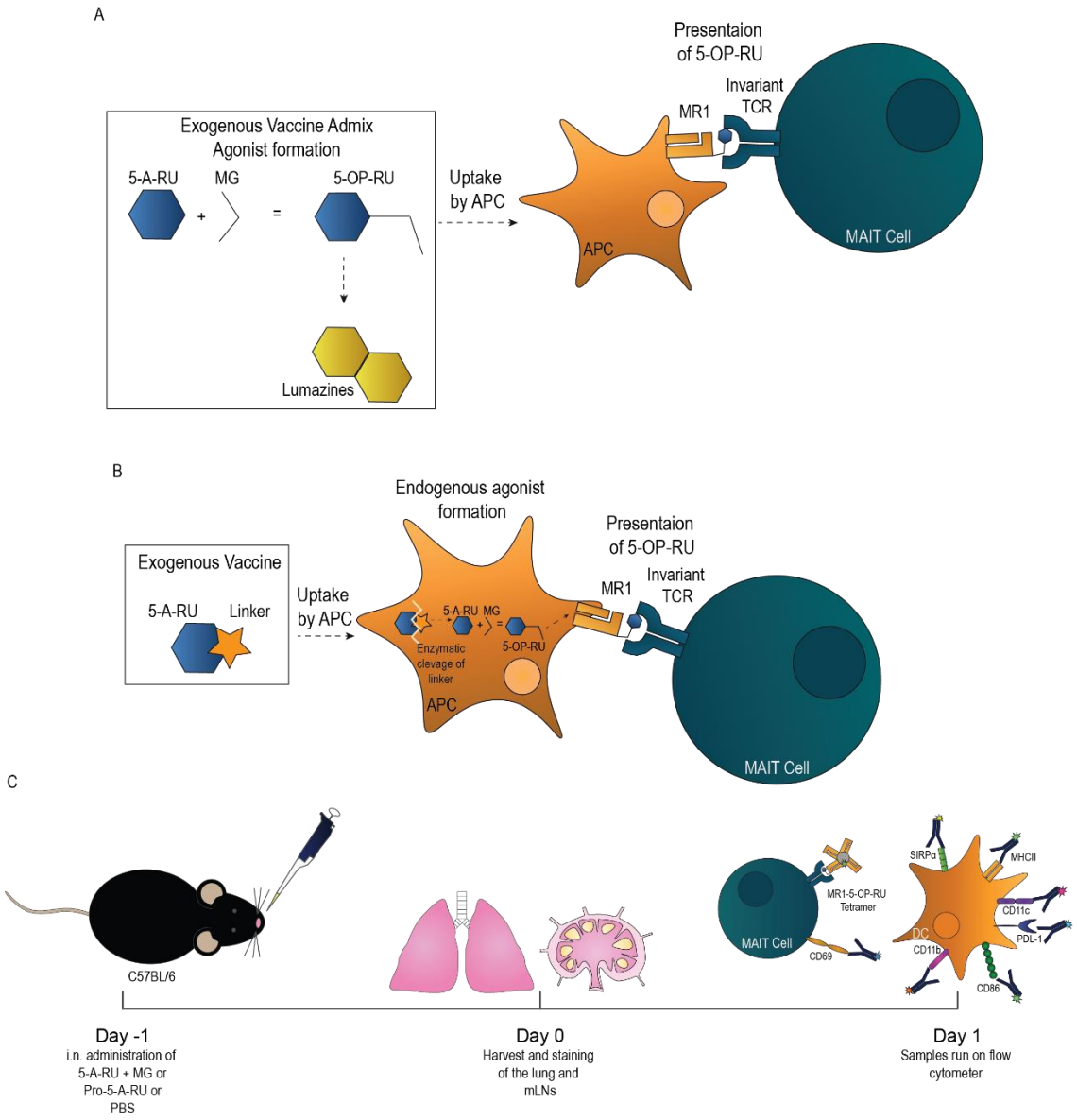

Figure 3.1: Schematic of Vaccine Mechanisms and Treatment. Mice were administered MAIT cell agonists intranasally either as an admix of 5-A-RU plus methylglyoxal (MG) or as pro-5-A-RU blocked by a self-immolative linker. **(A)** The admix vaccine combines 75 nmol 5-A-RU with 750 nmol MG in PBS, resulting in the exogenous formation of MAIT cell agonist 5-OP-RU. The 5-OP-RU can continue to form more stable lumazines with weaker agonist activity. Following intranasal delivery, the 5-OP-RU can be taken up by an antigen presenting cell (APC), stabilised by MR1 and trafficked to the cell surface for presentation to MAIT cells invariant T cell receptor (TCR). **(B)** The alternative pro-5-A-RU (75 nmol) vaccine contains 5-A-RU attached to a cleavable linker. This linker blocks exogenous lumazine formation. Only once the pro-5-A-RU has been taken up by an APC can the linker be cleaved endogenously by cathepsin, allowing for 5-A-RU to form 5-OP-RU with endogenous MG and be presented via MR1 to the MAIT cell invariant TCR. **(C)** Vaccine scheme involving intranasal administration of the vaccine, followed by harvesting of the lung tissue and mediastinal lymph nodes (mLN) 24 hrs later. The tissue samples are then processed into single cell suspensions and stained and fixed for flow cytometry analysis the next day.

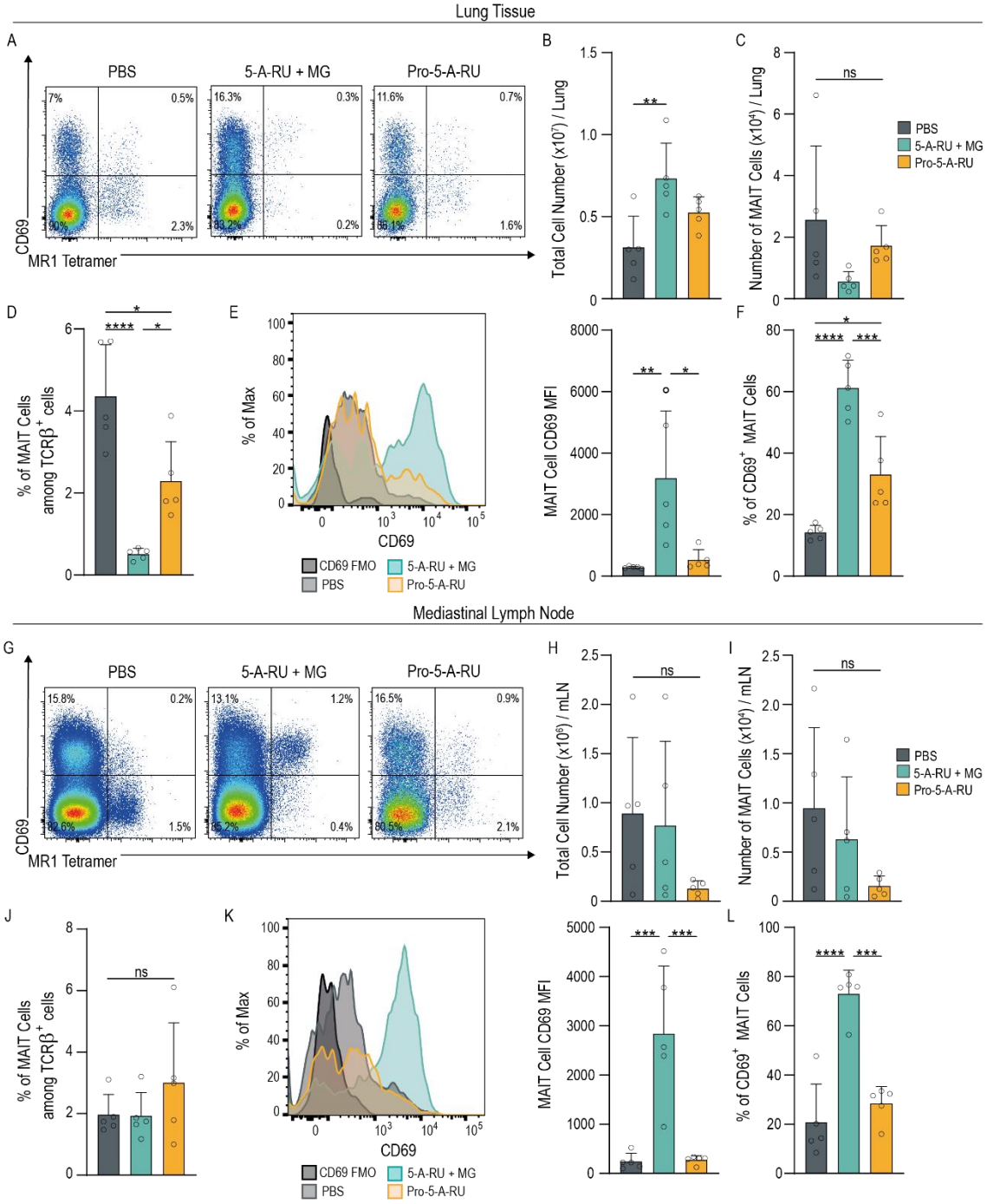
Lung Tissue
A
PBS
5-A-RU + MG
Pro-5-A-RU
CD69
MR1 Tetramer
B
Total Cell Number (x10⁷) / Lung
C
Number of MAIT Cells (x10⁴) / Lung
ns
PBS
5-A-RU + MG
Pro-5-A-RU
D
% of MAIT Cells among TCRβ⁺ cells
E
% of Max
CD69
CD69 FMO
PBS
5-A-RU + MG
Pro-5-A-RU
MAIT Cell CD69 MFI
F
% of CD69⁺ MAIT Cells
Mediastinal Lymph Node
G
H
Total Cell Number (x10⁶) / mLN
I
Number of MAIT Cells (x10⁴) / mLN
J
K
L

Figure 3.2: Intranasal Administration of Admix 5-A-RU plus MG Induces Superior MAIT Cell Activation in the Lung and mLN Compared to the Pro-5-A-RU Vaccine. C57BL/6 mice were administered either PBS (negative control), an admix of 5-A-RU (75 nmol) plus MG (750 nmol) or pro-5-A-RU (75 nmol) intransally. 24 hrs later the mLN and purfused lungs were harvested and processed for analysis by flow cytometry. **(A)** Representative flow plots of the lung showing identification of MAIT cells through the MR1-5-OP-RU tetramer and their activation through CD69. Cell were previously gated as $B220^{-}CD64^{-}TCR\beta^{+}$ cells. **(B)** Total number of cells per lung. **(C)** Number of MAIT cells per lung. **(D)** Frequency of MAIT cells among $TCR\beta^{+}$ cells per lung. **(E)** Representaive histograms normalised to the mode for MAIT cell CD69 expression, including CD69 fluorescence minus one (FMO) and MAIT cell CD69 median fluorescence intensity (MFI) in the lung. **(F)** Frequency of $CD69^{+}$ MAIT cells in the lung. **(G)** Representative MAIT cell flow plots in the mLN. **(H)** Number of total cells per mLN. **(I)** Number of MAIT cells per mLN. **(J)** Frequency of MAIT cells among $TCR\beta^{+}$ cells per mLN. **(K)** Representaive histograms normalised to the mode for MAIT cell CD69 expression and MAIT cell CD69 median fluorescence intensity (MFI) in the mLN.**(L)** Frequency of activated $CD69^{+}$ MAIT cells per mLN. Statistcial analysis was conducted using One-way ANOVA with Tukey's post hoc test. Bars represent the mean per group, symbols each induvidual mouse and error bars the standard deviation. ns>0.05, *p≤0.05, **p≤0.01, ***p≤0.001, ****p≤0.0001.

While MAIT cells are the primary target for the agonists, the DCs within the system are a vital component to determine whether the MAIT cell agonists can be used to drive an adjuvant system in the mucosa. DCs are the vital link between the innate and adaptive response and drive the presentation of vaccine antigen to produce an adaptive response and induction of immunological memory[105]. Therefore, I next wanted to determine whether conventional DCs became activated in the lung mucosa following i.n. vaccination with 5-A-RU + MG admix and pro-5-A-RU. C57BL/6 mice were treated i.n. with the vaccines alongside PBS as a control and the lung and mLN was harvested one day later for flow cytometry analysis. As illustrated in the gating strategy (figure 3.3A), conventional DCs (cDCs) were identified as $B220^{-}TCR\beta^{-}CD64^{-}MHCII^{+}CD11c^{+}$ cells. cDCs were further divided into cDC1s ($SIRP\alpha^{-}$) and cDC2s ($SIRP\alpha^{+}CD11b^{+}$) (figure 3.3A). The number of cDCs in the lung did not change between the different vaccinations (figure 3.3B). However, due to the adhesive nature of the lung tissue, counting of the cells was difficult and to avoid inaccuracy, only the cell frequencies in the lung tissue will be presented in the remainder of this thesis. The frequency of cDCs (among $B220^{-}TCR\beta^{-}$ cells) did not change (figure 3.3C), but the frequency of the cDC1 population among cDCs reduced in both the 5-A-RU + MG and pro-5-A-RU treated groups whereas the cDC2 frequency increased in these groups (figure 3.3D). To determine whether the cDCs became activated, CD86 and PDL-1 were used as markers. While the cDC1 CD86 MFI was similar to baseline levels across the groups, the cDC2 CD86 MFI was significantly elevated following both the 5-A-RU + MG and pro-5-A-RU vaccinations, with the highest expression in the 5-A-RU + MG admix group (figure 3.3E). PDL-1 MFI showed the same pattern in both cDC1s and cDC2s, with a significant increase only seen in the 5-A-RU + MG treated mice (figure 3.3F). While there may be a small increase in CD86 MFI in cDC2s after the pro-5-A-RU vaccine, the admix 5-A-RU + MG vaccine is able to induce a more potent cDC activation in the lung.

Since the lymph node represents the location where the DCs interact with the adaptive immune response, cDCs isolated from the mLN were also assessed. In the mLN, cDCs can be divided into resident DCs that reside within the mLN and migratory DCs that

enter the mLN from peripheral sites[125]. These populations can be divided by their MHCII expression with migratory DCs having high MHCII expression and resident DCs intermediate expression[252]. These DC populations could be further divided into cDC1s and cDC2s based on their SIRPα and CD11b expression (figure 3.4A). The number of resident cDC1s and cDC2s remained consistent between the PBS, 5-A-RU + MG and pro-5-A-RU groups (figure 3.4B). The resident cDC1s had a reduced CD86 MFI after pro-5-A-RU treatment and the resident cDC2s had no change from PBS (figure 3.4C). However, the resident cDC1s did have an elevated PDL-1 MFI in the 5-A-RU + MG group compared to PBS and pro-5-A-RU but no change in the cDC2s (figure 3.4D). The migratory cDC1s and cDC2 numbers also did not change (figure 3.4E) but both cDC1s and cDC2s had significantly higher CD86 and PDL-1 MFI's only in the 5-A-RU + MG i.n. vaccine treated mice (figures 3.4F&G). In summary, while the pro-5-A-RU does not induce adjuvant activity, the 5-A-RU + MG vaccine modestly activated resident cDCs and induced a strong activation of the migratory cDCs.

Together this data suggests that the pro-5-A-RU i.n. vaccine was unable to induce significant adjuvant activity. In contrast, the admix of 5-A-RU and MG was able to induce activation of both MAIT cells and cDCs in the lung and mLN. Therefore, the 5-A-RU + MG admix was used in all subsequent experiments. Additionally, analysis of DC activation and phenotype was commonly assessed 24 hours following vaccination as both MAIT cell (figure 3.2E&K) and cDC activation (supplementary figure 3) could be detected at this timepoint.

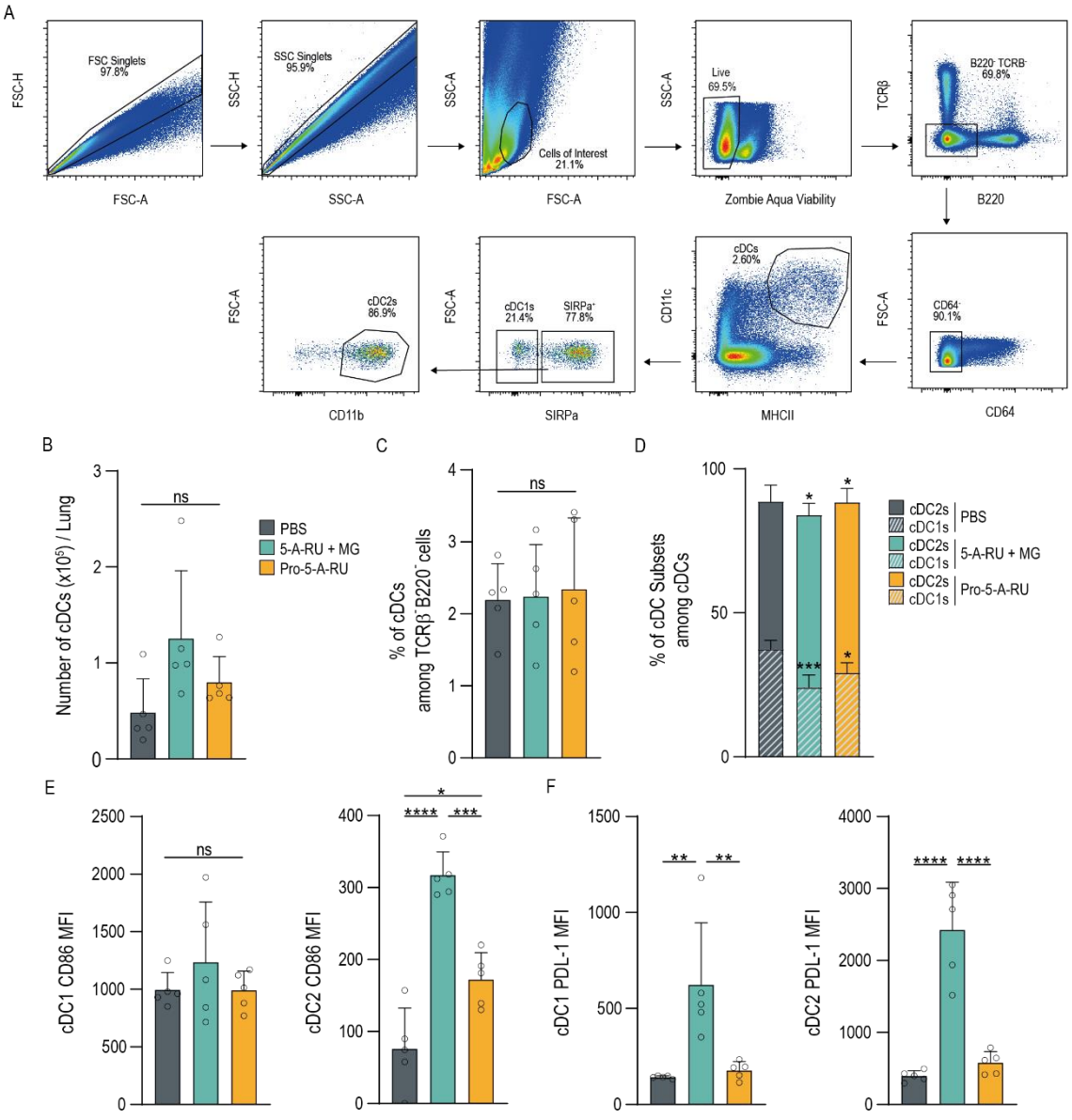

Figure 3.3: Vaccine Admix Preferentially Activates Conventional Dendritic Cells in the Lung Compared to Pro-5-A-RU. C57BL/6 mice were administered either PBS (negative control), an admix of 5-A-RU (75 nmol) plus MG (750 nmol) or pro-5-A-RU (75 nmol) intransally. 24 hrs later the mLN and purfused lungs were harvested and processed for analysis by flow cytometry. **(A)** Representative gating strategy for cDC1s and cDC2s. Cells of interest gate was defined by backgating on TCRβ+ cells. **(B)** Number of cDC per lung. **(C)** Frequency of cDCs among TCRβ-B220- cells per lung. **(D)** Frequency of cDC1s and cDC2s for each treatment group. **(E)** Median fluorescence intensity (MFI) of activation marker CD86 on cDC1s and cDC2s. **(F)** MF) of activation marker PDL-1 on cDC1s and cDC2s. Statistcial analysis was conducted using One-way ANOVA with Tukey's post hoc test or a Two-way ANOVA (D). Bars represent the mean per group, symbols each induvidual mouse and error bars the standard deviation. ns>0.05, *p≤0.05, **p≤0.01, ***p≤0.001, ****p≤0.0001. Significance stars in D, show significance between 5-A-RU + MG vs PBS and Pro-5-A-RU vs PBS for each cDC subset.

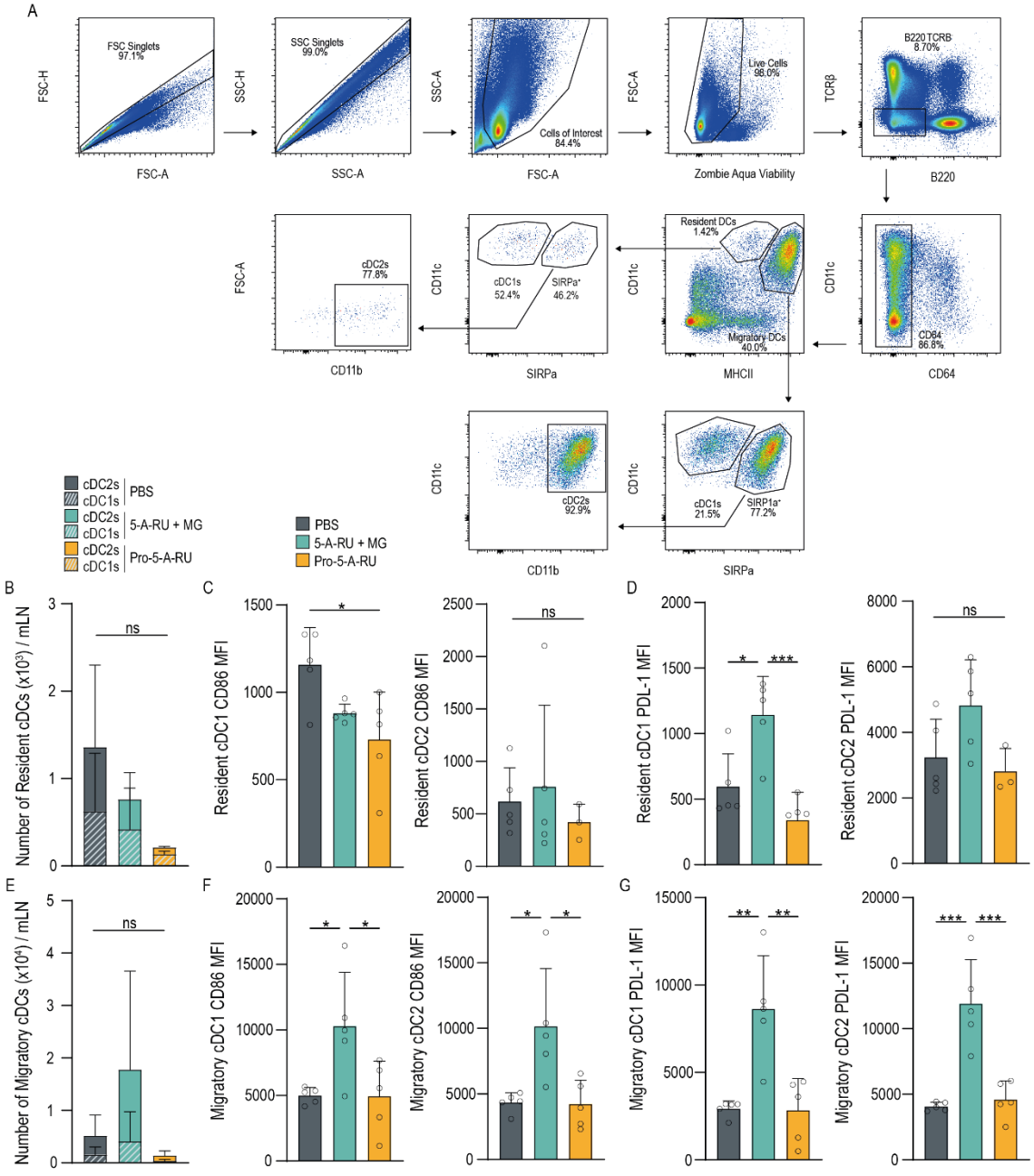

Figure 3.4: Vaccine Admix Preferentially Activates Migratory Dendritic Cells in the mLN Compared to Pro-5-A-RU. C57BL/6 mice were administered either PBS (negative control), an admix of 5-A-RU (75 nmol) plus MG (750 nmol) or pro-5-A-RU (75 nmol) intransally. 24 hrs later the mLN and purfused lungs were harvested and processed for analysis by flow cytometry. **(A)** Representive gating strategy to identify migratory cDC1s and cDC2s and resident cDC1s and cDC2s. **(B)** Number of resident cDC subsets per mLN. **(C)** Resident median fluorecence intensity (MFI) of CD86 on cDC1s and cDC2s. **(D)** PDL-1 MFI of resident cDC1s and cDC2s. **(E)** Number of migratory cDC subsets per mLN. **(F)** CD86 MFI of migratory cDC1s and cDC2s. **(G)** PDL-1 MFI of migratory cDC1s and cDC2s. Statistcial analysis was conducted using One-way ANOVA with Tukey's post hoc test or a Two-way ANOVA (B & E). Bars represent the mean per group, symbols each induvidual mouse and error bars the standard deviation. ns>0.05, *p≤0.05, **p≤0.01, ***p≤0.001.

I next wanted to determine the optimal dose of the i.n. 5-A-RU + MG admix vaccination, which was determined by the expression of activation markers on both MAIT cells and cDCs in the lung and mLN. C57BL/6 mice were treated i.n. with 5-A-RU + MG admix at either 5, 20, 75, 140 or 180 nmols together with MG at x10 the 5-A-RU concentration (50, 200, 750, 1,400 and 1,800 nmols respectively). Mice were immunised one day prior to the harvest of the lung and mLN for flow cytometry analysis. In the lung tissue there was a trend towards a reduction in MAIT cell frequencies with all doses, however, only the 20 nmol dose showed significance (figure 3.5A). There was also an increase in CD69 expression and MFI following the admix treatments, however, significance was only seen in the 180 nmol dose compared to PBS (figure 3.5B). In the lung, 5-A-RU + MG admix vaccination resulted in increased levels of CD86 and PDL-1 by all cDC subsets at all doses tested, however, significance was mostly achieved with the 75 nmol dose, the point where the response also plateaued (figure 3.5C). In the mLN there was no change in MAIT cell numbers or frequencies among TCRβ^+ cells between the PBS control and the admix treated mice (figure 3.5D&E). However, there was a dose response curve for CD69 expression on the MAIT cells, with a plateau around 75 nmols (figure 3.5F&G). As resident cDCs expressed a similar phenotype in both PBS and 5-A-RU + MG admix groups, only migratory cDC CD86 and PDL-1 MFI is shown. The migratory cDC CD86 MFI trended towards a dose response with 180 nmol being significantly higher in MFI than PBS for all cDC subsets. Additionally, PDL-1 MFI on migratory cDCs showed a significant dose response curve for all cDC subsets (figure 3.5H). Based on these results 75 nmol 5-A-RU admixed with 750 nmol MG was chosen as the optimal dose for the following experiments. Furthermore, the higher doses of 140 and 180 nmols are more viscous making i.n. administration more difficult.

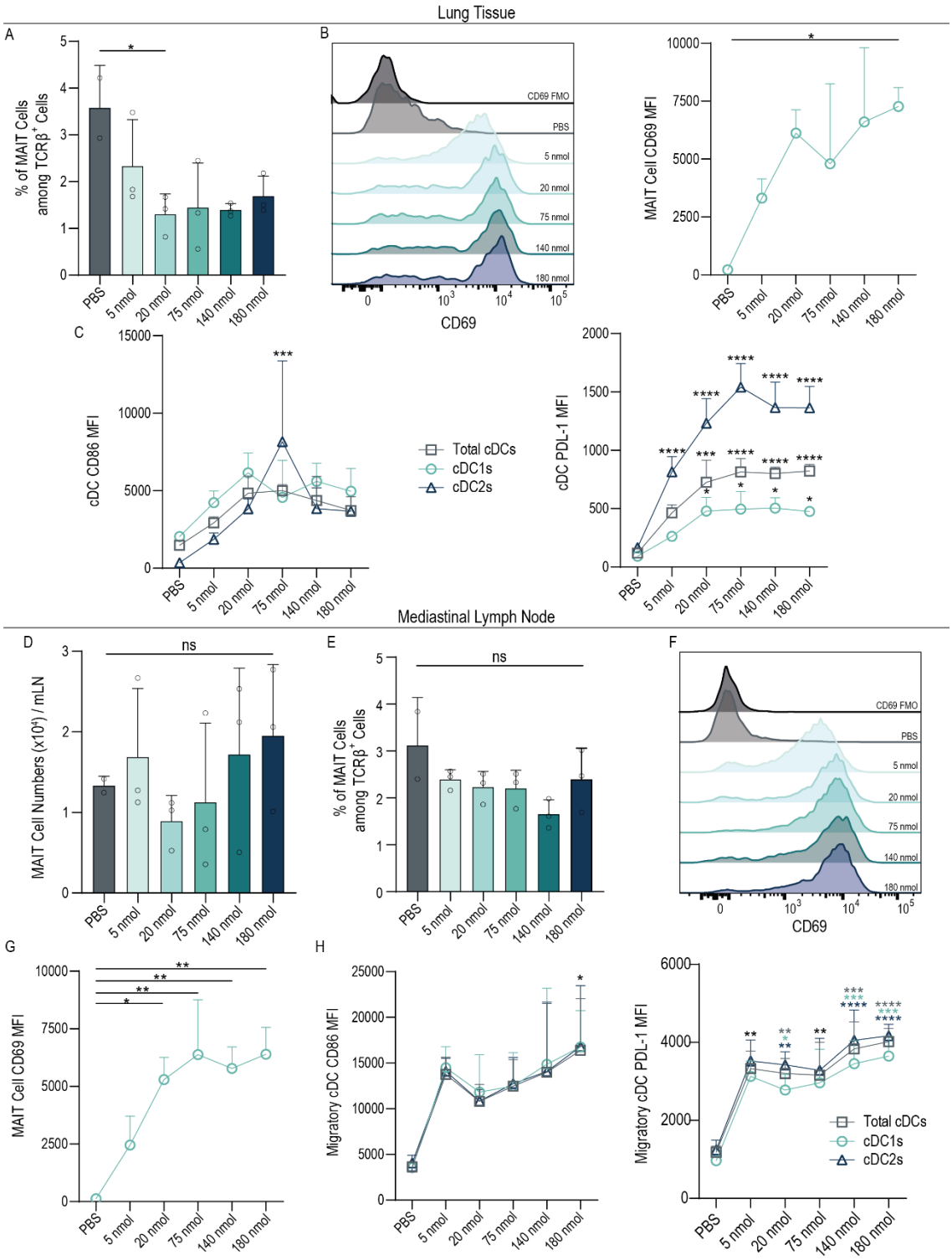
Lung Tissue
A
% of MAIT Cells among TCRβ+ Cells
B
CD69 FMO
PBS
5 nmol
20 nmol
75 nmol
140 nmol
180 nmol
CD69
MAIT Cell CD69 MFI
C
cDC CD86 MFI
Total cDCs
cDC1s
cDC2s
cDC PDL-1 MFI
PBS
5 nmol
20 nmol
75 nmol
140 nmol
180 nmol
Mediastinal Lymph Node
D
MAIT Cell Numbers (x10⁴) / mLN
ns
E
% of MAIT Cells among TCRβ+ Cells
F
G
MAIT Cell CD69 MFI
H
Migratory cDC CD86 MFI
Migratory cDC PDL-1 MFI

Figure 3.5: MAIT Cell and Dendritic Cell Activation Follow a Dose Response Curve After Intranasal Administration of the Admix Vaccine. C57BL/6 mice were administered increasing concentrations of 5-A-RU plus MG admix intransally and 1 day later the lung tissue and mLN were harvested and processed for flow cytometry analysis. **(A)** Frequency of MAIT cells among TCRβ^+ cells in the lung. **(B)** Representative MAIT cell CD69 histograms normalised to mode and median fluorcence intensity (MFI). **(C)** Lung cDC CD86 and PDL-1 MFI. **(D)** Number of total cells per mLN. **(E)** Frequency of MAIT cells among TCRβ^+ cells in the mLN. **(F)** Representative MAIT cell CD69 histograms normalised to mode with the CD69 FMO negative control in mLN. **(G)** MAIT cell CD69 MFI in the mLN. **(H)** Migratory cDCs and subsets CD86 and PDL-1 MFI in the mLN. Statistcial analysis was conducted using One-way ANOVA with Tukey's post hoc test or a Two-way ANOVA (C & H). Bars represent group means with symbols as individual mice, whereas, line graph symbols represent the group mean. Error bars show the standard deviation. ns>0.05, *p≤0.05, **p≤0.01, ***p≤0.001, ****p≤0.0001. Significance stars on cDC subset MFI graphs represent significance of each dose to PBS with in the subset. Black stars show significance between all DC groups and PBS. Whereas the coloured stars correspond to the specific cDC group and PBS. This experiment was repeated 3 independent times with similar results.

3.3.2 Activation of Conventional mLN Dendritic Cells is Dependent on the MR1 Pathway

To ensure the 5-A-RU + MG vaccine was functioning through the MAIT cells and was not working through untargeted effects to activate the cDCs, $MR1^{-/-}$ mice were utilised. These mice lack MR1 and therefore cannot develop MAIT cells[242]. $MR1^{-/-}$ mice along with C57BL/6 WT mice, were treated i.n. with either PBS or 5-A-RU + MG admix and 1 day later, mLNs were harvested and used for flow cytometry analysis. To ensure the $MR1^{-/-}$ mice lacked MAIT cells, the $B220^{-}TCR\beta^{+}CD64^{-}$MR1-5-OP-RU tetramer^{+} gating strategy was used. As expected, MAIT cells were not detected in the $MR1^{-/-}$ mice (figures 3.6A-C). To validate the C57BL/6 MAIT cells were activated as seen in the previous experiments, CD69 expression was analysed and showed increased CD69 MFI following admix vaccination compared to PBS (figure 3.6D). Next, the cDC activation was investigated to determine whether it was dependent on MAIT cells. Both the total number of cells and number of migratory cDCs per mLN did not change between C57BL/6 and $MR1^{-/-}$ mice (figure 3.6E), however, migratory cDC1s and cDC2s only showed elevated CD86 and PDL-1 MFI in the C57BL/6 admix treated group (figures 3.6F&G). This shows that the activation of cDCs in my model is dependent on MAIT cells. Furthermore, I showed that 5-A-RU + MG stimulates the MAIT cells through the TCR pathway. To do this, $Nur77^{GFP}$ (nuclear receptor 77-green fluorescent protein) mice which express GFP in response to TCR stimulation (in a dose dependent manner)[243], were either treated with the 5-A-RU + MG admix or PBS alongside a C57BL/6 admix treated group. Conformation of the GFP fluorescence on MAIT cells was determined using C57BL/6 admix treated mice, which do not have GFP expression and were used as FMOs to set gates for the Nur77^{+} cells (figure 3.6H). One day after treatment Nur77 expression and MFI was increased in only the $Nur77^{GFP}$ admix treated mice and not the $Nur77^{GFP}$ PBS treated or C57BL/6 admix control groups (figures 3.6H&I). Additionally, the majority of MAIT cells (between 65%-95%) in the $Nur77^{GFP}$ admix treated group were positive for GFP expression, compared to the 0-3% in the control groups (figure 3.6J). Taken together, this suggests MAIT cells are being presented the agonist through the MR1-TCR interaction to become activated.

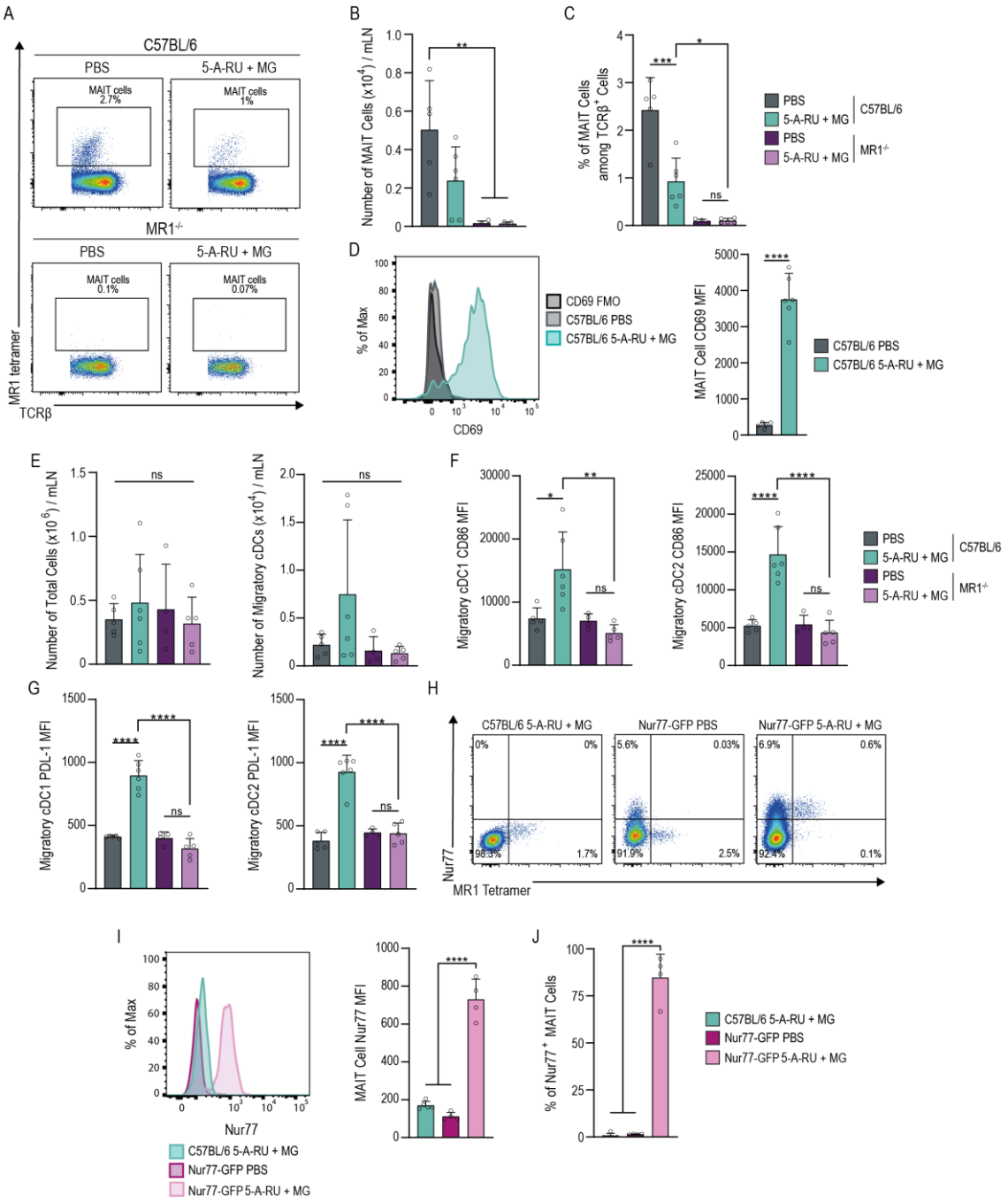
A
C57BL/6
PBS
5-A-RU + MG
MAIT cells 2.7%
MAIT cells 1%
MR1-/-
PBS
5-A-RU + MG
MAIT cells 0.1%
MAIT cells 0.07%
MR1 tetramer
TCRβ
B
Number of MAIT Cells (x10^4) / mLN
C
% of MAIT Cells among TCRβ+ Cells
PBS
5-A-RU + MG
C57BL/6
PBS
5-A-RU + MG
MR1-/-
D
% of Max
CD69
CD69 FMO
C57BL/6 PBS
C57BL/6 5-A-RU + MG
MAIT Cell CD69 MFI
C57BL/6 PBS
C57BL/6 5-A-RU + MG
E
Number of Total Cells (x10^6) / mLN
Number of Migratory cDCs (x10^4) / mLN
F
Migratory cDC1 CD86 MFI
Migratory cDC2 CD86 MFI
PBS
5-A-RU + MG
C57BL/6
PBS
5-A-RU + MG
MR1-/-
G
Migratory cDC1 PDL-1 MFI
Migratory cDC2 PDL-1 MFI
H
C57BL/6 5-A-RU + MG
Nur77-GFP PBS
Nur77-GFP 5-A-RU + MG
0%
0%
5.6%
0.03%
6.9%
0.6%
98.3%
1.7%
91.9%
2.5%
92.4%
0.1%
Nur77
MR1 Tetramer
I
% of Max
Nur77
C57BL/6 5-A-RU + MG
Nur77-GFP PBS
Nur77-GFP 5-A-RU + MG
MAIT Cell Nur77 MFI
J
% of Nur77+ MAIT Cells
C57BL/6 5-A-RU + MG
Nur77-GFP PBS
Nur77-GFP 5-A-RU + MG

Figure 3.6: Activation of Dendritic Cells is dependent on MR1 Presentation. C57BL/6 and MR1$^{-/-}$ mice were administered 5-A-RU plus MG and PBS intransally and the mLN harvested 24 hrs later. Single cell suspensions were prepared and cell surface antibody staining and fixing was completed for flow cytometry analysis the following day. **(A)** Representative MAIT cell gating (B220^{-}CD64^{-}TCRβ^{+}MR1-5-OP-RU tetramer^{+}) highlighting the loss of MAIT cells in MR1$^{-/-}$ mice. **(B&C)** Number and frequency of MAIT cells lost in the MR1$^{-/-}$ mice. **(D)** Representative MAIT cell CD69 histograms normalised to mode with the CD69 fluorecence minus one (FMO) was a negative control and CD69 median fluorcence intensity (MFI). **(E)** Number of total cells and migratory cDCs per mLN. **(F)** CD86 MFI of migratory cDC1s and cDC2s. **(G)** PDL-1 MFI of migratory cDC1s and cDC2s. **(H)** Nur77-GFP mice were treated intransally with either PBS or 5-A-RU plus MG admix, along with a admix treated C57BL/6 control group. 24 hrs later the mLN were harvested and prepared for flow cytometry analysis. Representative flow plots showing Nur77-GFP expression on MAIT cells, with the C57BL/6 plot being used as an FMO. **(I)** Representative histogram of MAIT cell Nur77 expression, normalised to mode, and Nur77 MFI. **(J)** Frequency of Nur77^{+} MAIT cells. Statistcial analysis was conducted using One-way ANOVA with Tukey's post hoc test or an unpaired T test (D). Bars represent the mean per group, symbols each induvidual mouse and error bars the standard deviation. ns>0.05, *p≤0.05, **p≤0.01, ***p≤0.001, ****p≤0.0001.

3.3.3 MAIT Cells Show a Dominant RORγT and GATA3 Phenotype in the Lung and mLN

In order to gain insight into the mechanisms that MAIT cells use to promote DC activation, I explored the kinetics of the MAIT cells in the lung and mLN and their transcription factor phenotype. C57BL/6 mice were treated i.n. with one dose of 5-A-RU + MG across a 7 day time period. Mice were either left as naïve, or treated with admix on either day -1, -3, -5 or -7 prior to harvesting of the mLN and lung tissue on day 0 as shown in figure 3.7A. The frequency of MAIT cells and MR1-5-OP-RU tetramer staining peaked at day 3 in the lung (figures 3.7B&C). MAIT cell CD69 MFI rapidly increased at day 1 then was back down to baseline levels by day 3 (figure 3.7D), whereas, the PD-1 MFI was also increase at day 1 but remained up at day 3 before gradually reducing (figure 3.7E). Ki67 was included as a marker of proliferation, both the frequency of $Ki67^+$ MAIT cells and Ki67 MFI peaked at day 3 in the lung (figure 3.7F&G). In the mLN, the number and frequency (among $TCR\beta^+$) of MAIT cells remained constant over time. The MAIT cell MR1-5-OP-RU, CD69, PD-1 and Ki67 frequency and MFIs showed the same trend as in the lung, with the peak MFIs at day 3 (figure 3.7J-N).

Cells were also stained for common T cell transcription factors, Tbet, RORγT and GATA3. Literature has shown that MAIT cells in the lungs of C57BL/6 mice express Tbet and RORγT with a high proportion of double positives, this suggesting a mixed T_H1 and T_H17-like phenotype[222]. The transcription factor (TF) expression is shown from mice treated with the admix at day 3, as this was the peak timing for the frequency, activation and proliferation of the MAIT cells. Conventional T cells (gated as $B220^-TCR\beta^+$MR1-5-OP-RU $tetramer^-$) were included in the analysis as a control as they were expected to have low levels of the effector TFs due to the short timing and lack of protein antigen in the vaccine. The PD-1 expression showed a trend towards increasing expression in only the MAIT cells of admix treated mice in both the lung and mLN. There was also a small proportion of PD-1 expression in the naïve MAIT cells but was insignificant compared to the admix group. There was a high expression of RORγT only in the MAIT cells (both in naïve and treated states) but not the conventional T cells. GATA3 expression was low in

the conventional T cells, however, there was a slight increase in expression in MAIT cells of the lung and mLN. Tbet did not have high expression in either the conventional T cells or the MAIT cells in the lung or mLN (figure 3.8A). The TF expression of MAIT cells was also presented as frequencies. The majority of MAIT cells in the lung at naïve state, were dual producers of GATA3 and RORγT. After treatment, there was a shift towards a greater single positive RORγT expression in the lung. In the mLN, the majority of the MAIT cells were dual producers of GATA3 and RORγT in both naïve and treated mice, however, there was a shift towards an increase frequency of GATA3 single positives and triple negatives following admix treatment. In both the lung and mLN and naïve versus admix treated mice there was very minimal MAIT cells expressing Tbet (figure 3.8B). This data suggests that treatment with 5-A-RU + MG admix promotes the maintenance and development GATA3 and RORγT positive MAIT cell populations.

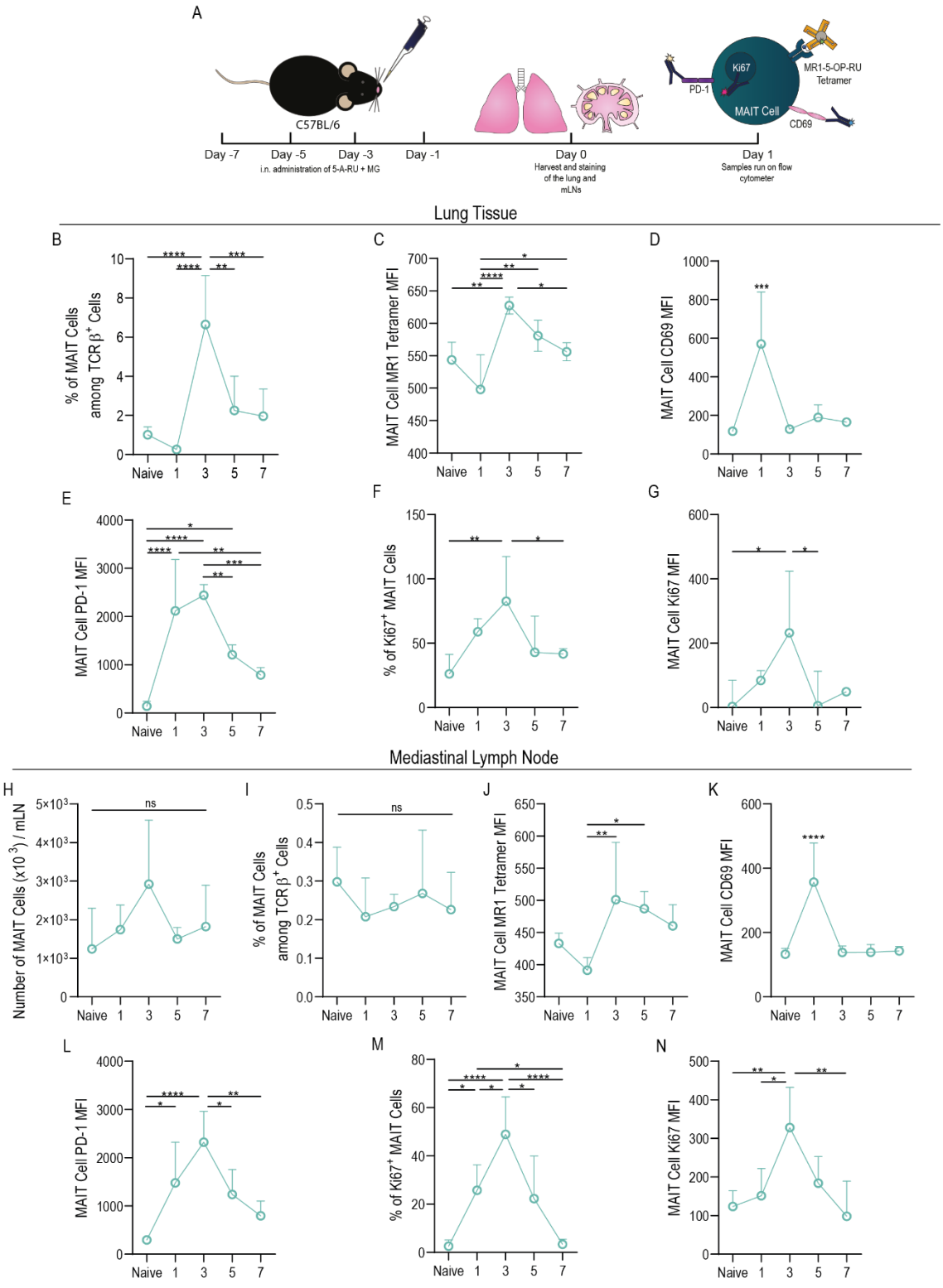
A
C57BL/6
Day -7
Day -5
i.n. administration of 5-A-RU + MG
Day -3
Day -1
Day 0
Harvest and staining of the lung and mLNs
Day 1
Samples run on flow cytometer
Ki67
PD-1
MR1-5-OP-RU Tetramer
MAIT Cell
CD69
Lung Tissue
B
% of MAIT Cells among TCRβ+ Cells
C
MAIT Cell MR1 Tetramer MFI
D
MAIT Cell CD69 MFI
E
MAIT Cell PD-1 MFI
F
% of Ki67+ MAIT Cells
G
MAIT Cell Ki67 MFI
Mediastinal Lymph Node
H
Number of MAIT Cells (x10^3) / mLN
I
% of MAIT Cells among TCRβ+ Cells
J
MAIT Cell MR1 Tetramer MFI
K
MAIT Cell CD69 MFI
L
MAIT Cell PD-1 MFI
M
% of Ki67+ MAIT Cells
N
MAIT Cell Ki67 MFI
Naive 1 3 5 7
ns

Figure 3.7: MAIT Cell Kinetics Following Intranasal 5-A-RU plus MG Administration. C57BL/6 mice were given intransal administration of one dose of 5-A-RU plus MG admix either 1, 3, 5 or 7 days prior to the lung and mLN harvest. Naïve mice were also included for baseline levels. Flow cytometry was used to analyse the MAIT cell phenotype. **(A)** Treatment scheme. **(B)** Frequency of MAIT cells among TCRβ^+ cells in the lung. **(C-E)** MAIT cell median fluorescence intensity (MFI) of MR1-5-OP-RU tetramer, CD69 and PD-1 in the lung. **(F&G)** Frequency and MFI of MAIT cell Ki67 expression in the lung. **(H)** Number of MAIT cells per mLN. **(I)** Frequency of MAIT cells among TCRβ^+ cells in the mLN. **(J-L)** MAIT cell MFI of MR1-5-OP-RU tetramer, CD69 and PD-1 in the mLN. **(M&N)** Frequency and MFI of MAIT cell Ki67 expression in the mLN. Statistcial analysis was conducted using One-way ANOVA with Tukey's post hoc test. Symbols represent the group mean and Error bars show the standard deviation. ns>0.05, *p≤0.05, **p≤0.01, ***p≤0.001, ****p≤0.0001.

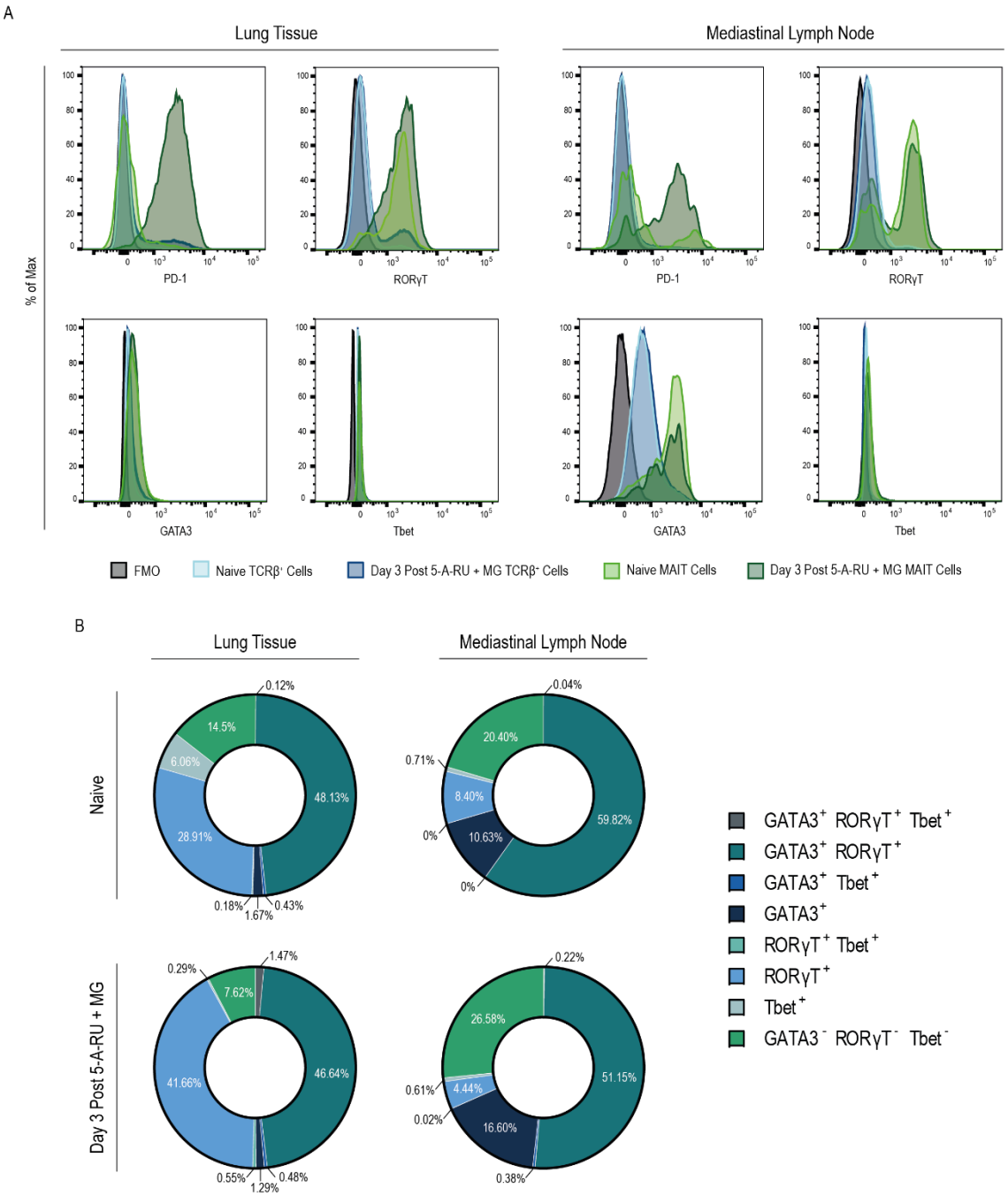

Figure 3.8: MAIT Cells in the Lung and mLN show a GATA3 and/or RORγT Phenotype Both Prior and After Intranasal Administration of 5-A-RU plus MG Admix. C57BL/6 mice were intranasally administered 5-A-RU plus MG admix or left as naive and the lung tissue and mLN were harvested at day 3 post administration when MAIT cells are at their peak. Single cell suspension of the lung and mLN were stained and fixed for flow cytometry analysis the following day. **(A)** Represenative histograms of MAIT cell and non-MAIT TCRβ+ cell PD-1, RORγT, GATA3 and Tbet expression in the lung and mLN. Histograms were normalised to the mode and an FMO included as a negative control for each maker. **(B)** MAIT cell transcription factor expression of naïve and day 3 admix treated mice in the lung and mLN. Expression was determined using boolean gating.

3.4 Discussion

The identification of non-conventional TCR α-chains that are conserved among humans, was first published in 1993. This paper described two different TCR α-chains found on $CD4^-CD8^-$ T cells, one being Vα24Jα19 and the other Vα7.2Jα33[280], which we now consider to be the invariant TCRs characteristic of NKT and MAIT cells respectively. However, it took until 1999 for the mouse ortholog (Vα19Jα33) of these Vα7.2Jα33 cells to be described, alongside both the human and mouse paired TCR β-chains (Vβ6 or 8 in mice, and Vβ2 or 13 in humans)[278]. These cells were then termed 'mucosal-associated invariant T cells' by Treiner, E. *et al.* (2003), after their preferential location at mucosal tissues and their dependence on MR1 presentation[242]. While MAIT cells are found in high abundance in humans, up to 10% of peripheral blood T cells[198,281], their frequency in mice is much lower, <0.1% of blood αβ-T cells in C57BL/6 mice[222]. However, despite the low frequency in mice, detection of MAIT cells can still be carried out using the MR1-5-OP-RU tetramer[204], with the lung tissue having one of the highest frequencies of MAIT cells among $TCR\beta^+$ lymphocytes[204,222] in C57BL/6 mice. In this chapter I showed that MAIT cells can be detected in the lungs and mLNs at both steady state and after i.n. administration of MAIT cell agonists in C57BL/6 mice. The Frequency of lung MAIT cells at steady state was equivalent to the frequencies seen in Rahimpour, A. *et al.* (2015)[204].

An interesting finding presented in the literature suggests that MAIT cell accumulation in vivo via 5-OP-RU also requires an additional co-stimulator signal. Chen, Z. *et al.* (2017), inoculated mice i.n. with either the TLR ligand, dipalmitoyl-S-glyceryl cysteine (Pam2Cys), followed by 4 doses of 5-OP-RU across 4 days or with 6 doses of 5-OP-RU only across 5 consecutive days. The 5-OP-RU only treated mice had baseline levels of MAIT cells in the lung, whereas the mice that were also given Pam2Cys had a significant accumulation of MAIT cells (~50% αβ-T cells) in the lung. Despite there being no accumulation of MAIT cells after 5-OP-RU only treatment, the MAIT cells still had an elevated CD69 MFI compared to naïve, however, the addition of Pam2Cys did further elevate the MFI[222]. My data shows consistency with this, with the CD69 MFI on lung

MAIT cells being significantly elevated after the i.n. administration of 5-A-RU + MG admix. However, I observed an accumulation of MAIT cells in the lung, peaking at day 3, and rapidly declining to almost baseline by day 7. The discrepancies between the two studies could be due to the rapid kinetics of the response. Alternatively, MAIT cell accumulation observed in my model could be due to the high dose of 75 nmol 5-A-RU + 750 nmol MG compared to the comparatively lower 15.2-0.76 μmol dose of 5-OP-RU in Chen, Z. *et al.* (2017).

The downregulation of the MAIT cell TCR was only seen in the lung tissue and not the mLN following i.n. administration of 5-A-RU + MG. This may reflect the dispersal of the agonist at the mucosal site. It may result in strong doses in the lung tissue with little passive dissemination to the mLN. This is seen in Lee, H. *et al.* (2009), where herpes simplex virus-1 (HSV-1) when administered via a mucosal route has low levels of lymph node resident DC presentation due to low lymph node dissemination, whereas, when administered cutaneous there is movement into the lymph node and presentation via resident DCs[282]. As I detected activation of the MAIT cells in the mLN, the agonist is likely reaching this site, however, this may be through migratory DCs trafficking to the mLN from the lung, which is supported by the detection of activated migratory DCs isolated from the mLN.

CD69 is used as a general marker of activation in lymphocytes and NK cells due to its rapid upregulation following stimulation of the cells. It is an early marker of activation with CD69 transcripts being detectable within an hour following activation, then declining rapidly in the hours following. The protein expression is also seen on the cell surface within hours of activation[283]. This is seen in the MAIT cell kinetics, with CD69 rapidly increasing at 24 hrs post i.n. treatment of agonist and returning to baseline levels by day 3. CD69 has also been used as a common marker for MAIT cell activation[209,222,284]. CD69 expression can be seen on MAIT cells both in vitro[209] at 16 hrs and in vivo at 16 hrs[284] and 2 hrs[222] after treatment with MAIT cell agonists. PD-1 expression on MAIT cells was more sustained, with a rapid increase at day 1 post i.n. administration of 5-A-

RU + MG, which remained elevated at day 2 before reducing by day 3 post vaccination. This may reflect the nature of PD-1 as an exhaustion marker. This sustained expression has been seen on $CD8^+$ T cells after infection with lymphocytic choriomeningitis virus (LCMV). The CD8 cells rapidly upregulated PD-1, with high frequencies of $PD\text{-}1^+$ LCMV specific $CD8^+$ T cells at day 1 post infection which was sustained at day 2 and 3 post infection[285].

MR1 is highly conserved[207] and is ubiquitously expressed at low levels by a wide range of cells[208]. This makes it difficult to determine what cells are capable of interacting with MAIT cells and inducing activation via the MR1 pathway. Wang, H. *et al.* (2019), was able to show that both bone marrow and non-bone marrow derived cells were capable of activating MAIT cells in vivo through MR1. However, the cell type required for this activation was dependent on the type of bacterial infection[209]. This indicates that a wide range of cell types could be responsible at activating MAIT cells and makes it difficult to narrow it down to specific cell types. Investigation into DC interactions with MAIT cells, has shown that co-culturing MAIT cells with immature DCs, and the addition of 5-A-RU + MG, results in DC maturation with upregulation of CD86 and PDL-1[236]. This suggesting an interaction between MAIT cells and DCs in an in vitro setting. Additionally, MAIT cells in a pulmonary *F. tularensis* live vaccine strain infection have been shown to produce GM-CSF, allowing for the differentiation of inflammatory monocytes into monocyte-derived DCs and in turn the faster recruitment of $CD4^+$ T cells[286]. Although this does not prove direct interactions between the MAIT cell and DCs in vivo, it does highlight that these two cell populations are able to influence each other. In this thesis I show cDC activation following i.n. administration of 5-A-RU + MG in both the lung and mLN. This DC activation was abrogated in mice lacking MAIT cells, implying an interaction between the DCs and MAIT cells. Additionally, the MAIT cells had TCR stimulation after admix administration suggesting presentation of a MAIT cell agonist through the MR1-TCR interaction. Although, from this work, it is still not clear whether DCs are directly presenting the agonist to the MAIT cell.

DCs in the mLN were divided into migratory and resident DCs through the expression of MHCII and CD11c. Migratory DCs were gated as $CD11c^{+}MHCII^{hi}$, whereas, resident DCs were identified as $CD11c^{+}MHCII^{Int}$. This characterisation is based on gating strategies in the literature[261,287,288], where migratory DCs upregulate MHCII in the tissue in response to inflammation and maintain higher levels compared to the lymph node resident populations[126]. In addition to MHCII upregulation, mature migratory DCs will also upregulate co-stimulatory molecules[127] and chemokine receptor CCR7[129,130], to allow for migration to the draining lymph nodes. Whereas resident DCs display only intermediate levels of MHCII[252,261]. However, gating DCs solely on MHCII expression may not cleanly divide these populations as in an Influenza infection, resident DCs in the mLN have been shown to upregulate MHCII early during infection[289]. Thus, it is possible that the gating strategy used may result in some resident DC contaminating the migratory gate. In a bid to separate the migratory and resident populations, some groups employ techniques such as using labelled beads that cannot drain to the lymph nodes[290] or fluorescent dyes locally applied to the skin to track migratory DCs[282]. However, these cannot always be used in experimental settings. My data indicated that migratory DCs are more involved in the response to i.n. administration of 5-A-RU + MG compared to resident DCs based on the elevation of activation markers in the migratory population. Migratory and resident DCs play important roles in infection. Their functions and ability to prime a T cell response can depend on the route of infection and accessibility to antigen[282].

Activation of conventional DCs (cDCs) occurred after administration of i.n. 5-A-RU + MG. Activation was considered to be cells that had significantly increase CD86 and PDL-1 expression. CD86 and CD80 are co-stimulatory molecules that become upregulated on mature DCs. They are able to bind to CD28 on T cells to provide co-stimulation and enhance the T cell response[291–293]. cDC2s in the lung and migratory cDC1 and cDC2s in the mLN had elevated CD86 MFIs after i.n. 5-A-RU + MG administration. However, cDC1s in the lung had no significant difference in CD86 MFI, which was surprising given that PDL-1 expression was elevated on this population. The low expression of CD86 on cDC1s may be due to the self-regulation of CD86 through IL-10, or through T_{Reg} induced

downregulation of CD80 and CD86 through a lymphocyte function-associated antigen 1 (LFA-1) and cytotoxic T-lymphocyte-associated protein-4 (CTLA-4) dependent pathway[294], thus it is possible that CD86 expression is rapidly downregulated on these cells and its expression is missed in my model. PDL-1 was also chosen as a marker for DC activation, as it is seen to be upregulated in mature DCs[295,296]. PDL-1 is one of the ligands for PD-1, a marker upregulated on activated T cells[297]. Engagement of PD-1 with its ligands results in immunosuppression that inhibits T cell proliferation and cytokine secretion as a protective measure to over stimulation[296]. The selection of CD86 and PDL-1 as activation markers was based on previous literature. In vitro culture of DCs with MAIT cells and 5-A-RU + MG has also been shown to cause elevated levels of CD86 and PDL-1 on the DCs[236]. This is consistent with my results which show this same trend in an in vivo model.

Despite cDC1s and cDC2s having specialised roles in an immune response, it seems that both subsets in the lung and the migratory subsets in the mLN are capable of becoming activated following i.n. administration of 5-A-RU + MG. cDC1s are known for their ability to cross-present exogenous antigen on MHCI to $CD8^+$ T cells to induce a cytotoxic response, making these cells a target for cancer immunotherapy and viral infected cells[244]. BATF3-dependent migratory ($CD11c^+MHCII^{hi}$) $CD103^+$ DCs have been shown to constitutively express IL-12, independent of inflammatory TLR or microbial stimuli[298]. These DCs are equivalent to the cells termed cDC1s. The IL-12 production by cDC1s skews a T_H1 response, whereas cDC2s induce more of a T_H2 phenotype in T cells[299–301] and have been linked to priming T_{FH} cells[290,302]. Why these different DC subsets induce specific T cell responses is not fully understood[303]. As both subsets are activated in my model, it may suggest the potential for a non-specific downstream adaptive response.

5-A-RU + MG was able to promote MAIT cell and DC activation in the lung and mLN following i.n. administration, however, the pro-5-A-RU was not able to mimic this stimulation status. Pro-5-A-RU was unable to activate these cell types to the same level as the admix, and in most cases showed the same baseline response as PBS. The concept

of the pro-5-A-RU, is the cathepsin cleavable linker prevents 5-A-RU binding to MG before it is inside an APC. Only once it is inside a cell can the linker be cleaved via cathepsin and form the strong agonist 5-OP-RU for presentation. This reduces the likelihood of the unstable 5-OP-RU forming weaker lumazine agonists before it is able to be presented. Proof of concept has been shown by Lange, J. *et al.* (2020). Human PBMCs incubated for 18 hrs with the pro-5-A-RU led to activation of the MAIT cells in a dose dependent manner. The addition of MG did not give any additional activation as expected due to the linker blocking the binding site. 5-A-RU alone caused little activation, however, 5-A-RU + MG had more potent activation effects at lower doses than the pro-5-A-RU. The cleavage of the pro-5-A-RU was also confirmed with cathepsin. To test the pro-5-A-RU in vivo, mice were intravenously administered either a low dose (5 nmol) or a high dose (180 nmol) of pro-5-A-RU or 5-A-RU and the lung MAIT cells were assessed 18 hrs later. The high dose caused equivalent CD69 upregulation, whereas the low dose of pro-5-A-RU led to significantly higher levels of CD69 compared to 5-A-RU[304]. While this showed that pro-5-A-RU was able to elevate MAIT cell activation in vivo compared to 5-A-RU, I compared the pro-5-A-RU to an admix of 5-A-RU + MG where the admix outcompeted the pro-5-A-RU. Addition of MG with 5-A-RU in the in vitro cultures did show higher activation levels compared to the pro-5-A-RU, which links the vivo treatment presented here. Additionally, they gave the treatments intravenously, whereas I gave them intranasally. The administration of the pro-5-A-RU at a mucosal site is likely to reduce the dose seen by the immune system due to the physical barriers of the mucosa such as mucus, tight junctions, acidic conditions and peristalsis, unlike intravenous administration which is directly injected into the blood stream. Furthermore, the addition of MG to the 5-A-RU admix is likely to be at a much higher concentration than the MG concentration intracellularly, allowing more opportunity for the 5-A-RU to form MAIT cell agonists compared to the pro-5-A-RU. Moreover, I only tried the pro-5-A-RU at one dose (75 nmol), therefore, a dose titration of the pro-5-A-RU may show more optimal effects at different doses via intranasal administration.

The MAIT cell transcription factor phenotype had a bias for RORγT and GATA3 double positives at steady state in both the lung and mLN. This expression did not change dramatically following i.n. administration of 5-A-RU + MG, with only moderate changes towards more RORγT single positive MAIT cells in the lung and more GATA3 single positives and TF negative (RORγT$^-$GATA3$^-$Tbet$^-$) MAIT cells in the mLN. In the literature, MAIT cells are often described as having a RORγT and Tbet phenotype. In a naïve state murine MAIT cells present with the majority being RORγT$^+$. Upon activation through infections such as *Salmonella*[209,222] and *Legionella*[209,218]*,* MAIT cells still maintain their RORγT phenotype however the majority shifts to a RORγT Tbet double positive phenotype[209,218]. This RORγT bias is seen in my data, however, the frequency of Tbet$^+$ MAIT cells is very low to absent after the i.n. treatment of 5-A-RU + MG. This could be because the admix does not contain the same TLR ligands and general immune stimulatory patterns as an infection model does, resulting in the Tbet effector phenotype. Interestingly, GATA3 expression on MAIT cells is commonly not investigated in the literature, with the majority publishing data focusing on RORγT and Tbet expression. However, Kelly, J. *et al.* (2019), recently published data where they found that chronically stimulating human MAIT cells in vitro with anti-CD3/CD28 monoclonal antibodies, Phytohaemagglutinin, IL-2 and IL-7 for 2 weeks resulted in comparable concentrations (although initially delayed) of T_H2 associated cytokines IL-13 and IL-5 to cytokines such as TNF around day 8-13 of stimulation. Although they did not show GATA3 protein expression, qPCR did show GATA3 expression in both naïve and stimulated MAIT cells[305]. This showing consistencies with my data and the baseline levels of GATA3 in MAIT cells.

3.5 Conclusions

In this chapter, it has been demonstrated that intranasal administration of 5-A-RU plus MG is capable of producing a MAIT cell agonist resulting in activation of MAIT cells in both the lung tissue and mLN. This treatment also leads to the activation of conventional DCs which is dependent on MR1 and MAIT cell presence. While this does not show direct interaction between the MAIT cells and DCs, it does suggest these two cell populations communicate and that MAIT cells are able to act on the DCs to cause stimulation. Despite the success of the 5-A-RU + MG admix, the pro-5-A-RU was unable to initiate an equivalent response. In addition to the dependence on MR1, the data also suggests that the MAIT cells are being stimulated through the direct MR1 to TCR pathway. Moreover, both cDC1s and cDC2s are activated in the lung and migratory DCs show a strong upregulation of activation markers in the mLN. This indicates DCs are activated at the primary lung tissue and then migrate to the lung draining lymph node (mLN) where they have the potential to interact with T lymphocytes. Furthermore, the MAIT cells show a homeostatic expression of RORγT and GATA3, with only slight changes to increases in RORγT single positives in the lung and GATA3 single positives along with TF negative cells in the mLN following i.n. administration of 5-A-RU + MG.

Leading on from these results, I wanted to determine whether the mucosal administration of the 5-A-RU + MG admix could induce an adaptive immune response favourable in a vaccination setting and what mechanisms are involved between the MAIT cell and DC interaction.

4 Intranasal Administration of 5-A-RU + MG Induces an Antigen-specific B Cell Response Dependent on cDC1s and cDC2s

4.1 Introduction

A goal of vaccinations is to induce a long-lasting protective immunity to a specific pathogen. A long-lasting response requires immune memory, a characteristic of the adaptive immune system. It is therefore paramount that a vaccine induces an adaptive response that upon reinfection can rapidly control the infection and protect the individual against severe illness[105]. The effector cells in a protective vaccine response are typically B cells resulting in antibody production[163,167] and in some cases cytotoxic $CD8^+$ T cells that are able to kill infected cells[306]. $CD4^+$ T cell subsets are also important responders as they provide support to the B cells and $CD8^+$ T cells to initiate and maintain their protective functions[187,307]. While B cell responses can be induced in a T-cell independent manner through antigens such as polysaccharides[308], the involvement of $CD4^+$ T cells, specifically T_{FH} cells, allows for the production of higher affinity antibodies and long lasting B cell memory[156]. Due to the high frequency of vaccines inducing an antibody response, the efficacy of a vaccine is commonly measured by an individual's antigen-specific antibody titre in the serum[309].

The type of T cell response induced by a vaccine is dependent on the site and type of vaccination along with the antigens and adjuvant used. For example, an intranasal live attenuated influenza vaccine is able to induce a $CD4^+$, $CD8^+$ and $\gamma\delta$ T cell response, whereas, an intramuscular trivalent inactivated influenza vaccine is unable to induce this T cell response[310]. The oral *Salmonella* Typhi vaccine, Ty21A, is also able to provoke a $CD4^+$ T cell response that either express IFN-γ or IL-17A[311]. The Ty21A vaccine is also a strong inducer of $CD8^+$ T cells. These $CD8^+$ T cells are *Salmonella* Typhi-specific and are able to lysis infected cells as well as produce IFN-γ[312]. Additionally, the adjuvant component of a vaccine also results in bias towards specific $CD4^+$ T cells responses. The common adjuvant alum, results in a response skewed towards a T_H2 phenotype, however, the adjuvant AS04 leads to a more T_H1 bias[40]. The different T cell responses in a vaccination setting have different roles to lead to protection. While $CD8^+$ T cell responses are important for killing intracellular pathogens and cancerous cells[187,313], $CD4^+$ T cell responses are involved in priming, maintaining and improving the cytotoxic

and B cell responses. T_{FH} cells are of utmost importance as they improve the affinity and memory of the humoral response[153,156]. Additionally, the type of $CD4^+$ T subset can also drive the antibody isotype switching. For example T_H1 cells cause a bias for IgG antibodies[188], whereas, T_H2 results in IgE isotype switching[174]. These immune responses are also reliant on co-stimulatory interactions. Interactions such as inducible T cell co-stimulator (ICOS) with its ligand (ICOSL) between T and B cells are important for the survival and maturation of GC B cells[314] whereas, CD40-CD40L is involved in DCs driving effector T cell functions and T_{FH} cells supporting B cell isotype switching[315]. Furthermore, the receptor activator of nuclear factor kappa-B (RANK) interaction with its ligand (RANKL) between DCs and T cells is known to aid in T cell proliferation and survival[316,317].

A common denominator of mucosal vaccines is their ability to induce an antibody response which is often dominated by systemic IgG and mucosal IgA antibody isotypes[17]. For example the Ty21A oral vaccine promotes an increase in antibody secreting cells and serum IgG and IgA antibodies specific for *Salmonella* Typhi[318]. It is also capable of inducing mucosal IgA antibodies[46]. These antibodies have different functions, IgG antibodies are the most predominant isotype in the circulation and have a broad range of functions including neutralisation, opsonisation and complement activation[160]. Whereas, IgA antibodies are specialised for the mucosal system where secretory IgA can cross into the lumen of the mucosa to bind and block pathogens and their products invading the human host[193]. T_{FH} cells are vital for the formation of germinal centers in the lymph nodes, which allows for the B cells to undergo this isotype switching and affinity maturation. This leads to the production of antibodies that have improved binding capacities for their specific antigens, resulting in improved function. T_{FH} cells also support the development of B cells into memory B cells and plasma cells[145,319]. The addition of adjuvants into a vaccine, is also able to influence the humoral response. Amongst others, adjuvants such as alum and MF59, drive an IgG antibody response[320,321]. Similarly, to T cell responses, the vaccine type and whether or not an adjuvant is involved, alters the persistence of an antibody response. Live attenuated viral vaccines, vaccines containing virus like particles and vaccines containing adjuvants

can induce long-term and in some cases lifelong antibody responses due to the T_{FH} and germinal center reaction[163,322–325]. Furthermore, the vaccine schedule also can affect this, with prime-boost strategies resulting in improved antibody responses. Vaccines can be administered close together (within weeks) to give a rapid increase in the protective response, however, allowing for more time between doses (months) induces a more persistent response as it allows for a greater generation of high affinity plasma cells and memory B cells[325,326].

The classical idea of immune memory focuses on the adaptive immune response. This is a key concept for effective vaccines and is a result of gene rearrangements to create antigen specific responses. However, recent investigations into the innate system has shown a 'trained immunity' characteristic – an innate equivalent to adaptive memory. Unlike adaptive memory, trained immunity doesn't involve gene rearrangements for specific antigen responses but instead a reprogramming of transcription factors and epigenetics. Additionally, trained immunity is non-specific for a particular pathogen/stimuli and is induced through pattern recognition receptors and cytokines [327]. Innate cell types such as monocytes, macrophages [328] and NK cells [329] have been implicated in trained immunity. Furthermore, a recent study has suggested even non-immune cells have the potential of trained immunity. A Nature publication found that after acute inflammation, epithelial stem cells had increased barrier healing after tissue damage due to a maintained accessibility of stress response genes enabling rapid transcription [330]. This idea of trained immunity has potential benefits for vaccine design. With the concept of trained immunity-based vaccines inducing a broad range of innate immune response to improve the protection against a wide spectrum of pathogens[331].

Many factors influence the type and preference of the adaptive response induced by a vaccine. One major influence is the DC response and how these cells are stimulated by the vaccine antigen and/or adjuvant. The PRR stimulated on DCs can lead to different responses both in the DC population and the adaptive response[332]. Interestingly activation of DCs through TLR9 leads to antiviral myeloid DC IL-12 production[333],

whereas on plasmacytoid DCs TLR9 and 7 stimulation induces type 1 IFN production[334]. Moreover, TLR9 has been linked with cross-presentation of exogenous antigen via bone marrow derived DCs to $CD8^+$ T cells[335]. The successful yellow fever vaccine, YF-17D, also employs multiple PRRs on different DC subsets. YF-17D is capable of stimulating monocyte-derived and plasmacytoid DCs leading to the release of IL-12 and IFNα respectively. The activation of these DCs results from the stimulation of multiple TLRs including TLR2, 7, 8 and 9, resulting in the involvement of multiple downstream pathways such as MyD88 and TIRAP. Furthermore the T_H1 and T_H2 mixed response induced by YF-17D is determined by the different TLRs stimulated[336]. This shows that depending on what subset of DCs are activated the signals that they provide such as cytokines will change and hence, lead to a specific adaptive response. Additionally, the success of a vaccine can be dependent on specific DC subsets. For example, in $BATF3^{-/-}$ mice which lack cDC1s, the protective IFN-γ $CD8^+$ T cell response against *Plasmodium* sporozoites is lost[337]. Indicating dependence on DC1s for this vaccine protection. In contrast, CD11c-cre $IRF4^{fl/fl}$ mice that lack the majority of DC2s, vaccinated with soluble flagellin have impaired antigen specific $CD4^+$ T cell numbers and germinal center B cells along with reduced IgG titres in the mesenteric lymph node[338]. This suggesting a dependence on DC2s for this response. Taken together the literature indicates that the adaptive response in vaccination is driven and skewed by the activated DC subsets and how these DCs were stimulated.

In order to determine whether the admix of 5-A-RU + MG could stimulate a desirable adaptive immune response; a prime boost vaccination scheme was first established. This treatment scheme where mice were given 3 doses of intranasal 5-A-RU + MG + antigen over 4 weeks was able to show that the admix was capable of inducing an antigen specific humoral response. This response was dependent on MR1 and showed involvement of both conventional cDC1s and cDC2s. I also began to investigate the initial interactions that lead to DC activation in my model and was able to discover the potential involvement of co-stimulatory interactions CD40:CD40L and RANK:RANKL on DCs which influence the ICOSL expression.

4.2 Aims

Based on my findings that MAIT cells along with cDCs were able to be activated after intranasal administration of 5-A-RU + MG in vivo, I wanted to determine whether this vaccine could also lead to an adaptive immune response. Additionally, I wanted to further investigate the role and dependence of cDCs in a long-term adaptive response within our model and the potential interactions between the DCs and MAIT cells.

Specific aims:

1) Determine whether intranasal administration of 5-A-RU plus MG with the addition of antigen can induce an adaptive immune response at the lung mucosal site
2) To assess the requirement of conventional DCs for the induction of an adaptive immune response following intranasal administration of 5-A-RU plus MG and antigen
3) To characterise the potential interactions and co-stimulatory requirements for the MAIT cell to communicate with conventional DCs

4.3 Results

4.3.1 Administering Multiple Doses of 5-A-RU + MG Admix Intranasally Maintains the Conventional DC and MAIT Cell Activation Status

To determine whether the 5-A-RU + MG admix administered i.n. could induce an adaptive response, the establishment of a treatment regime to optimise this type of response was required. Due to the nature of the mucosal system, multiple doses of the currently licensed mucosal vaccines are required to induce the desired long term protective adaptive response[17]. It is based on this prime-boost strategy our lab group was able to design an optimised treatment scheme of the 5-A-RU + MG i.n. vaccine to result in a humoral response. EndoGrade® Ovalbumin (OVA) whole protein was added to the 5-A-RU (75 nmol) and MG (750 nmol) at a concentration of 5 nmol to provide the system with a model antigen and allow for analysis of an antigen specific adaptive response. The treatment scheme involved i.n. administration of OVA only or the admix of 5-A-RU + MG + OVA to C57BL/6 mice 3 times at 2 week intervals. The immune response in the lung and mLN was assessed one week following the third dose. Blood was also collected, and serum isolated for ELISA analysis of antigen specific antibodies. This treatment scheme allowed for the analysis of the T and B lymphocyte response to our vaccine (figure 4.1).

With 'trained immunity' being shown in other innate immune cells such as monocytes, macrophages[328] and NK cells[329], I initially wanted to determine whether implementing this prime-boost scheme could induce a 'trained immunity' phenotype in cDCs. To assess whether cDCs retained some memory of the priming dose, I analysed their ability to upregulate the activation markers CD86 and PDL-1 in the mLN after a single dose of 5-A-RU + MG compared to three doses. The hypothesis being that if the DCs did retain a memory phenotype it would result in a faster and stronger activation following multiple doses. C57BL/6 mice were either treated with one dose or three doses (12 and 14 days apart) i.n. of 5-A-RU + MG. The mLN was then harvested one day later to assess the DC activation status by flow cytometry (figure 4.2A). The number of resident DCs

and the cDC1 and cDC2 subsets did not change between the PBS, one dose of admix and three doses of admix (figure 4.2B). As seen in previous experiments the resident DC1s and DC2s did not upregulate CD86 MFI with either of the doses given compared to the PBS (figure 4.2C). However, there was an upregulation of PDL-1 MFI in both resident cDC1s and cDC2s following both the one and three doses of the admix. In the cDC2s the PDL-1 MFI was also higher at one dose compared to the three doses of the admix (figure 4.2D). The upregulation of PDL-1 only and not CD86 was also seen in figure 3.4C&D. The lack of CD86 in resident cDCs may be due to a weaker stimulus in the mLN, whereas migratory cDCs get stimulated at the primary lung site, resident cDCs remain in the mLN and therefore may not receive the same stimulatory signals. However, the cells do still upregulate PDL-1, so it may be that the timing in the mLN for resident cDCs is different to the other subsets and the experimental model may be missing the upregulation. The number of migratory DCs also did not significantly increase following admix treatment compared to the PBS controls, however, there may be a trend towards increasing after the admix but with high variability within the groups (figure 4.2E). Both the migratory cDC1s and cDC2s had significantly elevated CD86 and PDL-1 MFIs following admix i.n. treatment compared to the PBS control. The increase in MFI of both markers was seen at equivalent levels between the one dose and three doses of the admix (figures 4.2F&G). Together this showed that the DCs have no added activation status after three doses of 5-A-RU + MG compared to one dose in the mLN. Suggesting the DCs in this model have no ‘trained immunity’ phenotype in terms of activation.

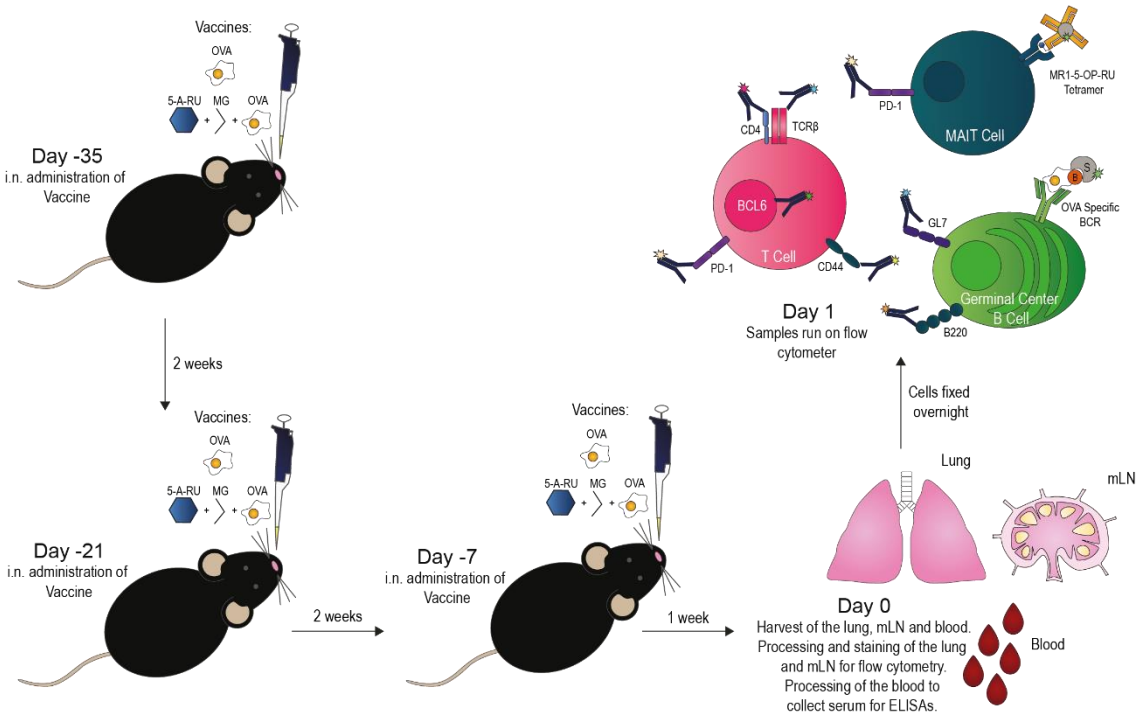

Figure 4.1: Treatment Scheme for a Boosted Vaccine Model to Induce an Adaptive Response. Mice are intranasally administered either the 5-A-RU (75 nmol) plus MG (750 nmol) admix including EndoGrade® Ovalbumin (OVA) at 5 nmol as an antigen or OVA alone. 2 weeks later the mice are given a second dose and then a third dose after 2 additional weeks. 1 week following the third dose of vaccine, the lung tissue, mLN and blood is harvested. Single cell suspensions of the lung and mLN are stained and fixed for flowcytometry analysis the following day. Serum is extracted from the blood and stored for antibody detection via ELISA.

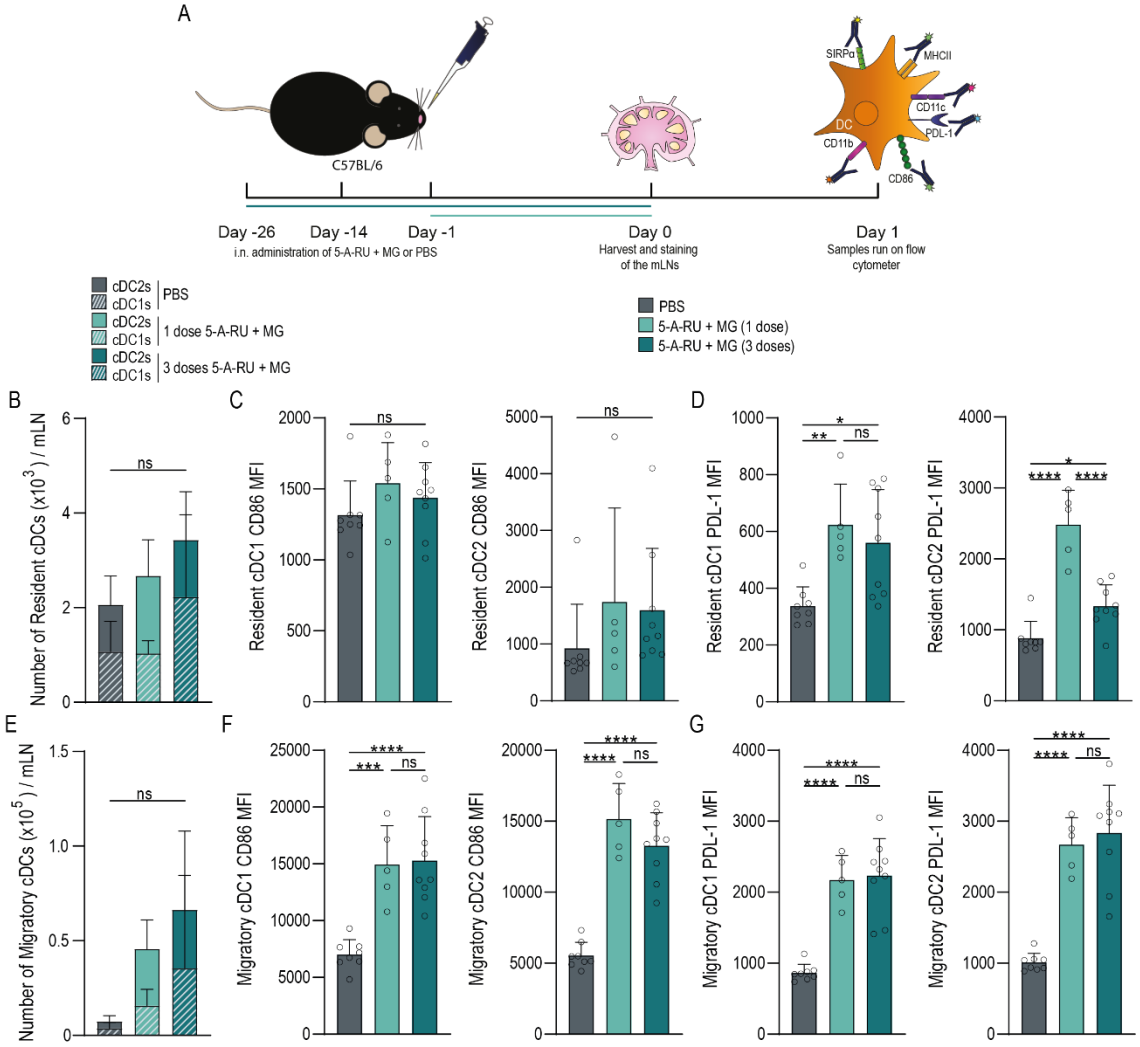

Figure 4.2: Dendritic Cells Don't Display an Innate 'Trained' Response Following Admix Boosting. C57BL/6 mice were either intranasally administered 3 doses of PBS or 5-A-RU plus MG admix or intranasally administered 1 dose of admix. The following day the mLN were harvested and the cells processed for flow cytometry analysis. **(A)** Treatment scheme. **(B)** Number of resident cDCs per subset per mLN. **(C)** Resident cDC1 and cDC2s CD86 median fluorescence intensity (MFI). **(D)** Resident cDC1 and cDC2s PDL-1 MFI. **(E)** Number of migratory cDCs per subset per mLN. **(F)** Migratory cDC1 and cDC2s CD86 MFI. **(G)** Migratory cDC1 and cDC2s PDL-1 MFI. Statistcial analysis was conducted using One-way ANOVA with Tukey's post hoc test or a Two-way ANOVA (B & E). Bars represent the mean per group, symbols each induvidual mouse and error bars the standard deviation. ns>0.05, *p≤0.05, **p≤0.01, ***p≤0.001, ****p≤0.0001.

After assessing the DC activation following three doses of 5-A-RU + MG admix, I next wanted to determine the MAIT cell phenotype in both the lung and mLN after multiple admix doses. This was also of particular interest as NKT cells in vivo have been shown to have an anergic response to a single high dose of the agonist α-GalCer in vivo[339]. Additionally, while NKT cell activation can occur in vivo, the same anergic phenotype is seen upon re-stimulation with α-GalCer ex vivo[340]. Therefore, the MAIT cell phenotype was investigated following multiple doses of the 5-A-RU + MG + OVA admix. C57BL/6 mice were i.n. administered 3 doses of the admix with the first and second doses being 15 days apart and then the third dose was either administered 14, 16 or 18 days later to give a time course. This allowed the MAIT cells in the lung and mLN to be assessed after three doses of the admix either 1, 3 or 5 days after the final dose. PBS and OVA only control groups were also included (figure 4.3A). Following the three doses of the admix the frequency of MAIT cells among TCRβ^+ cells in the lung increased at day 3 following i.n. vaccination compared to PBS and also at day 5 compared to PBS and OVA only (figure 4.3B). The MAIT cell CD69 MFI also remained significantly higher than the controls at all time points with a gradual decline over time. The frequency of lung CD69$^+$ MAIT cells remained at a frequency between 65-90% over the 5 days in the admix treated group compared to the baseline levels of 5-20% in the control groups (figure 4.3C). This same trend was also seen for the MAIT cell PD-1 expression in the lung with the frequency of PD-1$^+$ MAIT cells ranging from 75-95% after admix treatment (figure 4.3D). The MAIT cell transcription factor expression was assessed on day 3 after i.n. admix treatment. The majority of the MAIT cells in the lung had a RORγT$^+$ phenotype like in the previous chapter, however, there were less of the RORγT$^+$GATA3$^+$ population. Slight shifts in TF expression were seen following the admix treatment, with a reduction in RORγT$^+$GATA3$^+$ and an increase in TF negative cells (RORγT$^-$GATA3$^-$Tbet$^-$). However, the overall phenotype remained dominated by RORγT expression with little to no Tbet expression (figure 4.3E).

As I had seen previously, there was no change in MAIT cell frequencies in the mLN in the admix treated group compared to the PBS and OVA only controls (figure 4.3F).

Interestingly in the mLN the MAIT cell CD69 MFI had a shorter upregulation time compared to the lung, with a significant increase only seen at day 1 (figure 4.3G). Whereas the MAIT cell PD-1 MFI was consistent with the trend seen in the lung – significantly unregulated at all timepoints in the admix compared to the controls with a gradual reduction over time (figure 4.3G). The TF profile of the MAIT cells in the mLN, showed parallels with the previous chapter, where the majority of the MAIT cells were RORγT$^+$GATA3$^+$ both in the control and admix treated groups, with an increase in the GATA3 single positive population following admix treatment. However, there was also an increase in the RORγT single positives seen in this 3 dose model after treatment. Additionally, there was a consistent absence of Tbet$^+$ MAIT cells (figure 4.3H). Figure 4.3 indicates that MAIT cells don't undergo this same anergic phenotype seen in the NKT cells, with activation still significantly increased in the lung and mLN compared to the negative controls following 3 doses of the intranasal administration of 5-A-RU + MG + OVA. Furthermore, the MAIT cells still maintain an absence of Tbet expression after three doses of admix, with a dominant RORγT$^+$ phenotype in the lung and a dominant RORγT$^+$GATA3$^+$ phenotype in the mLN.

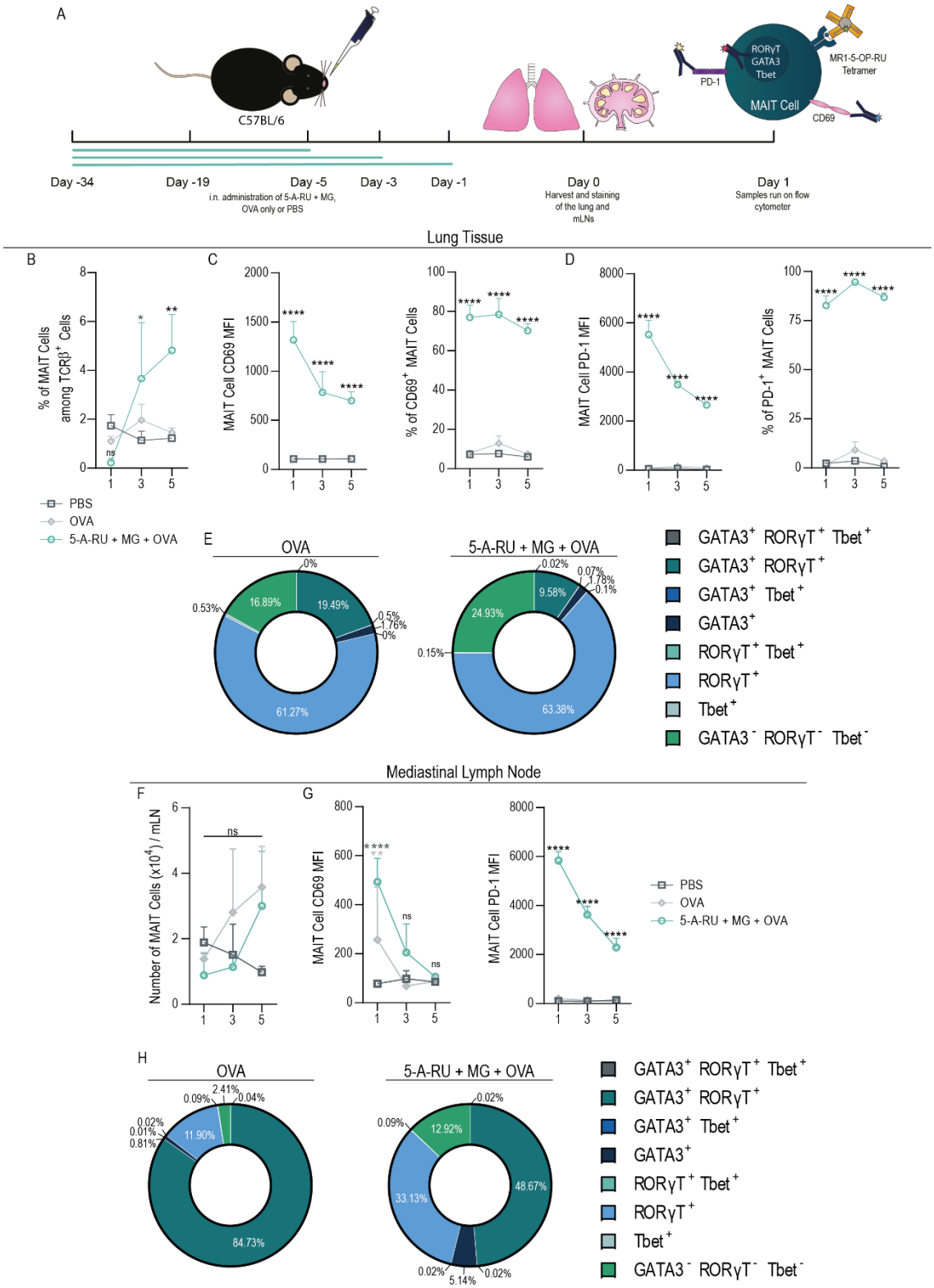
A
C57BL/6
RORγT
GATA3
Tbet
PD-1
MR1-5-OP-RU
Tetramer
MAIT Cell
CD69
Day -34
Day -19
Day -5
Day -3
Day -1
Day 0
Harvest and staining of the lung and mLNs
Day 1
Samples run on flow cytometer
i.n. administration of 5-A-RU + MG, OVA only or PBS
Lung Tissue
B
% of MAIT Cells among TCRβ+ Cells
C
MAIT Cell CD69 MFI
% of CD69+ MAIT Cells
D
MAIT Cell PD-1 MFI
% of PD-1+ MAIT Cells
PBS
OVA
5-A-RU + MG + OVA
E
OVA
5-A-RU + MG + OVA
GATA3+ RORγT+ Tbet+
GATA3+ RORγT+
GATA3+ Tbet+
GATA3+
RORγT+ Tbet+
RORγT+
Tbet+
GATA3- RORγT- Tbet-
Mediastinal Lymph Node
F
Number of MAIT Cells (x10^4) / mLN
G
MAIT Cell CD69 MFI
MAIT Cell PD-1 MFI
PBS
OVA
5-A-RU + MG + OVA
H
OVA
5-A-RU + MG + OVA
GATA3+ RORγT+ Tbet+
GATA3+ RORγT+
GATA3+ Tbet+
GATA3+
RORγT+ Tbet+
RORγT+
Tbet+
GATA3- RORγT- Tbet-

Figure 4.3: MAIT Cells remain Activated Following 3 Doses of Intranasal 5-A-RU plus MG Admix. C57BL/6 mice were intranasally administered 3 doses over 5 weeks of either PBS, OVA only or 5-A-RU + MG + OVA admix. The third dose was given at different time points, either 5, 3 or 1 day prior to tissue harvest. Both the lung and mLN were harvested for flow cytometry analysis. **(A)** Treatment scheme. **(B)** Frequency of MAIT cells among $TCR\beta^+$ cells in the lung. **(C)** MAIT cell CD69 MFI and frequency of $CD69^+$ MAIT cells in the lung. **(D)** MAIT cell PD-1 MFI and frequency of $PD\text{-}1^+$ MAIT cells in the lung. **(E)** Lung MAIT cell transcription factor expression at day 3 post thrid intransal dose. Expression was determined using boolean gating. **(F)** Number of MAIT cells per mLN. **(G)** MAIT cell CD69 and PD-1 MFI in the mLN. **(H)** mLN MAIT cell transcription factor expression at day 3 post thrid intransal dose. Expression was determined using boolean gating. Statistcial analysis was conducted using a Two-way ANOVA. Symbols represent the group mean and error bars show the standard deviation. ns>0.05, *p≤0.05, **p≤0.01, ****p≤0.0001. Dark grey stars represent admix vs PBS treated significance, light grey for OVA vs admix and black stars for both PBS and OVA vs admix.

4.3.2 A Prime-Boost Intranasal Vaccination Scheme of 5-A-RU + MG + OVA Induces Accumulation of T_{FH} Cells and an Antigen-Specific Humoral Response in the mLN that is Dependent on MR1

Implementing the treatment scheme in figure 4.1 I wanted to investigate whether the 5-A-RU + MG + OVA vaccine was able to enhance a T_{FH} response. A T_{FH} response is important as this would be a link between the DC activation and the induction of a B cell response. C57BL/6 mice were treated following the scheme in figure 4.1, where i.n. administration of 5-A-RU + MG + OVA and OVA only was given 3 times over a 4 week time period. The lungs and mLNs were then harvested and processed for flow cytometry analysis. The mLN data also included a PBS group to ensure the OVA only was not inducing any background responses. However, this was not included in the lungs due to experimental feasibility and the DC antigen presentation would be occurring in the mLN where the naïve T cells are located, therefore, it is likely that if there was any effect with antigen alone it would be present in the mLN. To identify conventional $CD4^+$ T cells, cells were gated as $B220^-TCR\beta^+$MR1-5-OP-RU $tetramer^-CD4^+CD44^{hi}$. CD44 was used as a marker of antigen experienced T cells[341,342]. To measure the T cells effector phenotype CD69 was used as an activation marker and the TFs Tbet and RORγT as effector function. In the lung tissue the conventional $CD4^+$ T cells did show an upregulation of CD69 MFI following admix treatment compared to OVA but there was no significant change between the frequency of $Tbet^+$ and $ROR\gamma T^+$ $CD4^+$ T cells (figure 4.4A). In a bid to investigate the $CD8^+$ T cell response, the CD69 MFI of $B220^-TCR\beta^+$MR1-5-OP-RU $tetramer^-CD4^-CD44^{hi}$ cells was analysed. Although this does not directly identify $CD8^+$ T cells, it is likely that the majority of the $CD4^-$ cells would be $CD8^+$ T cells. This gating strategy showed no significant difference in CD69 MFI between the OVA only and admix treated mice (figure 4.4B). This indicates that while the $CD4^+$ T cells in the lung show an activated phenotype they do not show an enhanced effector phenotype.

The T cell response in the mLN was of great interest to determine the potential of the admix vaccine inducing a T_{FH} response. The antigen experienced conventional $CD4^+$ T cells were again gated on using the same strategy as the lung ($B220^-TCR\beta^+$MR1-5-OP-

RU tetramer$^-$CD4$^+$CD44^{hi} cells). Unfortunately, CD69 was unable to be included due to panel design, however, both the Tbet and RORγT MFI and frequency (among parent population) either showed no change between the admix and control groups or in some cases the admix actually showed a significant decrease compared to the OVA only or PBS groups (figures 4.4C&D). Next T_{FH} cells were gated on as PD-1$^+$BCL6$^+$ double positives (previously gated as B220$^-$TCRβ$^+$MR1-5-OP-RU tetramer$^-$CD4$^+$CD44^{hi} cells) using the FMOs as a guide (figure 4.4E). While the frequency of T_{FH} cells didn't change between the groups, the number of T_{FH} cells was significantly higher in the admix group compared to the OVA only treated mice (figures 4.4F&G). In a separate experiment, mice were again treated following the same prime-boost scheme, however the flow cytometry panel also included both the I-A(b)-HAAHAEINEA and I-A(b)-AAHAEINEA tetramers. These tetramers contain specific OVA peptides (HAAHAEINEA and AAHAEINEA) that are known CD4$^+$ T cell epitopes bound to MHCII. This allowing for the identification of OVA specific CD4$^+$ T cells. Although the MHCII-OVA tetramer stain didn't show a significant difference between T_{FH} cells in the OVA only and admix treated groups, there did seem to be a trend towards an increase in frequency of OVA-peptide$^+$ T_{FH} cells and especially the number of OVA-peptide$^+$ T_{FH} cells (figures 4.4H&I). The frequency of these cells is difficult to quantify as a single positive cell in the OVA only group constitutes a similar frequency compared to the admix group due to the low number of T_{FH} cells in the OVA only group. It is clear from the flow plots that the admix treated group contains a greater number of positive T_{FH} cells (figure 4.4H). Additionally, although the number of OVA-peptide$^+$ T_{FH} cells is not significantly increased after admix treatment, there is a definite trend. The number of positive T_{FH} cells in the OVA only group ranges from 0 to 90, whereas, in the admix group they range from 80 to 1,300 (figure 4.4I). Taken together that data suggests that although the CD4$^+$ T cells in the lungs show activation they don't present with an effector phenotype. This lack of effector phenotype is also seen in the mLN, however, there does seem to be an accumulation of T_{FH} cells after admix treatment and a trend towards an increase in antigen positive T_{FH} cells which warrants further investigation into the B cell response.

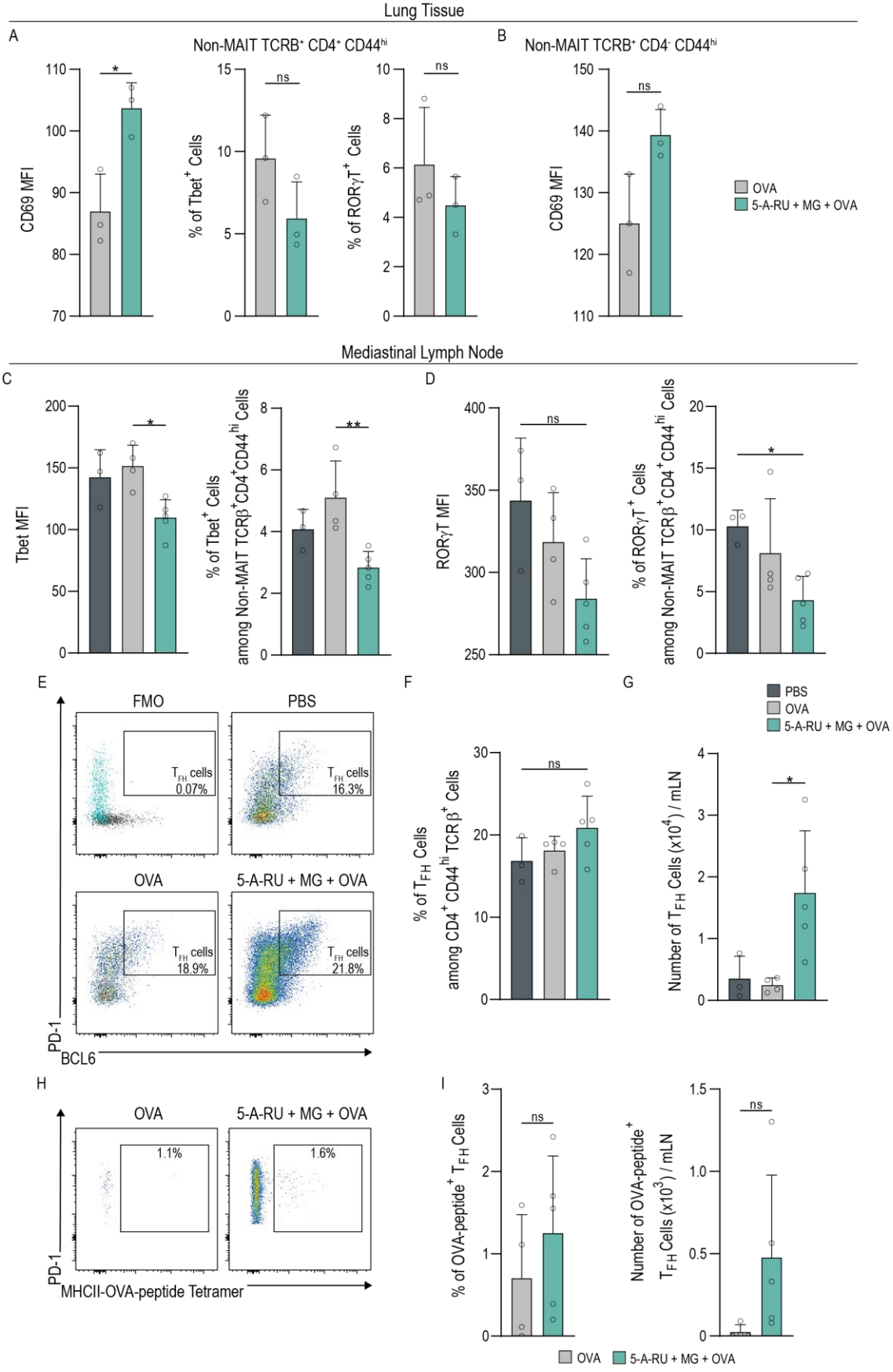
Lung Tissue
A
Non-MAIT TCRB+ CD4+ CD44hi
CD69 MFI
% of Tbet+ Cells
% of RORγT+ Cells
B
Non-MAIT TCRB+ CD4- CD44hi
CD69 MFI
OVA
5-A-RU + MG + OVA
Mediastinal Lymph Node
C
Tbet MFI
% of Tbet+ Cells among Non-MAIT TCRβ+CD4+CD44hi Cells
D
RORγT MFI
% of RORγT+ Cells among Non-MAIT TCRβ+CD4+CD44hi Cells
E
FMO
PBS
OVA
5-A-RU + MG + OVA
TFH cells 0.07%
TFH cells 16.3%
TFH cells 18.9%
TFH cells 21.8%
PD-1
BCL6
F
% of TFH Cells among CD4+CD44hi TCRβ+ Cells
G
PBS
OVA
5-A-RU + MG + OVA
Number of TFH Cells (x10^4) / mLN
H
OVA
5-A-RU + MG + OVA
1.1%
1.6%
PD-1
MHCII-OVA-peptide Tetramer
I
% of OVA-peptide+ TFH Cells
Number of OVA-peptide+ TFH Cells (x10^3) / mLN
OVA
5-A-RU + MG + OVA

Figure 4.4: Boosting Admix Intranasal Administration Leads to Elevated Number of T_{FH} Cells in the mLN. C57BL/6 mice were administered 3 doses of either intranasal 5-A-RU + MG + OVA, OVA only or PBS (mLN). Each dose was given two weeks apart and 1 week following the third dose, the lung tissue and mLN were harvested for flow cytometry. **(A)** $B220^{-}TCR\beta^{+}MR1\text{-}5\text{-}OP\text{-}RU\ tetramer^{-}CD4^{+}CD44^{hi}$ cells CD69 MFI and frequency of $Tbet^{+}$ and $ROR\gamma T^{+}$ cells in the lung. **(B)** $B220^{-}TCR\beta^{+}MR1\text{-}5\text{-}OP\text{-}RU\ tetramer^{-}CD4^{-}CD44^{hi}$ cells CD69 MFI in the lung. **(C)** Tbet MFI and frequency in the mLN of $B220^{-}TCR\beta^{+}MR1\text{-}5\text{-}OP\text{-}RU\ tetramer^{-}CD4^{+}CD44^{hi}$ cells. **(D)** RORγT MFI and frequency in the mLN of $B220^{-}TCR\beta^{+}MR1\text{-}5\text{-}OP\text{-}RU\ tetramer^{-}CD4^{+}CD44^{hi}$ cells. **(E)** Representative gating of T_{FH} cells ($BCL6^{+}PD\text{-}1^{+}$) previously gated on $B220^{-}TCR\beta^{+}MR1\text{-}5\text{-}OP\text{-}RU\ tetramer^{-}CD4^{+}CD44^{hi}$ cells. **(F)** Frequency of T_{FH} cells among $B220^{-}TCR\beta^{+}MR1\text{-}5\text{-}OP\text{-}RU\ tetramer^{-}CD4^{+}CD44^{hi}$ cells. **(G)** Number of T_{FH} cells per mLN. **(H & I)** An independent experiment using the same treatment scheme but including the MHCII-OVA peptide tetramer. **(H)** Representative gating of OVA-$peptide^{+}$ T_{FH} cells (previously gated on $B220^{-}TCR\beta^{+}MR1\text{-}5\text{-}OP\text{-}RU\ tetramer^{-}CD4^{+}CD44^{hi}$ cells). **(I)** Frequency and number of OVA-$peptide^{+}$ T_{FH} cells. Statistcial analysis was conducted using an unpaired T test (A, B & I) or a One-way ANOVA with Tukey's post hoc test (C,D,F & G). Bars represent the mean per group, symbols are induvidual mice and error bars show the standard deviation. ns>0.05, *p≤0.05, **p≤0.01.

The next logical step was to determine whether our prime-boost intranasal treatment of 5-A-RU + MG + OVA was able to result in a humoral response. To ensure that any response seen was dependent on the vaccine and was reliant on MAIT cells being involved, I included $MR1^{-/-}$ mice, which lack MR1 expression and therefore MAIT cells[242]. This also allows us to confirm that there are no contaminants in the vaccine with off targeted effects. C57BL/6 and $MR1^{-/-}$ mice were treated using the scheme in figure 4.1. To confirm the lack of MAIT cells in the $MR1^{-/-}$ mice, MAIT cells were gated on and showed a significant increase in numbers but no change in frequency (among $TCR\beta^+$ cells) in C57BL/6 mice following admix treatment compared to OVA only. This also confirmed a lack of MAIT cells in the $MR1^{-/-}$ mice (figure 4.5A). Additionally, as confirmation of the admix activating MAIT cells, the MAIT cell PD-1 MFI significantly increased after admix treatment compared to the OVA only group (figure 4.5B). As with the previous figure (4.4F&G) there was no change in the frequency of $PD\text{-}1^+BCL6^+$ T_{FH} cells (among $B220^-TCR\beta^+$ $CD4^+CD44^{hi}$ cells) between the OVA only and admix treated C57BL/6 mice, but the admix did result in an increase number of T_{FH} cells compared to OVA only. The number of T_{FH} cells in the C57BL/6 admix treated mice was also significantly increased compared to the $MR1^{-/-}$ mice which remained at baseline levels with the C57BL/6 OVA only treated mice. While the frequency and number of T_{FH} cells didn't change between the OVA only and admix treated $MR1^{-/-}$ mice, the frequency of T_{FH} cells was significantly higher in the admix treated C57BL/6 mice compared to the admix treated $MR1^{-/-}$ mice (figure 4.5C). Germinal center (GC) B cells were identified as $B220^+IgD^-GL7^+$ cells, which were further defined as antigen positive using OVA protein bound to biotin (figure 4.5D). The admix treated C57BL/6 mice had an increased number of GC B cells compared to the OVA only C57BL/6 and admix treated $MR1^{-/-}$ mice. The number of GC B cells in the $MR1^{-/-}$ mice remained to the same levels as C57BL/6 OVA treated mice despite the treatment given. Whereas the frequency of GC B cells (among $B220^+$ cells) remained constant between all groups (figure 4.5E). However, when the GC B cells were further identified as antigen positive, the C57BL/6 mice treated with the admix showed a significant upregulation of both number and frequency (among GC B cells) compared to the C57BL/6 OVA only group and both the $MR1^{-/-}$ groups (figure 4.5F).

This proved that the prime-boost treatment of 5-A-RU + MG + OVA was able to induce an antigen specific B cell response which was dependent on MR1 in the mLN. To assess the antibody production systemically, the serum was also harvested and used for an ELISA. The ELISA identified OVA specific total IgG antibodies through the use of whole OVA protein as the antigen bound to the plate. The ELISA showed that only the C57BL/6 admix treated mice produced OVA specific IgG antibodies in the serum (figure 4.5G). With this data I can conclude that the i.n. treatment of mice with 5-A-RU + MG + OVA induces a T_{FH} accumulation and humoral response with a prime-boost treatment scheme that is dependent on MR1 and is not a result of contaminants causing an untargeted response.

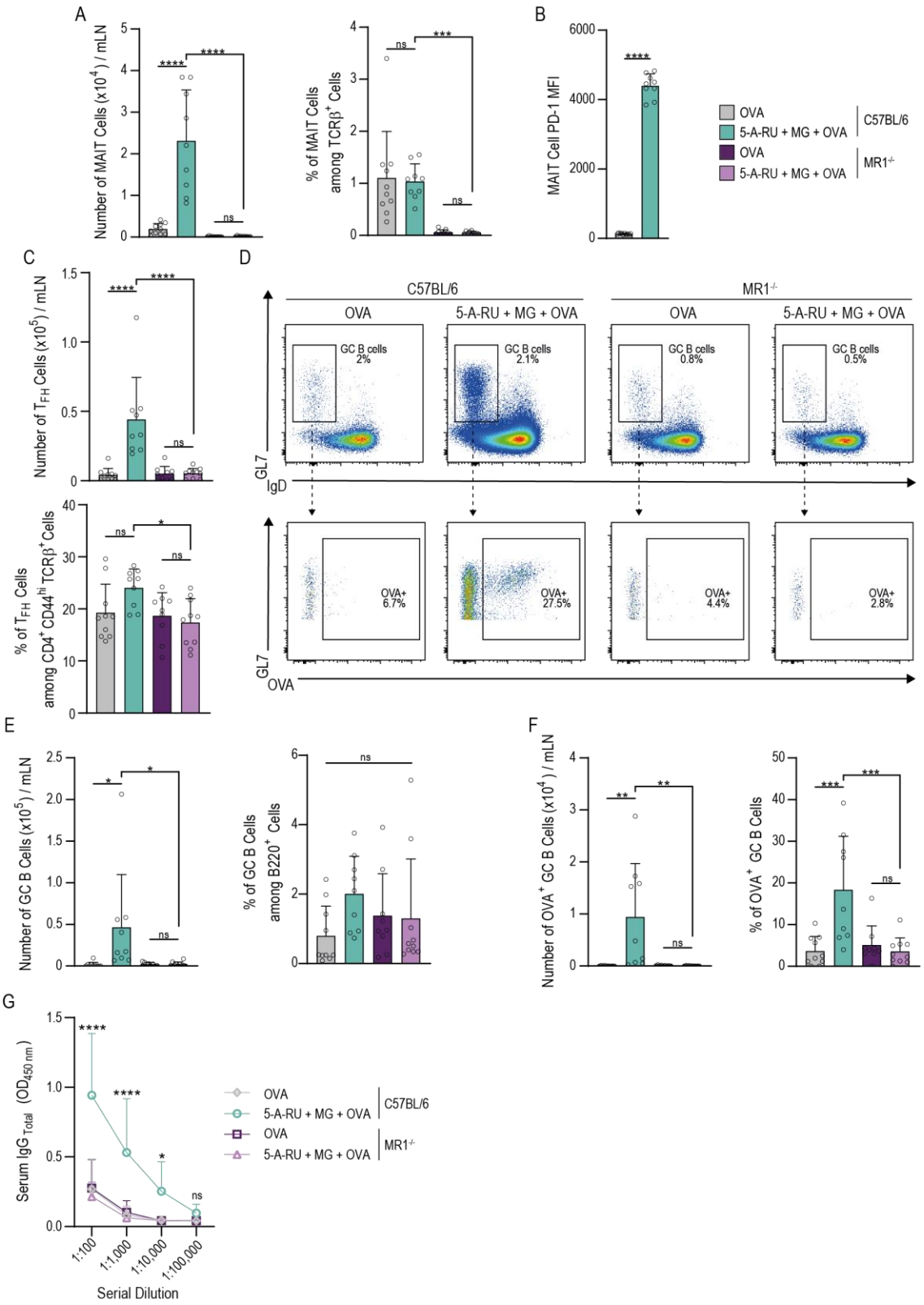
A
Number of MAIT Cells (x10⁴) / mLN
% of MAIT Cells among TCRβ⁺ Cells
B
MAIT Cell PD-1 MFI
OVA
5-A-RU + MG + OVA
C57BL/6
OVA
5-A-RU + MG + OVA
MR1-/-
C
Number of TFH Cells (x10⁵) / mLN
% of TFH Cells among CD4⁺ CD44hi TCRβ⁺ Cells
D
C57BL/6
MR1-/-
OVA
5-A-RU + MG + OVA
GC B cells 2%
GC B cells 2.1%
GC B cells 0.8%
GC B cells 0.5%
GL7
IgD
OVA+ 6.7%
OVA+ 27.5%
OVA+ 4.4%
OVA+ 2.8%
OVA
E
Number of GC B Cells (x10⁵) / mLN
% of GC B Cells among B220⁺ Cells
F
Number of OVA⁺ GC B Cells (x10⁴) / mLN
% of OVA⁺ GC B Cells
G
Serum IgG Total (OD450 nm)
1:100
1:1,000
1:10,000
1:100,000
Serial Dilution
OVA
5-A-RU + MG + OVA
C57BL/6
OVA
5-A-RU + MG + OVA
MR1-/-

Figure 4.5: Boosting the Intranasal Administration of 5-A-RU + MG + OVA Induces an Antigen Specific Antibody Response Dependent on MAIT Cells. C57BL/6 and $MR1^{-/-}$ mice were either given 3 intranasal doses of 5-A-RU + MG + OVA or OVA alone over the course of 4 weeks. 1 week following the last dose, mLNs and blood were harvested and used for flow cytometry and ELISA analysis respectively. **(A)** Number of MAIT cells per mLN and frequency among $TCR\beta^+$ cells. **(B)** MAIT cell PD-1 MFI. $MR1^{-/-}$ mice were excluded due to having no MAIT cells. **(C)** Number and Frequency of T_{FH} cells, determined by $BCL6^+$ expression. **(D)** Representative gating strategy for germinal center (GC) (defined as IgD^-GL7^+) OVA^+ B cells. Previously gated on $B220^+$ cells. **(E)** Number and frequency of GC B cells per mLN. **(F)** Number and frequency of OVA^+ GC B cells per mLN. **(G)** Serum antibody levels of total IgG isotype. Statistcial analysis was conducted using One-way ANOVA with Tukey's post hoc test, a Two-way ANOVA (G) or an unpaired T test (B). Bars represent group means with symbols as individual mice, whereas, line graph symbols represent the group mean. Error bars show the standard deviation. ns>0.05, *p≤0.05, **p≤0.01, ***p≤0.001, ****p≤0.0001. Significance stars in G represent significance between C57BL/6 admix treated and $MR1^{-/-}$ admix treated groups.

4.3.3 The Antigen-Specific Humoral Response is Dependent on Both Conventional DC1s and DC2s

As I have previously shown that conventional DC1s (cDC1s) and DC2s (cDC2s) become activated after i.n. administration of the 5-A-RU + MG admix both after one dose and three doses and that 3 doses is able to induce a humoral antigen specific response, I therefore wanted to determine whether the cDCs were involved in driving this response and whether there was a bias for one subset over the other. To investigate this, I firstly employed BATF3$^{-/-}$ mice. These mice lack CD8α^+ cDCs in the spleen, lymph nodes and thymi[244], as well as CD103$^+$CD11b$^-$ DCs in the lung[343,344], intestine, mesenteric lymph node, skin and skin draining lymph nodes[344], however, have normal development of other DC subsets. The knocked out DCs are characteristic of cDC1s. However, it has been noted that different pathogens such as *T.gondii* and *Mycobacterium tuberculosis* (Mtb) can cause the regeneration of CD8α^+ cDCs in BATF3$^{-/-}$ mice after just 10 days and 3 weeks respectively. Mtb was also able to restore CD103$^+$ cDCs in the lungs. Additionally, IL-12 administration was also able to restore CD8α^+ cDCs in BATF3$^{-/-}$ mice and these cDCs were functional at cross-presenting. It was suggested that *Batf* and *Batf2* were able to compensate for the loss of *Batf3*[345]. Due to these short comings of the BATF3$^{-/-}$ model I first characterised the cDC subsets in the mLN after i.n. administration of 5-A-RU + MG. To do this, C57BL/6 mice and BATF3$^{-/-}$ mice were either i.n. administered PBS or 5-A-RU + MG and then the mLNs were harvested two days later for flow cytometry analysis. The delayed harvest day of day 2 instead to the usual day 1, was chosen to ensure the cDC1s would not regenerate after the peak response at day 1. cDCs were split into resident and migratory cDCs based on CD11c$^+$MHCII^{int} and CD11c$^+$MHCII^{hi} expression respectively. In both the resident and migratory cDC populations, cDC1s and cDC2s were gated as SIRPα^- and SIRPα^+CD11b$^+$ respectively (figure 4.6A). The representative flow plots (figure 4.6A) along with the quantified cell numbers show an almost complete lack of cDC1s in the BATF3$^{-/-}$ mice in both the PBS and 5-A-RU + MG treated groups. There was no change in total cell numbers in the mLNs between groups and while there was also no significant difference between the number of resident cDC1s, cDC2s and migratory cDC1s, there is a defined trend towards a lack of cDC1s in

both the resident and migratory subsets of the BATF3$^{-/-}$ mice (figure 4.6C-E). The number of migratory cDC2s was elevated in the BATF3$^{-/-}$ mice after admix treatment compared to PBS (figure 4.6E). The frequency of resident and migratory cDC1s (among cDCs) showed a significant reduction in the BATF3$^{-/-}$ mice compared to the C57BL/6 mice (figure 4.6F), whereas the frequency of resident and migratory cDC2s (among cDCs) in the BATF3$^{-/-}$ admix treated mice compared to the C57BL/6 admix treated mice (figure 4.6G). The activation status of the cDC2s was also checked to determine whether this was affected by the lack of cDC1s in the BATF3$^{-/-}$ mice. In both the resident and migratory cDC2s there was no change in the CD86 and PDL-1 MFI between the PBS C57BL/6 mice compared to the PBS BATF3$^{-/-}$ mice or between the C57BL/6 admix treated mice and the BATF3$^{-/-}$ admix treated mice (figures 4.6H&I). This showed that the BATF3$^{-/-}$ mice lacked cDC1s even after the i.n. admix treatment in the mLN and that while the frequency of the cDC2s was elevated as expected in the BATF3$^{-/-}$ mice this had no effect on the activation status of these cDCs. Although, this showed the lack of cDC1s in the BATF3$^{-/-}$ mice after one dose of the 5-A-RU + MG admix, I also checked that this absence was seen in the prime-boost model. Due to limited mouse numbers only three BATF3$^{-/-}$ mice were available to treated as per the prime-boost scheme in figure 4.1, and comparably to the single dose, showed a significant reduction in frequency of cDC1s in both the resident and migratory cDCs (figure 4.6J&K).

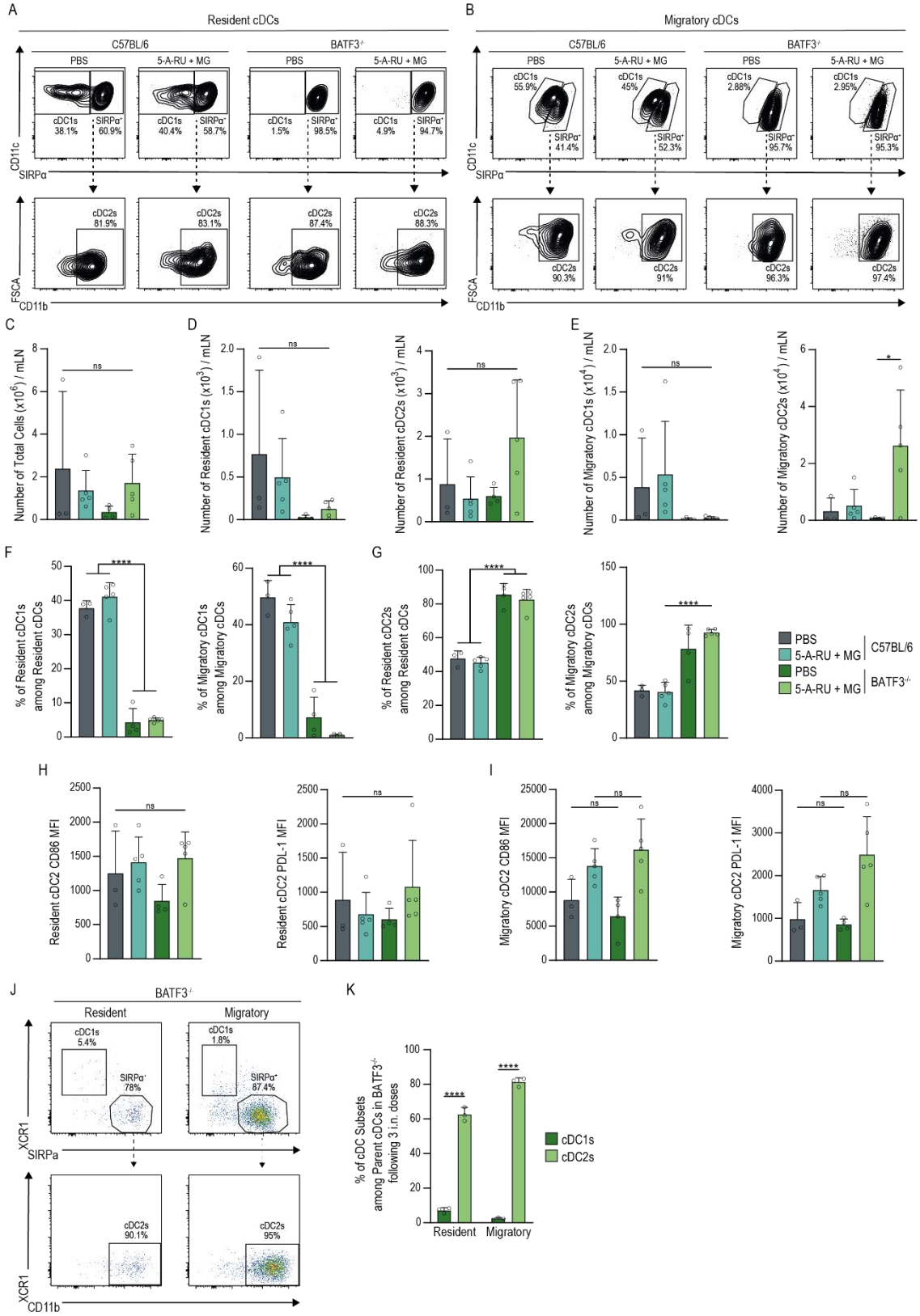
A
Resident cDCs
C57BL/6
BATF3-/-
PBS
5-A-RU + MG
cDC1s 38.1%
SIRPα+ 60.9%
cDC1s 40.4%
SIRPα+ 58.7%
cDC1s 1.5%
SIRPα+ 98.5%
cDC1s 4.9%
SIRPα+ 94.7%
CD11c
SIRPα
cDC2s 81.9%
cDC2s 83.1%
cDC2s 87.4%
cDC2s 88.3%
FSCA
CD11b
B
Migratory cDCs
cDC1s 55.9%
SIRPα- 41.4%
cDC1s 45%
SIRPα- 52.3%
cDC1s 2.88%
SIRPα- 95.7%
cDC1s 2.95%
SIRPα- 95.3%
cDC2s 90.3%
cDC2s 91%
cDC2s 96.3%
cDC2s 97.4%
C
Number of Total Cells (x10^6) / mLN
D
Number of Resident cDC1s (x10^3) / mLN
Number of Resident cDC2s (x10^3) / mLN
E
Number of Migratory cDC1s (x10^4) / mLN
Number of Migratory cDC2s (x10^4) / mLN
ns
F
% of Resident cDC1s among Resident cDCs
% of Migratory cDC1s among Migratory cDCs
G
% of Resident cDC2s among Resident cDCs
% of Migratory cDC2s among Migratory cDCs
PBS
5-A-RU + MG
C57BL/6
BATF3-/-
H
Resident cDC2 CD86 MFI
Resident cDC2 PDL-1 MFI
I
Migratory cDC2 CD86 MFI
Migratory cDC2 PDL-1 MFI
J
BATF3-/-
Resident
Migratory
cDC1s 5.4%
SIRPα+ 78%
cDC1s 1.8%
SIRPα+ 87.4%
XCR1
SIRPa
cDC2s 90.1%
cDC2s 95%
CD11b
K
% of cDC Subsets among Parent cDCs in BATF3-/- following 3 i.n. doses
Resident
Migratory
cDC1s
cDC2s

Figure 4.6: BATF3$^{-/-}$ Dendritic Cell Phenotype. C57BL/6 and BAFT3$^{-/-}$ mice were given intranasal administration of either PBS or 5-A-RU + MG admix and their mLNs were harvested two days later for flow cytometry analysis. **(A & B)** Representitiave gating stragtey for resident and migraotry cDC1s and cDC2s in the mLN. Cells were previously gated on B220^{-}TCRβ^{-}CD64^{-}CD11c^{+} and MHCII^{Int} for resident and MHCII^{hi} for migratory cDCs. **(C)** Total number of cells per mLN. **(D)** Number of resident cDC1s and cDC2s per mLN. **(E)** Number of migratory cDC1s and cDC2s. **(F)** Frequency of resident and migratory cDC1s. **(G)** Frequency of resident and migratory cDC2s. **(H & I)** Resident and migratory cDC2 CD86 and PDL-1 MFI. **(J)** BATF3$^{-/-}$ mice were given 3 doses of intranasal admix over 4 weeks with the mLNs harvested a week later. Representative gating strategy for resident and migratory cDC1 and cDC2 identification. Previously gated on B220^{-}TCRβ^{-}CD64^{-}CD11c^{+} and MHCII^{Int} for resident and MHCII^{hi} for migratory cDCs. **(K)** Frequency of cDC subsets in the mLN after 3 doses of admix. Statistcial analysis was conducted using One-way ANOVA with Tukey's post hoc test. Bars represent the mean per group, symbols are induvidual mice and error bars show the standard deviation. ns>0.05, *p≤0.05, ****p≤0.0001.

As the BATF3$^{-/-}$ mice were confirmed to have a lack of cDC1s in the mLNs after the 5-A-RU + MG admix treatment, these mice were used to determine whether cDC1s were required for the antigen specific B cell response. C57BL/6 and BATF3$^{-/-}$ mice were treated with 3 doses of 5-A-RU + MG + OVA admix over 4 weeks (figure 4.1) with the addition of OVA only in the lung and OVA only and PBS control groups in the mLN for each strain. One week following the final dose, the blood, lung tissue and mLNs were harvested for ELISA and flow cytometry analysis. The frequency of MAIT cells in the lungs was significantly elevated in the C57BL/6 admix treated mice compared to OVA only, however the MAIT cells in the BATF3$^{-/-}$ mice remained at baseline levels (figure 4.7A). Although the frequency of MAIT cells in the BATF3$^{-/-}$ admix treated mice remained equivalent to the PBS group, the MAIT cells did become activated with an increase in both CD69 and PD-1 MFI following admix treatment in the BATF3$^{-/-}$ mice. The C57BL/6 mice also showed this same activation after admix treatment, however, their activation status was slightly higher than the BATF3$^{-/-}$ mice following admix treatment (figure 4.7B). The number and frequency (among TCRβ^{+}) of the MAIT cells in the mLN showed no significant changes between groups (figure 4.7C), however, the MAIT cells in both the C57BL/6 and BATF3$^{-/-}$ admix treated groups showed an equivalent upregulation of PD-1 MFI (figure 4.7D). The number of T_{FH} cells were significantly elevated in only the C57BL/6 admix treated group, however, the frequency of T_{FH} cells among TCRβ^{+}CD4^{+}CD44^{hi} cells remained at a constant frequency across groups (figure 4.7E). The number and frequency (among B220^{+} cells) of GC B cells in the mLN also did not change between strains or treatments (figure 4.7F). Despite this, the frequency of OVA specific GC B cells only showed significant increases in the C57BL/6 admix treated mice. While the numbers of these cells statistically had no significant difference between groups, there is an obvious elevation only seen in the C57BL/6 admix treated group, whereas the BATF3$^{-/-}$ mice remain at baseline levels (figures 4.7G&H). To complement this, the serum OVA specific total IgG and IgG1 antibody isotypes were detected at significantly increased levels only in the C57BL/6 admix treated group and not the BATF3$^{-/-}$ admix treated mice (figure4.7I). Taken together, this indicates that the humoral

response induced by the i.n. prime-boost 5-A-RU + MG + OVA admix both locally in the mLN and systemically is dependent on conventional DC1s.

To ensure that the knockout of BATF3 expression would not independently affect a B cell response, the BATF3 RNA expression in B cells, $\alpha\beta$ and $\gamma\delta$ T cells and DCs was checked using the Immunological Genome Project RNA-Seq database[346]. This indicated high BATF3 expression in specific DC populations, but also showed a low expression of BAFT3 in a subset of plasmablast B cells (Supplementary figure 4A). Therefore, to ensure that the BATF3$^{-/-}$ mice were still capable to producing an equivalent IgG response to the wildtype C57BL/6 mice, both BATF3$^{-/-}$ and C57BL/6 mice were given two i.p. injections of either OVA only or OVA + alum two weeks apart. One week later serum was used for the detection of OVA specific total IgG antibodies. This showed that BATF3$^{-/-}$ mice had an equivalent IgG antibody response to the C57BL/6 mice, indicating the lack of BATF3 does not affect the mouse's ability to produce antibody (Supplementary figure 4B).

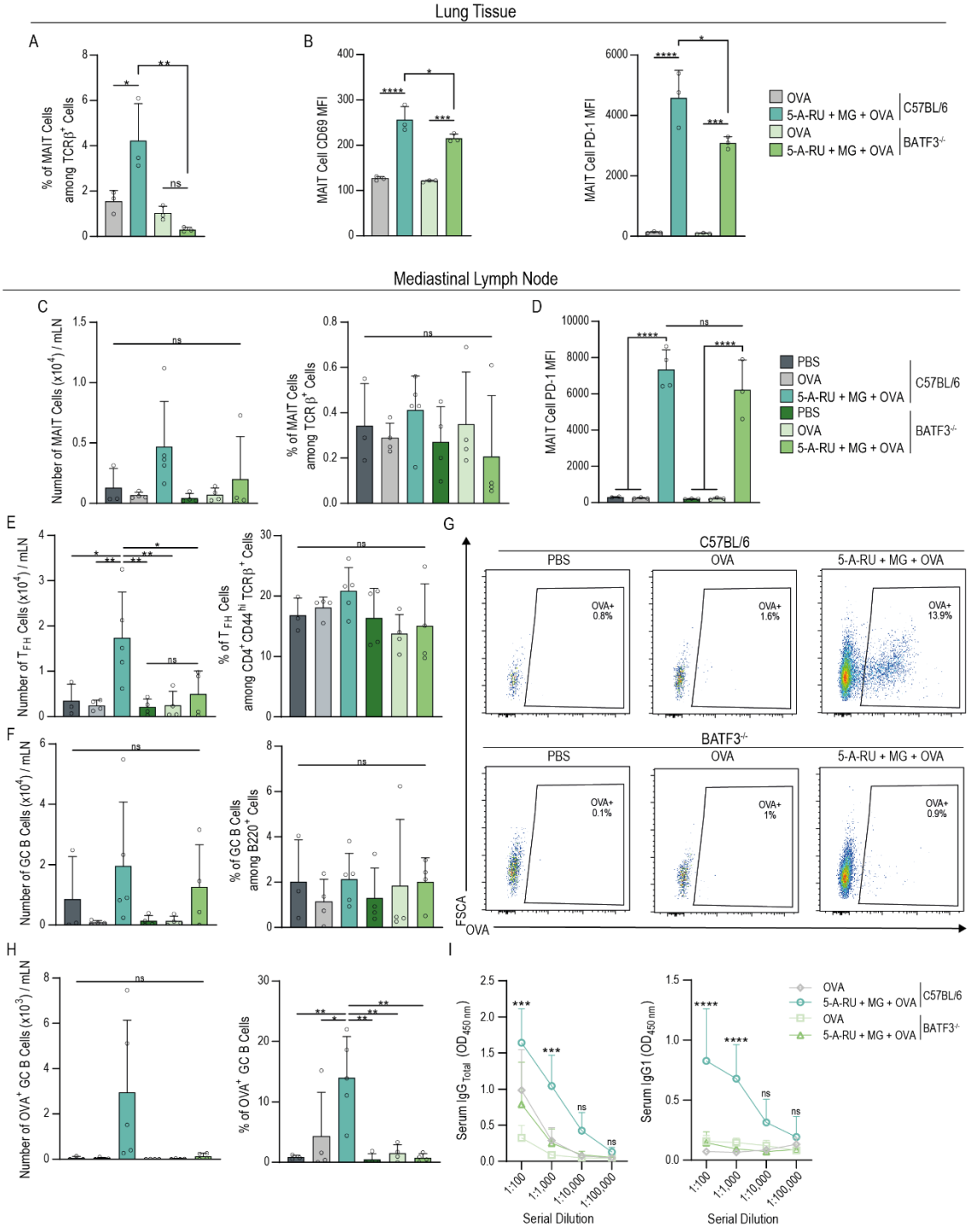
Lung Tissue
A
% of MAIT Cells among TCRβ+ Cells
B
MAIT Cell CD69 MFI
MAIT Cell PD-1 MFI
OVA
5-A-RU + MG + OVA
C57BL/6
OVA
5-A-RU + MG + OVA
BATF3-/-
Mediastinal Lymph Node
C
Number of MAIT Cells (x10^4) / mLN
% of MAIT Cells among TCRβ+ Cells
D
MAIT Cell PD-1 MFI
PBS
OVA
5-A-RU + MG + OVA
C57BL/6
PBS
OVA
5-A-RU + MG + OVA
BATF3-/-
E
Number of TFH Cells (x10^4) / mLN
% of TFH Cells among CD4+ CD44hi TCRβ+ Cells
F
Number of GC B Cells (x10^4) / mLN
% of GC B Cells among B220+ Cells
G
C57BL/6
PBS
OVA
5-A-RU + MG + OVA
OVA+ 0.8%
OVA+ 1.6%
OVA+ 13.9%
BATF3-/-
PBS
OVA
5-A-RU + MG + OVA
OVA+ 0.1%
OVA+ 1%
OVA+ 0.9%
FSCA
OVA
H
Number of OVA+ GC B Cells (x10^3) / mLN
% of OVA+ GC B Cells
I
Serum IgGTotal (OD450 nm)
Serum IgG1 (OD450 nm)
OVA
5-A-RU + MG + OVA
C57BL/6
OVA
5-A-RU + MG + OVA
BATF3-/-
1:100
1:1,000
1:10,000
1:100,000
Serial Dilution
Serial Dilution

Figure 4.7: cDC1s Contribute to the Antigen Specific Humoral Response. C57BL/6 and BATF3$^{-/-}$ mice were intranasally administered either PBS, OVA only or 5-A-RU + MG + OVA admix 3 times over 4 weeks. The following week the lung tissue, mLNs and blood were harvested for flow cytometry and ELISA analysis. **(A)** Frequency of MAIT cells in the lung. **(B)** MAIT cell CD69 and PD-1 MFI in the lung. **(C)** Number and frequency of MAIT cells in the mLN. **(D)** MAIT cell PD-1 MFI in the mLN. **(E)** Number and frequency of T_{FH} Cells (defined as B220^{-}TCRβ^{+}CD4^{+}CD44^{hi}BCL6^{+}PD-1^{+}) in the mLN. **(F)** Number and frequency of germinal center (GC) B cells (defined as B220^{+} IgD^{-}GL7^{+}) in the mLN. **(G)** Representative gating for OVA^{+} GC B cells. **(H)** Number and frequency of OVA^{+} GC B cells. **(I)** Total serum IgG and IgG1 antibody isotype levels via ELISA analysis. Statistcial analysis was conducted using One-way ANOVA with Tukey's post hoc test or a Two-way ANOVA (I). Bars represent group means with symbols as individual mice, whereas, line graph symbols represent the group mean. Error bars show the standard deviation. ns>0.05, *p≤0.05, **p≤0.01, ***p≤0.001, ****p≤0.0001. Significance stars in (I) represent significance between C57BL/6 admix treated and BATF3$^{-/-}$ admix treated groups.

Not only were cDC1s activated in the model, but also cDC2s. I therefore wanted to see whether the cDC2s also had a role in driving the humoral response. To investigate this, CD11c-Cre^{+} Irf4$^{fl/fl}$ mice were employed. These mice utilise a Cre-lox system which results in the selective ablation of IRF4 in CD11c^{+} cells, this resulting in the absence of cDC2s[245]. CD11c-Cre^{+} Irf4$^{fl/fl}$ mice and CD11c-Cre^{-} Irf4$^{fl/fl}$ mice that lack the Cre recombinase and therefore retain IRF4 expression in CD11c^{+} cells, were treated i.n. with three doses of the 5-A-RU + MG + OVA admix as described in figure 4.1. Both the lung tissue and mLNs were harvested one week following the last dose for flow cytometry analysis. The MAIT cells in the lung showed a significant increase in both frequency (among TCRβ^{+} cells) and activation (PD-1 MFI) following i.n. admix treatment in both CD11c-Cre^{+} Irf4$^{fl/fl}$ mice and CD11c-Cre^{-} Irf4$^{fl/fl}$ mice compared to their OVA only treated control groups. While there was a slightly lower MAIT cell frequency in the CD11c-Cre^{-} Irf4$^{fl/fl}$ mice compared to the CD11c-Cre^{+} Irf4$^{fl/fl}$ following admix treatment, the MAIT cells had equivalent PD-1 MFIs in these groups (figures 4.8A&B). In the mLN, the MAIT cell numbers increase only in the CD11c-Cre^{-} Irf4$^{fl/fl}$ mice after admix treatment compared to OVA only, however the frequency of MAIT cells remained constant across all groups (figure 4.8C). As in the lung tissue, the MAIT cells in the mLN also showed an increased expression of PD-1 in both the CD11c-Cre^{+} Irf4$^{fl/fl}$ mice and CD11c-Cre^{-} Irf4$^{fl/fl}$ mice treated with the admix (figure 4.8D). There was an increase in T_{FH} cells in the CD11c-Cre^{-} Irf4$^{fl/fl}$ mice after admix treatment, however, the statistical analysis found no significant difference between the CD11c-Cre^{-} Irf4$^{fl/fl}$ and CD11c-Cre^{+} Irf4$^{fl/fl}$ mice after admix treatment. Despite this, there does seem to be a trend towards a reduction in T_{FH} numbers with the lack of cDC2s. Much like in the BATF3$^{-/-}$ experiment the frequency of T_{FH} cells among TCRβ^{+}CD4^{+}CD44^{hi} cells stayed at a constant level between the groups (figure 4.8E). A similar trend was seen for both the number and frequency (among B220^{+} cells) of GC B cells which did not change across strains or treatments (figure 4.8F), but the OVA specific GC B cells did. The number of GC B cells specific for OVA protein was significantly elevated only in the CD11c-Cre^{-} Irf4$^{fl/fl}$ admix treated control group. Whereas the CD11c-Cre^{+} Irf4$^{fl/fl}$ admix treated mice had equivalent OVA specific GC B cells to baseline levels. Although there is statistically no significance

between the groups for the frequency of OVA specific GC B cells, there does seem to be a trend towards an increase in the CD11c-Cre^{+} Irf4$^{fl/fl}$ admix treated group, with the statistics potentially being influenced by the outlier in the CD11c-Cre^{+} Irf4$^{fl/fl}$ OVA only group (figures 4.8G&H). When considered with the BATF3$^{-/-}$ results, the data suggests that both conventional cDC1s and cDC2s in the mLN are involved in driving the B cell response to the 5-A-RU + MG + OVA admix. This suggests that neither of these subsets are able to compensate for the other and both are required to induce the humoral response.

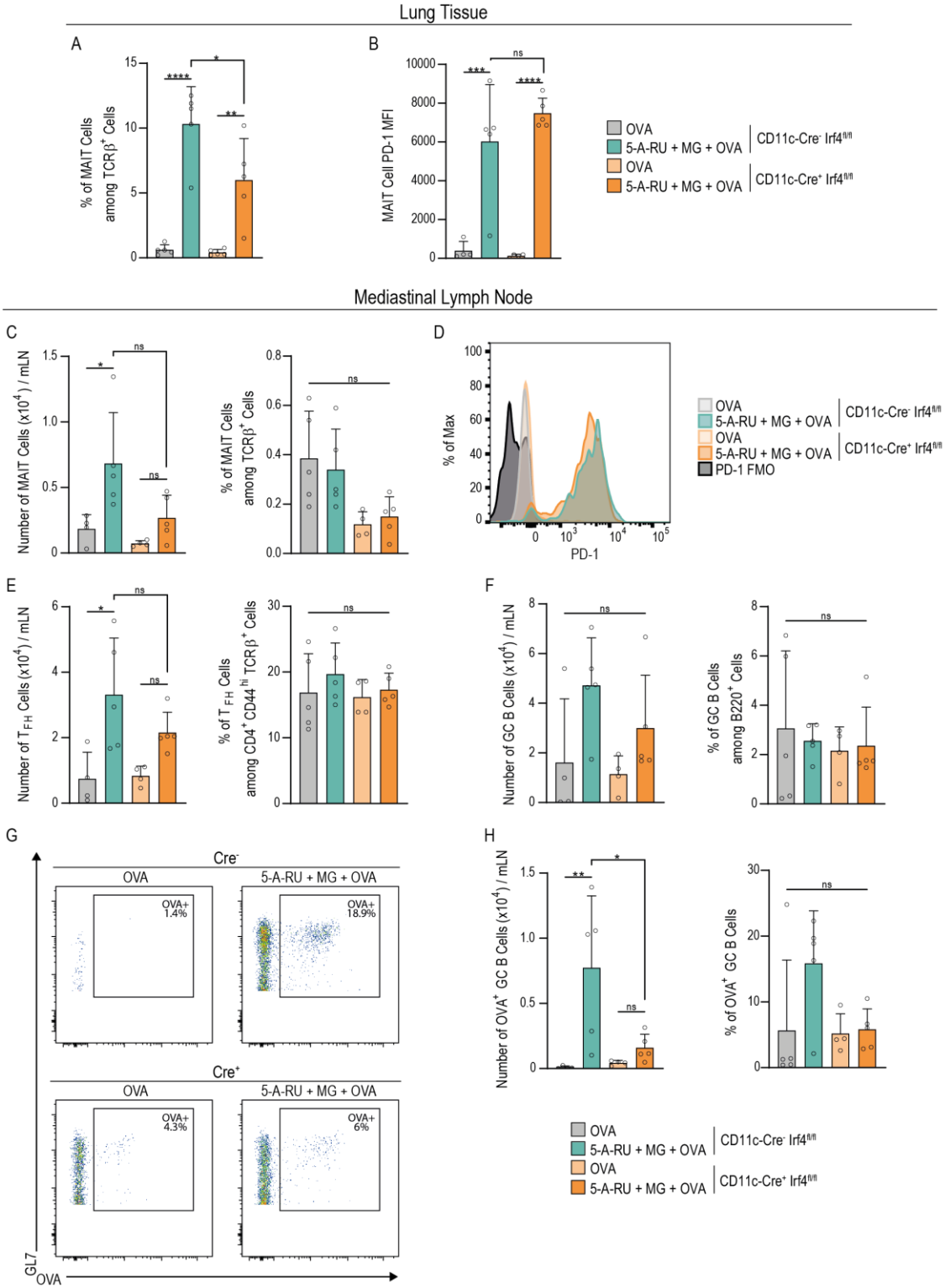
Lung Tissue
A
% of MAIT Cells among TCRβ+ Cells
B
MAIT Cell PD-1 MFI
OVA
5-A-RU + MG + OVA
CD11c-Cre- Irf4fl/fl
OVA
5-A-RU + MG + OVA
CD11c-Cre+ Irf4fl/fl
Mediastinal Lymph Node
C
Number of MAIT Cells (x10^4) / mLN
% of MAIT Cells among TCRβ+ Cells
D
% of Max
PD-1
PD-1 FMO
E
Number of TFH Cells (x10^4) / mLN
% of TFH Cells among CD4+ CD44hi TCRβ+ Cells
F
Number of GC B Cells (x10^4) / mLN
% of GC B Cells among B220+ Cells
G
Cre-
Cre+
OVA
5-A-RU + MG + OVA
OVA+ 1.4%
OVA+ 18.9%
OVA+ 4.3%
OVA+ 6%
GL7
OVA
H
Number of OVA+ GC B Cells (x10^4) / mLN
% of OVA+ GC B Cells

Figure 4.8: cDC2s Contribute to the Antigen Specific Germinal Center B Cell Response. C57BL/6 and CD11c-Cre$^{-/+}$ Irf4$^{fl/fl}$ mice were intranasally administered either OVA only or 5-A-RU + MG + OVA admix 3 times over 4 weeks. The following week the lung tissue and mLNs were harvested for flow cytometry analysis. **(A)** Frequency of MAIT cells in the lung tissue. **(B)** MAIT cell PD-1 MFI in the lung tissue. **(C)** Number and frequency of MAIT cells in the mLN. **(D)** Representative histograms showing MAIT cell PD-1 expression, normalised to mode. PD-1 FMO included for negative expression level. **(E)** Number and frequency of T_{FH} Cells (defined as B220^{-}TCRβ^{+}CD4^{+}CD44^{hi}BCL6^{+}PD-1^{+}) in the mLN. **(F)** Number and frequency of germinal center (GC) B cells (defined as B220^{+} IgD^{-}GL7^{+}) in the mLN. **(G)** Representative gating for OVA^{+} GC B cells. **(H)** Number and frequency of OVA^{+} GC B cells. Statistcial analysis was conducted using One-way ANOVA with Tukey's post hoc test. Bars represent the mean per group, symbols are induvidual mice and error bars show the standard deviation. ns>0.05, *p≤0.05, **p≤0.01, ***p≤0.001, ****p≤0.0001.

4.3.4 Investigating the Mechanism Behind the MAIT Cell and Conventional DC Response to the Intranasally Administered 5-A-RU + MG Admix

Due to the high frequency of GATA3 expression after i.n. 5-A-RU + MG admix treatment and as Kelly, J. *et al.* (2019), have previously shown MAIT cells to produce IL-13, IL-4 and IL-5[305], I wanted to determine whether the model could be driving a functional T_H2-like MAIT cell phenotype. 4C13R mice that have fluorescent reporters AmCyan and dsRed associated with the IL-4 and IL-13 cytokine production respectively[241]. The 4C13R mice were treated i.n. with 5-A-RU + MG at day 3, 7 and 11 prior to lung and mLN harvest (figure 4.9A). This timing was based on Kelly, J. *et al.* (2019), as they found IL-13 and IL-4 began to be produced by stimulated MAIT cells at days 5 and 8 respectively[305]. While the frequency of MAIT cells among TCRβ^+ cells in the lung had no significant change following treatment the PD-1 expression was upregulated, with day 3 treatment showing the highest level of expression (figures 4.9B&C). However, in the mLN there was a significant reduction in MAIT cell frequency at days 3 and 7 which may reflect the activation status of the MAIT cells as they had an increased expression of PD-1 following 5-A-RU + MG treatment (figures 4.9D&E). The MAIT cell IL-13 and IL-4 reporter expression was gated on based on a C57BL/6 control. The frequency of MAIT cells that expressed the reporters in the lung and mLN was less than 1%, with the majority of these cells being IL-4 single producers peaking at day 3 (figures 4.9F-H). These 4C13R mice bred from the same facility have previously been used and showed high reporter expression when stimulated with strong T_H2 inducing treatments[347]. This providing evidence that the reporters are functional, however, the MAIT cells in my model just express very low levels of IL-4 and IL-13. To confirm that this minimal level of IL-4 positive MAIT cells has no functional effect through T_H2 signalling pathways on the cDC activation, I used STAT6$^{-/-}$ mice. STAT6 is downstream of IL-4 receptor alpha subunit and is involved in mediating the T_H2 response[348]. STAT6$^{-/-}$ and C57BL/6 mice were treated either with PBS or 5-A-RU + MG admix intranasally and one day later the mLNs were harvested for flow cytometry. STAT6$^{-/-}$ mice showed no change in the number or frequency (among TCRβ^+) of MAIT cells compared to C57BL/6 controls (figure 4.9I). Additionally, the migratory cDCs showed equivalent upregulation of activation markers

CD86 and PDL-1 after admix treatment in the STAT6$^{-/-}$ and C57BL/6 mice. This suggests that the cDC activation in is not dependent on the STAT6 T_H2 pathway. Finally, to confirm that a T_H2 humoral response was not initiated after the prime-boost treatment scheme, mice were treated as per the treatment scheme in figure 4.1. The serum was collected and used for an ELISA to detect total IgE antibody production. As schistosomiasis infection is known to induce a strong IgE response[349], so serum from C57BL/6 mice infected with schistosomiasis was used as a positive control. The ELISA showed that the prime-boost administration of 5-A-RU + MG + OVA was unable to induce a systemic IgE antibody response (figure 4.9N). With the data taken together, it suggests that despite the high frequency of GATA3$^+$ MAIT cells, the admix treatment doesn't result in the production of T_H2 effector cytokines IL-4 and IL-13, nor activates DCs through the STAT6 T_H2 pathway, nor induces a T_H2 IgE antibody response after the prime-boost treatment scheme. Therefore, it does not seem that the MAIT cells are using a T_H2 mechanism to activate the cDCs or induce the humoral response in the vaccine model.

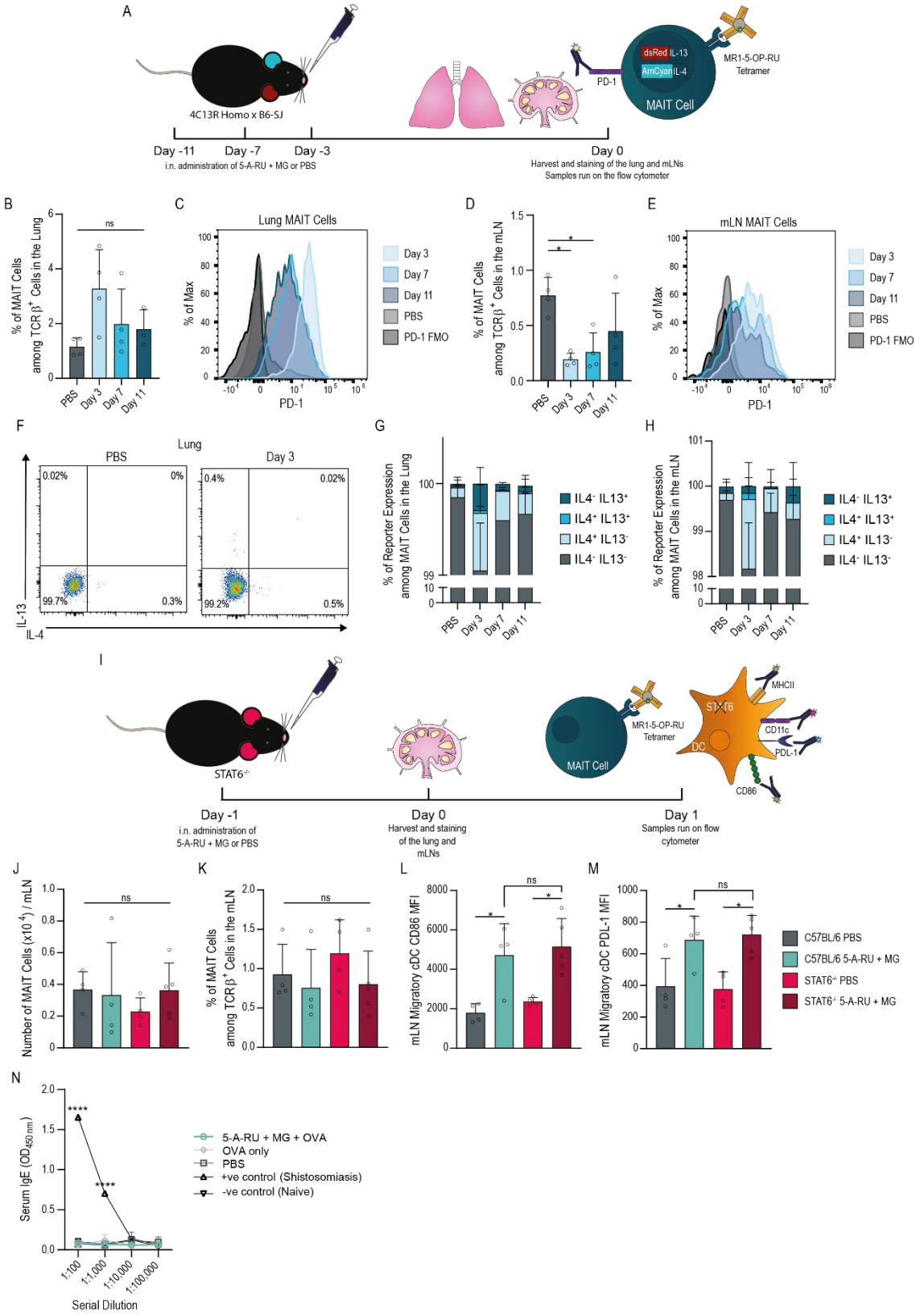
A
4C13R Homo x B6-SJ
Day -11
Day -7
Day -3
i.n. administration of 5-A-RU + MG or PBS
Day 0
Harvest and staining of the lung and mLNs
Samples run on the flow cytometer
dsRed IL-13
AmCyan IL-4
PD-1
MAIT Cell
MR1-5-OP-RU Tetramer
B
% of MAIT Cells among TCRβ+ Cells in the Lung
ns
PBS
Day 3
Day 7
Day 11
C
Lung MAIT Cells
% of Max
PD-1
Day 3
Day 7
Day 11
PBS
PD-1 FMO
D
% of MAIT Cells among TCRβ+ Cells in the mLN
E
mLN MAIT Cells
F
Lung
PBS
Day 3
IL-13
IL-4
0.02%
0%
99.7%
0.3%
0.4%
0.02%
99.2%
0.5%
G
% of Reporter Expression among MAIT Cells in the Lung
IL4- IL13+
IL4+ IL13+
IL4+ IL13-
IL4- IL13-
H
% of Reporter Expression among MAIT Cells in the mLN
I
STAT6-/-
Day -1
i.n. administration of 5-A-RU + MG or PBS
Day 0
Harvest and staining of the lung and mLNs
Day 1
Samples run on flow cytometer
MAIT Cell
MR1-5-OP-RU Tetramer
DC
STAT6
MHCII
CD11c
PDL-1
CD86
J
Number of MAIT Cells (x10-4) / mLN
K
% of MAIT Cells among TCRβ+ Cells in the mLN
L
mLN Migratory cDC CD86 MFI
M
mLN Migratory cDC PDL-1 MFI
C57BL/6 PBS
C57BL/6 5-A-RU + MG
STAT6-/- PBS
STAT6-/- 5-A-RU + MG
N
Serum IgE (OD450 nm)
5-A-RU + MG + OVA
OVA only
PBS
+ve control (Shistosomiasis)
-ve control (Naive)
1:100
1:1,000
1:10,000
1:100,000
Serial Dilution

Figure 4.9: Intranasal Administration of 5-A-RU plus MG Admix Doesn't Induce a MAIT Cell Th2-like Phenotype. (A) Treatment scheme. 4C13R Homo x B6-SJ mice were intranasally administered PBS or 5-A-RU + MG admix either 3, 7 or 11 days prior lung tissue and mLN harvest. MAIT cells were analysed through flow cytometry to identify IL-4 (AmCyan) and IL-13 (dsRed) expression on the same day as harvest. **(B)** Frequency of MAIT cells in the lung. **(C)** Representative histograms for lung MAIT cell PD-1 MFI, normalised to mode. PD-1 FMO included for negative expression level. **(D)** Frequency of mLN MAIT cells. **(E)** Representative histograms for mLN MAIT cell PD-1 MFI, normalised to mode. PD-1 FMO included for negative expression level. **(F)** Representative flow plots for lung MAIT cell IL-4 and IL-13 expression in PBS and admix treated mice 3 days prior to harvest. **(G & H)** Frequency of IL-4 and IL-13 expressing MAIT cells in the lung and mLN. **(I)** Treatment scheme of C57BL/6 and $STAT6^{-/-}$ mice. Each mouse strain had two groups, one given PBS and the other admix intranasally. 1 day later the mLN were harvested and used for flow cytometry analysis. **(J & K)** Number and frequency of MAIT cells in the mLN. **(L & M)** migratory cDCs CD86 and PDL-1 MFIs. **(N)** Serum from C57BL/6 mice treated intranasally with either PBS, OVA only or 5-A-RU + MG + OVA over 4 weeks was harvested 1 week later and used to perform an ELISA for IgE levels. Serum from schistosomiasis infected and naïve C57BL/6 mice were included as a positive and negative control respectively. Statistcial analysis was conducted using One-way ANOVA with Tukey's post hoc test or a Two-way ANOVA (N). Bars represent group means with symbols as individual mice, whereas, line graph symbols represent the group mean. Error bars show the standard deviation. ns>0.05, *p≤0.05, ****p≤0.0001. Significance stars in N represents significance between the positive control and all other groups.

To further explore the potential MAIT cell mechanisms and phenotypes that are leading to the cDC activation after administering 5-A-RU + MG admix intranasally a cell sort and qPCR analysis of the MAIT cells was done. Firstly, the MAIT cell sort required optimisation. Initially, a 12 hr time point was chosen to hopefully capture the RNA transcription before translation into the protein. However, mice treated i.n. with the 5-A-RU + MG admix yielded too few MAIT cells at 12hrs post vaccination likely due to the downregulation of the MAIT cell TCR (data not shown). A timepoint of 2 days was also trailed (data not shown) but a lung harvest of day 3 following i.n. admix administration was decided due to this previously being shown as the peak MR1-5-OP-RU tetramer staining. The samples were sorted on a BD FACSMelody^{TM}. Firstly, a purity sort was used to isolate the TCRβ^+CD44$^+$ cells. These cells had previously been gated on cells of interest, singlets, live cells and B220$^-$Ly6C$^-$CD64$^-$ cells (supplementary figure 5A). CD44 was used as it is a marker highly expressed on MAIT cells, a characteristic of their memory phenotype[204]. Next MAIT cells were isolated from the TCRβ^+CD44$^+$ cells through another purity sort. The same initial gating was used to help clean up the sample and MAIT cells were gated and sorted as MR1-5-OP-RU tetramer positive and PD-1$^+$ for the admix treated mice and PD-1$^-$ for the PBS treated mice (supplementary figure 5B). 100 MAIT cells were collected at a time, where possible multiple lots of 100 MAIT cells were sorted from the samples. An extra sample was included to check the purity of the sort. After going through these steps to isolate the MAIT cells, the sample was run again to check whether the cells isolated were in fact MAIT cells. This showed that 94.44% of the sorted MAIT cells fell within the parent T cell gate. However, as the gates were stringent to improve purity, the 5.56% of cells that did fall outside of the gates, still had the markers of MAIT cells (supplementary figure 5C). This suggesting the sorts were pure for MAIT cells.

Following the MAIT cell sort, RNA was extracted, converted to cDNA, pre-amplified for the selected gene targets and finally the prepared cDNA was used for qPCR analysis. A selection of three housekeeping genes (Gapdh, B2m and Rplp0) were first tested on extra samples. Rplp0 was chosen as the housekeeping gene for the qPCRs as it showed

the smallest expression variation between samples and it has previously been used as a housekeeping gene for MAIT cell qPCR[350]. The target genes chosen were selected based on known MAIT cell gene expression from the literature and also based on my own hypotheses of potential mechanisms. It has already been shown through RNA sequencing that murine MAIT cells can upregulate Csf2, Il17a, IL17f, Il21, Lif, Tnf, Ifng, Tnfsf11 and Il15 in mice following infection[351]. Additionally, analysis of MAIT cell proteins has identified IL-23r, ICOS[209], CD40L[236], IL-12R[352] and IL-6[353] expression. These cytokines, cytokine receptors and co-stimulatory molecules were included as targets in the qPCR analysis of the MAIT cells to determine whether any of these activation pathways may be involved in the DC activation and downstream humoral response to the admix. MAIT cells have also been shown to respond to type I IFNs both in a TCR-independent activation pathway along with IL-12 and IL-18 synergy[354] and as co-stimulation in a TCR-dependent pathway[355]. As MAIT cells can respond to type I IFNs, I wanted to determine whether they could also produce these cytokines. Furthermore, targets from the B cell-activating factor (BAFF) system that are part of the tumour necrosis factor family were also investigated. The BAFF system includes two ligands BAFF encoded by Tnfsf13b and a proliferation-inducing ligand (APRIL) encoded by Tnfsf13. The receptors for these ligands include the BAFF receptor (BAFFR) encoded by Tnfrsf13c and the transmembrane activator and calcium-modulating cyclophilin ligand interactor (TACI) encoded by Tnfrsf13b. BAFF binding to BAFFR is important for B cell survival whereas BAFF and APRIL binding to TACI can generate plasma B cells and induce the isotype switching and production of immunoglobulin independent of T cells[356]. Due to their important role in B cell responses these targets were also investigated in the qPCR analysis. The qPCR analysis only showed a significant difference in the relative Icos expression of the MAIT cells between the PBS and 5-A-RU + MG admix treated mice. Following the admix treatment the MAIT cells had reduced Icos expression (figure 4.10L). All other target genes that had a detectable signal in the MAIT cells (Il17a, Il17f, Il15, Tnf, Ifna, Ifnb1, Lif, Csf2, Il12rb1, Il23r, Cd40lg, Tnfsf11, Tnfsf13b and Tnfrsf13c) showed no significant difference in expression between the PBS and admix treated mice (figures 4.10A-K&M-O). However, targets such as Il17a, seems to show a trend towards

an increased expression after the admix treatment (figure 4.10A). Due to this and the low sample numbers, it would be interesting to both repeat and extend the sample sizes in a future experiment. Gene targets Il6, Il21, Il12rb2, Ifng, Tnfrsf13b and Tnfsf13 were also included in the qPCR but had undetectable signals (data not shown).

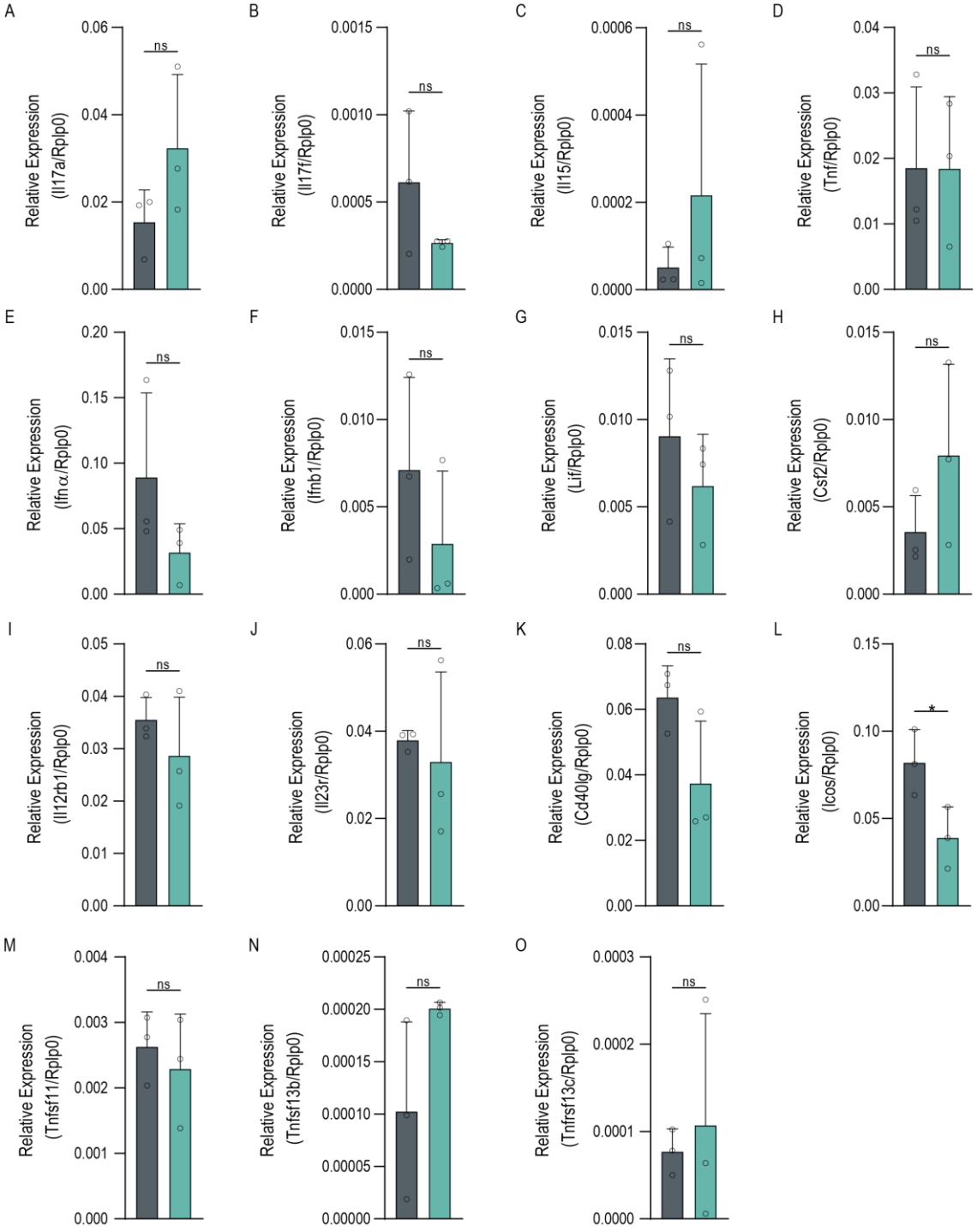

Figure 4.10: MAIT Cell RNA Expression Levels of Target Genes. MAIT cells were sorted and isolated from mice treated 3 days after intranasal administration of either PBS or 5-A-RU + MG admix. Each sample contained 100 MAIT cells with a duplicate for each mouse (except 1 mouse in admix group). RNA was then extracted, converted to cDNA, pre-amplified with target primers and finally a qPCR was conducted. **(A-O)** Relative expression of the identified target gene compared to the Rplp0 housekeeping gene. Each sample was run in duplicate for the given target gene and the average cycle threshold used. Statistcial analysis was conducted using unpaired T tests. Bars represent the mean per group, symbols are the average of duplicte samples from induvidual mice and error bars show the standard deviation. ns>0.05, *p≤0.05.

MAIT cells from murine lungs have already been shown to express high levels of ICOS in a naïve state, unlike the low expression at steady state seen in conventional T cells. Additionally, ICOS is important in an infection setting to drive the accumulation of MAIT cells in the lung[209]. ICOS is clearly an important co-stimulatory pathway for MAIT cell responses. ICOS expression on conventional T cells is well known for its co-stimulatory functions, where it becomes upregulated on the cell surface following antigen stimulation of the T cell and enhances proliferation, cytokine secretion and expression of cell-cell interaction molecules[357]. It has also been linked with both the induction[358] and inhibition[359] of a T_H1 response, driving a T_H2 response[360] and T_{FH} cell differentation[361]. ICOS binds to the ICOS ligand (ICOSL) which is expressed on B cells. T cells expressing ICOS bind to ICOSL on B cells and this interaction is essential for the survival and maturation of GC B cells[314]. DCs are also involved in this pathway, with conventional CD8α^- DCs inducing antigen specific T_{FH} cells through ICOSL and OX40L signalling, which in turn leads to the development of a humoral response[362]. I therefore wanted to determine whether the ICOS co-stimulatory pathway was involved in the model. Leading on from the qPCR findings, the ICOS protein expression on MAIT cells in the lung and mLN was determined after i.n. 5-A-RU + MG administration via flow cytometry. C57BL/6 mice were either administered 5-A-RU + MG or PBS i.n. and one day later the lung tissue and mLN was harvested. The ICOS protein expression on the cell surface of the MAIT cells reflected what was seen in the qPCR analysis, with the ICOS expression being significantly reduced following admix treatment (figures 4.11A&B). This downregulation may link with the activation status of the MAIT cells as like MAIT cells ICOS expression, B cells also have high expression of ICOSL in a naïve state, however, following BCR stimulation, ICOSL expression becomes downregulated[363]. I was also able to show that ICOSL expression on cDCs increased at 12 hrs following i.n. admix treatment and returned to baseline levels at 24 hrs in the lung (figure 4.11A). However, no change was seen with the migratory cDC ICOSL MFI in the mLN (figure 4.11B). The increase ICOSL expression on the cDCs in the lung, contrasts to the MAIT cells down regulation of ICOS. This opposite relationship may be linked to a negative feedback

relationship seen when ICOS overexpression leads to ICOSL downregulation[364]. From this data it seems ICOS expression could be used as an additional marker of activation.

Due to the admix causing alterations in the ICOS co-stimulatory pathway in the initial response with cDCs and MAIT cells and due to the known function of this pathway in T_{FH} and B cell responses, I hypothesised that the ICOSL expression on the lung DCs may be a mechanism influencing the downstream adaptive response. I therefore wanted to determine what the initial controls of ICOSL expression may be involved and how the MAIT cell and DC initial responses could be affected. CD40 signalling has been shown to both restore[363] and also upregulate ICOSL expression on B cells[365,366]. Supporting a role for CD40 signalling in the regulation of ICOSL expression. The literature also shows that MAIT cells are able to drive the maturation of monocyte-derived and primary DCs through a CD40L-dependent mechanism in vitro[236]. Given this literature, I wanted to determine whether the CD40-CD40L interaction could be regulating the ICOSL expression on the cDCs. To investigate this, α-CD40L blocking antibodies (500 μg) were administered i.p. 12 hrs prior to i.n. 5-A-RU + MG treatment, 1 hr later, to allow for anaesthetic recovery, a second 250 μg dose of the α-CD40L was administered i.p. to C57BL/6 mice. This treatment regime was completed for two time points, one where the i.n. admix treatment was given 24 hrs prior to the harvest and the other at 12 hrs prior to the harvest (figure 4.11C). These two timepoints were chosen as the cDCs in the lung had expression of ICOSL at 12 hrs and to analyse the MAIT cells a 24 hr timepoint is required as the TCR expression is low at 12 hrs making it difficult to assess MAIT cells with the MR1-5-OP-RU tetramer. The blocking of CD40L resulted in a reduction in the frequency of cDC among $B220^{-}TCR\beta^{-}$ cells in the lung at both 12 and 24 hr timepoints (figure 4.11D). The blocking of CD40L was also able to significantly reduce the ICOSL MFI on cDCs in the lung at 12hrs, however, the MFI was back to the same level as the admix treated control by 24 hrs in the lung (figure 4.11E). However, the blocking of the CD40L interaction did not affect the cDC CD86 MFI, or ICOS MFI on MAIT cells in the lung (figures 4.11F&G). In three independent experiments, unlike in the lung, there was no elevation in ICOSL expression on cDCs in the mLN after admix treatment. This is also

seen here, where there was only baseline expression across all groups for both migratory and resident cDCs in the mLN (figures 4.11H&I). Despite this, the migratory cDC CD86 MFI was reduced at 12 hrs following α-CD40L treatment (figure 4.11H), but no change was seen in the resident cDC CD86 MFI (figure 4.11I) which is consistent with the common trend seen throughout, where the resident cDC don't have elevated CD86 expression after admix treatment. Blocking the CD40-CD40L interaction didn't affect the MAIT cell numbers, frequencies (among TCRβ$^+$ cells) or the ICOS and CD69 MFIs at either timepoints in the mLN (figures 4.11J&K). Taken together, the data suggests blocking CD40L has no effect on MAIT cell activation but does play a role in cDC ICOSL expression in the lung and migratory cDC activation in the mLN.

As a continuation of the α-CD40L experiment, I also wanted to investigate whether another co-stimulatory pathway, RANK-RANKL, may be involved in the MAIT cell and cDC relationship. The RANKL gene, Tnfsf11, had previously been shown to be upregulated in MAIT cells during the resolution phase of *Legionella longbeachae* infection[351]. Additionally, RANK, the receptor of RANKL, is upregulated on activated DCs and RANKL is able to drive DCs to induce T cell proliferation and survival in vitro[316]. That has also been supported in vivo, with ex vivo RANKL treated DCs injected back into mice, induces an accumulation of antigen positive DCs in the draining lymph nodes leading to improved primary and memory T cell responses in vivo[317]. Additionally, RANK shows sequence homology with CD40[316] and like CD40 can signal through tumour necrosis factor receptor associated factors (TRAF) signal transducers, to activate NF-κB pwathways[367,368]. Although, the qPCR results showed no change in relative expression of Tnfsf11 following admix treatment, this was at day 3 post admix treatment, hence wouldn't capture the initial MAIT cell responses. I therefore hypothesised that the RANK-RANKL pathway may be involved in the cDC activation and due to the homology with CD40, may also be involved in ICOSL expression on cDCs. To investigate this, C57BL/6 mice were treated in the same experiment as the α-CD40L treatment. Mice received 500 μg α-RANKL blocking antibody i.p. and 12 hrs later were administered 5-A-RU + MG intranasally, then 1 hr later received a second 250 μg dose of α-RANKL. Two

time points of 12 hrs and 24 hrs after the i.n. admix treatment were chosen for the harvest of the lung tissue and mLNs. Control mice only received the 5-A-RU + MG admix or PBS (figure 4.12A). Blocking of RANKL, resulted in no change in cDC frequencies (among $B220^{-}TCR\beta^{-}$ cells) or CD86 MFI, however, did cause a reduction in cDC ICOSL MFI at 12 hrs in the lung (figures 4.12B-D). The recurring reduction in ICOS MFI in MAIT cells was also seen after admix treatment but did not change with the RANKL blocking (figure 4.12E). Much like the α-CD40L data there was no change in the migratory and resident cDC ICOSL express, which remained at baseline levels throughout the different treatments and timepoints. Additionally, the migratory and resident cDC CD86 MFI didn't change (figures 4.12F&G). However, there was a trend towards a decreased CD86 MFI in the migratory cDCs at 24 hrs with α-RANKL treatment. While this is not significant, it does show similar trends to the α-CD40L. Furthermore, the blocking of RANKL didn't affect the MAIT cell numbers or frequencies among $TCR\beta^{+}$ cells in the mLN (figure 4.12H). Interestingly, the blocking of RANKL did increase the MAIT cell ICOS and CD69 MFI at 12 hrs (figure 4.12I). In the blocking experiment, the ICOS expression on the MAIT cells was seen to reduce at 12 hrs and was back up by 24 hrs, unlike the previous experiments which shown a downregulation at 24 hrs and 3 days for the RNA expression. This may suggest the window for changes in ICOS is broad and not finely controlled but needs further investigation. Together, this data suggests similar roles of RANKL and CD40L signalling with the blocking causing reduction in ICOSL expression in the lung and a trend towards reducing CD86 expression in the mLN. However, RANKL also seems to be negatively associated with MAIT cell activation in the mLN.

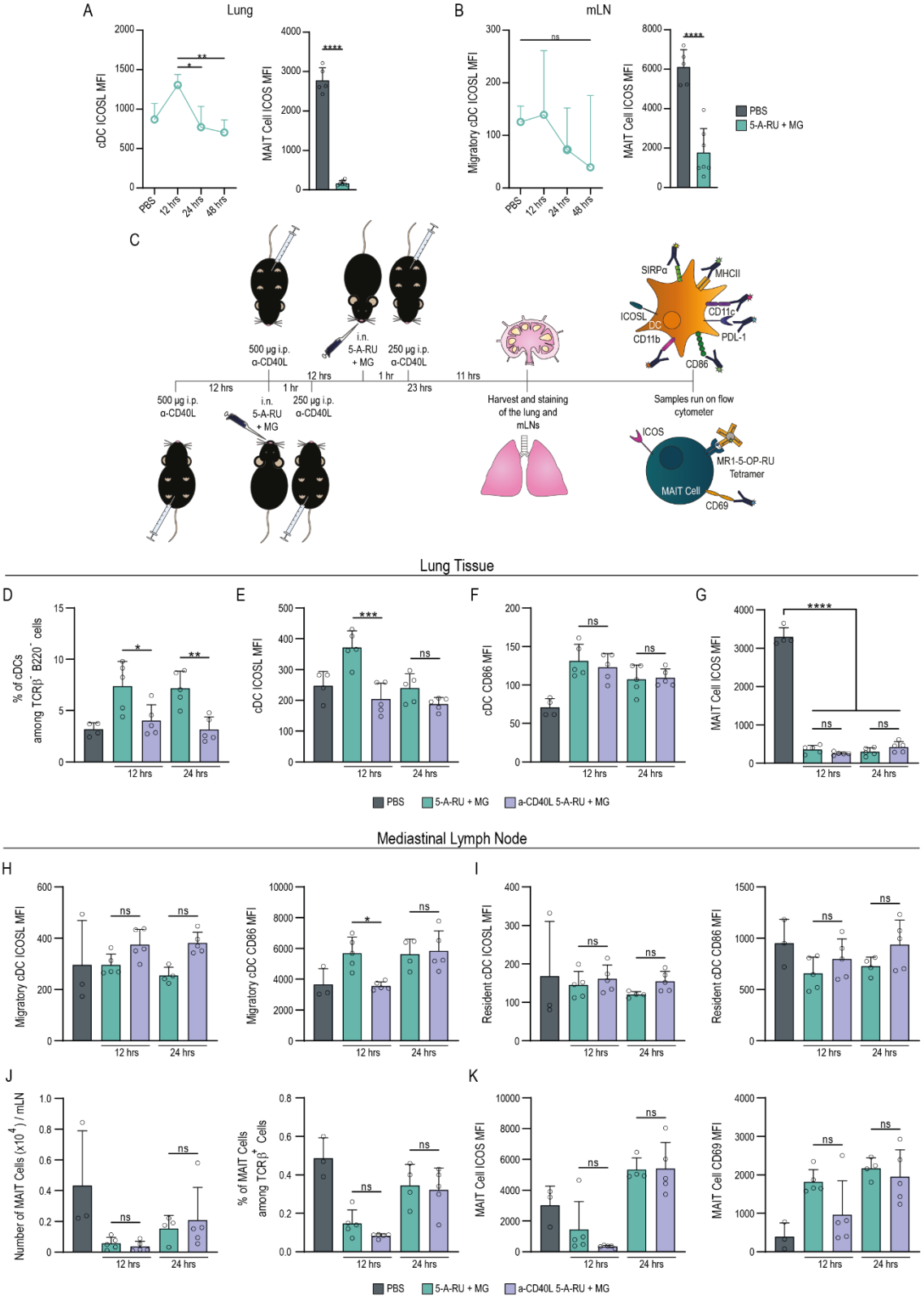
A
Lung
cDC ICOSL MFI
MAIT Cell ICOS MFI
PBS
12 hrs
24 hrs
48 hrs
B
mLN
Migratory cDC ICOSL MFI
MAIT Cell ICOS MFI
PBS
5-A-RU + MG
C
500 µg i.p. α-CD40L
i.n. 5-A-RU + MG
250 µg i.p. α-CD40L
12 hrs
1 hr
23 hrs
11 hrs
Harvest and staining of the lung and mLNs
Samples run on flow cytometer
SIRPα
MHCII
ICOSL
CD11c
DC
CD11b
PDL-1
CD86
ICOS
MR1-5-OP-RU Tetramer
MAIT Cell
CD69
Lung Tissue
D
% of cDCs among TCRβ⁻ B220⁻ cells
E
cDC ICOSL MFI
F
cDC CD86 MFI
G
MAIT Cell ICOS MFI
PBS
5-A-RU + MG
a-CD40L 5-A-RU + MG
Mediastinal Lymph Node
H
Migratory cDC ICOSL MFI
Migratory cDC CD86 MFI
I
Resident cDC ICOSL MFI
Resident cDC CD86 MFI
J
Number of MAIT Cells (x10⁴) / mLN
% of MAIT Cells among TCRβ⁺ Cells
K
MAIT Cell ICOS MFI
MAIT Cell CD69 MFI
PBS
5-A-RU + MG
a-CD40L 5-A-RU + MG

Figure 4.11: ICOSL Expression on Lung Conventional Dendritic Cells is Dependent on CD40L Co-stimulatory Interactions. **(A & B)** C57BL/6 mice were treated intranasally with either PBS or 5-A-RU plus MG. For DC data mice were treated either 12 hrs, 24 hrs or 48 hrs prior to the experiment endpoint, whereas for the MAIT cell data mice were treated 24 hrs prior to the experiment endpoint. **(A)** Conventional dendritic cell (cDC) ICOSL median fluorescence intensity (MFI) and MAIT cell ICOS MFI in the lung. **(B)** Migratory cDC ICOSL MFI and MAIT cell ICOS MFI in the mLN. **(C)** Treatment scheme for administration of α-CD40L antibodies. **(C-K)** C57BL/6 mice were administered 500 µg of α-CD40L antibody intraperitoneally (i.p.) 12 hrs before intranasal (i.n.) administration of 5-A-RU + MG. Mice were then given a second 250 µg dose of the antibody i.p. 1 hr after i.n. treatment. Two time points were chosen, one at 12 hrs and the other at 24 hrs post i.n. treatment for the tissue harvest of the lung and mLNs. **(D)** Frequency of cDCs among $TCR\beta^{-}B220^{-}$ cells in the lung. **(E & F)** cDC ICOSL and CD86 MFI in the lung tissue. **(G)** MAIT cell ICOS MFI in the lung. **(H)** Migratory cDC ICOSL and CD86 MFI in the mLN. **(I)** Resident cDC ICOSL and CD86 MFI in the mLN. **(J)** The number and frequency of MAIT cells in the mLN. **(K)** MAIT cell ICOS and CD69 MFI in the mLN. Statistcial analysis was conducted using One-way ANOVA with Tukey's post hoc test, or an unpaired T test. Bars represent group means with symbols as individual mice, whereas, line graph symbols represent the group mean. Error bars show the standard deviation. ns>0.05, *p≤0.05, **p≤0.01, ***p≤0.001, ****p≤0.0001.

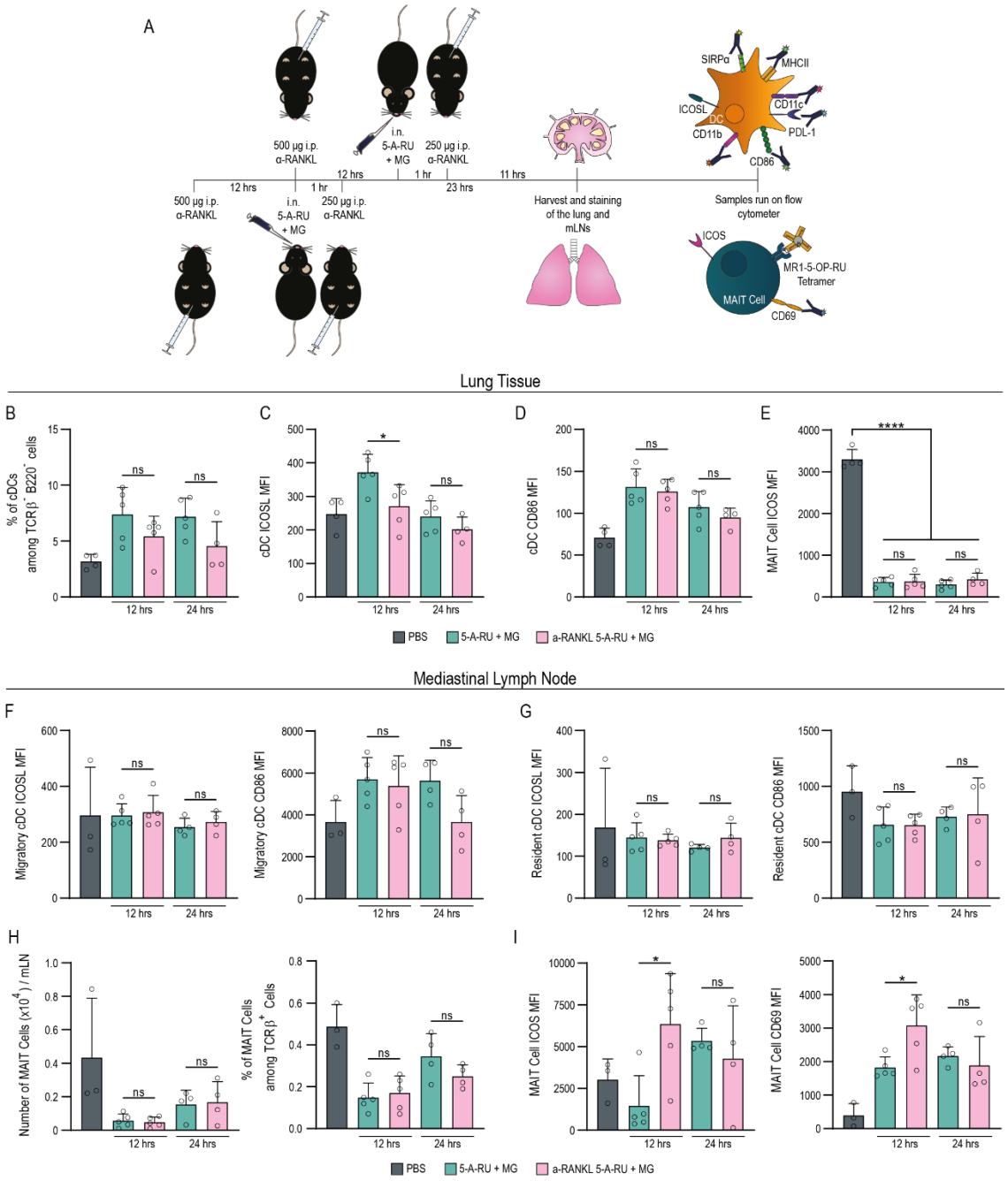

Figure 4.12: ICOSL Expression on Lung Conventional Dendritic Cells is Dependent on RANKL Co-stimulatory Interactions. **(A)** Treatment scheme for administration of α-RANKL antibodies. C57BL/6 mice were administered 500 µg of α-RANKL antibody intraperitoneally (i.p.) 12 hrs before intranasal (i.n.) administration of 5-A-RU + MG. Mice were then given a second 250 µg dose of the antibody i.p. 1 hr after i.n. treatment. Two time points were chosen, one at 12 hrs and the other at 24 hrs post i.n. treatment for the tissue harvest of the lung and mLNs. **(B)** Frequency of cDCs among TCRβ$^-$B220$^-$ cells in the lung. **(C & D)** cDC ICOSL and CD86 MFI in the lung tissue. **(E)** MAIT cell ICOS MFI in the lung. **(F)** Migratory cDC ICOSL and CD86 MFI in the mLN. **(G)** Resident cDC ICOSL and CD86 MFI in the mLN. **(H)** The number and frequency of MAIT cells in the mLN. **(I)** MAIT cell ICOS and CD69 MFI in the mLN. Statistcial analysis was conducted using One-way ANOVA with Tukey's post hoc test. Bars represent group means with symbols as individual mice. Error bars show the standard deviation. ns>0.05, *p≤0.05, ****p≤0.0001.

4.4 Discussion

The idea of innate 'trained immunity' differs from the classic sense of immune memory seen in T and B lymphocytes as it's seen in innate cells and involves stimulation of germline encoded receptors and cytokines. Due to this germline characteristic, innate memory is not specific to a given pathogen, but induces a general enhancement in the response to a secondary stimuli as a result of epigenetic changes[327]. For example, monocytes primed or 'trained' with *C. albicans* produce significantly higher levels of cytokines such as TNF-α and IL-6 upon secondary stimulation with *C. albicans* compared to non-primed monocytes[369]. Additionally, mice were first primed with a low dose of *C. albicans* followed by a second lethal dose or were given just the second lethal dose. This showed that in a Rag1$^{-/-}$ mice, which have defective T and B lymphocytes, the primed mice had improved survival, whereas in CCR2$^{-/-}$ mice, which have defective monocytes, both the primed and non-primed infections resulted in equivalent poor survival[369]. This suggesting a role for 'trained' monocytes in this protection. While innate cells such as monocytes, macrophages and NK cells have shown a 'trained' immunity phenotype[327], DCs have not been intensely investigated for this memory phenotype. Hole, C. *et al.* (2019), did suggest DCs could present a 'memory-like' phenotype in vivo, however, due to some experiments only enriching for CD3^{-}F4/80^{-} cells it is likely that what was defined as DCs also contained other cell subsets[370]. I was unable to detect any enhanced cDC activation capability when mice were administered with one dose of 5-A-RU + MG intranasally compared to three doses. There seems to be no improvement in activation following the priming of mice with the vaccine. However, implementing activation markers to determine this 'trained' immunity may not be the optimal readout. Effector cytokine production or mRNA expression as shown in previous literature may have been a more compelling readout[369,371]. Additionally, the lack of an improved DC activation response following priming in our model, may also be due to the lack of PAMPs in the admix vaccine. It is unlikely that the vaccine would induce strong PRR stimulation as it doesn't contain pathogenic antigens and it seems this may be a major player in inducing trained immunity as in the literature it is often studied in the context of an infection

model[327,369,371] and it has been shown that stimulation of different PRRs results in a 'trained' immunity phenotype[372].

Although a T_H2 response is associated with allergy[373], Alum is a successful adjuvant which also induces a dominant T_H2 response. Alum induces a T_H2 $CD4^+$ T cell response[374], IgG1 and IgE antibody production[375] and IL-4, IL-5 and IL-13 cytokine production[376]. While alum is the most widely used adjuvant in vaccines[19], it can also be used as an inducer of allergic inflammation in animal models due to its T_H2 phenotype[377,378]. This along with the dominant IgG1 antibody production and high GATA3 positive MAIT cells in our model which is typically associated with T_H2 induction[173], suggested that the model could be working through a T_H2 system. However, despite the high level of GATA3 expression, it did not result in a functional T_H2 response. Less than 1% of the MAIT cells were positive for IL-4 and/or IL-13 production, the lack of STAT6 had no effect on DC activation and there was no production of IgE in the serum after a prime-boost administration of the 5-A-RU + MG + OVA i.n. vaccine. MAIT cells have previously been investigated for a T_H2 phenotype, in vitro stimulation of MAIT cells with PMA and ionomycin or anti-CD3 and CD28 antibodies for 48 hrs showed no IL-4, IL-5 or IL-13 production[379]. Additionally, GATA3 is notoriously difficult to stain for in human cells with no expression found in MAIT cells[281]. However, a recent study by Kelly, J. *et al.* (2019), found that after tong term chronic stimulation with anti-CD3 and CD28 antibodies, phytohaemagglutinin, IL-2 and IL-7 for two weeks induced a strong IL-13 and IL-5 production along with a weaker IL-4 production in MAIT cells. They also assessed GATA3 gene expression and found MAIT cells did express GATA3 but the levels of expression didn't change between the unstimulated and stimulated cells[305]. The MAIT cells in our model reflect this unstimulated phenotype, where they have baseline GATA3 expression with no functional output of T_H2 effector cytokines or IgE antibodies. This may be a reflection of the vaccine providing only an MR1 metabolite and no additional signals as seen in the chronic stimulation, which is also reflected by the lack of effector Tbet expression in the model. While, GATA3 is commonly considered as the T_H2 inducing transcription factor, it also has been shown to have an important role in survival of $CD4^+$

T cells, T cell commitment in early development and NKT cell development and function[380]. This background homeostatic role may support the baseline levels of GATA3 we see in the MAIT cells with no association with an effector T_H2 response.

An important pathway to induce a long lasting humoral response in vaccination is the induction of T_{FH} cell differentiation by DCs, which allows for the germinal center reaction involving the T_{FH} cells driving B cell affinity maturation, isotype switching and memory cell production[145,156,319,381]. I was able to show that the prime-boost vaccine administration was able to induce conventional $CD4^+$ T cell activation in the lung and prime a T_{FH} response in the mLN. The lack of effector cytokine production in the conventional $CD4^+$ T cells in the model was unsurprising as the vaccine doesn't contain PAMPs and doesn't drive strong effector phenotypes in the MAIT cells which are the main target. Although the vaccine doesn't induce Tbet and RORγT effector functions it does support the accumulation of T_{FH} cells in the mLN. This is like the adjuvant MF59 which is able to promote an increase in T_{FH} cells in draining lymph nodes and drive antigen-specific germinal center B cells[382]. Additionally, there does also seem to be a trend towards an increase in OVA-peptide specific T_{FH} cells. Despite the low level of staining for the two OVA peptides (HAAHAEINEA and AAHAEINEA) this is only identifying the T_{FH} cells specific to these two OVA peptides, however, the processing of proteins such as OVA in the APC cell would result in more T cell epitopes due to different enzymatic reactions[240] that are not identified by the specific epitopes on these tetramers. The staining that was present for OVA-peptide specific T_{FH} cells would suggest that the vaccine is able to induce an antigen-specific T_{FH} response but doesn't seem to drive other conventional $CD4^+$ T cell responses such as T_H1 or T_H17 or cellular $CD8^+$ T cell responses.

MAIT cells ability to induce a B cell response has been previously investigated. Leung, D. *et al.* (2014), were able to identify that an increase in MAIT cell frequencies correlated with an increase in LPS specific IgA and IgG antibodies in cholera infected patients[383]. An in vitro study was also able to show that supernatant from MAIT cells incubated with

APCs and *E. coli* was able to induce plasmablast expansion of B cells and IgA, IgG and IgM antibody production. Indicating a more direct relationship between the two cell types[384]. Additionally, Murayama, G. *et al.* (2019), were able to link MAIT cells with the production of autoantibodies in a model of lupus. They crossed FcγRIIb$^{-/-}$*Yaa* mice, a spontaneous lupus mouse model, with MR1$^{-/-}$ mice. The lack of MAIT cells resulted in a reduction in disease severity, GC B cells, T_{FH} cells, effector T cells and cytokine production and autoantibody production. Furthermore, they were able to show direct MAIT cell interaction with B cells. Co-culture of MAIT cells with B cells isolated from FcγRIIb$^{-/-}$*Yaa* mice along with LPS stimulation induced an elevated IgG and autoantibody production that was partially dependent on CD40-CD40L and TCR-MR1 interactions[284]. These studies support my findings, which also shows that MAIT cells are able to induce a humoral response. While the previous studies indicate this relationship in disease settings, I was able to show that the intranasal administration of 5-A-RU + MG + OVA was able to induce antigen specific GC B cells and a systemic OVA specific IgG antibody response. Moreover, this humoral response was dependent on MAIT cells. Taken together with the current literature, it seems MAIT cells have the capacity to drive humoral responses both through indirect cytokine production and direct interactions.

The type of DC subset activated by a vaccine can determine the outcome of the adaptive immune response[337,338]. I therefore wanted to determine whether the cDC1s and cDC2s that are activated after i.n. administration of 5-A-RU + MG, were involved in driving the humoral response to our prime-boost vaccination scheme and whether the response was more dependent on one subset over the other. To assess cDC1 function in our model, I used BATF3$^{-/-}$ mice. These mice have been previously shown to lack CD8α^+ cDCs in secondary lymphoid tissues[244] and CD103$^+$CD11b$^-$ DCs in peripheral tissues and draining lymph nodes[344]. However, these mice are not a perfect model and have shown in some cases to restore cDC1s[345]. Despite this short fall, I was able to show an absence of cDC1s in the mLN both after one dose of 5-A-RU + MG and three doses of 5-A-RU + MG + OVA admix. This giving me confidence that this specific DC subset was absent in the model and specific tissue, allowing for analysis of the dependence of cDC1s in the

humoral response. An interesting observation in these mice, showed that following our prime-boost model, there was a lack of MAIT cell accumulation in the lung and a slightly lower MFI for CD69 and PD-1 compared to the wildtype C57BL/6 mice after admix treatment. This could be due to the constitutive IL-12 expression found in BATF3-dependent migratory ($CD11c^{+}MHCII^{hi}$) $CD103^{+}$ DCs[298], which would be considered as migratory cDC1s which would constitute some of the lung cDC1s. As IL-12 is known to be involved in the TCR-independent activation of MAIT cells[224], the reduction in accumulation and activation in the MAIT cells may be due to the lack of the constitutive IL-12 producing cDC1s in the $BATF3^{-/-}$ mice. However, this reduction in MAIT cell activation was only seen in the lung and not mLN. Alternatively, it could be that the cDC1s in the lung are partially involved in the initial priming of the MAIT cells and presentation of the agonist via MR1, leading to the reduction in accumulation and activation.

Through implementing the $BATF3^{-/-}$ mice I was able to show a dependence on the cDC1 subset for the development of the T_{FH} and humoral response following intranasal administration of 5-A-RU + MG + OVA. In support of cDC1s promoting humoral responses, in a mouse model that lacked epidermal Langerhans cells, an influenza peptide conjugated to antibodies targeting langerin and therefore $CD103^{+}$ DCs in the skin (cDC1s equivalent), the cDC1s were able to promote antigen specific T_{FH} cell differentiation and IgG antibody production[385]. Targeting of both OVA and HSV-1 glycoprotein antigen to cDC1s via Clec9A was also able to promote the development of T_{FH} cells and enhanced the germinal center reactions and antibody production[386]. However, another study found $BATF3^{-/-}$ mice were able to maintain the ability to produce antigen specific antibodies to red blood cell (RBC) antigens[387]. Therefore, it seems that cDC1s are not always involved in priming humoral responses, but show dependency depending on the vaccine setting and antigen.

In our model it seems the T_{FH} and humoral response is dependent on cDC1s. However, I have shown that both cDC1s and cDC2s are activated after i.n. 5-A-RU + MG treatment,

hence I wanted to determine whether cDC2s were also vital for this T_{FH} and humoral response. *IRF4*$^{fl/fl}$ CD11c-Cre^{+} mice implement a Cre-lox system whereby IRF4 is not expressed in CD11c^{+} cells. This is to avoid the removal of IRF4 in macrophages, so the knockout of IRF4 is DC dependent[245]. However, IRF4$^{-/-}$ mice have been shown to have elevated number of dermal CD11b^{+} and CD103^{+} resident DCs, but reduced numbers of CD11b^{+} DCs migrating to the draining lymph node. This suggesting IRF4 is not required for the development and tissue residency of CD11b^{+} DCs but is involved in the migration of these cells[388]. It would therefore be of importance to, like with the BATF3$^{-/-}$ mice, characterise the DC phenotype in the lung and mLN in our model, to determine whether the cDC2s are fully knocked out. However, there was a paper that investigated *IRF4*$^{fl/fl}$ CD11c-Cre^{+} mice and showed an absence of lung resident CD11c^{hi}CD11b^{+}SIRPα^{+}CD24^{+} DCs, which would fall under the classification of cDC2s in this thesis[389]. No doubt it would still be important to determine the lack of cDC2s in our model. The *IRF4*$^{fl/fl}$ CD11c-Cre^{+} mice showed a trend towards a decrease in T_{FH} cells and a significant reduction in antigen-specific GC B cells. Thus, implementing cDC2s in helping to drive the B cell response to 5-A-RU + MG + OVA. The literature suggests that due to cDC2s superior CD4^{+} T cell priming ability[390] and location at the T-B cell border in the lymph node[290,381] they are better suited for T_{FH} priming compared to cDC1s. This is supported as *IRF4*$^{fl/fl}$ CD11c-Cre^{+} mice lose the ability to drive a humoral response consisting of RBC autoantidodies[387] and mice lacking CD11b^{+} cDC2s have also been shown to have impaired T_{FH} priming and impaired antibody production[290]. Furthermore, antigen targeted to cDC2s via anti-DCIR2 antibodies enhances the development of antigen-specific T_{FH} cells, germinal center formation and antibody production[362]. The data in this thesis, indicates that both conventional DC1s and DC2s are required for the T_{FH} and antigen-specific GC B cell response in our model. From the knockout experiments, it seems either subset is unable to compensate for the loss of the other, therefore both are required to induce the adaptive response to 5-A-RU + MG + OVA admix in the mLN.

The qPCR analysis hinted at no significant changes in the target genes, except ICOS expression in lung MAIT cells between PBS and 5-A-RU + MG treated mice. This was

surprising for some of the targets such as CD40L, as in vitro cultures of whole blood with the addition of 5-A-RU + MG for 16 hrs, results in the significant upregulation of CD40L on MAIT cells[236]. Additionally, the α-CD40L experiment in this thesis also suggests a role for CD40L in our model at 12 hrs post vaccination. It could be that the CD40L on MAIT cells is upregulated early on in MAIT cell activation giving only a small window for analysis which may have been missed with the qPCR due to the MAIT cells being sorted 3 days post admix administration. It would therefore, be interesting to repeat the sort at an earlier timepoint (if possible with the TCR downregulation) or alternatively determine the cell surface protein expression of CD40L on MAIT cells via flow cytometry. Il-17A was another surprising marker which showed no statistically significant difference between PBS and admix treatment, despite the increase in RORγT expression following the i.n. admix treatment in the lung. The literature shows an association with the high RORγT expression in MAIT cells and the production of IL-17. Even in a naïve state MAIT cells have high expression of IL-17A compared to non-MAIT T cells, this being associated with their high baseline RORγT expression[218]. The total number of IL-17A producing MAIT cells is significantly increased following infection models[209,218,222,284]. However, when in vitro cultures of DCs and MAIT cells are co-cultured with 5-A-RU + MG, no IL-17 production is detected[236]. While there seems to be a slight trend towards increasing Il17a RNA after 5-A-RU + MG treatment, it may be that MAIT cells only strongly upregulate IL-17 production following infection which provides additional signals unlike the admix which contains only the MAIT cell agonist. The consistent relative expression of Tnf between PBS and 5-A-RU + MG treatment is supported by the absence of Tbet expression in the MAIT cells. This is also supported in the literature with MAIT cells having low Tbet expression and TNF production at steady state which is elevated upon bacterial infection[222]. However, in vitro culture of 5-A-RU and MG with MAIT cells has been shown to induce TNF-α production[236]. This disparity may reflect the difference between in vitro culture and in vivo mucosal environments. Other targets such as Il17f, Il15, Lif, Csf2 and Tnfsf11 also had no change between the PBS control and the 5-A-RU + MG admix. The RNA expression of these markers was identified as upregulated either during or after infection with *L. longbeachae*[351]. Which again may reflect that the MAIT

cells in our model are only being stimulated by the agonists and not an infection model. Cytokine receptor genes Il12rb1 and Il23r were also investigated due to IL-12 being shown to activate MAIT cells independent of bacterial antigen[391] and as IL-23R is upregulated following Salmonella infection and also Il-23p19$^{-/-}$ mice, which lack a functional receptor for IL-23, have decreased MAIT cell accumulation in the lung following infection[209]. As there was no change in expression of the genes for the IL-23 and IL-12 receptors, it is unlikely that the MAIT cells in our model are being activated through these cytokines involved activation pathways with IL-23 and IL-12. Furthermore, the admix treatment of 5-A-RU + MG doesn't seem capable of inducing an upregulation of type 1 IFNs or genes within the BAFF system. It would however, be interesting to investigate the protein levels of some of these markers by flow cytometry as the gene expression doesn't necessarily directly correlate with protein production.

As the qPCR results highlighted a difference in ICOS expression on MAIT cells and it is known to play a role in MAIT cell accumulation[209], I wanted to further investigate its ligand, ICOSL, as it is also known to be expressed on cDCs upon activation and plays a role in T_{FH} differentation[362]. I therefore hypothesised that MAIT cells activate cDCs to upregulate ICOSL and induce the T_{FH} and humoral response seen in the prime-boost model. Initially, I wanted to see whether the cDCs were able to upregulate ICOSL after the admix administration. This showed a rapid upregulation of ICOSL only in the lung cDCs at 12 hrs after i.n. admix treatment, which returned to baseline levels by 24 hrs. Interestingly, this upregulation of ICOSL was not present in the migratory or resident cDCs in the mLN. Further investigation into why this occurred is required, as ICOSL is highly expressed in lymphoid tissues such as lymph nodes[392] and ICOSL expression on DCs is associated with T_{FH} development which occurs in the lymph node[362]. It may be that the ICOSL has already returned to baseline levels in the mLN cDC subsets, as even in the lung it is only present for a brief amount of time. The window where ICOSL is expressed is very short in my model, this is unlike in vitro studies which have shown ICOSL to be upregulated on DCs at 24 hrs following stimulation with Poly(I:C) or LPS[362]. However, the conditions are different as in my model, the cDCs aren't receiving a direct

stimulus like Poly(I:C) or LPS but are instead reliant on the stimulus provided by the MAIT cell activation.

As the literature suggests with B cells, the data shows that CD40L signalling is involved in the regulation of ICOSL on cDCs, as displayed by the blocking of CD40L resulting in the absence of ICOSL upregulation. Activating B cells with CD40, results in upregulation of ICOSL[365] which is also most highly expressed on the GC B cells with higher affinity BCRs[366]. Additionally, CD8α^- DCs have also been shown to express ICOSL under the stimulation of the non-canonical NF-κB pathway[362]. This pathway can be activated by both CD40[393] and RANK[394] signalling. This also supporting the finding that RANKL signalling is involved in ICOSL expression on cDCs. In future experiments it would be interesting to determine whether this blocking of ICOSL expression on cDCs reduces the T_{FH} population and humoral response in the prime-boost model. The blocking of CD40L resulted in a significant reduction of CD86 MFI on migratory cDCs at 12 hrs, whereas blocking RANKL led to a trend towards reduction at 24 hrs. Interestingly this reduction was not seen in the lung cDCs. It may be due to the dose of antibody used. It would be interesting to see whether increasing the dose of the α-CD40L and α-RANKL would prolong the absence of CD86 in the mLN and induce this reduction in the lung cDCs and determine whether RANKL can truly regulate DC activation. It is of particular interest as despite their signalling pathway similarities, unlike CD40[395], RANKL signalling has be shown to result in no changes in CD80 or CD86 expression in DCs[317]. However, on the contrary, another study found DCs that were transduced with RANKL/RANK had higher frequencies of CD80 and CD86 compared to DCs transduced with CD40L/CD40[396]. Furthermore, as CD40 and RANK signalling stimulate the same pathway, they could play compensatory roles. Therefore, a future experiment blocking both pathways simultaneously may provide a more substantial effect on the cDC activation. An interesting observation following RANKL blocking was the upregulation of MAIT cell CD69 and ICOS MFI at 12 hrs, this suggesting RANKL has a role in negative regulation of MAIT cells. This requires further investigation as the literature suggests RANKL as a pro-inflammatory signal[397]. While direct interactions between MAIT cells and DCs haven't

been proven the data does suggest MAIT cells may interact with cDCs through CD40-CD40L and RANK-RANKL which allows for the upregulation of ICOSL on cDCs. These interactions may also regulate cDC activation in our model.

4.5 Conclusions

In this chapter, it has been demonstrated that implementing a prime-boost vaccination scheme where 5-A-RU + MG + OVA is administered three times intranasally over 4 weeks, is able to induce a humoral response. This humoral response is linked with an increase in T_{FH} cell accumulation and antigen specificity in the mLN and consists of an increase in antigen-specific germinal center B cells and production of systemic IgG antibodies. In addition, the humoral response is dependent on MR1 and MAIT cells, suggesting the MAIT cells are able to induce an adjuvant effect to the intranasal vaccine. The data also shows that the cDCs remain activated to an equivalent extent following prime-boost vaccination, whereas, the MAIT cells have increased accumulation, prolonged activation status and also maintain the RORγT and GATA3 expression in the lung and mLN. Moreover, the humoral response is dependent on the involvement of both conventional DC1s and DC2s. The initial mechanism between the MAIT cells and cDCs also began to be investigated. Despite the high GATA3 expression in MAIT cells, this chapter showed that the vaccine doesn't function through a typical T_H2 response. Furthermore, the expression of ICOSL on cDCs is regulated by both CD40L and RANKL signalling, which also effects cDC activation. This suggesting a role for CD40-CD40L and RANK-RANKL interactions in the early response between MAIT cells and cDCs in my model.

5 General Discussion

5.1 Summary of Findings

In this thesis I have shown that intranasal administration of 5-A-RU + MG is capable of inducing MAIT cell and cDC activation in the lung tissue and mLNs in an MR1 dependent manner. Initial experiments concluded that unlike these optimal effects from the 5-A-RU + MG admix, the pro-5-A-RU which was designed to have improved stability, was unable to match the MAIT cell and cDC response induced by the admix. Optimisation of the dose (75 nmol 5-A-RU + 750 nmol MG) as well as the optimal timing to assess both MAIT cell and cDC activation (day 1 post vaccination), enabled the establishment of a model to determine the initial MAIT cell and cDC responses and relationship following the admix vaccination. Through this model, I was able to characterise the MAIT cells phenotype of a maintained RORγT and GATA3 dominant expression in the lung and mLN both in the control and admix treated groups. Additionally, despite high GATA3 expression, the stimulated MAIT cell and cDC response did not require the typical T_H2 signalling pathway through STAT6, nor induce characteristic T_H2 IL-4 and IL-13 cytokine production in MAIT cells or IgE antibody production. Furthermore, I explored the role of different co-stimulatory pathways in the initial response to the admix vaccine, identifying a potential role for CD40L and RANKL signalling to control activation of migratory cDCs, including the upregulation of ICOSL.

This thesis also explored the adaptive response induced by the 5-A-RU + MG admix with the addition of the model antigen, OVA, using a prime-boost intranasal vaccine scheme. Through this model, I found that the cDCs maintain an equivalent activation status between one and three doses of the vaccine, suggesting the lack of a 'trained' innate response and also that the prime-boost model induces an accumulation of MAIT cells in the lung, prolongs their activation and maintains the same RORγT and GATA3 dominant phenotype. Additionally, the prime-boost admix induces a T_{FH} accumulation in the mLN and promotes and antigen-specific humoral response, with an increase in antigen-specific germinal center B cells and systemic antigen-specific IgG antibodies. Importantly, this adaptive response is MR1 dependent. Finally, this thesis identifies both

cDC1s and cDC2s as important drivers of adaptive immune response in the lung and mLN following intranasal administration of 5-A-RU + MG + OVA.

5.2 Can MAIT Cells be Exploited as Cellular Adjuvants in Mucosal Vaccines?

MAIT cells are known to drive pro-inflammatory effector responses. In infections such as *Legionella* and *Salmonella* MAIT cells are known to produce inflammatory cytokines such as IL-17A, IFN-γ and TNF[209,218,222] and are able to induce protection against lethal doses of *Legionella*[218]. MAIT cells have also been linked to pathogenesis of pro-inflammatory diseases such as lupus erythematosus[284] and ankylosing spondylitis[398,399]. However, while MAIT cell granzyme production has been linked to type 1 diabetes, the lack of MAIT cells can also enhance the anti-islet responses in the NOD mouse model of type 1 diabetes[400]. This dual role of MAIT cells is also described in multiple sclerosis (MS), with reports indicating a presence of MAIT cells in central nervous system lesions of MS patients suggesting a pro-inflammatory role[401,402], however, in the experimental autoimmune encephalomyelitis model of MS, MAIT cells seem to provide protection[403]. Therefore, while MAIT cells are able to drive inflammatory responses, they are also linked to maintaining homeostasis. This homeostatic function is further supported by their production of tissue repair genes[351], their role in maintaining gut integrity[400] and their absence in germ-free mice[242].

The MAIT cells phenotype following intranasal administration of 5-A-RU + MG admix represents a more homeostatic, non-inflammatory status. This is highlighted by the transcription factor profile, which maintains a RORγT and GATA3 dominant phenotype with little to no expression of Tbet even after admix administration. This also correlates with the lack of upregulation of effector cytokine gene expression. As discussed previously, the lack of an effector response may be linked to the vaccine containing only the MAIT cell agonist and not a pathogen[209,218,222] which would contain PAMPs and stimulate alternative pathways. This is also supported by Ussher, J. *et al.* (2014), who showed that stimulants of TRL4 and TLR8 can lead to MAIT cell activation measured by IFN-γ production in vitro[224]. TLR stimulation is a mechanism by which some licenced adjuvants function. For example, the MPL proportion of the adjuvant AS04 targets TLR4 to induce its immune enhancing effects[37–39]. However, when implementing direct

stimulators of TLRs as adjuvants, caution is needed, as if TLR agonists disseminate systemically they can induce potentially fatal cytokine storms[404]. As 5-A-RU + MG admix doesn't contain known TLR agonists and induces little pro-inflammatory phenotype, it may have improved safety as an adjuvant.

An important consideration in vaccine design, especially when incorporating an adjuvant, is to limit the immune stimulus to avoid toxic side effects, while maintaining an appropriate level of stimulation to drive the desired immune responses to initiate long term protection. Although the admix doesn't induce strong pro-inflammatory effector functions, it is able to induce MAIT cell activation, which leads to cDC activation, T_{FH} accumulation and a humoral response, these being key responses in a vaccination. The activation of DCs is an important initial step in a vaccine response as they are the superior antigen presenting cell and allow for antigen to be trafficked to the draining lymph nodes where it can be presented to naïve T cells to initiate the adaptive response[252,253]. Additionally, the type of adaptive response will be skewed by the DC population activated and also how they were stimulated. A common technique implemented to drive a DC and therefore adaptive responses is the conjugation of the vaccine antigen to antibodies that target specific DC markers. For example, antigen bound to CD11c and DEC-205 DC markers is able to enhance the $CD4^+$ and $CD8^+$ T cell responses[248,249]. The importance for DCs in vaccination is also supported by knockout mouse strains that lack either cDC1s or cDC2s, the lack of these populations have been shown to impair the IFN-γ $CD8^+$ T cell response[337] and T_{FH} and humoral response[290] respectively. The 5-A-RU + MG vaccine was able to induce both cDC1 and cDC2 activation at the mucosa, and in turn I showed the importance of the cDC populations for driving the T_{FH} and humoral response seen in our model. Both cDC populations were required for the T_{FH} and humoral response.

Most successful vaccines induce a B cell response that constitutes long lived plasma cells and antibody production[164–166]. This B cell response is supported by the induction of T_{FH} cells that improve affinity, induce isotype switching and drive memory B cell

development[153,156]. While the 5-A-RU + MG + OVA vaccine does show a success in inducing a T_{FH} and antigen-specific germinal center B cells along with systemic antigen-specific IgG antibodies, it doesn't induce other $CD4^+$ T cell responses. The drive towards different $CD4^+$ T cell responses can be induced by the chosen adjuvant. For example, alum induces a T_H2 phenotype, while AS04 results in a T_H1 bias[40]. However, the 5-A-RU + MG + OVA vaccine only promoted a T_{FH} response. Further investigation into the $CD8^+$ T cell response is required as I didn't comprehensively investigate this subset. It would be interesting to follow-up as the NKT cell agonist α-GalCer, has shown promise as an adjuvant to induce a cytotoxic T cells response to cancerous cells when conjugated to an MHCI binding peptide[234]. Despite this gap, the 5-A-RU + MG intranasal vaccine still stimulates desirable immune pathways for vaccination.

Currently only recombinant cholera toxin subunit B (CTB) is used as an adjuvant in licenced mucosal vaccines as a component of the vaccine Dukoral, an inactivated oral vaccine against *Vibrio cholerae*. Whereas, the other licenced mucosal vaccines are live attenuated due to the lack of effective mucosal adjuvants[45]. Cholera toxin (CT) is known as a potent stimulator of mucosal immune responses[405], however, due to its toxic effects[406] it has limited use as an adjuvant in human vaccines despite showing potential in animal models[407]. The toxic effects can be mitigated by only employing the B subunit. When administered intranasally, CTB is able to induce IgG and IgA antibody production both systemically and in mucosal secretions[408]. CTB conjugated to antigen is also able to enhance to antigen presentation by DCs, increase DC IFN-γ and IL-12 production and drive proliferation of T cells in vitro[409]. Much like CTB, our 5-A-RU + MG vaccine is able to promote DC activation and induce a systemic IgG antibody response, however, the levels of IgA are undetermined. The majority of vaccines induce an IgG serum antibody response. IgG antibodies have a wide range of functions as they are able to carry out opsonisation of bacteria, neutralise viruses as well as activate the complement system[157,160,325]. It is therefore, promising that our vaccine is able to induce a systemic IgG response, however, due to the mucosal administration route, most mucosal vaccines also induce a secretory IgA mucosal response which limits pathogen entry[325].

It would therefore be important to determine whether IgA can be produced in response to the i.n. 5-A-RU + MG + OVA vaccine in future experiments. The consistent IgA response in mucosal vaccines could be influenced by the fact that most mucosal vaccines are live attenuated and therefore contain a range of PAMPs and would actively infect cells providing a range of immune stimulants. It may be that the addition of PAMPs in our vaccine could enhance isotype switching.

The combination of 5-A-RU and MG produces the MAIT cell agonist, 5-OP-RU and/or lumazines, which can then be presented through the MR1-TCR pathway in the lung, allowing for the activation of the MAIT cells. My data suggests that activated MAIT cells then drive cDC activation, potentially through CD40-CD40L and RANK-RANKL co-stimulatory pathways. Blocking these co-stimulatory pathways with specific monoclonal antibodies resulted in the inhibition of ICOSL upregulation on cDCs in the lung, which may have implications for downstream events including the priming of the T_{FH} cells in the mLN, whereby, ICOS-ICOSL is involved in the development of T_{FH} responses[361].

Furthermore, my data suggests there is a strong migratory cDC response in the mLN, implying migration from the peripheral lung into the mLN where T_{FH} priming can occur. The data supports two distinct MAIT cell populations, one that resides within the lung tissue and the other in the mLN. However, both these MAIT cell populations have similar activation phenotypes and kinetics. The literature supports that MAIT cell migration is unlikely as Constantinides, M. *et al.* (2019), showed with parabiosis mice, that MAIT cells in the skin remain tissue resident[410]. Furthermore, MAIT cells exhibit a gene signatures associated with tissue residency and parabiosis mice have also shown tissue resident MAIT cells in the spleen, liver and lungs[411]. In contrast, there are also MAIT cells that exhibit a non-resident phenotype and some MAIT cells that circulate in the blood[412], although the circulating population in mice is minimal (<0.1% of T cells)[204,222]. Two distinct MAIT cell populations in my model may also explain some of the differences seen in the migratory versus resident cDC phenotypes, suggesting they are primed by different MAIT cell populations.

The precise roles of cDC1 and cDC2 populations involved in the initiation of T_{FH} and humoral responses is not clear, however there is significant evidence from the literature that show each population can contribute toward T_{FH} development[290,385–387]. Surprisingly, in our model, I found that both cDC1 and cDC2 populations were required, but on their own, were not sufficient to induce adaptive immunity in response to 5-A-RU + MG, suggesting each plays a vital role. As there is not a substantial change in the MAIT cell activation in the cDC knockout studies, the lack of the adaptive immune response is more likely due to the loss of the DC-T cell interaction, rather than a defect in DC-MAIT cell antigen presentation. Further investigation in the mechanisms of the two populations is needed. The likely pathway to induce the humoral response, is that both cDC populations are able to present antigen to naïve $CD4^+$ T cells in the mLN and induce T_{FH} differentiation, which in turn provide help to B cells. This being the classical pathway to induce long lasting vaccine humoral responses[153,156]. My data supports this hypothesis since I observed a correlation between T_{FH} cell expansion and the presence of an antigen-specific humoral response. To directly assess this, one could use the $Bcl6^{fl/fl}$CD4-Cre^+ mice strain which lacks T_{FH} cells[413] to determine whether the humoral response is still induced. In our model it is not likely that the humoral immunity is induced by a direct interaction between MAIT cells and B cells due to the lack of the humoral but not MAIT cell response in the cDC knockout mice. While this is a controversial mechanism, there is evidence to suggest MAIT cells and B cells can interact directly, as there is a lack of MAIT cells in B cell deficient mice and patients[242]. It is also possible that B cells interact directly with DCs, it has been shown both in vitro and in vivo that DCs have the potential to present unprocessed antigen on the cell surface where it can be transferred to naïve B cells and induce an isotype switching to IgG[414].

Lastly, it is important to note that presentation of 5-A-RU + MG is not dependent on a singular cDC population, since *Irf4*$^{fl/fl}$ CD11c-Cre^+ mice showed no change in MAIT cell activation and the MAIT cells from $BATF3^{-/-}$ mice had only a slight decrease in activation in the lung. However, the loss of a singular cDC population, could be compensated for

by the remaining DC populations. The engagement of antigen presentation to TCRs is coupled with the interaction of co-stimulation pathways to induce activation and avoid tolerance[415,416]. To induce an optimal adaptive response, DCs require both antigen presentation and stimulation through costimulatory pathways[249]. This is also the case for NKT cells, where the agonist, α-GalCer, results in DC activation with dependence on co-stimulatory pathways for the induction of the adaptive response[276]. As my data suggests that co-stimulatory pathways are involved in the cDC activation, I hypothesise that to become activated, the cDCs are also presenting the MAIT cell agonist via MR1 to engage with the MAIT cell invariant TCR, which in turn allow for the engagement of the co-stimulatory pathways and cDC activation. While, it is likely that other cell types are presenting the agonist via MR1, as MR1 is ubiquitously expressed at low levels by a wide range of cells[208] and Wang, H. *et al.* (2019), revealed both bone marrow derived and non-bone marrow derived cells have the capacity to activate MAIT cells via MR1 in vivo[209], to get the cDC activation and subsequent adaptive response, I believe that the cDCs would require both the MR1-TCR and co-stimulatory interaction. However, this hypothesis does require further elucidation to determine the mechanism.

Taken together, 5-A-RU + MG acts as a suitable mucosal adjuvant capable of evoking an antigen-specific immune response to co-administered antigen. The activation of the MAIT cells via TCR signalling, provides a set of key signals that conditions cDCs to specifically induce T_{FH} cell differentiation, antigen specific germinal B cells and systemic antigen-specific IgG antibodies (working hypothesis mechanism presented in figure 5.1).

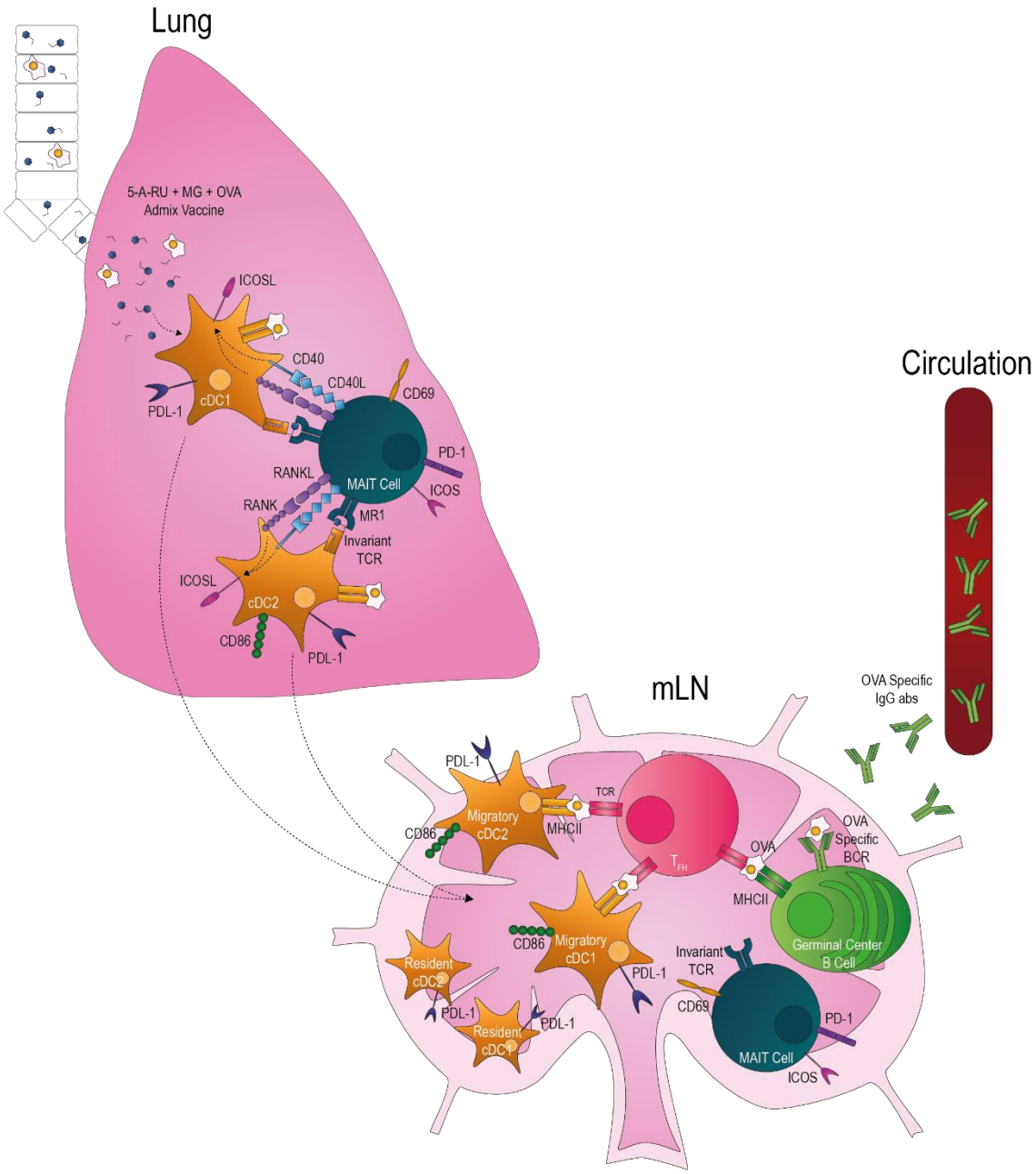

Figure 5.1: Working Hypothesis Mechanism. The current hypothesised mechanism for the immune response to the 5-A-RU + MG + OVA admix vaccine.

5.3 Limitations and Future Directions

There are some important factors to consider in this thesis that are difficult to control experimentally. MAIT cells have a strong association with the microbiome. They are absence in germ-free mice, they are found in high abundance at mucosal sites which are in contact with the microbiome[206] and are activated by riboflavin derivatives produced by microbes and fungi[220]. Additionally, the colonisation of different bacteria in the microbiome is associated with the accumulation of MAIT cells which is evident by the different frequencies of MAIT cells seen in distinct cages of mice[410]. It is therefore likely that the microbiome will have effects on the MAIT cell response and may influence our experimental readouts. However, in an attempt to reduce this cage effect, I split the treatments across multiple cages. While there was variation in MAIT cell frequencies, I did not see the dramatic 5%-40% differences across cages as in Constantinides, M. *et al.* (2019)[410]. The microbiome is difficult to control in experiments, it is therefore important to consider there may be background effects in our experimental readouts that are not solely due to the treatments.

It is also important to highlight that due to the downregulation of the MAIT cell TCR following initial activation, I may be missing the highly activated cells in my analysis as the MAIT cells are identified via a MR1-5-OP-RU tetramer that binds the MAIT cell TCR. While this is important to keep in mind, the MAIT cell phenotype at day 1 post i.n. treatment does seem to be representative of what I observe at later timepoints when the TCR cell surface expression has returned.

Another important consideration is that the intranasal administration of the admix vaccine is likely reaching more than just the lung mucosal site. For example, Visweswaraiah, A. *et al.* (2002), showed through intranasal administration of dye, the position of the anaesthetised mouse upon administration could influence what mucosal sites the dye travelled to. They also showed that intranasal administration commonly led to dye in the stomach[417]. This along with the evidence that shows that administration of a vaccine at one mucosal site also induces a response at other distal

mucosal sites[49,50,53], would suggest that our admix vaccine may be inducing immune responses at other mucosal sites such as the gut. It would therefore be interesting to investigate the response in the gut and also determine whether the mucosal route induces different responses and/or strengths of the response, for example, comparing intranasal administration to oral.

While MAIT cell characteristics such as the semi-invariant TCR is common across humans and mice[278], there are a few characteristics that are dissimilar. Humans have a high abundance of MAIT cells, with MAIT cells contributing up to 10% of peripheral T cells in the blood[198,281], whereas, mice have a comparatively lower frequency of <0.1% of peripheral blood T cells[222]. Additionally, the majority of MAIT cells in humans are $CD8^{+}$[281] unlike the dominant $CD4^{-}CD8^{-}$ MAIT cells in mice[204]. In humans it has been shown that $CD8^{+}$ and $CD4^{-}CD8^{-}$ MAIT cells have similar functions and phenotypes, but $CD8^{+}$ MAIT cells do have a more pro-inflammatory phenotype, with higher production of TNF-α, IFN-γ and granzyme B[418]. Therefore, due to the increased number of MAIT cells in humans and the dominant $CD8^{+}$ MAIT cells, the response to the 5-A-RU + MG vaccine may be more potent in a human compared to the mouse model. However, this is always a vital consideration in science, that an animal model is not identical to the human system and therefore differences in response may occur if the treatment is ever translated.

In this thesis I only began to understand the mechanism behind the 5-A-RU + MG admix response. While I was able to show a dependence for cDCs and a link between RANKL and CD40L with ICOSL expression, many more experiments are required to elucidate the full mechanism. Firstly, the $BATF3^{-/-}$ and $Irf4^{fl/fl}$ CD11c-Cre^{+} experiments require repeats as these experiments have only been done once. Additionally, larger sample sizes may also help to narrow down variation between mice and improve the statistical significance of the readouts with the stringent ANOVA tests. Also, an experiment assessing the baseline phenotype of the $Irf4^{fl/fl}$ CD11c-Cre^{+} mice is necessary to ensure the cDC2s in our model are in fact absent. A repeat of the MAIT cell sort and qPCR would

also be of interest at an earlier timepoint to determine whether changes in gene expression can be seen at the start of the response to 5-A-RU + MG. Alternatively, some of the markers such as CD40L and the cytokine production could also be deduced from flow cytometry analysis. Further understanding around the role of co-stimulatory interactions is also required. Initial experiments suggest a potential role for CD40L and RANKL signalling for ICOSL expression on cDCs. However, I have not shown that the ICOSL expression nor the CD40L and RANKL signalling has any functional effect on the downstream immune response. As the data shows changes in ICOS expression on MAIT cells and ICOSL on cDCs early on in the response, it would be interesting to block this interaction to see whether it is involved in the activation of the cDCs. The data suggests that this may also occur with CD40L and RANKL blocking with a reduction and trend towards reduction in CD86 MFI on migratory cDCs respectively. It would be of interest to increase the blocking antibody concentration and see whether this response can be prolonged and generalised across all cDC subsets. Another interesting point, is that CD40-CD40L and ICOS-ICOSL co-stimulatory interactions are also known in the literature to be involved in inducing humoral responses, with CD40 and ICOSL[314,419], along with RANKL and RANK[420,421] being expressed on B cells. Therefore, it would be interesting to not only block these co-stimulatory pathways during the initial MAIT cell and DC response but also after their activation to see whether these pathways are also involved in the adaptive response to the 5-A-RU + MG admix. This thesis also did not investigate the cells involved in the presentation of the MAIT cell agonist. This could be achieved by tagging the agonist with a fluorescent probe to identify the cells capable of cell surface expression of the agonist. Then these cells could be targeted for agonist uptake through antibodies specific for cell surface markers on the presenting cells, which may in turn enhance the cDC, T_{FH} and humoral response. Finally, as mentioned previously, experiments implementing $Bcl6^{fl/fl}CD4\text{-}Cre^{+}$ mice would help to elucidate the mechanism which drives the humoral response.

OVA is commonly used in vaccine studies as a model antigen[386,422–425], however, it is not a clinically relevant antigen[426] and may result in different responses compared to a

pathogen antigen. It is therefore important to test the 5-A-RU + MG admix with the addition of a clinically relevant antigen. Future directions are to test the admix with influenza derived antigens to determine whether the admix can boost an influenza specific immune response when administered intranasally. MAIT cells have already been shown to have a protective role in influenza infection through cytokine activation[219], it would therefore be interesting to see whether also driving activation through the MR1-TCR pathway with the admix would improve this protection and induce a long term antibody response. Furthermore, as the main goal of vaccination is long term protection, it would also be of importance to challenge with the pathogen following the intranasally administered admix to determine whether it improves protection and also test the longevity of the antibody response.

5.4 Final Conclusions

The evidence outlined in this thesis demonstrates that MAIT cells do have promising potential as cellular adjuvants in mucosal vaccines. This is of importance for the future of mucosal vaccines as there is currently few licenced mucosal adjuvants, limiting the potential for safer inactivated or subunit vaccines compared to the primarily live attenuated strategies seen in mucosal vaccination.

In Summary:

1) Intranasal administration of MAIT cell agonist components, 5-A-RU and MG, induce both MAIT cell and cDC activation in the lung tissue and mLN.
2) Following intranasal administration of the 5-A-RU + MG admix the MAIT cells maintain a more homeostatic phenotype with minimal pro-inflammatory characteristics.
3) The prime-boost vaccine strategy involving intranasal administration of 5-A-RU + MG + OVA drives a T_{FH} and humoral response in the mLN
4) Both conventional DC1s and DC2s play a role in the induction of the T_{FH} and humoral response

Supplementary Figures

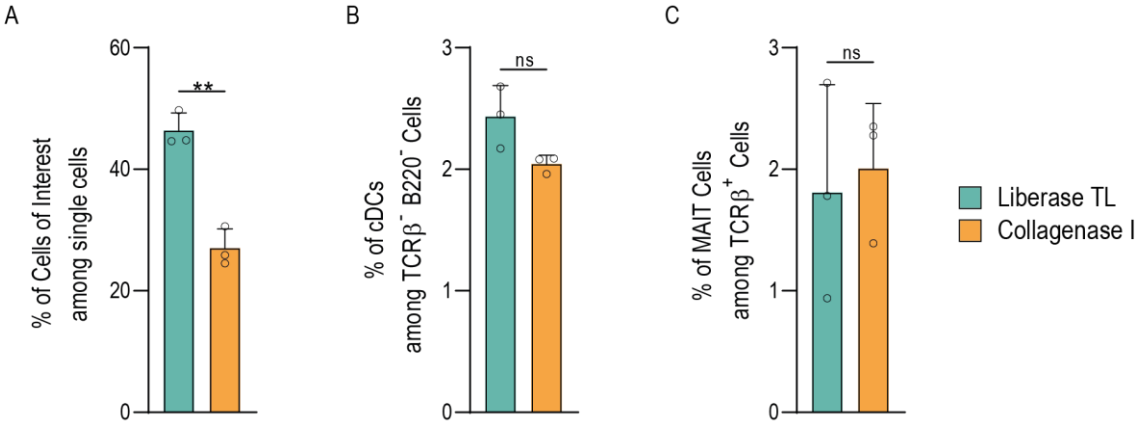

Supplementary Figure 1: Comparison Between Liberase TL and Collagenase I Enzymes for Lung Digestion. Naïve C57BL/6 lungs were harvested and stained to identify cDCs and MAIT cells. **(A)** Frequency of cells of interest, backgated on TCRβ+ Cells. **(B)** Frequency of cDCs. **(C)** Frequency of MAIT cells. Statistcial analysis was conducted using unpaired T tests. Bars represent the mean per group, symbols are induvidual mice and error bars show the standard deviation. ns>0.05, **p≤0.01.

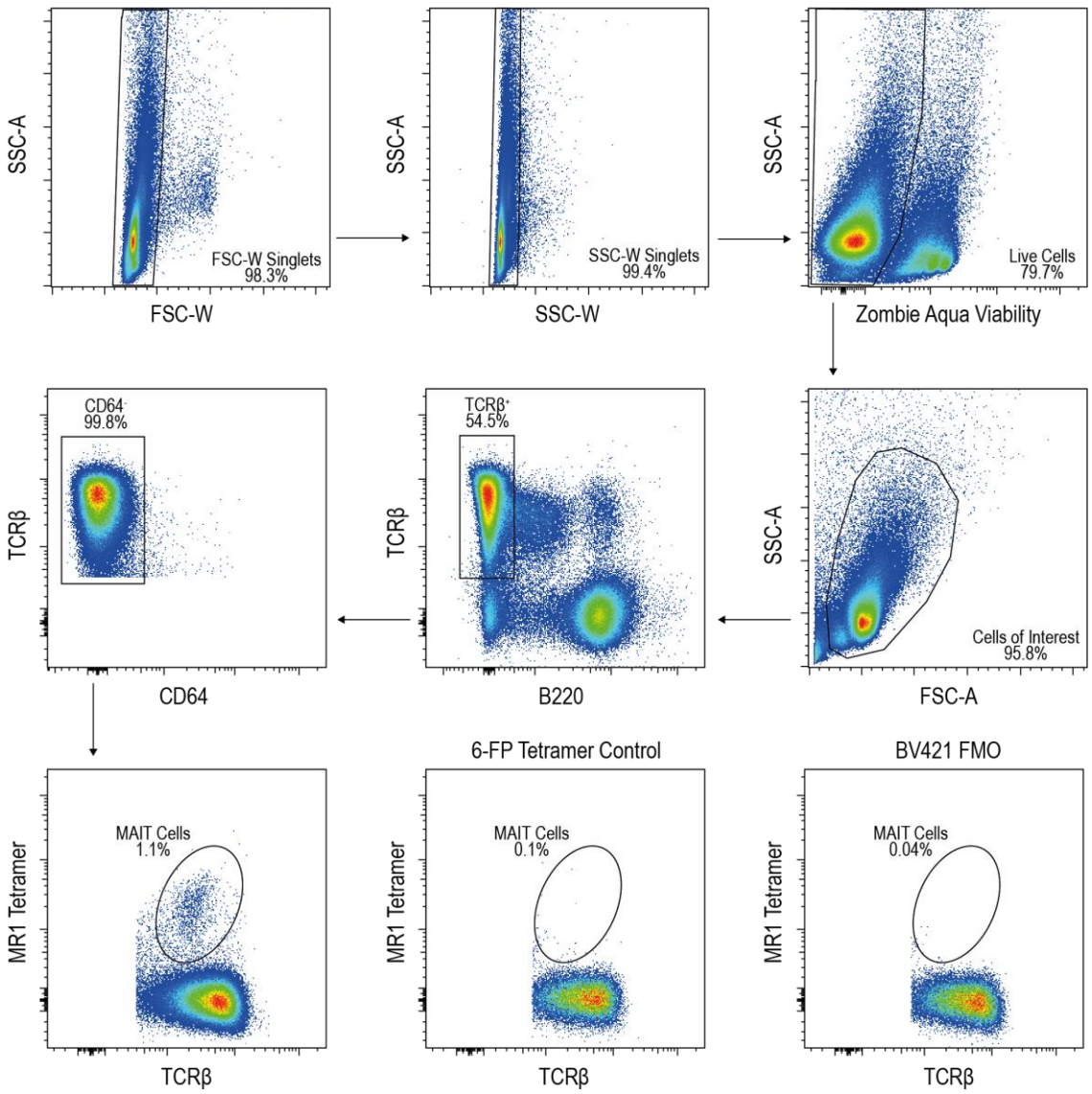

Supplementary Figure 2: Representative MAIT Cell Gating Strategy. Following isolation of single live cells and cells of interest, MAIT cells were gated on as B220$^-$TCRβ$^+$CD64$^-$MR1-5-OP-RU tetramer$^+$. Both a MR1-6-FP tetramer and MR1-5-OP-RU tetramer FMO control was used to place the MAIT cell gate. Plots shown are from mLNs, however, lung data was gated the same except for back gating of TCRβ$^+$ cells to set the cells of interest gate.

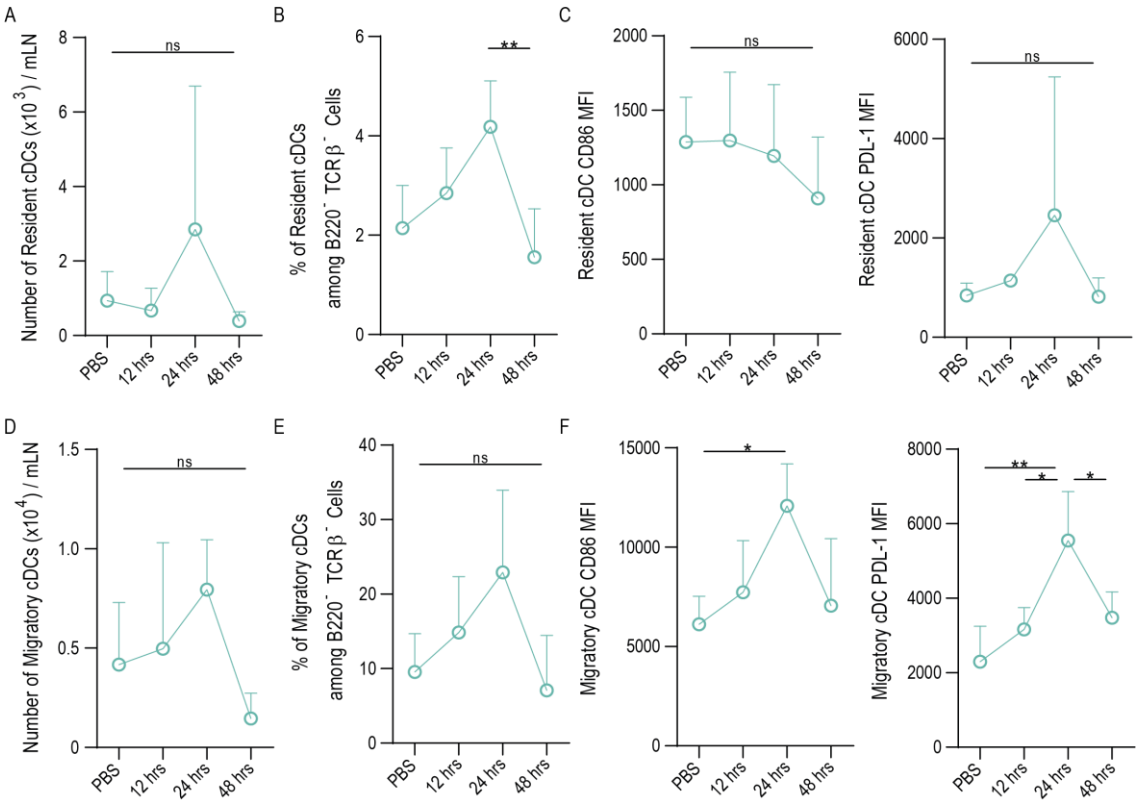

Supplementary Figure 3: Dendritic Cell Kinetics Following Intranasal Administration of 5-A-RU + MG Admix. C57BL/6 mice were intranasally administered either PBS or admix at 48, 24 and 12 hrs prior to harvesting of the mLN. mLNs were processed, stained for cDC markers and fixed, for flow cytometry analysis the following day. **(A & B)** Number and frequency of resident cDCs. **(C)** CD86 and PDL-1 MFI of resident cDCs. **(D & E)** Number and frequency of migratory cDCS. **(F)** Migratory cDCs CD86 and PDL-1 MFI. Statistcial analysis was conducted using One-way ANOVA with Tukey's post hoc test. Symbols represent group means and error bars show the standard deviation. ns>0.05, *p≤0.05, **p≤0.01.

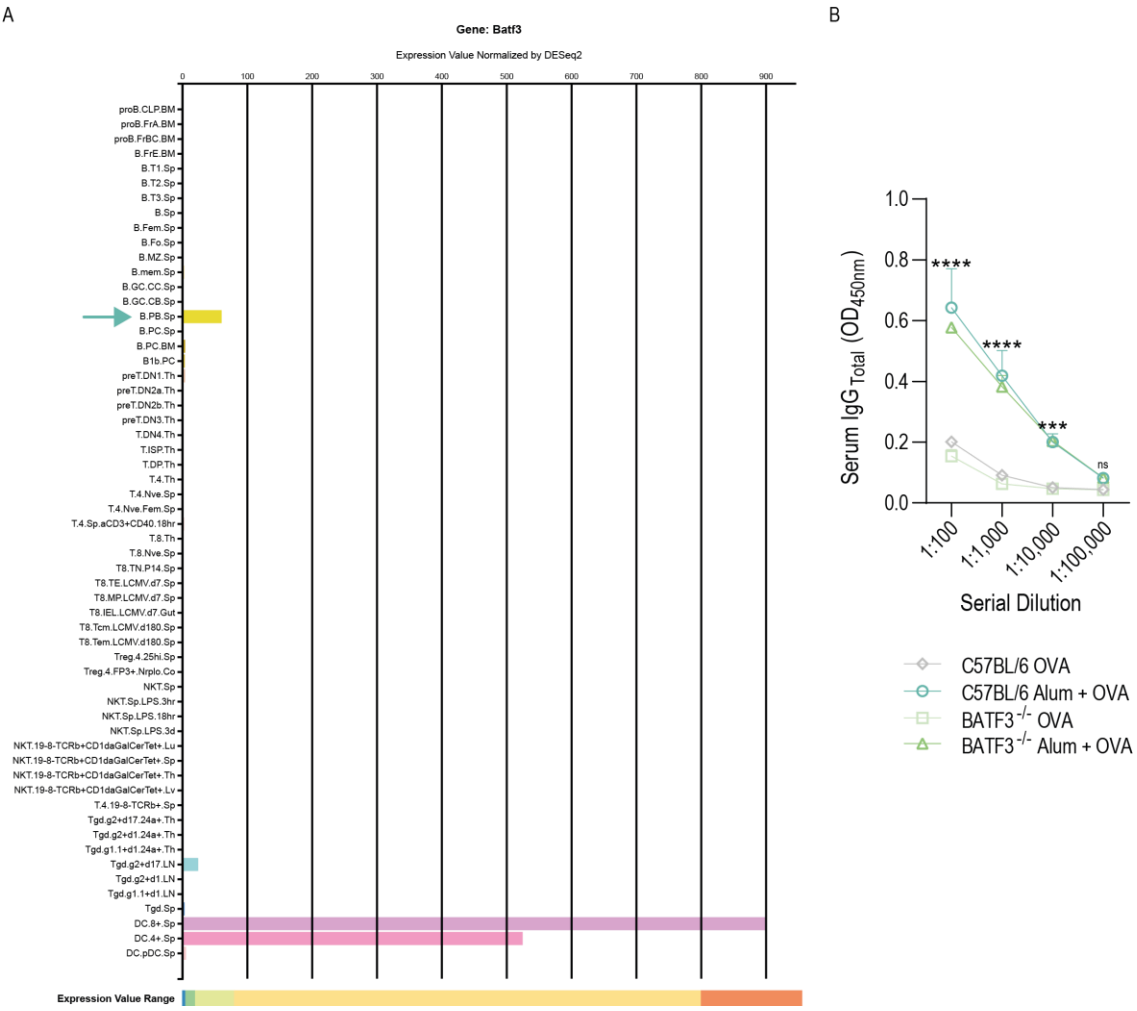

Supplementary Figure 4: IgG Antibody Response is not Affected by BATF3$^{-/-}$. (A) BATF3 RNA expression levels in B cells, αβ and γδ T cells and dendritic cells from the Immunological Genome Project (ImmGen) RNA-Seq database. **(B)** C57BL/6 and BATF3$^{-/-}$ mice were given two intraperitoneal injections of either OVA alone or in combination with alum 2 weeks apart. Blood was then harvested through cardiac puncture 1 week later. An ELISA was used to identify total IgG serum levels. Statistcial analysis was conducted using a Two-way ANOVA. Symbols represent the group mean and error bars show the standard deviation. ns>0.05, ***p≤0.001, ****p≤0.0001. Significance stars represent significance between both C57BL/6 and BATF3$^{-/-}$ admix treated mice compared to the OVA treated mice of both strains.

A TCRβ+ Cell Purity Sort Gating

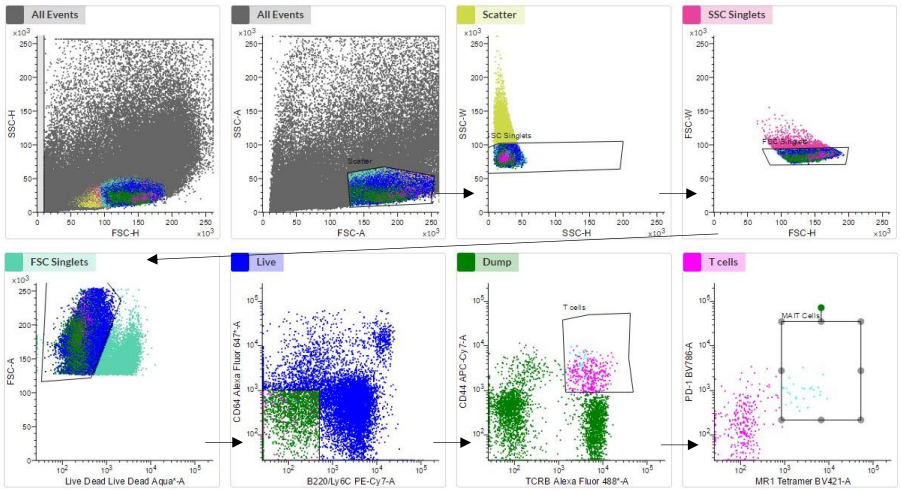

B MAIT Cell Purity Sort Gating

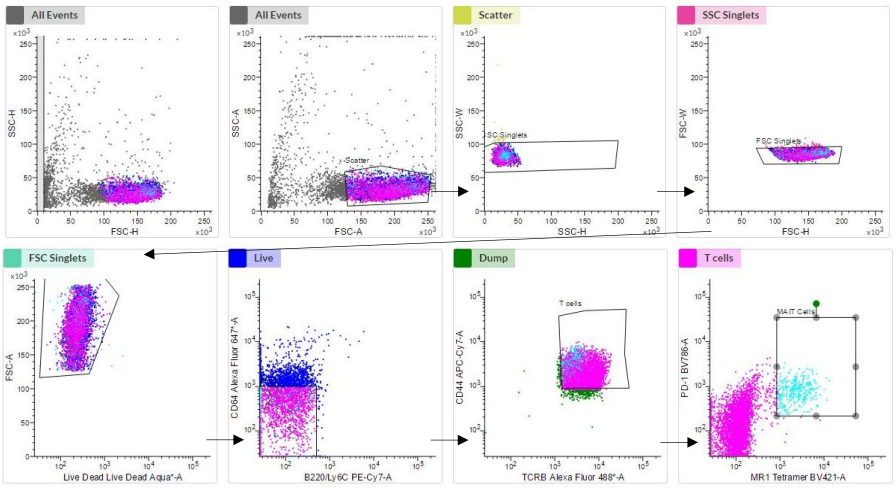

C MAIT Cell Post Sort

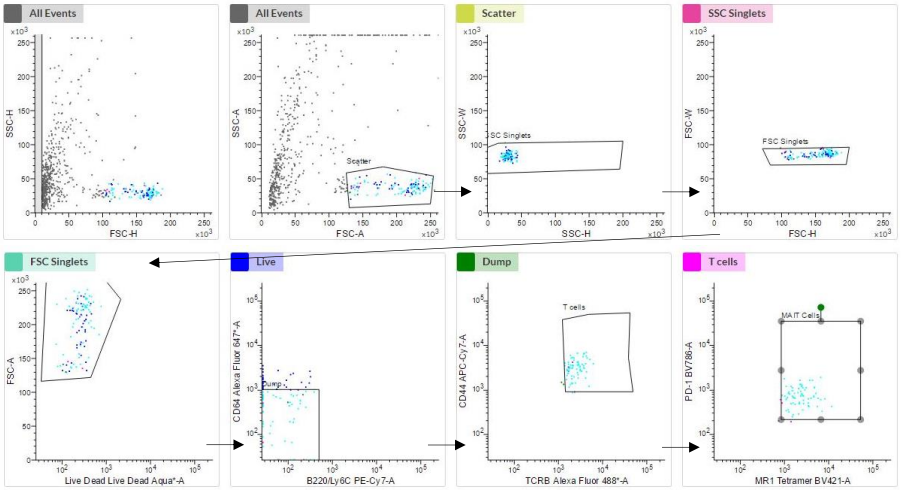

Supplementary Figure 5: MAIT Cell Sort Gating Strategy. (A) The initial gating strategy for a purity sort of T cells. **(B)** Next the T cells obtained in A, were put through another purity sort to isolate MAIT cells. **(C)** The MAIT cells sorted from B, were run through to check the purity of the sample.

References

1. Rappuoli, R., Miller, H. & Falkow, S. The intangible value of vaccination. *Science (80-.).* **297**, 937–9 (2002).
2. Lutwick, L. I., Laberge, M., Davidson, T., Checchia, P. & Hodgkins, F. Vaccination. *he Gale Encyclopedia of Public Health (Vol. 2.)* (2013).
3. Organization, W. H. Immunization Coverage. https://www.who.int/en/news-room/fact-sheets/detail/immunization-coverage (2019).
4. Rappuoli, R., Mandl, C., Black, S. & De Gregorio, E. Vaccines for the twenty-first century society. *Nat. Rev. Immunol.* **12**, 225 (2012).
5. Mallory, M. L., Lindesmith, L. C. & Baric, R. S. Vaccination-induced herd immunity: Successes and challenges. *J. Allergy Clin. Immunol.* **142**, 64–66 (2018).
6. Baxter, D. Active and passive immunity, vaccine types, excipients and licensing. *Occup. Med. (Chic. Ill).* **57**, 552–556 (2007).
7. Pulendran, B. & Ahmed, R. Immunological mechanisms of vaccination. *Nat. Immunol.* **12**, 509–517 (2011).
8. Clem, A. S. Fundamentals of vaccine immunology. *J. Glob. Infect. Dis.* **3**, 73–78 (2011).
9. Moyle, P. M. & Toth, I. Modern Subunit Vaccines: Development, Components, and Research Opportunities. *ChemMedChem* **8**, 360–376 (2013).
10. Jones, R. G. A., Liu, Y., Rigsby, P. & Sesardic, D. An improved method for development of toxoid vaccines and antitoxins. *J. Immunol. Methods* **337**, 42–48 (2008).
11. Minor, P. D. Live attenuated vaccines: Historical successes and current challenges. *Virology* **479–480**, 379–392 (2015).
12. Blower, S. M., Koelle, K., Kirschner, D. E. & Mills, J. Live attenuated HIV vaccines: Predicting the tradeoff between efficacy and safety. *Proc. Natl. Acad. Sci. U. S. A.* **98**, 3618–3623 (2001).
13. Parker, E. P. K., Molodecky, N. A., Pons-salort, M., Reilly, K. M. O. & Grassly, N. C. Impact of inactivated poliovirus vaccine on mucosal immunity : implications for the polio eradication endgame. *Expert Rev. Vaccines* **14**, 1113–1123 (2015).
14. Wang, N. & Wang, T. *Immunization - Vaccine Adjuvant Delivery System and Strategies*. (IntechOpen, 2018).
15. Pasquale, A. Di, Preiss, S., Da Silva, F. & Gar qon, N. Vaccine Adjuvants : from 1920 to 2015 and Beyond. *Vaccines* **3**, 320–343 (2015).
16. Coffman, R. L., Sher, A. & Seder, R. A. Vaccine Adjuvants : Putting Innate Immunity to Work. *Immunity* **33**, 492–503 (2010).
17. Kim, S.-H. & Jang, Y.-S. The development of mucosal vaccines for both mucosal and systemic immune induction and the roles played by adjuvants. *Clin. Exp. Vaccine Res.* **6**, 15–21 (2017).
18. Bergmann-leitner, E. S. & Leitner, W. W. Adjuvants in the Driver's Seat: How Magnitude, Type, Fine Specificity and Longevity of Immune Responses Are Driven by Distinct Classes of Immune Potentiators. *Vaccines* **2**, 252–296 (2014).

19. Marrack, P., Mckee, A. S., Munks, M. W. & Marrack, P. Timeline: Towards an understanding of the adjuvant action of aluminium. *Nat. Rev. Immunol.* **9**, 287–293 (2009).
20. Glenny, A. T., Pope, C. G., Waddington, H. & Wallace, U. Immunology Notes: XVII-XXIV. *J. Pathol. Bacteriol.* **29**, 31–40 (1926).
21. Hutchison, S. *et al.* Antigen depot is not required for alum adjuvanticity. *FASEB J.* **26**, 1272–1279 (2012).
22. Eisenbarth, S. C., Colegio, O. R., O'connor, W., Sutterwala, F. S. & Flavell, R. A. Crucial role for the Nalp3 inflammasome in the immunostimulatory properties of aluminium adjuvants. *Nature* **453**, 1122 (2008).
23. Kool, M. *et al.* Alum adjuvant boosts adaptive immunity by inducing uric acid and activating infl ammatory dendritic cells. *J. Exp. Med.* **205**, 869–882 (2008).
24. Freund, J., Casals, J. & Hosmer, E. Sensitization and antibody formation after injection of Tubercle Bacilli and paraffin oil. *Soc. Exp. Biol. Med.* **37**, 509–513 (1937).
25. Miller, L. H., Saul, A. & Mahanty, S. Revisiting Freund ' s incomplete adjuvant for vaccines in the developing world. *Trends Parasitol.* **21**, 7–9 (2005).
26. Hagan, D. T. O. *et al.* The history of MF59 ® adjuvant : a phoenix that arose from the ashes. *Expert Rev. Vaccines* **12**, 13–30 (2013).
27. Calabro, S. *et al.* The adjuvant effect of MF59 is due to the oil-in-water emulsion formulation , none of the individual components induce a comparable adjuvant effect. *Vaccine* **31**, 3363–3369 (2013).
28. Hagan, D. T. O., Ott, G. S., Gregorio, E. De & Seubert, A. The mechanism of action of MF59 – An innately attractive adjuvant formulation. *Vaccine* **30**, 4341–4348 (2012).
29. Dupuis, M. *et al.* Immunization with the adjuvant MF59 induces macrophage trafficking and apoptosis. *Eur. J. Immunol.* **31**, 2910–2918 (2001).
30. Calabro, S. *et al.* Vaccine adjuvants alum and MF59 induce rapid recruitment of neutrophils and monocytes that participate in antigen transport to draining lymph nodes. *Vaccine* **29**, 1812–1823 (2011).
31. Dupuis, M. *et al.* Dendritic Cells Internalize Vaccine Adjuvant after Intramuscular Injection. *Cell. Immunol.* **186**, 18–27 (1998).
32. Garcia-sicilia, J. *et al.* Immunogenicity and safety of AS03-adjuvanted H1N1 pandemic vaccines in children and adolescents. *Vaccine* **29**, 4353–4361 (2011).
33. Izurieta, P. *et al.* Immunogenicity and safety of an AS03-adjuvanted H5N1 pandemic influenza vaccine in Korean adults : A phase IV , randomized , open-label , controlled study. *Vaccine* **33**, 2800–2807 (2015).
34. Morel, S. *et al.* Adjuvant System AS03 containing a-tocopherol modulates innate immune response and leads to improved adaptive immunity. *Vaccine* **29**, 2461–2473 (2011).
35. Kammer, A. R. *et al.* A new and versatile virosomal antigen delivery system to induce cellular and humoral immune responses. *Vaccine* **25**, 7065–7074 (2007).
36. Moser, C., Amacker, M. & Zurbriggen, R. Influenza virosomes as a vaccine adjuvant and carrier system. *Expert Rev. Vaccines* **10**, 437–446 (2014).
37. Evans, J. T. *et al.* Enhancement of antigen-specific immunity via the TLR4 ligands

MPL ™ adjuvant and Ribi . 529. *Expert Rev. Vaccines* **2**, 219–229 (2003).
38. Casella, C. R. & Mitchell, T. C. Putting endotoxin to work for us : Monophosphoryl lipid A as a safe and effective vaccine adjuvant. *Cell. Mol. Life Sci.* **65**, 3231–3240 (2008).
39. Qureshi, N., Takayama, K. & Ribi, E. Purification and structural determination of nontoxic lipid A obtained from the lipopolysaccaride of Salmonella typhimurium. *J. Biol. Chem.* **257**, 11808–11815 (1982).
40. Didierlaurent, A. M. *et al.* AS04, an aluminum salt-and TLR4 agonist-based adjuvant system, induces a transient localized innate immune response leading to enhanced adaptive immunity. *J. Immunol.* **183**, 6186–6197 (2009).
41. Giudice, G. Del, Rappuoli, R. & Didierlaurent, A. M. Correlates of adjuvanticity : A review on adjuvants in licensed vaccines. *Semin. Immunol.* **39**, 14–21 (2018).
42. Galli, G. *et al.* Fast rise of broadly cross-reactive antibodies after boosting long-lived human memory B cells primed by an MF59 adjuvanted prepandemic vaccine. *Proc. Natl. Acad. Sci. United States* **106**, 7962–7968 (2009).
43. Khurana, S. *et al.* Vaccines with MF59 adjuvant expand the antibody repertoire to target protective sites of pandemic avian H5N1 influenza virus. *Sci. Transl. Med.* **2**, 15ra5 (2010).
44. Zhang, L., Wang, W. & Wang, S. Effect of vaccine administration modality on immunogenicity and efficacy. *Expert Rev. Vaccines* **14**, 1509–1523 (2015).
45. Miquel-Clopes, A., Bentley, E. G., Stewart, J. P. & Carding, S. R. Mucosal vaccines and technology. *Clin. Exp. Immunol.* **196**, 205–214 (2019).
46. Lycke, N. Recent progress in mucosal vaccine development : potential and limitations. *Nat. Rev. Immunol.* **12**, 592–605 (2012).
47. Levine, M. & Dougan, G. Optimism over vaccines administered via mucosal surfaces. *Lancet* **351**, 1375–1376 (1998).
48. Yuki, Y. & Kiyono, H. Mucosal vaccines : novel advances in technology and delivery. *Expert Rev. Vaccines* **8**, 1083–1097 (2009).
49. Mestecky, J. *et al.* Selective Induction of an Immune Response in Human External Secretions by Ingestion of Bacterial Antigen. *J. Clin. Invest.* **61**, 731–737 (1978).
50. Clancy, R. L., Cripps, A. W., Husband, A. J. & Buckley, D. Specific Immune Response in the Respiratory Tract After Administration of an Oral Polyvalent Bacterial Vaccine. *Infect. Immun.* **39**, 491–496 (1983).
51. Kantele, A., Arvilommi, H. & Jokinen, I. Specific Immunoglobulin-Secreting Human Blood Cells after Peroral Vaccination against Salmonella typhi. *J. Infect. Dis.* **153**, 1126–1131 (1986).
52. Czerkinsky, C. *et al.* IgA Antibody-Producing Cells in Peripheral Blood after Antigen Ingestion : Evidence for a Common Mucosal Immune System in Humans. *Proc. Natl. Acad. Sci. U. S. A.* **84**, 2449–2453 (1987).
53. Kantele, A. *et al.* Differences in Immune Responses Induced by Oral and Rectal Immunizations with Salmonella typhi Ty21a : Evidence for Compartmentalization within the Common Mucosal Immune System in Humans. *Infect. Immun.* **66**, 5630–5635 (1998).
54. Sabin, A. *et al.* Live, orally given poliovirus vaccine: effects of rapid mass

immunization on population under conditions of massive enteric infection with other viruses. *J. Am. Med. Assoc.* **173**, 1521–1526 (1960).
55. Jorba, J. *et al.* Update on Vaccine-Derived Polioviruses — Worldwide , January 2017 – June 2018. *Morb. Mortal. Wkly. Rep.* **67**, 1189–1194 (2018).
56. Neutra, M. R. & Kozlowski, P. A. Mucosal vaccines : the promise and the challenge. *Nat. Rev. Immunol.* **6**, 148–158 (2006).
57. Borges, O., Lebre, F., Bento, D., Borchard, G. & Junginger, H. E. Mucosal Vaccines : Recent Progress in Understanding the Natural Barriers. *Pharm. Res.* **27**, 211–223 (2010).
58. Weiner, H. L. & van Rees, E. P. Mucosal tolerance. *Immunol. Lett.* **69**, 3–4 (1999).
59. Burks, A. W., Laubach, S. & Jones, S. M. Oral tolerance , food allergy , and immunotherapy : Implications for future treatment. *J. Allergy Clin. Immunol.* **121**, 1344–1350 (2008).
60. Sakaguchi, S., Powrie, F. & Ransohoff, R. M. Re-establishing immunological self-tolerance in autoimmune disease. *Nat. Med.* **18**, 54 (2012).
61. Slack, E. *et al.* Innate and adaptive immunity cooperate flexibly to maintain host-microbiota mutualism. *Science (80-.).* **325**, 617–621 (2009).
62. Gutgemann, I., Fahrer, A. M., Altman, J. D., Davis, M. M. & Chien, Y. Induction of Rapid T Cell Activation and Tolerance by Systemic Presentation of an Orally Administered Antigen. *Immunity* **8**, 667–673 (1998).
63. Levine, M., Black, R., Ferreccio, C. & Germanier, R. Large-scale field trail of Ty21a live oral typhoid vaccine in enteric-coated capsule formulation. *Lancet* **329**, 1049–1052 (1987).
64. Seong, S., Cho, N. & Kwon, I. C. K. C. Protective Immunity of Microsphere-Based Mucosal Vaccines against Lethal Intranasal Challenge with Streptococcus pneumoniae. *Infect. Immun.* **67**, 3587–3592 (1999).
65. Baca-estrada, M. E. *et al.* Intranasal immunization with liposome-formulated Yersinia pestis vaccine enhances mucosal immune responses. *Vaccine* **18**, 2203–2211 (2000).
66. Chabot, S. *et al.* A novel intranasal Protollin -based measles vaccine induces mucosal and systemic neutralizing antibody responses and cell-mediated immunity in mice. *Vaccine* **23**, 1374–1383 (2005).
67. McNeela, E. *et al.* A mucosal vaccine against diptheria: formulation of cross reacting material (CRM197) of diptheria toxin with chitosan enhances local and systemic antibody and Th2 responses following nasal delivery. *Vaccine* **19**, 11188–1198 (2000).
68. Martin, E. & Hine, R. Peyer's patches. *Oxford A Dictionary of Biology (7 ed.)* (2016).
69. Eldridge, J., Meulbroek, J., Staas, J., Tice, T. & Gilley, R. Vaccine-containing biodegradable microspheres specifically enter the gut-associated lymphoid tissue following oral administration and induce a disseminated mucosal immune response. *Adv Exp Med Biol* **251**, 191–202 (1989).
70. Ryan, E. J., Daly, L. M. & Mills, K. H. G. Immunomodulators and delivery systems for vaccination by mucosal routes. *Trends Biotechnol.* **19**, 293–304 (2001).

71. McDermott, M. & Bienenstock, J. Evidence for a common mucosal immunologic system. I. Migration of B immunoblasts into intestinal, respiratory, and genital tissues. *J. Immunol.* **122**, 1892–1898 (1979).
72. Izadpanah, A. *et al.* Regulated MIP-3a/CCL20 production by human intestinal epithelium : mechanism for modulating mucosal immunity. *Am. J. Physiol. Liver Physiol.* **280**, 710–719 (2001).
73. Eckmann, L., Kagnoff, M. F. & Fierer, J. Epithelial Cells Secrete the Chemokine Interleukin-8 in Response to Bacterial Entry. *Infect. Immun.* **61**, 4569–4574 (1993).
74. Jung, H. C. *et al.* A distinct array of proinflammatory cytokines is expressed in human colon epithelial cells in response to bacterial invasion. *J. Clin. Inestigation* **95**, 55–65 (1995).
75. Hamada, H. *et al.* Identification of Multiple Isolated Lymphoid Follicles on the Antimesenteric Wall of the Mouse Small Intestine. *J. Immunol.* **168**, 57–64 (2002).
76. Maric, I., Holt, P., Perdue, M. & Bienenstock, J. Class II MHC antigen (Ia)-bearing dendritic cells in the epithelium of the rat intestine. *J. Immunol.* **156**, 1408–1414 (1996).
77. Niess, J. *et al.* CX3CR1-mediated dendritic cell access to the intestinal lumen and bacterial clearance . *Science (80-.).* **307**, 254–258 (2005).
78. Rescigno, M. *et al.* Dendritic cells express tight junction proteins and penetrate gut epithelial monolayers to sample bacteria. *Nat. Immunol.* **2**, 361 (2001).
79. Kraehenbuhl, J. & Neutra, M. *Defense of mucosal surfaces: Pathogenesis, Immunity and Vaccines. Current topics in microbiology and immunology*. (Springer, Berlin, Heidelberg, 1999).
80. Warshaw, A., Walker, W. & Isselbacher, K. Protein uptake by the intestine: evidence for aborption of intact macromolecules. *Gastroenterology* **66**, 987–992 (1974).
81. Husby, S., Jensenius, J. & Svehag, S. Passage of undegraded dietary antigen into the blood of healthy adults. Quantification, estimation of size distribution, and relation of uptake to levels of specific antibodies. *Scand. J. Immunol.* **22**, 83–92 (1985).
82. Sender, R., Fuchs, S. & Milo, R. Revised estimates for the number of human and bacteria cells in the body. *PLoS Biol.* **14**, 1–14 (2016).
83. The Human Microbiome Project Consortium. Structure , function and diversity of the healthy human microbiome. *Nature* **486**, 207–214 (2012).
84. Rooks, M. G. & Garrett, W. S. Gut microbiota, metabolites and host immunity. *Nat. Rev. Immunol.* **16**, 341–352 (2016).
85. Leblanc, J. G. *et al.* Bacteria as vitamin suppliers to their host : a gut microbiota perspective. *Curr. Opin. Biotechnol.* **24**, 160–168 (2013).
86. Kommineni, S. *et al.* Bacteriocin production augments niche competition by enterococci in the mammalian gastrointestinal tract. *Nature* **526**, 719–722 (2015).
87. Johansson, M. *et al.* Normalization of Host Intestinal Mucus Layers Requires Long-Term Microbial Colonization. *Cell Host Microbe* **18**, 582–592 (2015).

88. Bouskra, D. *et al.* Lymphoid tissue genesis induced by commensals through NOD1 regulates intestinal homeostasis. *Nature* **456**, 507 (2008).
89. Pabst, O. *et al.* Adaption of solitary intestinal lymphoid tissue in response to Microbiota and Chemokine Receptor CCR7 Signaling. *J. Immunol.* **177**, 6824–6832 (2006).
90. Ivanov, I. I. *et al.* Specific Microbiota Direct the Differentiation of IL-17-Producing T-Helper Cells in the Mucosa of the Small Intestine. *Cell Host Microbe* **4**, 337–349 (2008).
91. Ivanov, I. I. *et al.* Induction of Intestinal Th17 Cells by Segmented Filamentous Bacteria. *Cell* **139**, 485–498 (2009).
92. Atarashi, K. *et al.* Induction of Colonic Regulatory T Cells by indigenous Clostridium species. *Science (80-.).* **331**, 337–342 (2011).
93. Geuking, M. B. *et al.* Intestinal Bacterial Colonization Induces Mutualistic Regulatory T Cell Responses. *Immunity* **34**, 794–806 (2011).
94. Uematsu, S. *et al.* Regulation of humoral and cellular gut immunity by lamina propria dendritic cells expressing Toll-like receptor 5. *Nat. Immunol.* **9**, 769–776 (2008).
95. Macpherson, A., Gatto, D., Sainsbury, E. & Harriman, G. A primitive T cell-independent mechanism of intestinal mucosal IgA responses to commensal bacteria . *Science (80-.).* **288**, 2222–2226 (2000).
96. Sanos, S. L. *et al.* RORyt and commensal microflora are required for the differentiation of mucosal interleukin 22 – producing NKp46+ cells. *Nat. Immunol.* **10**, 83–91 (2008).
97. Macpherson, A. & Uhr, T. Induction of protective IgA by intestinal dendritic cells carrying commensal bacteria. *Science (80-.).* **303**, 1662–1665 (2004).
98. Bisgaard, H. *et al.* Reduced diversity of the intestinal microbiota during infancy is associated with increased risk of allergic disease at school age. *J. Allergy Clin. Immunol.* **128**, 626–652 (2011).
99. de Goffau, M. *et al.* Fecal microbitoa composition differs between children with beta-cell autoimmunity and those without. *Diabetes* **62**, 1238–1244 (2013).
100. Wu, H. *et al.* Gut-Residing Segmented Filamentous Bacteria Drive Autoimmune Arthritis via T Helper 17 Cells. *Immunity* **32**, 815–827 (2010).
101. Kim, S. C. *et al.* Variable phenotypes of enterocolitis in interleukin 10-deficient mice monoassociated with two different commensal bacteria. *Gastroenterology* **128**, 891–906 (2005).
102. Ochoa-repáraz, J. *et al.* Role of gut commensal microflora in tbe development of experimental autoimmune encephalomyelitis. *J. Immunol.* **183**, 6041–6050 (2009).
103. Trompette, A. *et al.* Gut microbiota metabolism of dietary fiber influences allergic airway disease and hematopoiesis. *Nat. Med.* **20**, 159–166 (2014).
104. Lu, Y. *et al.* Short Chain Fatty Acids Prevent High-fat-diet-induced Obesity in Mice by Regulating G Protein- coupled Receptors and Gut Microbiota. *Sci. Rep.* **6**, 1–13 (2016).
105. Murphy, K. & Weaver, C. *Janeway's Immunobiology*. (Garland Science Taylor & Francis Group, 2017).

106. Takeuchi, O. *et al.* Cutting edge: preferentially the R-stereoisomer of the mycoplasmal lipopeptide macrophage-activating lipopeptide-2 activates immune cells through a toll-like receptor 2-and MyD88-dependent signaling pathway. *J. Immunol.* **164**, 554–557 (2000).
107. Poltorak, A., He, X., Smirnova, I. & Liu, M. Defective LPS signaling in C3H / HeJ and C57BL10ScCr mice : Mutations in Tlr4 gene. *Science (80-.).* **282**, 2085–2093 (1998).
108. Hemmi, H. *et al.* A Toll-like receptor recognizes bacterial DNA. *Nature* **408**, 740–745 (2000).
109. Alexopoulou, L., Holt, A., Medzhitov, R. & Flavell, R. A. Recognition of double-stranded RNA and activation of NF- k B by Toll-like receptor 3. *Nature* **413**, 732–738 (2001).
110. Hayashi, F. *et al.* The innate immune response to bacterial flagellin is mediated by Toll-like receptor 5. *Nature* **410**, 1099–1103 (2001).
111. Geijtenbeek, T. B. H. & Gringhuis, S. I. Signalling through C-type lectin receptors: shaping immune responses. *Nat. Rev. Immunol.* **9**, 465–479 (2009).
112. Royet, J. & Reichhart, J. Detection of peptidoglycans by NOD proteins. *Trends Cell Biol.* **13**, 610–614 (2003).
113. Yoneyama, M. *et al.* The RNA helicase RIG-I has an essential function in double-stranded RNA-induced innate antiviral responses. *Nat. Immunol.* **5**, 730–737 (2004).
114. Takeuchi, O. & Akira, S. Pattern Recognition Receptors and Inflammation. *Cell* **140**, 805–820 (2010).
115. Martinon, F., Mayor, A. & Tschopp, J. The Inflammasomes : Guardians of the Body. *Annu. Rev. Immunol.* **27**, 229–265 (2009).
116. Martinon, F., Burns, K. & Tschopp, J. The Inflammasome : A Molecular Platform Triggering Activation of Inflammatory Caspases and Processing of proIL-beta. *Mol. Cell* **10**, 417–426 (2002).
117. Franchi, L. *et al.* Cytosolic flagellin requires Ipaf for activation of caspase-1 and interleukin 1B in salmonella-infected macrophages. *Nat. Immunol.* **7**, 576–582 (2006).
118. Carta, S. *et al.* Cell stress increases ATP release in NLRP3 inflammasome-mediated autoinflammatory diseases , resulting in cytokine imbalance. *Proc. Natl. Acad. Sci. U. S. A.* **112**, 2835–2840 (2015).
119. Martinon, F., Petrilli, V., Mayor, A., Tardivel, A. & Tschopp, J. Gout-associated uric acid crystals activate the NALP3 inflammasome. *Nature* **440**, 237–241 (2006).
120. Hornung, V. *et al.* Silica crystals and aluminum salts activate the NALP3 inflammasome through phagosomal destabilization. *Nat. Immunol.* **9**, 847–856 (2008).
121. Idoyaga, J. & Steinman, R. M. SnapShot: Dendritic Cells. *Cell* **146**, 660-660.e2 (2011).
122. Steinman, R. M. Dendritic cells: versatile controllers of the immune system. *Nat. Med.* **13**, 1155–1159 (2007).
123. Jakubzick, C. *et al.* Modulation of dendritic cell trafficking to and from the

airways. *J. Immunol.* **176**, 3578–3584 (2006).
124. Macri, C., Pang, E. S., Patton, T. & O'Keeffe, M. Dendritic cell subsets. *Semin. Cell Dev. Biol.* **84**, 11–21 (2018).
125. Merad, M. & Manz, M. G. Dendritic cell homeostasis. *Blood* **113**, 3418–3427 (2009).
126. Cella, M., Engering, A., Pinet, V., Pieters, J. & Lanzavecchia, A. Inflammatory stimuli induce accumulation of MHC class II complexes on dendritic cells. *Nature* **388**, 782–787 (1997).
127. Larsen, C. P., Ritchie, S. C., Pearson, T. C., Linsley, P. S. & Lowry, R. P. Functional Expression of the Costimulatory Molecule, B7/BB1, on Murine Dendritic Cell Populations. *J. Exp. Med.* **176**, 1215–1220 (1992).
128. Martín-fontecha, A. *et al.* Regulation of Dendritic Cell Migration to the Draining Lymph Node : Impact on T Lymphocyte Traffic and Priming. *J. Exp. Med.* **198**, 615–622 (2003).
129. Yanagihara, S. *et al.* EBI1/CCR7 Is a New Member of Dendritic Cell Chemokine Receptor That Is Up-Regulated upon Maturation. *J. Immunol.* **161**, 3096–3102 (1998).
130. Forster, R. *et al.* CCR7 Coordinates the Primary Immune Response by Establishing Functional Microenvironments in Secondary Lymphoid Organs. *Cell* **99**, 23–33 (1999).
131. Randolph, G. J., Ochando, J. & Partida-Sanchez, S. Migration of Dendritic Cell Subsets and their Precursors. *Annu. Rev. Immunol.* **26**, 293–316 (2008).
132. Sixt, M. *et al.* The conduit system transports soluble antigens from the afferent lymph to resident dendritic cells in the T cell area of the lymph node. *Immunity* **22**, 19–29 (2005).
133. Heufler, C. *et al.* Interleukin-l2 is produced by dendritic cells and mediates T helper 1 development as well as interferon-y production by T helper 1 cells. *Eur. J. Immunol.* **26**, 659–668 (1996).
134. Connor, L. M., Tang, S., Camberia, M., Le Gros, G. & Ronchese, F. Helminth-Conditioned Dendritic Cells Prime CD4 + T Cells to IL-4 Production In Vivo. *J. Immunol.* **193**, 2709–2717 (2014).
135. Seubert, A. *et al.* The adjuvants aluminum hydroxide and MF59 induce monocyte and granulocyte chemoattractants and enhance monocyte differentiation toward dendritic cells. *J. Immunol.* **180**, 5402–5412 (2008).
136. Bouteau, A. A. *et al.* DC Subsets Regulate Humoral Immune Responses by Supporting the Differentiation of Distinct Tfh Cells . *Front. Immunol.* **10**, (2019).
137. Wille-reece, A. U. *et al.* HIV Gag protein conjugated to a Toll-like receptor 7 / 8 agonist improves the magnitude and quality of Thl and CD8 + T cell responses in nonhuman primates. *Proc. Natl. Acad. Sci.* **102**, 15190–15194 (2005).
138. Huleatt, J. W. *et al.* Vaccination with recombinant fusion proteins incorporating Toll-like receptor ligands induces rapid cellular and humoral immunity. *Vaccine* **25**, 763–775 (2007).
139. Kazzaz, J. *et al.* Encapsulation of the immune potentiators MPL and RC529 in PLG microparticles enhances their potency. *J. Control. Release* **110**, 566–573 (2006).

140. Franco, D., Liu, W., Gardiner, D., Hahn, B. & Ho, D. CD40L-containing virus-like particle as a candidate HIV-1 vaccine targeting dendritic cells. *J. Acquir. Immune Defic. Syndr.* **56**, 393–400 (2011).
141. Park, H. *et al.* Enhancing vaccine antibody responses by targeting Clec9A on dendritic cells. *npj Vaccines* **2**, 31–42 (2017).
142. Caminschi, I. *et al.* The dendritic cell subtype-restricted C-type lectin Clec9A is a target for vaccine enhancement. *Blood* **112**, 3264–3273 (2008).
143. Bassing, C. H., Swat, W. & Alt, F. W. The Mechanism and Regulation of Chromosomal V (D) J Recombination. *Cell* **109**, 45–55 (2002).
144. Lanzavecchia, A. & Sallusto, F. From synapses to immunological memory : the role of sustained T cell stimulation. *Curr. Opin. Immunol.* **12**, 92–98 (2000).
145. De Silva, N. S. & Klein, U. Dynamics of B cells in germinal centres. *Nat. Rev. Immunol.* **15**, 137–148 (2015).
146. Ollila, J. & Vihinen, M. B cells. *Int. J. Biochem. Cell Biol.* **37**, 518–523 (2005).
147. Turner, J. S., Marthi, M., Benet, Z. L. & Grigorova, I. Transiently antigen-primed B cells return to naive-like state in absence of T-cell help. *Nat. Commun.* **8**, 1–11 (2017).
148. Goodnow, C. C. Chance encounters and organized rendezvous. *Immunol. Rev.* **156**, 5–10 (1997).
149. Pape, K. A., Catron, D. M., Itano, A. A. & Jenkins, M. K. The Humoral Immune Response Is Initiated in Lymph Nodes by B Cells that Acquire Soluble Antigen Directly in the Follicles. *Immunity* **26**, 491–502 (2007).
150. Garside, P. *et al.* Visualization of specific B and T lymphocyte interactions in the lymph node . *Science (80-.).* **281**, 96–99 (1998).
151. Reif, K. *et al.* Balanced responsiveness to chemoattractants from adjacent zones determines B-cell position. *Nature* **416**, 94–99 (2002).
152. Lanzavecchia, A. Antigen-specific interaction between T and B cells. *Nature* **314**, 537–539 (1985).
153. King, C., Tangye, S. G. & Mackay, C. R. T follicular helper (TFH) cells in noraml and dysregulated immune responses. *Annu. Rev. Immunol.* **26**, 741–766 (2008).
154. Chan, T. D. *et al.* Antigen affinity controls rapid T-dependent antibody production by driving the expansion rather than the differentation or extrafollicular migration of early plasmablasts. *J. Immunol.* **183**, 3139–3149 (2009).
155. Cervenak, L., Magyar, A., Boja, R. & Laszlo, G. Differential expression of GL7 activation antigen on bone marrow B cell subpopulations and peripheral B cells. *Immunol. Lett.* **78**, 89–96 (2001).
156. Crotty, S. Follicular Helper CD4 T cells (TFH). *Annu. Rev. Immunol.* **29**, 621–663 (2011).
157. Xu, Z., Zan, H., Pone, E. J., Mai, T. & Casali, P. Immunoglobulin class-switch DNA recombination : induction , targeting and beyond. *Nat. Rev. Immunol.* **12**, 517–531 (2012).
158. Inamine, A. *et al.* Two waves of memory B-cell generation in the primary immune response. *Int. Immunol.* **17**, 581–589 (2005).
159. Pape, K. A. *et al.* Visualization of the Genesis and Fate of Isotype-switched B

Cells during a Primary Immune Response. *J. Exp. Med.* **197**, 1677–1687 (2003).
160. Vidarsson, G., Dekkers, G. & Rispens, T. IgG subclasses and allotypes: From structure to effector functions. *Front. Immunol.* **5**, 1–17 (2014).
161. Lafaille, J. J. & Curotto de Lafaille, M. A. *Current Topics in Microbiology and Immunology, IgE Antibodies : Generation and Function*. (Springer International Publishing Switzerland, 2015).
162. Macpherson, A. J., Mccoy, K. D., Johansen, F. & Brandtzaeg, P. The immune geography of IgA induction and function. *Mucosal Immunol.* **1**, 11–22 (2008).
163. Yu, X. *et al.* Neutralizing antibodies derived from the B cells of 1918 influenza pandemic survivors. *Nature* **455**, 532–536 (2008).
164. Slifka, M. K., Matloubian, M. & Ahmed, R. Bone Marrow Is a Major Site of Long-Term Antibody Production after Acute Viral Infection. *J. Virol.* **69**, 1895–1902 (1995).
165. Hammarlund, E. *et al.* Plasma cell survival in the absence of B cell memory. *Nat. Commun.* **8**, 1781–1792 (2017).
166. Slifka, M. K., Antia, R., Whitmire, J. K. & Ahmed, R. Humoral immunity due to long-lived plasma cells. *Immunity* **8**, 363–372 (1998).
167. Amanna, I. J., Carlson, N. E. & Slifka, M. K. Duration of Humoral Immunity to Common Viral and Vaccine Antigens. *N. Engl. J. Med.* **357**, 1903–1915 (2007).
168. Chen, W. H. *et al.* Vaccination in the elderly : an immunological perspective. *Trends Immunol.* **30**, 351–359 (2009).
169. Podda, A. The adjuvanted influenza vaccines with novel adjuvants : experience with the MF59-adjuvanted vaccine. *Vaccine* **19**, 2673–2680 (2001).
170. Moldoveanu, Z. T., Clementst, M. L., Prince, S. J., Murphy, B. R. & Mestecky, J. Human immune responses to influenza virus vaccines administered by systemic or mucosal routes. *Vaccine* **13**, 1006–1012 (1995).
171. Trapani, J. A. & Smyth, M. J. Functional significance of the perforin/granzyme cell death pathway. *Nat. Rev. Immunol.* **2**, 735–747 (2002).
172. Abbas, A. K., Murphy, K. M. & Sher, A. Functional diversity of helper T lymphocytes. 787–793.
173. Horiuchi, S. *et al.* Genome-Wide Analysis Reveals Unique Regulation of Transcription of Th2-Specific Genes by GATA3. *J. Immunol.* **186**, 6378–6389 (2011).
174. Allen, J. E. & Sutherland, T. E. Host protective roles of type 2 immunity: parasite killing and tissue repair, flip sides of the same coin. *Semin. Immunol.* **26**, 329–340 (2014).
175. Park, H. *et al.* A distinct lineage of CD4 T cells regulates tissue inflammation by producing interleukin 17. *Nat. Immunol.* **6**, 1133–1141 (2005).
176. Ye, P. *et al.* Requirement of Interleukin 17 Receptor Signaling for Lung CXC Chemokine and Granulocyte Colony-stimulating Factor Expression , Neutrophil Recruitment , and Host Defense. *J. Exp. Med.* **194**, 519–527 (2001).
177. Josefowicz, S. Z. & Rudensky, A. Control of Regulatory T Cell Lineage Commitment and Maintenance. *Immunity* **30**, 616–625 (2009).
178. Nakayamada, S., Takahashi, H., Kanno, Y. & Shea, J. J. O. Helper T cell diversity and plasticity. *Curr. Opin. Immunol.* **24**, 297–302 (2012).

179. Masopust, D., Vezys, V., Marzo, A. L. & Lefrancois, L. Preferential Localization of Effector Memory Cells in Nonlymphoid Tissue. *Science (80-.).* **291**, 2413–2418 (2001).
180. Sallusto, F., Lenig, D., Forster, R., Lipp, M. & Lanzavecchia, A. Two subsets of memory T lymphocytes with distinct homing potentials and effector functions. *Nature* **401**, 708–712 (1999).
181. Nguyen, Q. P., Deng, T. Z., Witherden, D. A. & Goldrath, A. W. Origins of CD4 + circulating and tissue-resident memory T-cells. *Immunology* **157**, 3–12 (2019).
182. Hansen, S. G. *et al.* Profound early control of highly pathogenic SIV by an effector memory T-cell vaccine. *Nature* **473**, 523–527 (2011).
183. Swadling, L. *et al.* A human vaccine strategy based on chipanzee adenoviral and MVA vectors that primes, boosts, and sustains functional HCV-specific T cell memory. *Sci. Transl. Med.* **6**, 261ra153 (2014).
184. Hu, Z., Molloy, M. J. & Usherwood, E. J. CD4+ T-cell dependence of primary CD8+ T-cell response against vaccinia virus depends upon route of infection and viral dose. *Cell. Mol. Immunol.* **13**, 82–93 (2016).
185. Wherry, E. J. T cell exhaustion. *Nat. Publ. Gr.* **12**, 6–13 (2011).
186. Panagioti, E., Klenerman, P., Lee, L., van Der Burg, S. & Arens, R. Features of effective T cell-inducing vaccines against chronic viral infections. *Front. Immunol.* **9**, (2018).
187. He, R. *et al.* Efficient control of chronic LCMV infection by a CD4 T cell epitope-based heterologous prime-boost vaccination in a murine model. *Cell. Mol. Immunol.* **15**, 815–826 (2018).
188. Martins, K. A. O. *et al.* Adjuvant-enhanced CD4 T Cell Responses are Critical to Durable Vaccine Immunity. *EBioMedicine* **3**, 67–78 (2016).
189. Pedersen, S. R. *et al.* Comparison of Vaccine-Induced Effector CD8 T Cell Responses Directed against Self- and Non − Self-Tumor Antigens: Implications for Cancer Immunotherapy. *J. Immunol.* **191**, 3955–3967 (2013).
190. Timens, W. I. M., Boes, A., Rozeboom-uiterwijk, T. & Poppema, S. Immaturity of the human splenic marginal zone in infancy - Possible contribution to the deficient infant immune response. *J. Immunol.* **143**, 3200–3206 (1989).
191. Einhorn, M., Anderson, E., Weinberg, G., Granoff, P. & Granoff, D. Immunogenicity in infants of Haemophilus influenzae type B polysaccharide in a conjugate vaccine with Neisseria meningitidis outer-membrane protein. *Lancet* **328**, 299–302 (1986).
192. Pollard, A. J., Perrett, K. P. & Beverley, P. C. Maintaining protection against invasive bacteria with protein-polysaccaride conjugate vaccines. *Nat. Rev. Immunol.* **9**, 213–221 (2009).
193. Apter, F. M., Lencer, W. I., Finkelstein, R. A., Mekalanos, J. J. & Neutra, M. R. Monoclonal Immunoglobulin A Antibodies Directed against Cholera Toxin Prevent the Toxin-Induced Chloride Secretory Response and Block Toxin Binding to Intestinal Epithelial Cells In Vitro. *Infect. Immun.* **61**, 5271–5278 (1993).
194. Crux, N. B. & Elahi, S. Human leukocyte antigen (HLA) and immune regulation: How do classical and non-classical HLA alleles modulate immune response to human immunodeficiency virus and hepatitis C virus infections? *Front. Immunol.*

8, (2017).
195. Liu, Y. *et al.* Association of human leukocyte antigen alleles and supertypes with immunogenicity of oral rotavirus vaccine given to infants in China. *Medicine (Baltimore).* **97**, 1–5 (2018).
196. Gulukota, K. & Delisi, C. HLA allele selection for designing peptide vaccines. *Genet. Anal. Biomol. Eng.* **13**, 81–86 (1996).
197. Bennett, M. S., Round, J. L. & Leung, D. T. Innate-like lymphocytes in intestinal infections. *Curr. Opin. Infect. Dis.* **28**, 457–463 (2015).
198. Le Bourhis, L. *et al.* Antimicrobial activity of mucosal-associated invariant T cells. *Nat. Immunol.* **11**, 701–708 (2010).
199. Gapin, L. Where Do MAIT Cells Fit in the Family of Unconventional T Cells? *PLoS Biol.* **7**, e1000070 (2009).
200. Reantragoon, R. *et al.* Antigen-loaded MR1 tetramers define T cell receptor heterogeneity in mucosal-associated invariant T cells. *J. Exp. Med.* **210**, 2305–2320 (2013).
201. Treiner, E. *et al.* Mucosal-associated invariant T (MAIT) cells: An evolutionarily conserved T cell subset. *Microbes Infect.* **7**, 552–559 (2005).
202. Kumar, V. & Ahmad, A. Role of MAIT cells in the immunopathogenesis of inflammatory diseases: New players in old game. *Int. Rev. Immunol.* **37**, 90–110 (2018).
203. Dias, J., Leeansyah, E. & Sandberg, J. K. Multiple layers of heterogeneity and subset diversity in human MAIT cell responses to distinct microorganisms and to innate cytokines. *Proc. Natl. Acad. Sci.* **114**, E5434–E5443 (2017).
204. Rahimpour, A. *et al.* Identification of phenotypically and functionally heterogeneous mouse mucosal-associated invariant T cells using MR1 tetramers. *J. Exp. Med.* **212**, 1095–1108 (2015).
205. Xiao, X. & Cai, J. Mucosal-associated invariant T cells: New insights into antigen recognition and activation. *Front. Immunol.* **8**, 12–15 (2017).
206. Treiner, E. *et al.* Selection of evolutionarily conserved mucosal-associated invariant T cells by MR1. *Nature* **422**, 164–169 (2003).
207. Huang, S. *et al.* MR1 antigen presentation to mucosal-associated invariant T cells was highly conserved in evolution. *Proc. Natl. Acad. Sci. U. S. A.* **106**, 8290–8295 (2009).
208. Riegert, P., Wanner, V. & Bahram, S. Genomics, isoforms, expression, and phylogeny of the MHC class I-related MR1 gene. *J. Immunol.* **161**, 4066–77 (1998).
209. Wang, H. *et al.* IL-23 costimulates antigen-specific MAIT cell activation and enables vaccination against bacterial infection. *Sci. Immunol.* **4**, 1–14 (2019).
210. Kjer-Nielsen, L. *et al.* MR1 presents microbial vitamin B metabolites to MAIT cells. *Nature* **491**, 717–723 (2012).
211. Truscott, S. M. *et al.* Biochemical Features of the MHC-Related Protein 1 Consistent with an Immunological Function. *J. Immunol.* **170**, 6090–6098 (2003).
212. Fremont, D. H. *et al.* MR1 uses an endocytic pathway to activate mucosal-associated invariant T cells. *J. Exp. Med.* **205**, 1201–1211 (2008).
213. Corbett, A. J. *et al.* T-cell activation by transitory neo-antigens derived from

distinct microbial pathways. *Nature* **509**, 361–365 (2014).
214. Pediongco, T. *et al.* Drugs and drug-like molecules can modulate the function of mucosal-associated invariant T cells. *Nat. Immunol.* **18**, 402–411 (2017).
215. Villadangos, J. A. *et al.* A molecular basis underpinning the T cell receptor heterogeneity of mucosal-associated invariant T cells. *J. Exp. Med.* **211**, 1585–1600 (2014).
216. Meierovics, A., Yankelevich, W.-J. C. & Cowley, S. C. MAIT cells are critical for optimal mucosal immune responses during in vivo pulmonary bacterial infection. *Proc. Natl. Acad. Sci.* **110**, E3119–E3128 (2013).
217. Mori, L., Lepore, M. & De Libero, G. The Immunology of CD1- and MR1-Restricted T Cells. *Annu. Rev. Immunol.* **34**, 479–510 (2016).
218. Wang, H. *et al.* MAIT cells protect against pulmonary Legionella longbeachae infection. *Nat. Commun.* **9**, 3350–3365 (2018).
219. Wilgenburg, B. van *et al.* MAIT cells contribute to protection against lethal influenza infection in vivo. *Nat. Commun.* **9**, 1–9 (2018).
220. Howson, L. J., Salio, M. & Cerundolo, V. MR1-restricted mucosal-associated invariant T cells and their activation during infectious diseases. *Front. Immunol.* **6**, 303 (2015).
221. Willberg, C. B. *et al.* MAIT cells are licensed through granzyme exchange to kill bacterially sensitized targets. *Mucosal Immunol.* **8**, 429–440 (2014).
222. Chen, Z. *et al.* Mucosal-associated invariant T-cell activation and accumulation after in vivo infection depends on microbial riboflavin synthesis and co-stimulatory signals. *Mucosal Immunol.* **10**, 58–68 (2017).
223. Berkson, J. D. & Prlic, M. The MAIT conundrum – how human MAIT cells distinguish bacterial colonization from infection in mucosal barrier tissues. *Immunol. Lett.* **192**, 7–11 (2017).
224. Ussher, J. E. *et al.* CD161++CD8+ T cells, including the MAIT cell subset, are specifically activated by IL-12+IL-18 in a TCR-independent manner. *Eur. J. Immunol.* **44**, 195–203 (2014).
225. Crowe, J. *et al.* Human mucosal-associated invariant T cells contribute to antiviral influenza immunity via IL-18–dependent activation. *Proc. Natl. Acad. Sci.* **113**, 10133–10138 (2016).
226. Chiba, A. *et al.* Activation status of mucosal-associated invariant T cells reflects disease activity and pathology of systemic lupus erythematosus. *Arthritis Res. Ther.* **19**, 58–68 (2017).
227. Gherardin, N. A., McCluskey, J., Rossjohn, J. & Godfrey, D. I. The diverse family of MR1-restricted T cells. *J. Immunol.* **201**, 2862–2871 (2018).
228. Fries, B. C. & Varshney, A. K. Bacterial Toxins-Staphylococcal Enterotoxin B. *Microbiol. Spectr.* **1**, 1–21 (2013).
229. Shaler, C. R. *et al. MAIT cells launch a rapid, robust and distinct hyperinflammatory response to bacterial superantigens and quickly acquire an anergic phenotype that impedes their cognate antimicrobial function: Defining a novel mechanism of superantigen-induced immunopatho*. *PLoS Biology* vol. 15 (2017).
230. Pullen, A. M. *et al.* The Vβ-specific superantigen staphylococcal enterotoxin B:

Stimulation of mature T cells and clonal deletion in neonatal mice. *Cell* **56**, 27–35 (1989).
231. Holmgren, J. & Czerkinsky, C. Mucosal immunity and vaccines. *Nat. Med.* **11**, 45–53 (2005).
232. O'Hagan, D. T., Friedland, L. R., Hanon, E. & Didierlaurent, A. M. Towards an evidence based approach for the development of adjuvanted vaccines. *Curr. Opin. Immunol.* **47**, 93–102 (2017).
233. Anderson, R. J. *et al.* A self-adjuvanting vaccine induces cytotoxic T lymphocytes that suppress allergy. *Nat. Chem. Biol.* **10**, 943–949 (2014).
234. Anderson, R. J. *et al.* NKT cell-dependent glycolipid–peptide vaccines with potent anti-tumour activity. *Chem. Sci.* **6**, 5120–5127 (2015).
235. Hermans, I. F. *et al.* Dendritic cell function can be modulated through cooperative actions of TLR ligands and invariant NKT cells. *J. Immunol.* **178**, 2721–2729 (2007).
236. Salio, M. *et al.* Activation of Human Mucosal-Associated Invariant T Cells Induces CD40L-Dependent Maturation of Monocyte-Derived and Primary Dendritic Cells. *J. Immunol.* **199**, 2631–2638 (2017).
237. Gautier, G. *et al.* A type I interferon autocrine-paracrine loop is involved in Toll-like receptor-induced interleukin-12p70 secretion by dendritic cells. *J. Exp. Med.* **201**, 1435–1446 (2005).
238. Huntington, J. A. & Stein, P. E. Structure and properties of ovalbumin. *J. Chromatogr. B Biomed. Sci. Appl.* **756**, 189–198 (2001).
239. Avalos, A. M. *et al.* Monovalent engagement of the BCR activates ovalbumin-specific transnuclear B cells. *J. Exp. Med.* **211**, 365–379 (2014).
240. Vidard, L., Rock, K. L. & Benacerraf, B. Diversity in MHC class II ovalbumin T cell epitopes generated by distinct proteases. *J. Immunol.* **149**, 498–504 (1992).
241. Roediger, B. *et al.* Cutaneous immunosurveillance and regulation of inflammation by group 2 innate lymphoid cells. *Nat. Immunol.* **14**, 564–573 (2013).
242. Treiner, E. *et al.* Selection of evolutionarily conserved mucosal-associated invariant T cells by MR1. *Nature* **422**, 164–169 (2003).
243. Moran, A. E. *et al.* T cell receptor signal strength in Treg and iNKT cell development demonstrated by a novel fluorescent reporter mouse. *J. Exp. Med.* **208**, 1279–1289 (2011).
244. Hildner, K. *et al.* Batf3 deficiency reveals a critical role for CD8α+ dendritic cells in cytotoxic T cell immunity. *Science (80-.).* **322**, 1097–1100 (2008).
245. Akbari, M. *et al.* IRF4 in Dendritic Cells Inhibits IL-12 Production and Controls Th1 Immune Responses against Leishmania major . *J. Immunol.* **192**, 2271–2279 (2014).
246. Kaplan, M. H., Schindler, U., Smiley, S. T. & Grusby, M. J. Stat6 is required for mediating responses to IL-4 and for the development of Th2 cells. *Immunity* **4**, 313–319 (1996).
247. Chen, P. *et al.* Dendritic cell targeted vaccines: Recent progresses and challenges. *Hum. Vaccines Immunother.* **12**, 612–622 (2016).
248. Castro, F. V. V. *et al.* CD11c provides an effective immunotarget for the

generation of both CD4 and CD8 T cell responses. *Eur. J. Immunol.* **38**, 2263–2273 (2008).
249. Bonifaz, L. C. *et al.* In Vivo Targeting of Antigens to Maturing Dendritic Cells via the DEC-205 Receptor Improves T Cell Vaccination. *J. Exp. Med.* **199**, 815–824 (2004).
250. Siegal, F. P. *et al.* The nature of the principal Type 1 interferon-producing cells in human blood. *Science (80-.).* **284**, 1835–1837 (1999).
251. Tabib, Y. *et al.* Cell-intrinsic regulation of murine epidermal Langerhans cells by protein S. *Proc. Natl. Acad. Sci. U. S. A.* **115**, E5736–E5745 (2018).
252. Merad, M., Helft, J., Sathe, P., Miller, J. & Mortha, A. The Dendritic Cell Lineage: Ontogeny and Function of Dendritic Cells and Their Subsets in the Steady State and the Inflamed Setting. *Annu. Rev. Immunol.* **31**, 563–604 (2013).
253. Sichien, D., Lambrecht, B. N., Guilliams, M. & Scott, C. L. Development of conventional dendritic cells: From common bone marrow progenitors to multiple subsets in peripheral tissues. *Mucosal Immunol.* **10**, 831–844 (2017).
254. Gurka, S., Hartung, E., Becker, M. & Kroczek, R. A. Mouse conventional dendritic cells can be universally classified based on the mutually exclusive expression of XCR1 and SIRPα. *Front. Immunol.* **6**, 6–11 (2015).
255. Vanderkerken, M. *et al.* IRF8 Transcription Factor Controls Survival and Function of Terminally Differentiated Conventional and Plasmacytoid Dendritic Cells, Respectively. *Immunity* **45**, 626–640 (2016).
256. Hildner, K. *et al.* Batf3 Deficiency Reveals a Critical Role for CD8α + Dendritic Cells in Cytotoxic T Cell Immunity. *Science (80-.).* **322**, 1097–1101 (2008).
257. Bagadia, P. *et al.* Batf3 maintains autoactivation of Irf8 for commitment of a CD8α+ conventional DC clonogenic progenitor. *Nat. Immunol.* **16**, 708–717 (2015).
258. Gudjonsson, S. *et al.* IRF4 Transcription-Factor-Dependent CD103+CD11b+ Dendritic Cells Drive Mucosal T Helper 17 Cell Differentiation. *Immunity* **38**, 958–969 (2013).
259. Schlitzer, A. *et al.* IRF4 Transcription Factor-Dependent CD11b+ Dendritic Cells in Human and Mouse Control Mucosal IL-17 Cytokine Responses. *Immunity* **38**, 970–983 (2013).
260. Guilliams, M. *et al.* Unsupervised High-Dimensional Analysis Aligns Dendritic Cells across Tissues and Species. *Immunity* **45**, 669–684 (2016).
261. Bachem, A. *et al.* Expression of XCR1 Characterizes the Batf3-Dependent Lineage of Dendritic Cells Capable of Antigen Cross-Presentation. *Front. Immunol.* **3**, 1–12 (2012).
262. Mowat, A. M. *et al.* Lymph-borne CD8α+ dendritic cells are uniquely able to cross-prime CD8+ T cells with antigen acquired from intestinal epithelial cells. *Mucosal Immunol.* **8**, 38–48 (2015).
263. Pigni, M., Ashok, D., Stevanin, M. & Acha-Orbea, H. Establishment and Characterization of a Functionally Competent Type 2 Conventional Dendritic Cell Line. *Front. Immunol.* **9**, 1–15 (2018).
264. Pooley, J. L., Heath, W. R. & Shortman, K. Cutting Edge: Intravenous Soluble Antigen Is Presented to CD4 T Cells by CD8- Dendritic Cells, but Cross-Presented

to CD8 T Cells by CD8+ Dendritic Cells. *J. Immunol.* **166**, 5327–5330 (2001).
265. Lepore, M., Mori, L. & De Libero, G. The conventional nature of non-MHC-restricted T cells. *Front. Immunol.* **9**, 1–11 (2018).
266. Trottein, F. & Paget, C. Natural killer T cells and mucosal-associated invariant T cells in lung infections. *Front. Immunol.* **9**, 1–17 (2018).
267. Wingender, G. *et al.* Intestinal microbes affect phenotypes and functions of invariant natural killer T cells in mice. *Gastroenterology* **143**, 418–428 (2012).
268. Wands, J. M. *et al.* Distribution and leukocyte contacts of γδ T cells in the lung. *J. Leukoc. Biol.* **78**, 1086–1096 (2005).
269. Carding, S. R. & Egan, P. J. γδ T cells: Functional plasticity and heterogeneity. *Nat. Rev. Immunol.* **2**, 336–345 (2002).
270. Godfrey, D. I. & Rossjohn, J. New ways to turn on NKT cells. *J. Exp. Med.* **208**, 1121–1125 (2011).
271. Kinjo, Y. *et al.* Recognition of bacterial glycosphingolipids by natural killer T cells. *Nature* **434**, 520–525 (2005).
272. Godfrey, D. I. *et al.* Antigen recognition by CD1d-restricted NKT T cell receptors. *Semin. Immunol.* **22**, 61–67 (2010).
273. Holzapfel, K. L., Tyznik, A. J., Kronenberg, M. & Hogquist, K. A. Antigen-Dependent versus -Independent Activation of Invariant NKT Cells during Infection. *J. Immunol.* **192**, 5490–5498 (2014).
274. Kawano, T. *et al.* CD1d-Restricted and TCR-Mediated Activation of V(sub alpha) 14 NKT Cells by Glycosylceramides. *Science (80-.).* **278**, 1626–1630 (1997).
275. Anderson, R. J. *et al.* NKT cell-dependent glycolipid-peptide vaccines with potent anti-tumour activity. *Chem. Sci.* **6**, 5120–5127 (2015).
276. Hermans, I. F. *et al.* NKT Cells Enhance CD4 + and CD8 + T Cell Responses to Soluble Antigen In Vivo through Direct Interaction with Dendritic Cells . *J. Immunol.* **171**, 5140–5147 (2003).
277. Speir, M., Hermans, I. F. & Weinkove, R. Engaging Natural Killer T Cells as 'Universal Helpers' for Vaccination. *Drugs* **77**, 1–15 (2017).
278. Tilloy, F. *et al.* An invariant T cell receptor α chain defines a novel TAP-independent major histocompatibility complex class Ib-restricted α/β T cell subpopulation in mammals. *J. Exp. Med.* **189**, 1907–1921 (1999).
279. Awad, W., Le Nours, J., Kjer-Nielsen, L., McCluskey, J. & Rossjohn, J. Mucosal-associated invariant T cell receptor recognition of small molecules presented by MR1. *Immunol. Cell Biol.* **96**, 588–597 (2018).
280. Porcelli, S., Yockey, C. E., Brenner, M. B. & Balk, S. P. Analysis of T cell antigen receptor (TCR) expression by human peripheral blood CD4-8− αβ T cells demonstrates preferential use of several Vβ genes and an invariant TCR α chain. *J. Exp. Med.* **178**, 1–16 (1993).
281. Gherardin, N. A. *et al.* Human blood MAIT cell subsets defined using MR1 tetramers. *Immunol. Cell Biol.* **96**, 507–525 (2018).
282. Lee, H. K. *et al.* Differential roles of migratory and resident DCs in T cell priming after mucosal or skin HSV-1 infection. *J. Exp. Med.* **206**, 359–370 (2009).
283. Cibrián, D. & Sánchez-madrid, F. CD69 : from activation marker to metabolic gatekeeper. *Eur. J. Immunol.* **47**, 946–953 (2017).

284. Murayama, G., Chiba, A., Suzuki, H., Nomura, A. & Mizuno, T. A Critical Role for Mucosal-Associated Invariant T Cells as Regulators and Therapeutic Targets in Systemic Lupus Erythematosus. *Front. Immunol.* **10**, 1–12 (2019).
285. Ahn, E. *et al.* Role of PD-1 during effector CD8 T cell differentiation. *Proc. Natl. Acad. Sci. United States* **115**, 4749–4754 (2018).
286. Meierovics, A. I. & Cowley, S. C. MAIT cells promote inflammatory monocyte differentiation into dendritic cells during pulmonary intracellular infection. *J. Exp. Med.* **213**, 2793–2809 (2016).
287. Gerner, M. Y., Torabi-Parizi, P. & Germain, R. N. Strategically Localized Dendritic Cells Promote Rapid T Cell Responses to Lymph-Borne Particulate Antigens. *Immunity* **42**, 172–185 (2015).
288. Ohl, L. *et al.* CCR7 governs skin dendritic cell migration under inflammatory and steady-state conditions. *Immunity* **21**, 279–288 (2004).
289. Waithman, J. *et al.* Resident CD8+ and Migratory CD103+ Dendritic Cells Control CD8 T Cell Immunity during Acute Influenza Infection. *PLoS One* **8**, 1–7 (2013).
290. Krishnaswamy, J. K., Gowthaman, U., Zhang, B., Mattsson, J. & Szeponik, L. Migratory CD11b+ conventional dendritic cells induce T follicular helper cell-dependent antibody responses. *Sci. Immunol.* **2**, eaam9169 (2017).
291. Lim, T. S. *et al.* CD80 and CD86 Differentially Regulate Mechanical Interactions of T-Cells with Antigen-Presenting Dendritic cells and B-cells. *PLoS One* **7**, 1–8 (2012).
292. Subauste, C. S., Malefyt, R. D. W. & Fuh, F. Role of CD80 (B7.1) and CD86 (B7.2) in the Immune Response to an Intracellular Pathogen. *J. Immunol.* **160**, 1831–1840 (1998).
293. Dudek, A. M., Martin, S., Garg, A. D., Agostinis, P. & Hargadon, K. M. Immature , semi-mature , and fully mature dendritic cells : toward a DC-cancer cells interface that augments anticancer immunity. *Front. Immunol.* **4**, 1–14 (2013).
294. Onishi, Y., Fehervari, Z., Yamaguchi, T. & Sakaguchi, S. Foxp3+ natural regulatory T cells preferentially form aggregates on dendritic cells in vitro and actively inhibit their maturation. *Proc. Natl. Acad. Sci. United States* **105**, 10113–10118 (2008).
295. Garcia-Bates, T. M. *et al.* Contrasting Roles of the PD-1 Signaling Pathway in Dendritic cell-mediated induction and regulation of HIV-1-specific effector T cell functions. *J. Virol.* **93**, e02035-18 (2019).
296. Freeman, B. G. J. *et al.* Engagement of the PD-1 Immunoinhibitory Receptor by a Novel B7 Family Member Leads to Negative Regulation of Lymphocyte Activation. *J. Exp. Med.* **192**, 1027–1034 (2000).
297. Nishimura, H. *et al.* Developmentally regulated expression of the PD-1 protein on the surface of double-negative (CD4-CD8-) thymocytes. *Int. Immunol.* **8**, 773–780 (1996).
298. Everts, B. *et al.* Migratory CD103 + dendritic cells suppress helminth-driven type 2 immunity through constitutive expression of IL-12. *J. Exp. Med.* **213**, 35–51 (2016).
299. Maldonado-López, R. *et al.* CD8α+ and CD8α- Subclasses of dendritic cells direct the development of distinct T helper cells in vivo. *J. Exp. Med.* **189**, 587–592

(1999).
300. Gao, Y. *et al.* Control of T helper 2 responses by transcription factor IRF4-dependent dendritic cells. *Immunity* **39**, 722–732 (2013).
301. Plantinga, M. *et al.* Conventional and Monocyte-Derived CD11b+ Dendritic Cells Initiate and Maintain T Helper 2 Cell-Mediated Immunity to House Dust Mite Allergen. *Immunity* **38**, 322–335 (2013).
302. Shin, C. *et al.* Intrinsic features of the CD8α- dendritic cell subset in inducing functional T follicular helper cells. *Immunol. Lett.* **172**, 21–28 (2016).
303. Eisenbarth, S. C. Dendritic cell subsets in T cell programming: location dictates function. *Nat. Rev. Immunol.* **19**, 89–103 (2019).
304. Lange, J. *et al.* The Chemical Synthesis, Stability, and Activity of MAIT Cell Prodrug Agonists That Access MR1 in Recycling Endosomes. *ACS Chem. Biol.* (2020) doi:10.1021/acschembio.9b00902.
305. Kelly, J. *et al.* Chronically stimulated human MAIT cells are unexpectedly potent IL-13 producers. *Immunol. Cell Biol.* **97**, 689–699 (2019).
306. Appay, V., Douek, D. C. & Price, D. A. CD8 + T cell efficacy in vaccination and disease. *Nat. Med.* **14**, 623–628 (2008).
307. Geginat, J. *et al.* Plasticity of human CD4 T cell subsets. *Front. Immunol.* **5**, 1–10 (2014).
308. Weintraub, A. Immunology of bacterial polysaccharide antigens. *Carbohydr. Res.* **338**, 2539–2547 (2003).
309. Plotkin, S. A. Correlates of Vaccine-Induced Immunity. *Clin. Infect. Dis.* **47**, 401–409 (2008).
310. Hoft, D. F. *et al.* Live and Inactivated Influenza Vaccines Induce Similar Humoral Responses , but Only Live Vaccines Induce Diverse T-Cell Responses in Young Children. *J. Infect. Dis.* **204**, 845–854 (2011).
311. Booth, J. S. *et al.* Effect of the live oral attenuated typhoid vaccine , Ty21a , on systemic and terminal ileum mucosal CD4 + T memory responses in humans. *Int. Immunol.* **31**, 101–116 (2018).
312. Salerno-goncalves, R., Pasetti, M. F. & Sztein, M. B. Characterization of CD8 + Effector T Cell Responses in Volunteers Immunized with Salmonella enterica Serovar Typhi Strain Ty21a Typhoid Vaccine. *J. Immunol.* **169**, 2196–2203 (2002).
313. Garrido, F. *et al.* The escape of cancer from T cell-mediated immune surveillance: HLA class I loss and tumor tissue architecture. *Vaccines* **5**, 1–10 (2017).
314. Zheng, B., Xu, G., Chen, X., Marinova, E. & Han, S. ICOSL-mediated signalling is essential for the survival and functional maturation of germinal center B cells through the classical NF-kB pathway. *J. Immunol.* **194**, 131.9 (2015).
315. Grewal, I. S. & Flavell, R. A. The Role of CD40 Ligand in Costimulation and T-Cell Activation. *Immunol. Rev.* **153**, 85–106 (1996).
316. Anderson, D. M. *et al.* A homologue of the TNF receptor and its ligand enhance T-cell growth and dendritic-cell function. **390**, 175–179 (1997).
317. Josien, B. R. *et al.* TRANCE , a Tumor Necrosis Factor Family Member , Enhances the Longevity and Adjuvant Properties of Dendritic Cells In Vivo. *J. Exp. Med.*

191, 495–501 (2000).
318. Viret, J. *et al.* Mucosal and Systemic Immune Responses in Humans after Primary and Booster Immunizations with Orally Administered Invasive and Noninvasive Live Attenuated Bacteria. *Infect. Immun.* **67**, 3680–3685 (1999).
319. Goodnow, C. C., Vinuesa, C. G., Randall, K. L., Mackay, F. & Brink, R. Control systems and decision making for antibody production. *Nat. Immunol.* **11**, 681–688 (2010).
320. Ko, E. *et al.* Roles of alum and monophosphoryl lipid A adjuvants in overcoming CD4+ T cell deficiency to induce isotype-switched IgG antibody responses and protection by T-dependent influenza vaccine. *J. Immunol.* **198**, 279–291 (2017).
321. Ko, E. *et al.* Effects of MF59 Adjuvant on Induction of Isotype-Switched IgG Antibodies and Protection after Immunization with T-Dependent Influenza Virus Vaccine in the Absence of CD4+ T Cells. *J. Virol.* **90**, 6976–6988 (2016).
322. Kasturi, S. P. *et al.* Programming the magnitude and persistence of antibody responses with innate immunity. *Nature* **470**, 543–547 (2011).
323. Crotty, S. *et al.* Cutting Edge: Long-Term B Cell Memory in Humans after Smallpox Vaccination. *J. Immunol.* **171**, 4969–4973 (2003).
324. Calisher, H., Monath, T. P., Downs, W. G. & Murphy, K. Persistence of neutralizing antibody 30- 35 years after immunization with 17D yellow fever vaccine. *Bull. World Heath Organ.* **59**, 895–900 (1981).
325. Siegrist, C. *Vaccines*. (Saunders, 2013).
326. Nothdurft, H. D. *et al.* A new accelerated vaccination schedule for rapid protection against hepatitis A and B. *Vaccine* **20**, 1157–1162 (2002).
327. Netea, M. G. *et al.* Trained immunity: A program of innate immune memory in health and disease. *Science (80-.).* **352**, p.aaf1098 (2016).
328. Quintin, J. *et al.* Candida albicans Infection Affords Protection against Reinfection via Functional Reprogramming of Monocytes. *Cell Host Microbe* **12**, 223–232 (2012).
329. Lee, J. *et al.* Epigenetic Modification and Antibody-Dependent Expansion of Memory-like NK Cells in Human Cytomegalovirus-Infected Individuals. *Immunity* **42**, 431–442 (2015).
330. Naik, S. *et al.* Inflammatory memory sensitizes skin epithelial stem cells to tissue damage. *Nature* **550**, 475–480 (2017).
331. Sánchez-Ramón, S. *et al.* Trained Immunity-Based Vaccines: A New Paradigm for the Development of Broad-Spectrum Anti-infectious Formulations. *Front. Immunol.* **9**, 1–11 (2018).
332. Pulendran, B. Variegation of the Immune Response with Dendritic Cells and Pathogen Recognition Receptors. *J. Immunol.* **174**, 2457–2465 (2005).
333. Krug, A. *et al.* TLR9-dependent recognition of MCMV by IPC and DC generates coordinated cytokine responses that activate antiviral NK cell function. *Immunity* **21**, 107–119 (2004).
334. Ito, T., Wang, Y. H. & Liu, Y. J. Plasmacytoid dendritic cell precursors/type I interferon-producing cells sense viral infection by Toll-like receptor (TLR) 7 and TLR9. *Springer Semin. Immunopathol.* **26**, 221–229 (2005).
335. Datta, S. K. *et al.* A Subset of Toll-Like Receptor Ligands Induces Cross-

presentation by Bone Marrow-Derived Dendritic Cells. *J. Immunol.* **170**, 4102–4110 (2003).
336. Querec, T. *et al.* Yellow fever vaccine YF-17D activates multiple dendritic cell subsets via TLR2, 7, 8, and 9 to stimulate polyvalent immunity. *J. Exp. Med.* **203**, 413–424 (2006).
337. Montagna, G. N., Biswas, A., Hildner, K., Matuschewski, K. & Dunay, I. R. Batf3 deficiency proves the pivotal role of CD8α+ dendritic cells in protection induced by vaccination with attenuated Plasmodium sporozoites. *Parasite Immunol.* **37**, 533–543 (2015).
338. Flores-Langarica, A. *et al.* Intestinal CD103+CD11b+ cDC2 conventional dendritic cells are required for primary CD4+ T and B cell responses to soluble flagellin. *Front. Immunol.* **9**, 1–9 (2018).
339. Parekh, V. V *et al.* Glycolipid antigen induces long-term natural killer T cell anergy in mice . *J. Clin. Invest.* **115**, 2572–2583 (2005).
340. Iyoda, T. *et al.* Invariant NKT cell anergy is induced by a strong TCR-mediated signal plus co-stimulation. *Int. Immunol.* **22**, 905–913 (2010).
341. Budd, R. C. *et al.* Distinction of virgin and memory T lymphocytes . Stable acquisition of the Pgp-1 glycoprotein concomitant with antigenic stimulation . *J. Immunol.* **138**, 3120–3129 (1987).
342. Schumann, J., Stanko, K., Schliesser, U. & Appelt, C. Differences in CD44 Surface Expression Levels and Function Discriminates IL-17 and IFN- γ Producing Helper T Cells. *PLoS One* **10**, 1–18 (2015).
343. Conejero, L. *et al.* Lung CD103 + dendritic cells restrain allergic airway inflammation through IL-12 production. *JCI Insight* **2**, e90420 (2017).
344. Edelson, B. T. *et al.* Peripheral CD103 + dendritic cells form a unified subset developmentally related to CD8a+ conventional dendritic cells. *J. Exp. Med.* **207**, 823–836 (2010).
345. Tussiwand, R. *et al.* Compensatory dendritic cell development mediated by BATF-IRF interactions. *Nature* **490**, 502–507 (2012).
346. Immunological Genome Project RNA-Seq Gene Skyline database. http://rstats.immgen.org/Skyline/skyline.html.
347. Ochiai, S. *et al.* Thymic stromal lymphopoietin drives the development of IL-13 + Th2 cells. *Proc. Natl. Acad. Sci. U. S. A.* **115**, 1033–1038 (2018).
348. Maier, E., Duschl, A. & Horejs-Hoeck, J. STAT6-dependent and -independent mechanisms in Th2 polarization. *Eur. J. Immunol.* **42**, 2827–2833 (2012).
349. Black, C. L. *et al.* Increases in Levels of Schistosome-Specific Immunoglobulin E and CD23 + B Cells in a Cohort of Kenyan Children Undergoing Repeated Treatment and Reinfection with Schistosoma mansoni . *J. Infect. Dis.* **202**, 399–405 (2010).
350. Mitchell, J. *et al.* Altered Populations of Unconventional T Cell Lineages in Patients with Langerhans Cell Histiocytosis. *Sci. Rep.* **8**, 1–13 (2018).
351. Hinks, T. S. C. *et al.* Activation and In Vivo Evolution of the MAIT Cell Transcriptome in Mice and Humans Reveals Tissue Repair Functionality. *Cell Rep.* **28**, 3249-3262.e5 (2019).
352. Cui, Y. *et al.* Mucosal-associated invariant T cell-rich congenic mouse strain

allows for functional evaluation. *J. Clin. Inestigation* **125**, 4171–4186 (2015).
353. Bennett, M. S., Trivedi, S., Iyer, A. S., Hale, J. S. & Leung, D. T. Human mucosal-associated invariant T (MAIT) cells possess capacity for B cell help. *J. Leukoc. Biol.* **102**, 1261–1269 (2017).
354. Wilgenburg, B. Van *et al.* MAIT cells are activated during human viral infections. *Nat. Commun.* **7**, 1–11 (2016).
355. Lamichhane, R., Galvin, H. & Hannaway, R. F. Type I interferons are important co-stimulatory signals during T cell receptor mediated human MAIT cell activation. *Eur. J. Immunol.* **50**, 178–191 (2020).
356. Sakai, J. & Akkoyunlu, M. The Role of BAFF System Molecules in Host Response to Pathogens. *Clin. Microbiol. Rev.* **30**, 991–1014 (2017).
357. Hutloff, A. *et al.* ICOS is an inducible T-cell co-stimulator structurally and functionally related to CD28. *Nature* **397**, 263–266 (1999).
358. Vidric, M., Bladt, A. T., Dianzani, U. & Watts, T. H. Role for Inducible Costimulator in Control of Salmonella enterica Serovar Typhimurium Infection in Mice. *Infect. Immun.* **74**, 1050–1061 (2006).
359. Nouailles, G. *et al.* Impact of inducible co-stimulatory molecule (ICOS) on T-cell responses and protection against Mycobacterium tuberculosis infection. *Eur. J. Immunol.* **41**, 981–991 (2011).
360. Scales, H. E. *et al.* Effect of inducible costimulator blockade on the pathological and protective immune responses induced by the gastrointestinal helminth Trichinella spiralis. *Eur. J. Immunol.* **34**, 2854–2862 (2004).
361. Akiba, H., Takeda, K. & Kojima, Y. The Role of ICOS in the CXCR5 + Follicular B Helper T Cell Maintenance In Vivo. *J. Immunol.* **175**, 2340–2348 (2005).
362. Shin, C. *et al.* CD8a- Dendritic Cells Induce Antigen-Specific T Follicular Helper Cells Generating Efficient Humoral Immune Responses. *Cell Rep.* **11**, 1929–1940 (2015).
363. Liang, L., Porter, E. M. & Sha, W. C. Constitutive expression of the B7h ligand for inducible costimulator on naive B cells is extinguished after activation by distinct B cell receptor and interleukin 4 receptor-mediated pathways and can be rescued by CD40 signaling. *J. Exp. Med.* **196**, 97–108 (2002).
364. Watanabe, M. *et al.* Down-Regulation of ICOS Ligand by Interaction with ICOS Functions as a Regulatory Mechanism for Immune Responses. *J. Immunol.* **180**, 5222–5234 (2008).
365. Zheng, J. *et al.* ICOS regulates the generation and function of human CD4+ Treg in a CTLA-4 dependent manner. *PLoS One* **8**, e82203 (2013).
366. Liu, D. *et al.* T-B-cell entanglement and ICOSL-driven feed-forward regulation of germinal centre reaction. *Nature* **517**, 214–218 (2015).
367. Rothe, M., Sarma, V., Dixit, V. M. & Goeddel, D. V. TRAF2-mediated activation of Nf-kappaB by TNF receptor 2 and CD40. *Science (80-.).* **269**, 1424–1427 (1995).
368. Akiyama, T., Shinzawa, M. & Akiyama, N. TNF receptor family signaling in the development and functions of medullary thymic epithelial cells. *Front. Immunol.* **3**, 1–9 (2012).
369. Quintin, J. *et al.* Candida albicans infection affords protection against reinfection via functional reprogramming of monocytes. *Cell Host Microbe* **12**, 223–232

(2012).
370. Hole, C. *et al.* Induction of memory-like dendritic cell responses in vivo. *Nat. Commun.* **10**, 2955–2968 (2019).
371. Chen, F. *et al.* Neutrophils prime a long-lived effector macrophage phenotype that mediates accelerated helminth expulsion. *Nat. Immunol.* **15**, 938–946 (2014).
372. Ifrim, D. C. *et al.* Trained immunity or tolerance: Opposing functional programs induced in human monocytes after engagement of various pattern recognition receptors. *Clin. Vaccine Immunol.* **21**, 534–545 (2014).
373. Palm, N. W., Rosenstein, R. K. & Medzhitov, R. Allergic host defences. *Nature* **484**, 465–472 (2012).
374. Grun, J. L. & Maurer, P. H. Different T helper cell subsets elicited in mice utilizing two different adjuvant vehicles: The role of endogenous interleukin 1 in poliferative responses. *Cell. Immunol.* **121**, 134–145 (1989).
375. Pollock, K. G. J., Conacher, M., Wei, X., Alexander, J. & Brewer, J. M. Interleukin-18 plays a role in both the alum-induced T helper 2 response and the T helper 1 response induced by alum-adsorbed interleukin-12. *Immunology* **108**, 137–143 (2003).
376. Brewer, J. M. *et al.* Aluminium Hydroxide Adjuvant Initiates Strong Antigen-Specific Th2 Responses in the Absence of IL-4- or IL-13-Mediated Signaling. *J. Immunol.* **163**, 6448–6454 (1999).
377. Chapman, T. J. *et al.* Pre-existing Tolerance Shapes the Outcome of Mucosal Allergen Sensitization in a Murine Model of Asthma. *J. Immunol.* **191**, 4423–4430 (1999).
378. Baker, K., Raemdonck, K., Snelgrove, R. J., Belvisi, M. G. & Birrell, M. A. Characterisation of a murine model of the late asthmatic response. *Respir. Res.* **18**, 1–17 (2017).
379. Dusseaux, M. *et al.* Human MAIT cells are xenobiotic-resistant , tissue-targeted , CD161 hi IL-17 – secreting T cells. *Blood* **117**, 1250–1259 (2011).
380. Ho, I. & Pai, S. GATA-3 – Not Just for Th2 Cells Anymore. *Cell. Mol. Immunol.* **4**, 15–29 (2007).
381. Krishnaswamy, J. K., Alsén, S., Yrlid, U. & Eisenbarth, S. C. Determination of T Follicular Helper Cell Fate by Dendritic Cells. *Front. Immunol.* **9**, 1–16 (2018).
382. Lofano, G. *et al.* Oil-in-Water Emulsion MF59 Increases Germinal Center B Cell Differentiation and Persistence in Response to Vaccination. *J. Immunol.* **195**, 1617–1627 (2015).
383. Leung, D. T. *et al.* Circulating Mucosal Associated Invariant T Cells Are Activated in Vibrio cholerae O1 Infection and Associated with Lipopolysaccharide Antibody Responses. *PLoS Negl. Trop. Dis.* **8**, e3076 (2014).
384. Bennett, M. S., Trivedi, S., Lyer, A. S., Hale, J. S. & Leung, D. T. Human mucosal-associated invariant T (MAIT) cells possess capacity for B cell help. *J. Leukoc. Biol.* **102**, 1261–1269 (2017).
385. Yao, C., Zurawski, S. M., Jarrett, E. S., Chicoine, B. & Crabtree, J. Skin dendritic cells induce follicular helper T cells and protective humoral immune responses. *J. Allergy Clin. Immunol.* **136**, 1387–1397 (2015).

386. Kato, Y. *et al.* Targeting antigen to Clec9A primes follicular Th cell memory responses capable of robust recall. *J. Immunol.* **195**, 1006–1014 (2015).
387. Calabro, S. *et al.* Bridging channel dendritic cells induce immunity to transfused red blood cells. *J. Exp. Med.* **213**, 887–896 (2016).
388. Bajaña, S. *et al.* IRF4 Promotes Cutaneous Dendritic Cell Migration to Lymph Nodes during Homeostasis and Inflammation. *J. Immunol.* **189**, 3368–3377 (2012).
389. Bajaña, S., Turner, S., Paul, J., Ainsua-Enrich, E. & Kovats, S. IRF4 and IRF8 act in CD11c+ cells to regulate terminal differentation of lung tissue dendritic cells. *J. Immunol.* **196**, 1666–1677 (2016).
390. Dudziak, D. *et al.* Differential antigen processing by dendritic cell subsets in vivo. *Science (80-.).* **315**, 107–112 (2007).
391. Chua, W. *et al.* Polyclonal mucosa-associated invariant T cells have unique innate functions in bacterial infection. *Infect. Immun.* **80**, 3256–3267 (2012).
392. Swallow, M. M., Wallin, J. J. & Sha, W. C. B7h , a Novel Costimulatory Homolog of B7 . 1 and B7 . 2 , Is Induced by TNFa. *Immunity* **11**, 423–432 (1999).
393. Coope, H. J. *et al.* CD40 regulates the processing of NF-kB2 p100 to p52. *EMBO J.* **21**, 5375–5385 (2002).
394. Novack, D. V. *et al.* The IkB Function of NF-kB2 p100 Controls Stimulated Osteoclastogenesis. *J. Exp. Med.* **198**, 771–781 (2003).
395. Caux, B. C. *et al.* Activation of human dendritic cells through CD40 cross-linking. *J. Exp. Med.* **180**, 1263–1272 (1994).
396. Wiethe, C., Dittmar, K., Doan, T. & Tindle, R. Enhanced effector and memory CTL responses generated by incorporation of receptor activator of NF-kB (RANK)/RANK ligand costimulatory molecules into dendritic cell immunogens expressing a hman tumor-specific antigen. *J. Immunol.* **171**, 4121–4130 (2003).
397. Papadaki, M., Rinotas, V., Violitzi, F. & Thireou, T. New Insights for RANKL as a Proinflammatory Modulator in Modeled Inflammatory Arthritis. *Front. Immunol.* **10**, 1–19 (2019).
398. Hayashi, E. *et al.* Involvement of Mucosal-associated Invariant T cells in Ankylosing Spondylitis. *J. Rheumatol.* **43**, 1–9 (2016).
399. Gracey, E. *et al.* IL-7 primes IL-17 in mucosal-associated invariant T (MAIT) cells, which contribute to the Th17-axis in ankylosing spondylitis. *Ann. Rheum. Dis.* **75**, 2124–2132 (2016).
400. Rouxel, O. *et al.* Dual role of mucosal-associated invariant T cells in type 1 diabetes. *Nat. Immunol.* **18**, 1321–1331 (2018).
401. Willing, A. *et al.* CD8 + MAIT cells infiltrate into the CNS and alterations in their blood frequencies correlate with IL-18 serum levels in multiple sclerosis. *Eur. J. Immunol.* **44**, 3119–3128 (2014).
402. Abrahamsson, S. V *et al.* Non-myeloablative autologous haematopoietic stem cell transplantation expands regulatory cells and depletes IL-17 producing mucosal-associated invariant T cells in multiple sclerosis. *Brain* **136**, 2888–2903 (2013).
403. Croxford, J. L., Miyake, S., Huang, Y., Shimamura, M. & Yamamura, T. Invariant Va19i T cells regulate autoimmune inflammation. *Nat. Immunol.* **7**, 987–994

(2006).
404. Smirnov, D., Schmidt, J. J., Capecchi, J. T. & Wightman, P. D. Vaccine adjuvant activity of 3M-052 : An imidazoquinoline designed for local activity without systemic cytokine induction. *Vaccine* **29**, 5434–5442 (2011).
405. Holmgren, J., Harandi, A. M. & Czerkinsky, C. Mucosal adjuvants and anti-infection and anti- immunopathology vaccines based on cholera toxin , cholera toxin B subunit and CpG DNA. *Expert Rev. Vaccines* **2**, 205–217 (2003).
406. Kopic, S. & Geibel, J. P. Toxin Mediated Diarrhea in the 21st Century: The Pathophysiology of Intestinal Ion Transport in the Course of ETEC, V. cholerae and Rotavirus Infection. *Toxins (Basel).* **2**, 2132–2157 (2010).
407. Elson, C. & Ealding, A. N. D. W. Generalized systemic and mucosal immunity in mice after mucosal stimulation with cholera toxin. *J. Immunol.* **132**, 2736–2741 (1984).
408. Bergquist, C., Johansson, E., Lagergård, T., Holmgren, J. A. N. & Rudin, A. Intranasal Vaccination of Humans with Recombinant Cholera Toxin B Subunit Induces Systemic and Local Antibody Responses in the Upper Respiratory Tract and the Vagina. *Infect. Immun.* **65**, 2676–2684 (1997).
409. George-chandy, A. *et al.* Cholera Toxin B Subunit as a Carrier Molecule Promotes Antigen Presentation and Increases CD40 and CD86 Expression on Antigen-Presenting Cells. *Infect. Immun.* **69**, 5716–5725 (2001).
410. Constantinides, M. G. *et al.* MAIT cells are imprinted by the microbiota in early life and promote tissue repair. *Science (80-.).* **366**, 1–13 (2019).
411. Salou, M. *et al.* A common transcriptomic program acquired in the thymus defines tissue residency of MAIT and NKT subsets. *J. Exp. Med.* **216**, 133–151 (2018).
412. Sobkowiak, M. J. *et al.* Tissue-resident MAIT cell populations in human oral mucosa exhibit an activated profile and produce IL-17. *Eur. J. Immunol.* **49**, 133–143 (2019).
413. Hollister, K. *et al.* Insights into the role of Bcl6 in follicular helper T cells using a new conditional mutant mouse model. *J. Immunol.* **191**, 3705–3711 (2013).
414. Wykes, M. *et al.* Dendritic Cells Interact Directly with Naive B Lymphocytes to Transfer Antigen and Initiate Class Switching in a Primary T-Dependent Response. *J. Immunol.* **161**, 1313–1319 (1998).
415. Lefrançois, L., Altman, J. D., Williams, K. & Olson, S. Soluble Antigen and CD40 Triggering Are Sufficient to Induce Primary and Memory Cytotoxic T Cells. *J. Immunol.* **164**, 725–732 (2000).
416. Sprent, J. Antigen-Presenting Cells: Professionals and amateurs. *Curr. Biol.* **5**, 1095–1097 (1995).
417. Visweswaraiah, A., Novotny, L. A., Hjemdahl-Monsen, E. J., Bakaletz, L. O. & Thanavala, Y. Tracking the tissue distribution of marker dye following intranasal delivery in mice and chinchillas: A multifactorial analysis of parameters affecting nasal retention. *Vaccine* **20**, 3209–3220 (2002).
418. Brozova, J., Karlova, I. & Novak, J. Analysis of the Phenotype and Function of the Subpopulations of Mucosal-Associated Invariant T Cells. *Scand. J. Immunol.* **84**, 245–251 (2016).

419. Elgueta, R. *et al.* Molecular mechanism and function of CD40/CD40L engagement in the Immune System. *Immunol. Rev.* **229**, 1–6 (2009).
420. Perlot, T. & Penninger, J. M. Development and Function of Murine B Cells Lacking RANK. *J. Immunol.* **188**, 1201–1205 (2012).
421. Kawai, T. *et al.* B and T lymphocytes are the primary sources of RANKL in the bone resorptive lesion of periodontal disease. *Am. J. Pathol.* **169**, 987–998 (2006).
422. Stark, F. C., McCluskie, M. J. & Krishnan, L. Homologous prime-boost vaccination with OVA entrapped in self-adjuvanting archaeosomes induces high numbers of OVA-specific CD8+ T cells that protect against subcutaneous B16-OVA melanoma. *Vaccines* **4**, 1–15 (2016).
423. Liu, Z. *et al.* A novel method for synthetic vaccine construction based on protein assembly. *Sci. Rep.* **4**, 1–8 (2014).
424. Silva, A. *et al.* The Combination of ISCOMATRIX Adjuvant and TLR Agonists Induces Regression of Established Solid Tumors In Vivo. *J. Immunol.* **194**, 2199–2207 (2015).
425. Weiberg, D. *et al.* Participation of the spleen in the IgA immune response in the gut. *PLoS One* **13**, 1–18 (2018).
426. Knudsen, N. P. H. *et al.* Different human vaccine adjuvants promote distinct antigen-independent immunological signatures tailored to different pathogens. *Sci. Rep.* **6**, 1–13 (2016).